Sea ice and carbon dioxide

Clive Hambler (1)*, Peter A. Henderson (1,2)

((1) Department of Zoology, University of Oxford, UK, ORCID 0000-0002-2361-828X (2) PISCES Conservation Ltd, UK, ORCID 0000-0002-7461-1758) * corresponding author clive.hambler@zoo.ox.ac.uk

Abstract

1) The annual cycles of atmospheric CO_2 at Mauna Loa and Point Barrow (Alaska) are statistically almost completely explained by changes in Arctic sea ice volume and extent. 2) The annual cycles of atmospheric CO_2 at the South Pole and at Palmer Station are statistically largely explained by changes in Antarctic sea ice extent. 3) Results are consistent with a monthly CO_2 flux dependent on the distance from equilibrium of a temperature dependent process. Degassing and calcium carbonate crystal formation during the sea ice freeze likely contribute to the peak net monthly emission rate of CO_2. High solubility of gas in cold sea ice meltwater and dissolution of calcium carbonate likely contribute to the peak net monthly sink rate of CO_2. 4) The global annual mean Lower Tropospheric temperature anomaly has high predictive value for annual CO_2 changes, consistent with marine outgassing (and possibly vertical transport mediated by sea ice). 5) The global carbon cycle is poorly understood, with abiotic factors likely dominating biotic fluxes - and little scope for substantive human involvement in the annual cycle. 6) A new investigative paradigm is required in which atmospheric CO_2 level is a response variable of temperature or an unknown covariate. 7) Climate predictions and attributions must be revisited. 8) The policy implications are as significant as the relationship between sea ice and CO_2 rates.

Keywords $CaCO_3$ • Carbon dioxide • Climate change • Degassing • Outgassing • Productivity

Introduction

The dynamics of atmospheric CO_2 and temperature are central to climate science and policy (Ciais et al 2013). Here we demonstrate that sea ice has been very seriously neglected in studies of the carbon cycle - including the seasonal variation of CO_2 fluxes.

Because the total observed atmospheric CO_2 level is the product of various sources and sinks, any re-evaluation of the scale of a specific CO_2 flux component has implications for the estimated magnitudes of other fluxes (Ciais et al 2013; Resplandy et al 2018; Bushinsky et al 2019). Modelled projections of future CO_2 levels and associated global climates depend on natural fluxes being partitioned and quantified (Ciais et al 2013; Steiner et al 2013; Notz and Bitz 2017; Resplandy et al 2018). Detection of the anthropogenic contribution to net CO_2 flux and hence atmospheric levels also depends on the partitioning of the natural fluxes (Ciais et al 2013). However, many parameters in the global carbon cycle are very sparsely sampled - including the details of air-sea fluxes (Takahashi et al 1993, 2009; Rosso et al 2017; Tison et al 2017; Resplandy et al 2018; Francey et al 2019). This is particularly problematic in logistically challenging sea ice zones (Geilfus et al 2018; Gray AR et al 2018; Bushinsky et al 2019; MOSAiC 2019; Ouyang et al 2020). Models have been relatively poor at reproducing the oceanic partial pressure of CO_2 (pCO_2) in sub-polar regions (Ciais et al 2013). Despite its potential importance, sea ice is not well represented qualitatively or quantitatively in many climate models (Nomura et al 2013; Steiner et al 2013; Vancoppenolle et al 2013; Moreau et al 2016; Notz and Bitz 2017; Vancoppenolle and Tedesco 2017).

Mauna Loa is the iconic site for monitoring global CO_2 levels, benefitting from a location where samples are likely to be relatively representative (Keeling et al 1976, 2005; Buermann et al 2007). On an annual cycle, CO_2 levels at Mauna Loa fluctuate seasonally in a distinctive 'sawtooth' curve (Keeling et al 2005; IPCC 2013). This and similar oscillations elsewhere have long been ascribed to terrestrial vegetation production and respiration in the northern land masses (Keeling 1960, 2008; Denning et al 1995; Dettinger and Ghil 1998; Keeling et al 2001, 2005; Schaefer et al 2005; Buermann et al 2007; Ciais et al 2013; Graven et al 2013; Zhao and Zeng 2014; Barlow et al 2015; Francey et al 2019; Haverd et al 2020). Such oscillation at Barrow (Alaska) has been ascribed to terrestrial vegetation (Peterson et al 1987; Keeling et al 2005). However, an involvement of sea ice in seasonal variation of atmospheric CO_2 at Barrow was suggested by Semiletov et al (2007). An alternative explanation for seasonal variation in CO_2 was also provided by Nelson and Nelson (2016) who found very high correlations between regional sea ice area and the regional level of CO_2.

Sea ice is often a source of atmospheric CO_2 in autumn and winter, and a sink in spring and summer, but these fluxes may not be exactly counter-balanced and their global significance is still to be established (Tison et al 2017; Ouyang et al 2020). The high latitude North Atlantic is the most intense observed oceanic sink area for CO_2 (Takahashi et al 2009), previously ascribed to phytoplankton blooms (Takahashi et al 1993). There is evidence that bidirectional CO_2 fluxes through Arctic sea ice - moderated by snow cover, flooding, melt ponds and ice properties - may have been neglected (Semiletov et al 2004, 2007; Miller et al 2011; Nomura et al 2013; Tison et al 2017). The effects of sea ice freeze and melt on atmospheric CO_2 flux are largely unknown (*e.g.* Geilfus et al 2015; Legge et al 2015; Tison et al 2017; Nomura et al 2018; Ouyang et al 2020).

The amplitude of seasonal variation in CO_2 levels is lower near the equator than for northern high latitudes, and relatively low in Southern Hemisphere sampling locations (Keeling et al 2001, 2005). The decline in amplitude is typically ascribed to less seasonal variation in photosynthesis (Keeling et al 1976, 2005; Haverd et al 2020) although Semiletov (1999) deduced there was a northern source for CO_2 and Nelson and Nelson (2016) implicated sea ice. Weaker CO_2 oscillations in more southerly CO_2 recording stations suggest a weaker Southern Hemisphere sink (Zhao and Zeng 2014).

Variation in CO_2 levels between years is the consequence of the balance of sources and sinks during a year. Some of these fluxes vary on short (hourly and monthly) scales, and others on multi-decadal or far longer scales. Inter-annual variability in CO_2 growth rate is typically ascribed largely to a presumed land sink, particularly in the tropics (Ciais et al 2013). The global ocean is widely believed to be a net CO_2 sink (*e.g.* Khatiwala et al 2009; IPCC 2013; DeVries 2014) of which the Arctic Ocean may contribute 5-15% (Ahmed and Else, 2019; Ahmed et al 2019), a flux that may change if sea ice retreats (Ouyang et al 2020).

Whilst regions differ, pCO_2 in the ocean surface water has generally been increasing at about the same rate as atmospheric CO_2 (Ciais et al 2013; Ouyang et al 2020), potentially consistent with one or more factors including increased CO_2 levels in the air, increased venting of CO_2 rich water from depth, and the basic physical process of increased outgassing from warming water (Wiesenburg and Guinasso 1979; Takahashi et al 1993; Soares 2010). Separating the influences of such factors is extremely challenging because controlled, replicated global experiments are impossible. In contrast to mainstream opinion, oceanic forcing of atmospheric CO_2 levels has long been proposed (*e.g.* Newell and Wear 1977; Newell et al 1978) and global surface temperature implicated in CO_2 dynamics (Salby 2012, 2016).

It is also difficult to isolate the processes leading to seasonal and inter-annual changes in CO_2 because there are spatial and temporal gaps in data - especially at high latitudes (*e.g.* Ouyang et al 2020). In-situ measurements of fluxes can give highly divergent magnitudes (Tison et al 2017). We therefore use cross-correlations to investigate

variables leading CO_2 changes, regionally and globally. Short lags between variables suggest more likely causal relationships, and if accurately measured a lagging variable cannot logically be causal.

We address these and related questions:

1) How strongly does sea ice correlate with the annual ('sawtooth') oscillation in atmospheric CO_2 recorded at Mauna Loa and elsewhere?

2) How strongly does terrestrial vegetation activity (NDVI) correlate with variation in atmospheric CO_2, within years?

3) How strongly is inter-annual variation in atmospheric CO_2 correlated with annual mean global and tropical ocean Lower Tropospheric temperature anomalies?

4) Is the global carbon cycle well understood?

Methods

Datasets

We use the datasets in Table 1.

Table 1 Data sources

Variable	**Source**
Atmospheric CO_2 Mauna Loa, USA. Monthly flask. NOAA data.	https://www.esrl.noaa.gov/gmd/dv/data/ Accessed 5 February 2020
Atmospheric CO_2 Point Barrow, USA Monthly flask. NOAA data	https://www.esrl.noaa.gov/gmd/dv/data/ Accessed 5 February 2020
Atmospheric CO_2 Point Barrow, USA Monthly flask. Scripps data 2017	Flask data in this file through 15-Dec-2017 from archive dated 2017-12-15 http://scrippsco2.ucsd.edu/data/atmospheric_co2/ptb Monthly atmospheric CO2 concentrations (ppm) derived from flask air samples and Pt. Barrow (Flasks), Alaska. 157W 71N Source: R. F. Keeling, S. C. Piper, A. F. Bollenbacher and S. J. Walker Scripps CO2 Program. Keeling et al (2001) https://web.archive.org/web/20180507042247/http://scrippsco2.ucsd.edu:80/assets/data/atmospheric/stations/flask_co2/monthly/monthly_flask_co2_ptb.csv Accessed 22 February 2020
Atmospheric CO_2 Point Barrow, USA Monthly flask. Scripps data 2018	Flask data in this file through 15-Oct-2018 last updated 29-Oct-2018 http://scrippsco2.ucsd.edu/data/atmospheric_co2/ptb Monthly atmospheric CO2 concentrations (ppm) derived from flask air samples and Pt. Barrow (Flasks), Alaska. 157W 71N Source: R. F. Keeling, S. C. Piper, A. F. Bollenbacher and S. J. Walker. Scripps CO2 Program. Keeling et al (2001)
Atmospheric CO_2 Alert, Canada. Monthly flask. NOAA data	https://www.esrl.noaa.gov/gmd/dv/data/ Accessed 5 February 2020
Atmospheric CO_2 South Pole. Monthly flask. NOAA data	https://www.esrl.noaa.gov/gmd/dv/data/ Accessed 5 February 2020
Atmospheric CO_2 Cape Kumukahi. Monthly flask. NOAA data	https://www.esrl.noaa.gov/gmd/dv/data/ Accessed 2 March 2020

(Table 1 continued). Variable	Source
Atmospheric CO_2 for other locations and used for graphs in the Appendix. Monthly flask. NOAA data.	Dlugokencky, E.J., J.W. Mund, A.M. Crotwell, M.J. Crotwell, and K.W. Thoning (2019), Atmospheric Carbon Dioxide Dry Air Mole Fractions from the NOAA ESRL Carbon Cycle Cooperative Global Air Sampling Network, 1968-2018, Version: 2019-07, https://doi.org/10.15138/wkgj-f215 Retrieved 11 May 2020
Sea ice volume Arctic. Modelled by DMI	http://ocean.dmi.dk/arctic/index.uk.php http://ocean.dmi.dk/arctic/icethickness/txt/IceVol.txt Accessed 23 July 2019
Sea Ice extent, Northern Hemisphere and its regions (MASIE data)	ftp://sidads.colorado.edu/DATASETS/NOAA/G02186/ MASIE NSIDC/NIC Sea Ice Product G02186 - Daily Ice Extent by Region in Square Kilometers National Ice Center and National Snow and Ice Data Center. Compiled by F. Fetterer, M. Savoie, S. Helfrich, and P. Clemente-Colón. 2010, updated daily. Multisensor Analyzed Sea Ice Extent - Northern Hemisphere (MASIE-NH), Version 1. Subset: 4km. Boulder, Colorado USA. NSIDC: National Snow and Ice Data Center. doi: https://doi.org/10.7265/N5GT5K3K Accessed 5 February 2020
Sea ice extent, Arctic and Antarctic (NSIDC)	https://nsidc.org/data/seaice_index/archives Sea Ice Index Version 3 ftp://sidads.colorado.edu/DATASETS/NOAA/G02135/ (Fetterer et al 2017) 'North' (= 'Arctic'): ftp://sidads.colorado.edu//DATASETS/NOAA/G02135/north/monthly/data/ at sidads.colorado.edu 'South' (= 'Antarctic'): ftp://sidads.colorado.edu/DATASETS/NOAA/G02135/south/monthly/data/ Files in form: S_01_extent_v3.0.csv Accessed 26 February 2020
NDVI	MDOIS satellite imagery MOD13C2 product as 5 kilometre monthly mean global imagery Accessed July 2019
Lower Troposphere atmospheric temperature anomaly, Global and Tropical ocean	UAH Temperature Dataset Version 6. 'Globe'; 'Ocean Trpcs' https://www.nsstc.uah.edu/data/msu/v6.0/tlt/uahncdc_lt_6.0.txt Accessed 23 July 2019
Snow extent Greenland	https://climate.rutgers.edu/snowcover/docs.php?target=datareq NH SCE CDR v01r01 https://climate.rutgers.edu/snowcover/files/moncov.namgnld.txt https://climate.rutgers.edu/snowcover/files/moncov.nam.txt Accessed 27 March 2020

Causality: elimination of variables

Changes in absolute CO_2 levels must lag their causal factor, but time series must be interpreted with care when identifying possible causality (Stips et al 2016; Faes et al 2017). Changes in the level of CO_2 (its first derivative) by definition lead absolute CO_2 levels and are used here to infer the regions that are possible net sources and sinks of atmospheric CO_2. The monthly derivative of atmospheric CO_2 level at a recording station is hereafter called the 'CO_2 rate' for that site. Variables having the strongest correlation with and the shortest lag to a site's CO_2 rates are more likely to be causes of the changes in both that site's CO_2 flux and ultimately its CO_2 level. Cross-correlations have previously been used to examine possible sources of CO_2 (e.g. Humlum et al 2013; Salby 2016; MacRae 2019).

We consider the derivative of CO_2 more informative than the CO_2 level in identifying potential causal variables. The same CO_2 level may occur due to the net effect of various strengths of sources and sinks, masking the changes that drove them. Whilst the same may be true of net fluxes at a site, synchrony of a CO_2 rate with a variable makes it a candidate causal factor. Of the many putative sources and sinks (both biotic and abiotic) a dominant one should change simultaneously with the change in local CO_2 rate. Moreover, due to lags, mixing and noise introduced as gas travels around the globe, we consider regions with high CO_2 levels (as might be measured by flask or satellite) to be less informative of locations of sources and sinks than regions with high CO_2 rates.

We compare CO_2 levels for six sites selected from those where there are long term CO_2 records from flasks:

a) Mauna Loa (Hawaii, USA, elevation 3397.00 masl), being the widely used standard site for discussion of global atmospheric CO_2 trends (Keeling et al 2005; Buermann et al 2007; Ciais et al 2013; Francey et al 2019).

b) Barrow (Point Barrow, Alaska, USA). This is selected as a site with very high amplitudes of CO_2 variation within years (Peterson et al 1987; Semiletov et al 2004; Keeling et al 2005). It is relatively close to the North Pole, is similar to neighbouring sites (Peterson et al 1987; Barlow et al 2015) and is often compared with Mauna Loa in publications (*e.g.* Keeling et al 2005; Graven et al 2013; Barlow et al 2015). Three data sets for Barrow are compared: the NOAA data as used for other sites in this paper, and data from the Scripps CO2 Program (http://scrippsco2.ucsd.edu) last updated in 2017 and in 2018.

c) Alert (Canada) being the long-term recording site closest to the North Pole, with similarly high amplitude to Barrow but with a different regional context (Keeling et al 2005). Data from this site are also presented in IPCC (2013).

d) The South Pole, being a site as remote as possible in latitude to those above and with some previous comparative analysis of trends (*e.g.* Dettinger and Ghil 1998; Keeling et al 1989, 2005; Francey et al 2019).

e) Palmer Station, Antarctic peninsula, being a coastal Antarctic site with a local measurement footprint (Le Quéré et al 2007) and plausibly influenced strongly by sea ice.

f) Cape Kumukahi (Hawaii, USA, elevation 0.30 masl), being a lowland site very near (c. 80 km east of) Mauna Loa.

Provisional comparisons are also performed for all sites with monthly CO_2 flask recording in the NOAA Global Monitoring Laboratory that have data since January 2003 (Appendix), after which the sea ice data are available.

The earliest start date for any analysis was taken to be July 1976, after which the Mauna Loa CO_2 record from flask measurements is continuous. Each start date for time series cross-correlations was selected as the date when continuous recording was available for both data sets. The latest date used was December 2018, since this is the last date for which monthly CO_2 flask levels were available from NOAA for our selected sites at the time of analysis (February 2020). Monthly flask measurements were used because these are available for many recording stations. Data for CO_2 levels for Barrow were also downloaded from Scripps in June 2018 and again using the web archive in February 2020, allowing comparison of the data sets. Start and end dates for time periods comparing CO_2 rates at different sites were chosen to include long periods with continuous records.

Derivatives of variables (rates of change) were approximated as follows. Changes in month 2 were taken as the mean value in month 2 minus the mean value in month 1, and plotted in month 2. Changes between years were taken as the mean value in year 2 minus the mean value in year 1 (as per Humlum et al 2013) and plotted in year 2.

Temperature data (temperature anomalies) for the Lower Troposphere were obtained from the University of Alabama in Huntsville (UAH) satellite dataset (Spencer et al 2015). We consider these data far less influenced by adjustments, homogenization and instrumentation changes than many other large-scale datasets. The UAH data are widely used in climate studies and show less of a warming trend than many global temperature reconstructions (IPCC 2013). We use the global and regional divisions (*e.g.* 'Globe', 'Trpcs', 'Ocean') as in the UAH data.

For sea ice volume in the Arctic we use a modelled value calculated by the Danish Meteorological Institute (DMI), which is presumably smoothed compared to raw data on ice extent and thickness. Cross-correlations of ice volume rate against CO_2 rate were performed for 2003-2018 inclusive (the period for which data on both variables were available).

Sea ice extent data were obtained from two providers. For the Arctic and its sub-regions data were obtained from MASIE at the National Snow and Ice Data Center (NSIDC), USA, derived from satellite at 4km resolution. Sea ice data were also obtained from MASIE for 16 regions within the Northern Hemisphere (mapped at ftp://sidads.colorado.edu/DATASETS/NOAA/G02186/). To compare and to sum Arctic and Antarctic sea ice extents derived in a consistent way we use other data from NSIDC for the 'North' (Arctic) and 'South' (Antarctic). Sea ice extents are considered more robust than measures of sea ice area, since the latter can be complicated by surface water.

Cross-correlations of sea ice extent rate against CO_2 rate were performed for 2006-2018 inclusive (the period for which the regional data on both variables were available). For time series of sea ice extent, where changes between days are likely to be relatively slow, monthly averages for the months with missing daily values were estimated by taking the average of the values present in that month; this makes detection of correlations with variables driven by sea ice less likely. All months have only a few, or no, days missing.

Terrestrial vegetation light spectral properties were assumed to be correlated with productivity and carbon drawdown, as in many other studies (*e.g.* Buermann et al 2007). It is acknowledged that productivity may have slightly different phenology to greenness, including a few days of non-synchrony at start of spring (Karkauskaite et al 2017). Data for Normalised Difference Vegetation Index (NDVI) were obtained from the MODIS satellite imagery MOD13C2 product as 5 kilometre resolution monthly mean global imagery (Didan 2015) for each month between January 2001 and May 2019. Mean values (provided with a scale factor of 10,000) for the defined areas were extracted using the Zonal Statistics function of ESRI's ArcMap 10.4. Only data from 2003 to 2018 are used in cross-correlations to enable direct comparison with sea ice volume and CO_2. For simplicity these rescaled values are hereafter referred to as NDVI.

It is generally suggested the dominant cause of the within-year pattern of CO_2 variation lies in northern latitudes (Keeling et al 2005), particularly north of 40 degrees North (Haverd et al 2020). There is little terrestrial vegetation north of 70 degrees North. There might be major, unsynchronized biotic sources and sinks in North America and Eurasia. It is assumed a region with a strong seasonal variation in productivity is likely to be the best predictor of northern and net global CO_2 rates if terrestrial vegetation dominates the observed global seasonal CO_2 rate sawtooth. Monthly data were therefore calculated for the following subjectively chosen regions:

Northern Hemisphere, latitudes 0 to 70 degrees North, hereafter abbreviated to NH070.

North America plus Eurasia, latitudes 35 to 70 degrees North, hereafter NAEUA3570.

North America, latitudes 35 to 70 degrees North, hereafter NA3570.

Eurasia, latitudes 35 to 70 degrees North, hereafter EUA3570.

North America plus Eurasia, latitudes 50 to 70 degrees North, hereafter NAEUA5070.

North America plus Eurasia, latitudes 35 to 60 degrees North, hereafter NAEUA3560.

In preliminary plots (Hambler and Henderson, unpublished), synchrony in NDVI between the latitudinal regions, and North America and Eurasia, was found to be very high, with higher amplitude at high latitudes. To reduce redundant effort, only data from regions NAEUA3570 or NH070 is used in most of our comparisons with CO_2 rates.

Monthly data for NDVI were inverted to give an approximate measure of a lack of productivity and thus the lack of a presumed CO_2 sink (hereafter termed 1/NDVI). For clarity in display these were then scaled by a multiple of 1000 for monthly levels and their rates of change. The timing of months of rapid decline and increase in NDVI are of particular interest here. Only data from 2003 or 2006 are plotted and analysed in cross-correlations to give direct comparison with data for sea ice volume or extent (respectively).

Monthly snow extent for Greenland was deduced by subtracting snow extent for 'North America no Greenland' from the snow extent for 'North America' (Robinson et al 2012), and monthly rates of change calculated as for sea ice.

Statistical analyses

All statistical analyses used the R platform. For monthly time series the autocorrelation function over a lag of up to 24 months was calculated using the acf function. Monthly time series showing seasonality were decomposed into additive seasonal, trend and random components using the decompose and stl functions. The degree of cross-correlation at different lags between time series was calculated using the sample cross-correlation function ccf. For monthly and annual data, lags were considered for periods up to 36 months. Visual inspection of the annual data showed that lags longer than this were unlikely to have stronger correlations, since some very distinctive spikes and troughs would not be matched with longer lags.

Results

Annual cycle (within-year seasonal variation)

Comparison of CO_2 rates in different sites

Comparing monthly CO_2 rates of the selected sites, cross-correlation analysis identified the following lags as having the maximum positive correlations in the specified time period:

Barrow and Alert: Rates have an extremely high significant positive correlation at zero lag, $r = 0.971$. (164 monthly measures commencing May 2005).

Mauna Loa and Barrow: Mauna Loa lags Barrow by 1 month, $r = 0.850$. There is also a statistically significant and almost as great positive cross-correlation with a 13 months lag, $r = 0.827$. (August 1976 to end 2018).

South Pole and Barrow: South Pole lags Barrow by 7 months, $r = 0.669$. (August 2001 to end 2018).

South Pole and Palmer Station: South Pole lags Palmer Station by 1 month, $r = 0.845$. (August 2001 to end 2018).

Comparison of rates of CO_2 and sea ice volume and ice extent.

Results of cross-correlations are given in Table 2 and variables compared in Figs. 1-8.

Within the Northern Hemisphere, we identified by visual inspection which of the 16 regions in the Arctic used by MASIE for ice extent appeared likely to have the strongest correlation of ice extent rate with the CO_2 rate at Barrow. Visual inspection suggested relatively strong correlation between Greenland Sea ice extent rate and Barrow CO_2 rate (Fig. 4), both having inflections early in the year unlike some other regions (Appendix, section E). PCA analysis (Hambler and Henderson, unpublished) identified Greenland Sea as one of a cluster of extent rate axes of similar shape (*ie* phenology). Testing the shape of the Barrow CO_2 rate axis against combinations of Greenland Sea and similar sea ice extent axes identified additional seas (Barents and Kara) that might give marginal improvements in correlation strength.

Table 2 Cross-correlations between ice volume and extent rates and CO_2 rates. (Extent rates 2006-2018 inclusive, volume rates 2003-2018, unless indicated otherwise due to missing data)

Variables	**Cross-correlation coefficient *r* and lag at which correlation strongest if not zero**	**p value**	**Fig. number**
Mauna Loa CO_2 rate *vs* Arctic ice volume rate	$r = 0.907$ when CO_2 lags ice by 1 month	$p < 0.01$	1
Barrow CO_2 rate *vs* Arctic ice volume rate	$r = 0.920$ with zero lag	$p < 0.01$	2
Barrow CO_2 rate *vs* N. Hemisphere sea ice extent rate			3
Barrow CO_2 rate *vs* Greenland Sea ice extent rate	$r = 0.833$ with zero lag	$p < 0.01$	4
Barrow CO_2 rate *vs* Greenland Sea ice extent rate. Scripps CO_2 data to November 2017, archive dated 2017			5a
Barrow CO_2 rate *vs* Greenland Sea ice extent rate. Scripps CO_2 data, archive dated 2018			5b
Mauna Loa CO_2 rate *vs* Northern Hemisphere sea ice extent rate			6
Mauna Loa CO_2 rate vs Antarctic sea ice extent rate (NSIDC data)			7
Mauna Loa CO_2 rate *vs* sum of Arctic and Antarctic ice extent rates (NSIDC data)			8
Mauna Loa CO_2 rate *vs* Greenland Sea ice extent rate			9a
Cape Kumukahi (Hawaii lowlands) CO_2 rate vs monthly Greenland Sea ice extent rate			9b
South Pole CO_2 rate *vs* Antarctic sea ice extent rate (NSIDC data)	$r = 0.836$ when CO_2 lags ice by 1 month	$p < 0.01$	10
Palmer Station CO_2 rate *vs* Antarctic sea ice extent rate (NSIDC data)	$r = 0.868$ with zero lag	$p < 0.01$	11

Figure 1

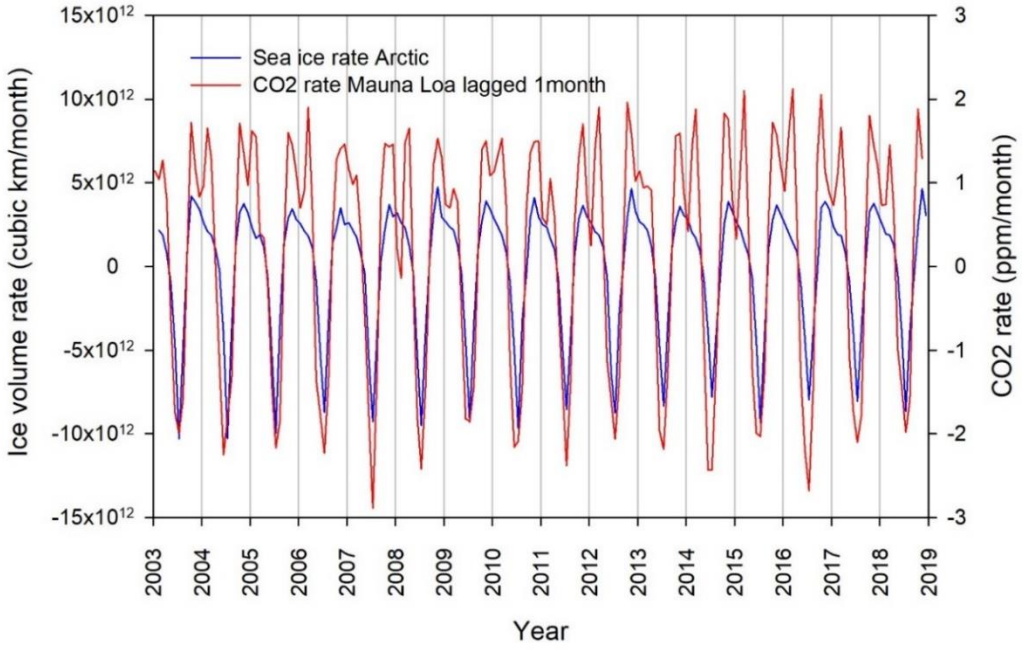

Fig. 1 Monthly CO_2 rate Mauna Loa (lagged 1 month) *vs* monthly Arctic sea ice volume rate. $r = 0.907$, $p < 0.01$

Figure 2

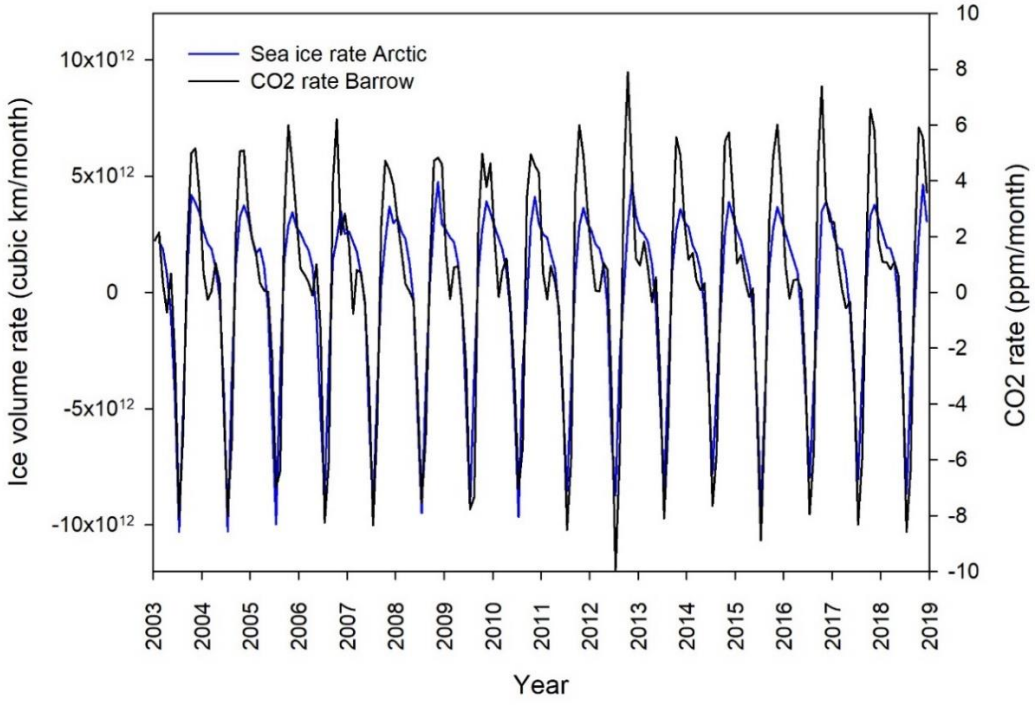

Fig. 2 Monthly CO_2 rate Barrow *vs* monthly Arctic sea ice volume rate. $r = 0.920$, $p < 0.01$

Figure 3

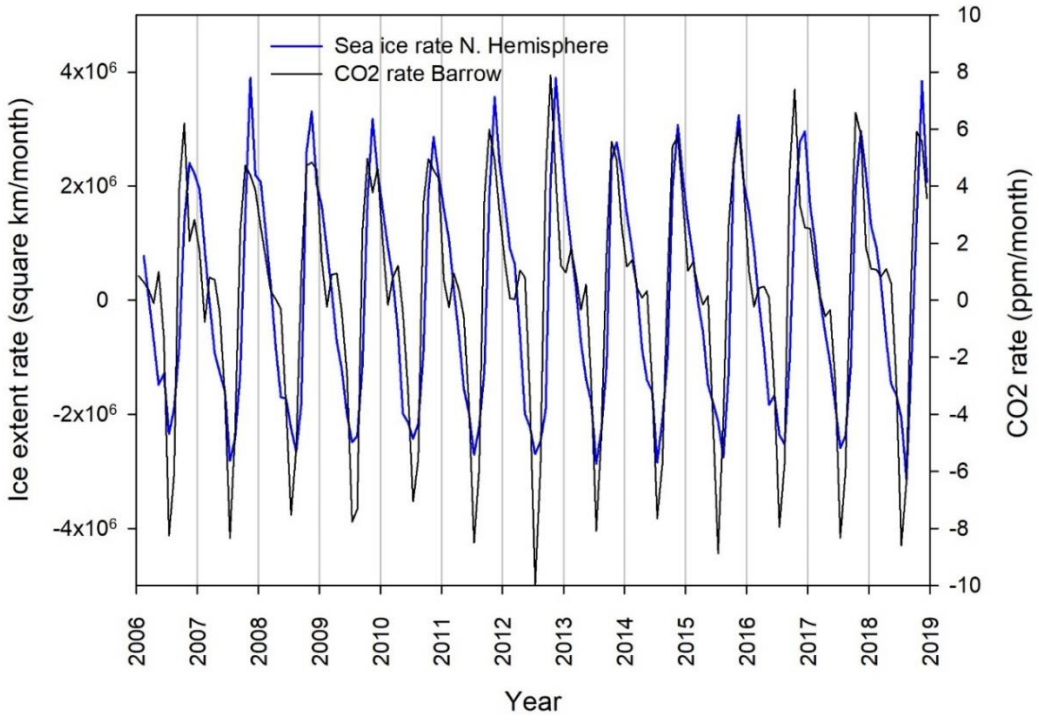

Fig. 3 Monthly CO_2 rate Barrow *vs* monthly Northern Hemisphere sea ice extent rate (MASIE data)

Figure 4

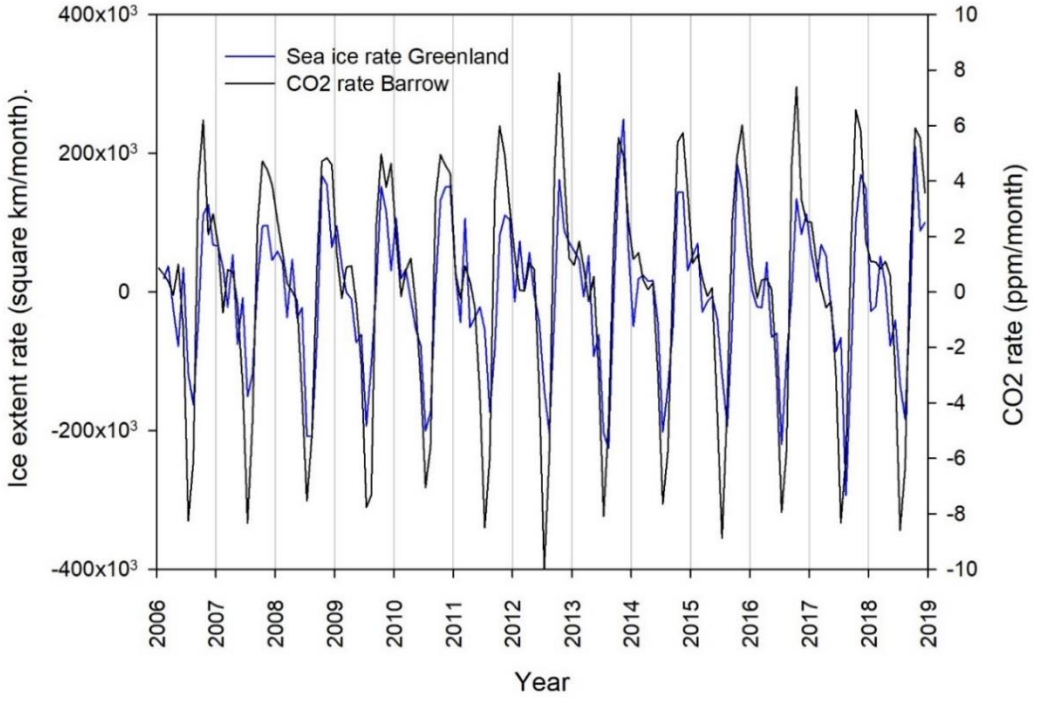

Fig. 4 Monthly CO_2 rate Barrow *vs* monthly Greenland Sea ice extent rate. NOAA data for CO_2. $r = 0.833$, $p < 0.01$

Figure 5a

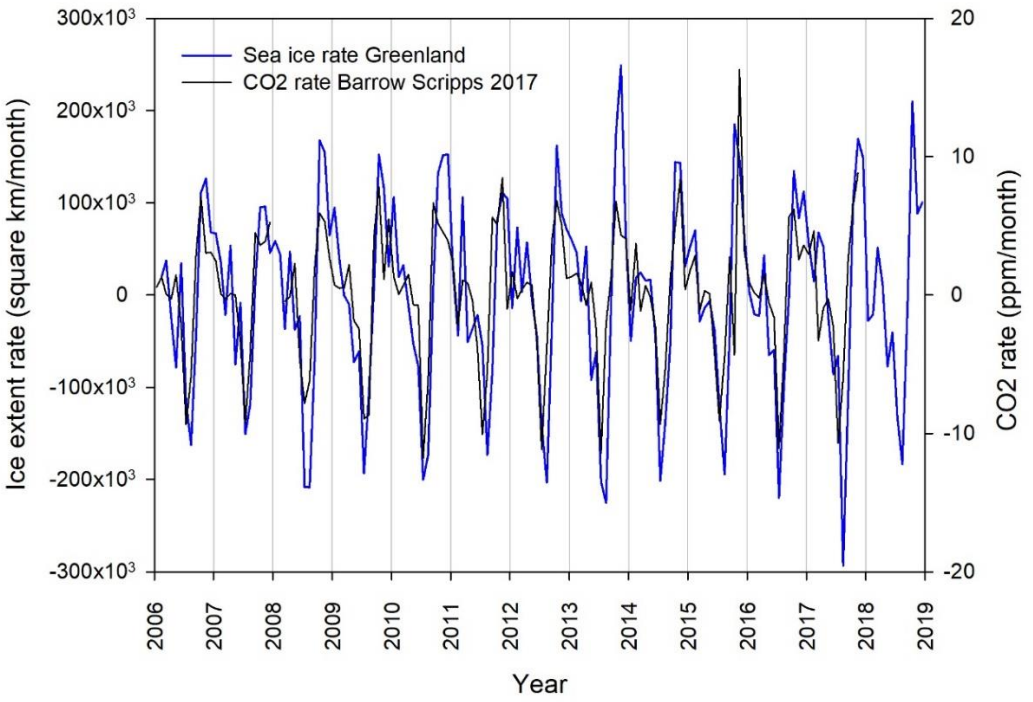

Figure 5b

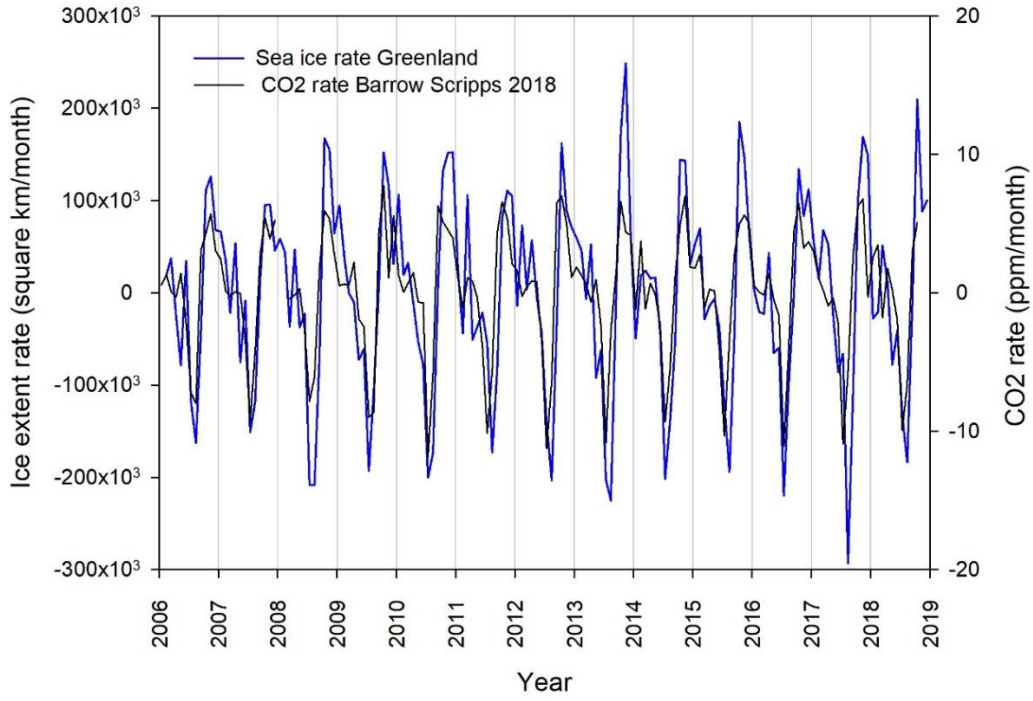

Fig. 5 Monthly CO_2 rate Barrow (Scripps data) *vs* monthly Greenland Sea ice extent rate: **Fig. 5a** CO_2 archive dated 15 December 2017. **Fig. 5b** CO_2 archive data to 15 October 2018, last updated 29 October 2018

Figure 6

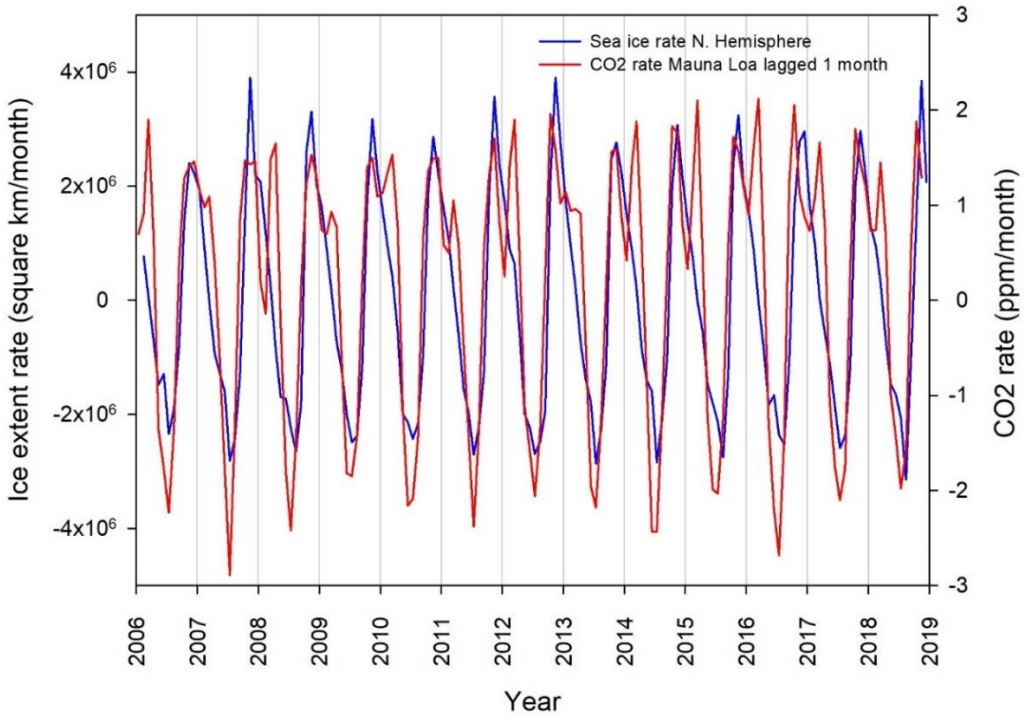

Fig. 6 Monthly CO_2 rate Mauna Loa (lagged 1 month) *vs* monthly Northern Hemisphere sea ice extent rate

Figure 7

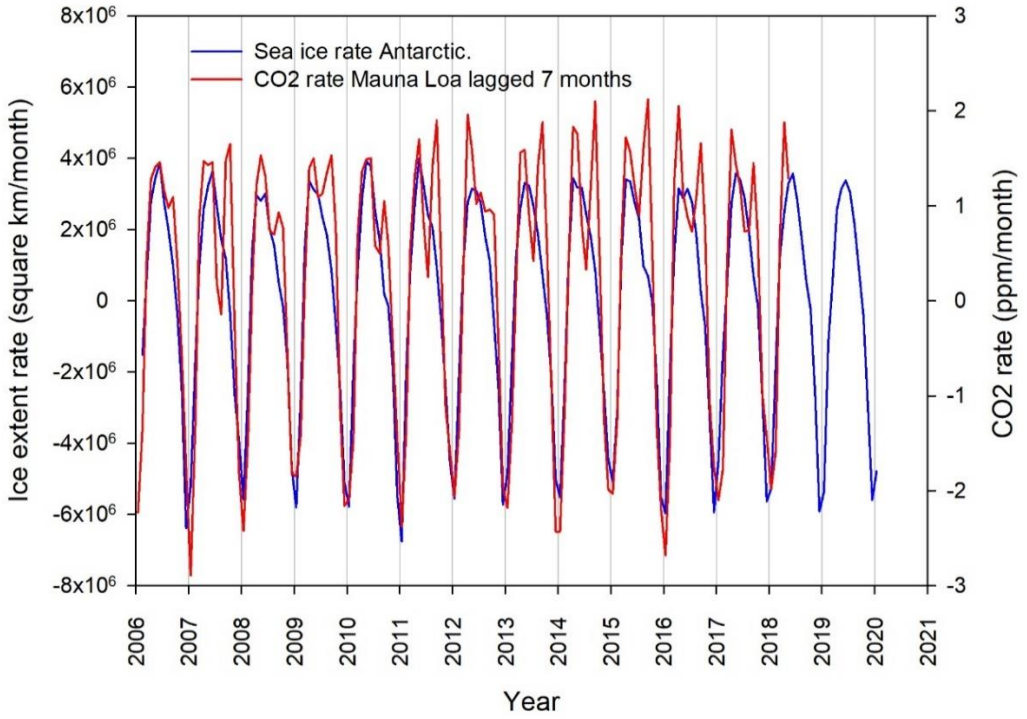

Fig. 7 Monthly CO_2 rate Mauna Loa (lagged 7 months) *vs* monthly Antarctic sea ice extent rate

Figure 8

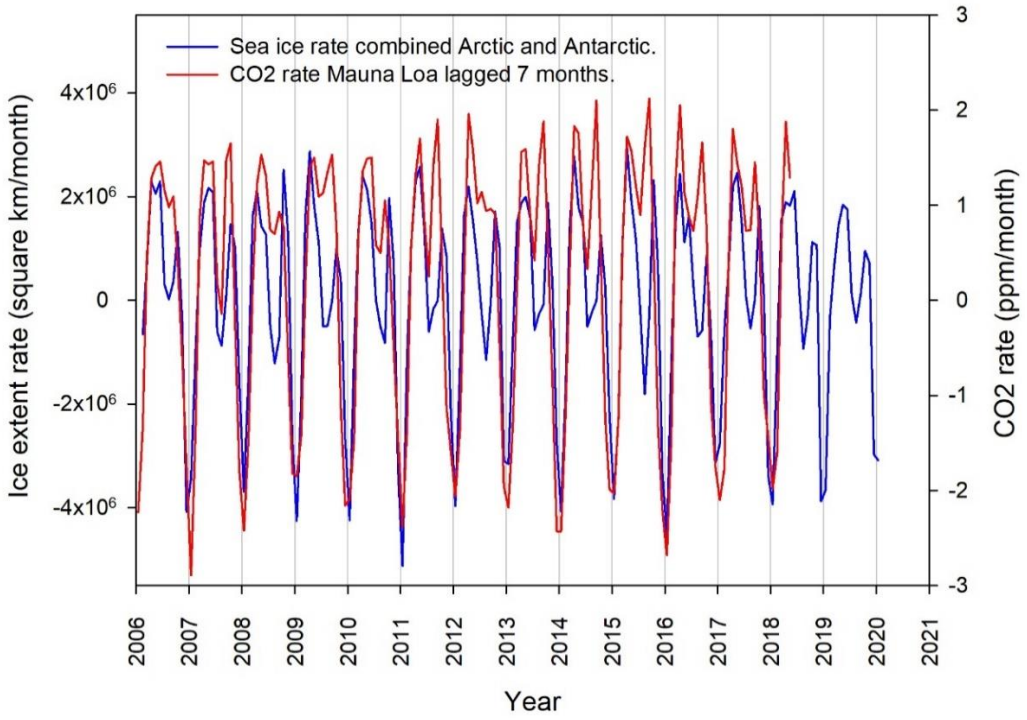

Fig. 8 Monthly CO_2 rate Mauna Loa (lagged 7 months) *vs* sum of monthly Arctic and Antarctic sea ice extent rates

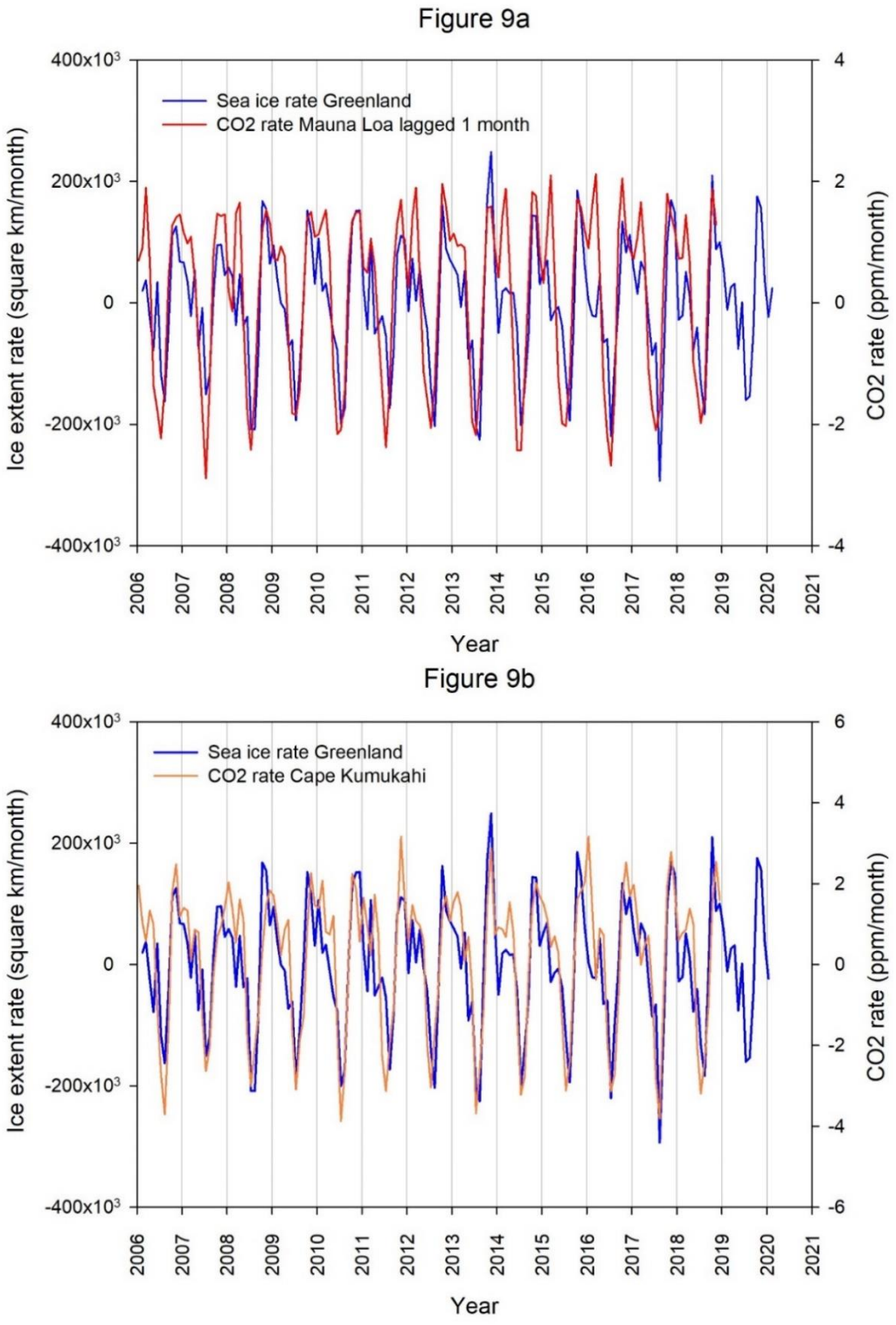

Fig. 9 CO_2 rates compared for an upland and lowland site in Hawaii (USA): **Fig. 9a** Monthly CO_2 rate Mauna Loa (Hawaii uplands, lagged 1 month) *vs* monthly Greenland Sea ice extent rate. **Fig. 9b** Monthly CO_2 rate Cape Kumukahi (Hawaii lowlands) *vs* monthly Greenland Sea ice extent rate

Figure 10

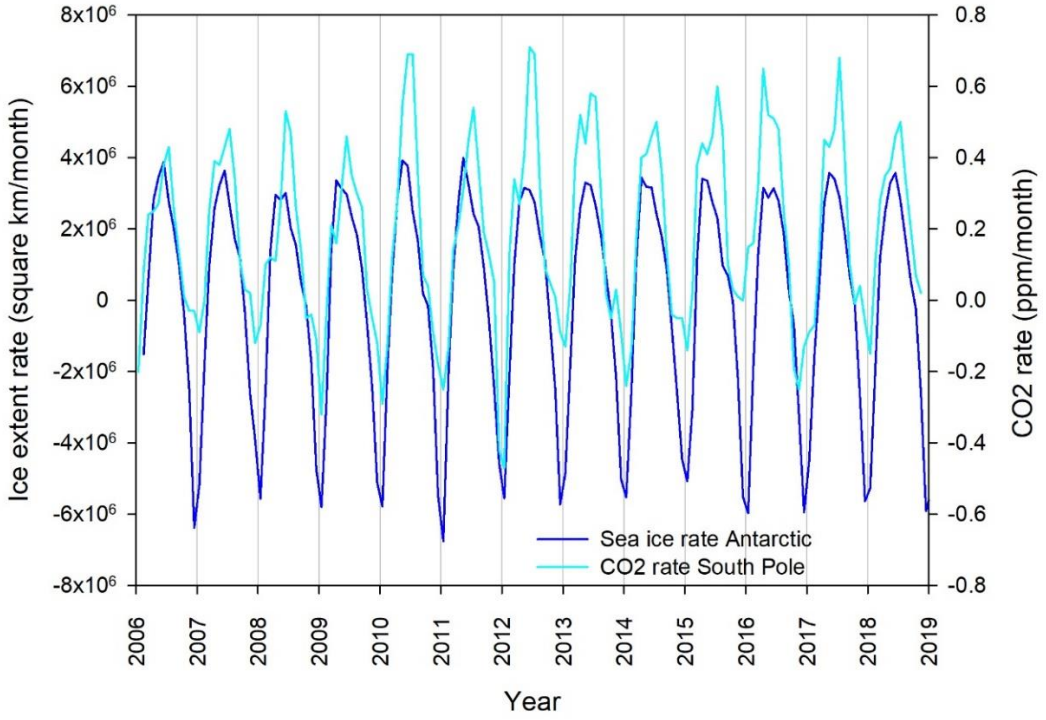

Fig. 10 Monthly CO_2 rate South Pole (lagged 1 month) *vs* monthly Antarctic Sea ice extent rate. $r = 0.836$, $p < 0.01$

Figure 11

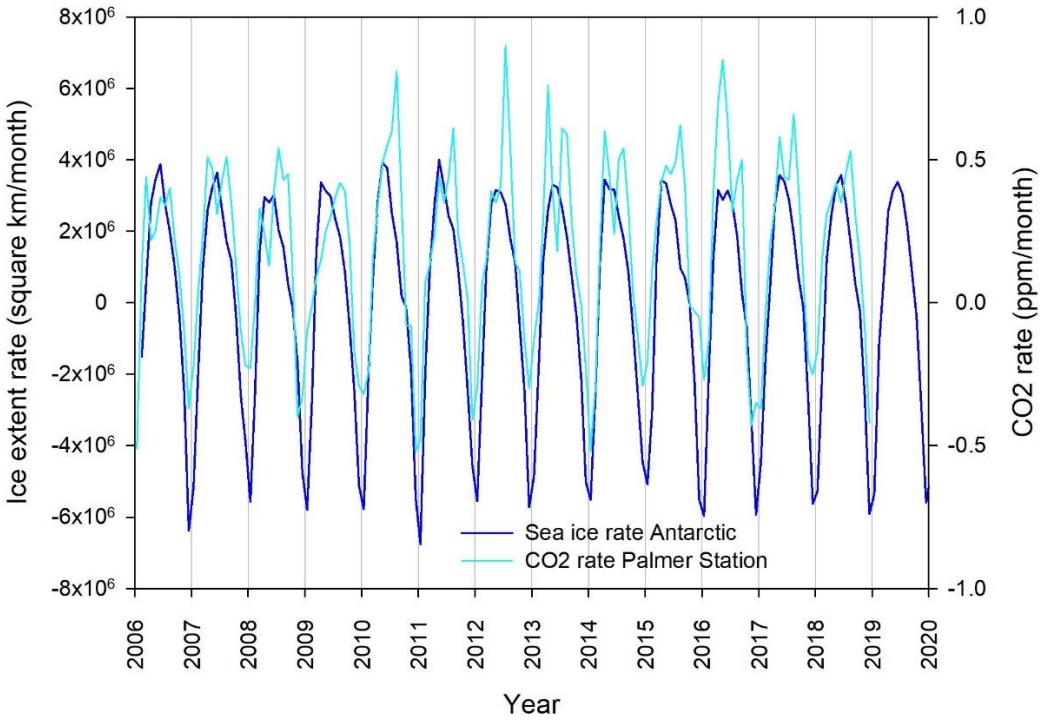

Fig. 11 Monthly CO_2 rate Palmer Station (Antarctica) *vs* monthly Antarctic Sea ice extent rate. $r = 0.868$, $p < 0.01$

Preliminary comparison of rates of CO_2 in multiple recording stations with sea ice rates

Examples of plots of CO_2 rates against selected sea ice rates with high visual similarity are presented in the Appendix. No statistical analyses were performed on these data, and lags of the CO_2 rate are presented which give relatively good visual fits based primarily on periods with negative CO_2 flux. Given the very numerous potential sources of error, individual graphs should not be treated as definitive and should be checked, but patterns found in several graphs are likely to be robust.

Comparison of rates of CO_2 and terrestrial productivity (NDVI)

The monthly rates of inverted NDVI are derived from overlapping latitudes and thus show high coherence (Fig. 12).

Figure 12

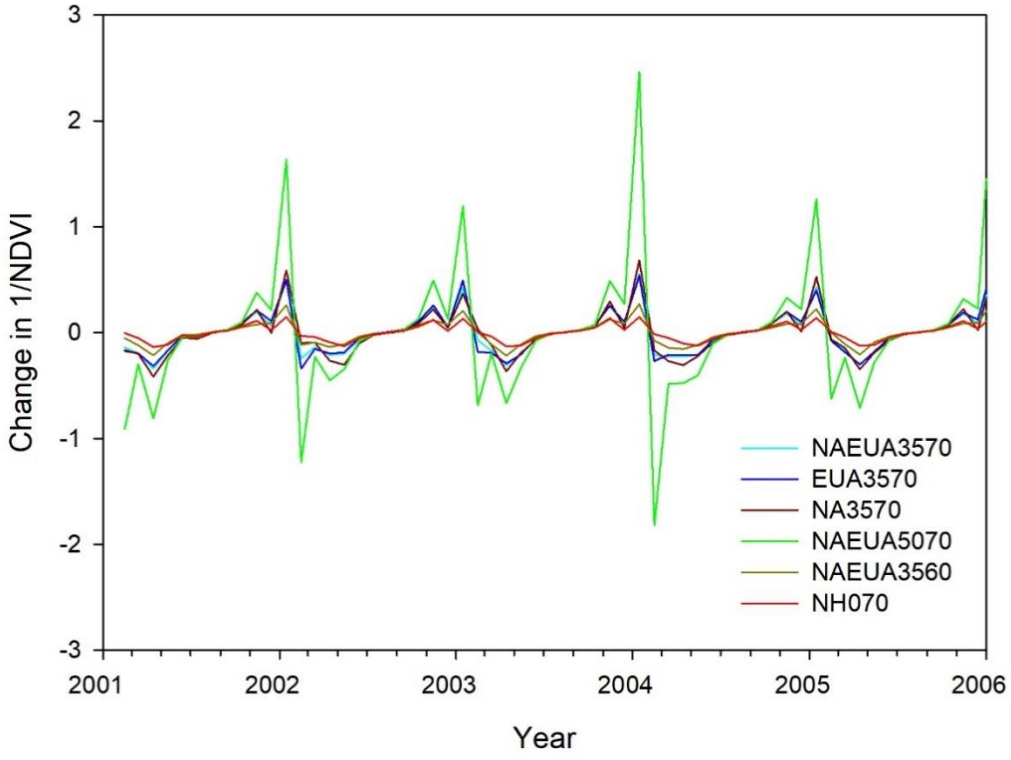

Fig. 12 Monthly rates of inverted NDVI derived from overlapping latitudinal belts show high coherence, illustrated for 2001-2006 to enlarge scale for clarity. (NDVI rescaled as per Methods)

Table 3 Cross-correlations between selected monthly inverted NDVI rate and monthly CO_2 rate (2003-2018 inclusive)

Variables	**Cross-correlation coefficient r and lag at which correlation strongest if not zero**	**p value**	**Fig. number**
Mauna Loa CO_2 rate *vs* monthly change inverted NDVI NAEUA3570	r = 0.621 when CO_2 lags by 3 months r = 0.614 when CO_2 lags by 4 months	p < 0.01 p < 0.01	13
Mauna Loa CO_2 rate *vs* monthly change inverted NDVI NAEUA3570			14
Mauna Loa CO_2 rate *vs* monthly change inverted NDVI NH070			15

Barrow CO_2 rate *vs* monthly change inverted NDVI NAEUA3570			16
Barrow CO_2 rate *vs* monthly change inverted NDVI NH070			17
Barrow and Mauna Loa CO_2 rate *vs* monthly change inverted NDVI NH070 level			18

Figure 13

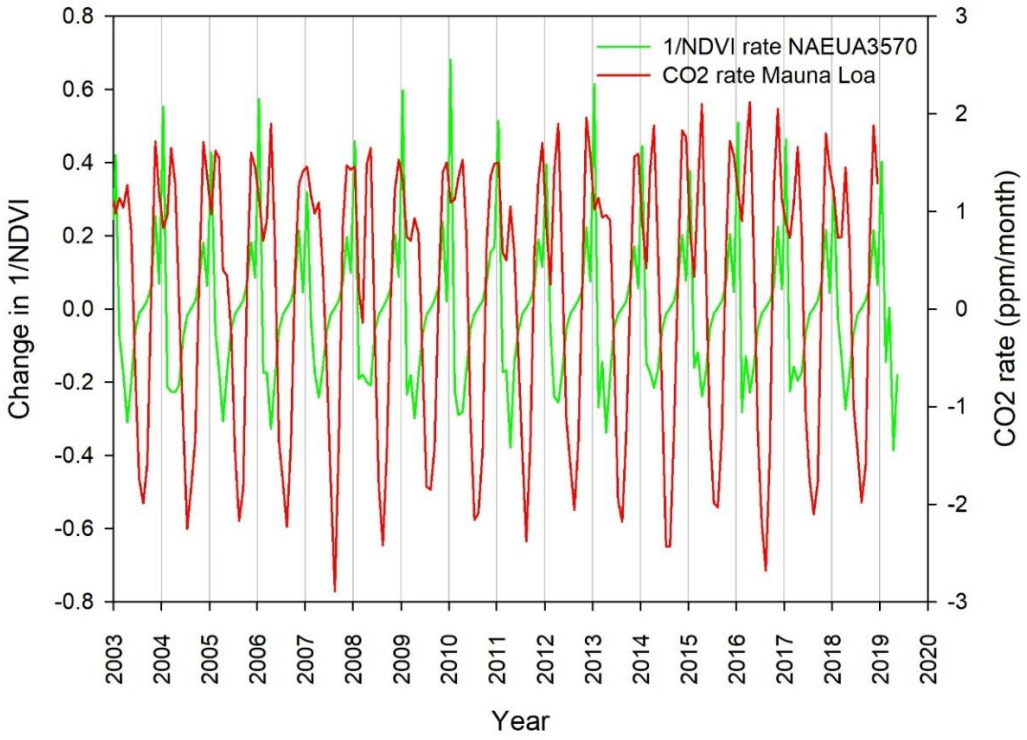

Fig. 13 Monthly CO_2 rate Mauna Loa *vs* monthly inverted NDVI rate for North America and Eurasia 35-70 degrees North (NAEUA3570). (NDVI rescaled as per Methods)

Figure 14

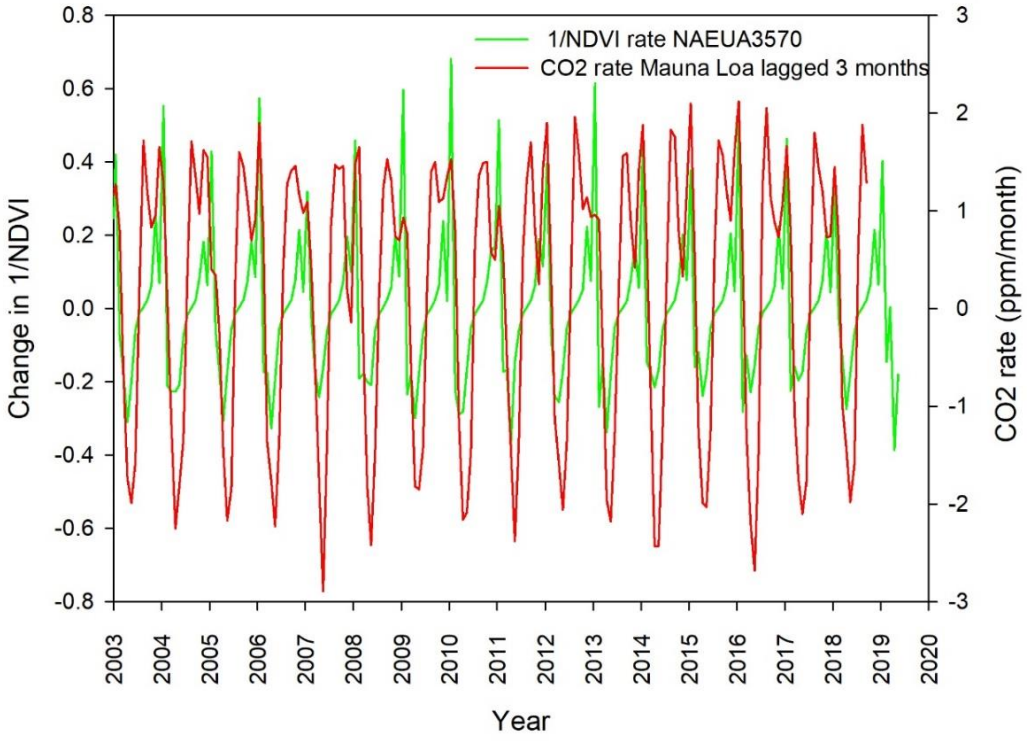

Fig. 14 Monthly CO_2 rate Mauna Loa (lagged 3 months) *vs* monthly inverted NDVI rate for North America and Eurasia 35-70 degrees North (NAEUA3570), CO_2. (NDVI rescaled as per Methods). $r = 0.621$, $p < 0.01$

Figure 15

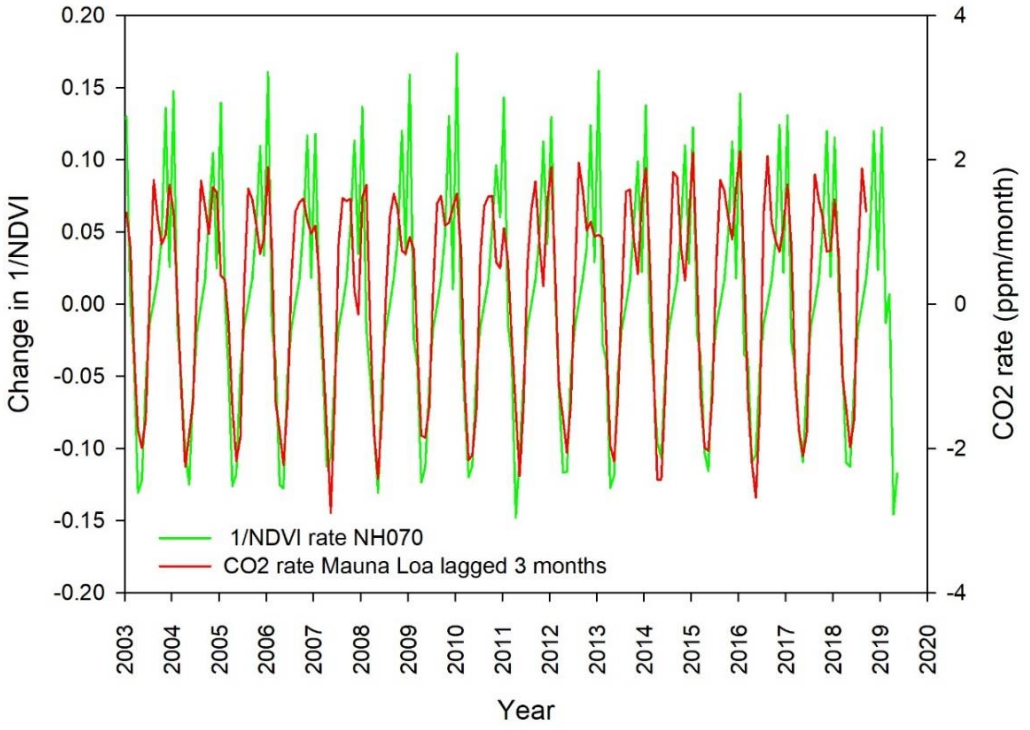

Fig. 15 Monthly CO_2 rate Mauna Loa (lagged 3 months) *vs* monthly inverted NDVI rate for Northern Hemisphere 0-70 degrees North (NH070). (NDVI rescaled as per Methods)

Figure 16

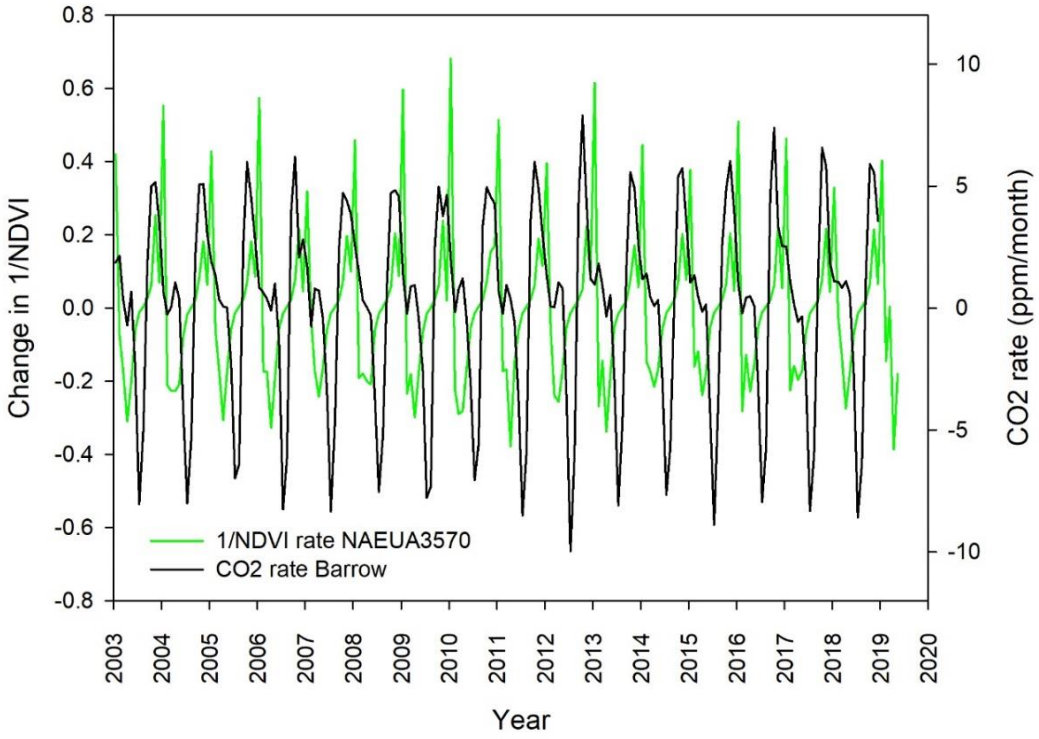

Fig. 16 Monthly CO_2 rate Barrow *vs* monthly inverted NDVI rate for North America and Eurasia 35-70 degrees North (NAEUA3570). (NDVI rescaled as per Methods)

Figure 17

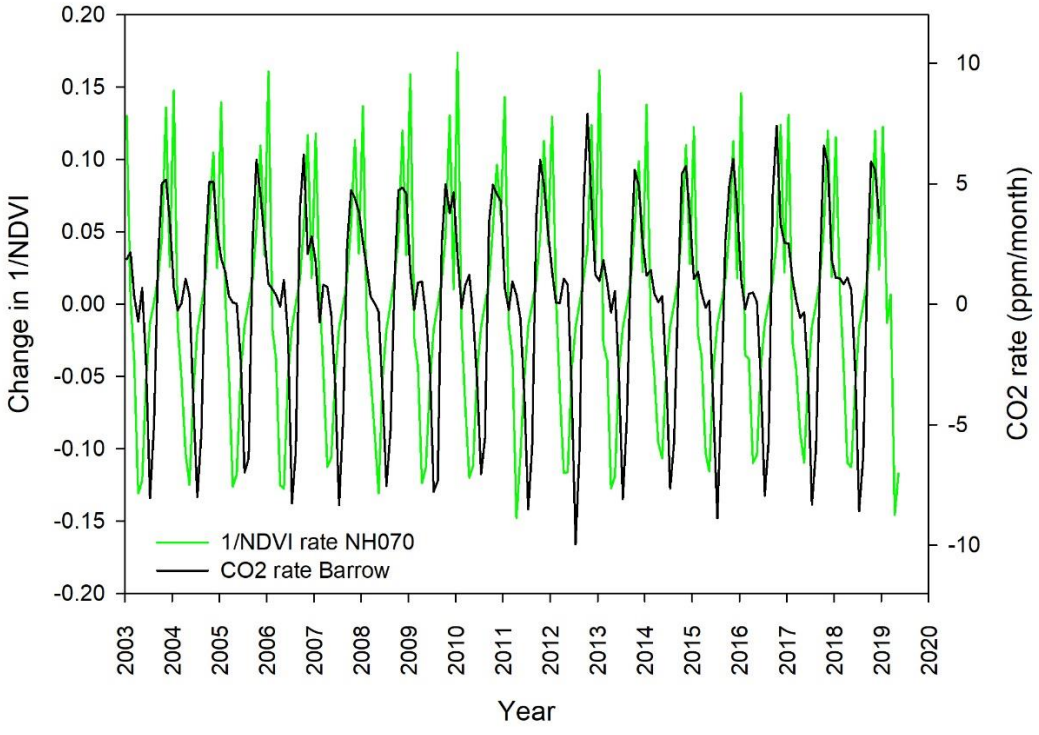

Fig. 17 Monthly CO_2 rate Barrow *vs* monthly inverted NDVI rate for Northern Hemisphere 0-70 degrees North (NH070). (NDVI rescaled as per Methods)

Figure 18

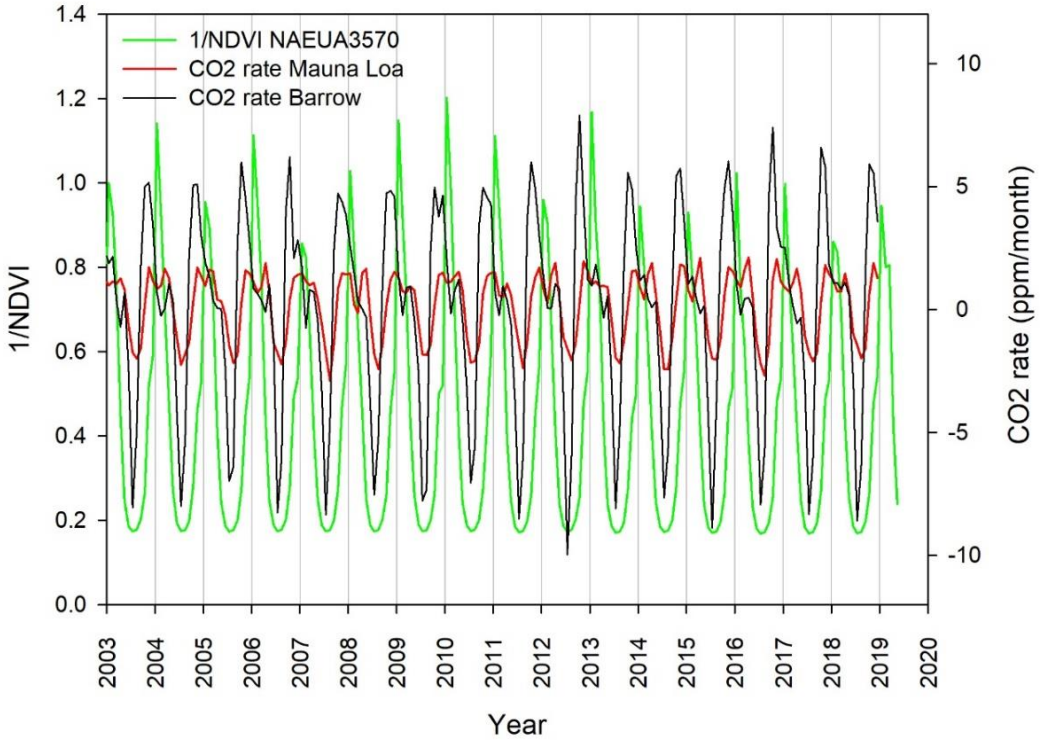

Fig. 18 Monthly CO_2 rate Mauna Loa and Barrow *vs* monthly inverted NDVI level for North America and Eurasia 35-70 degrees North (NAEUA3570). (NDVI rescaled as per Methods)

Inter-annual variation

Comparison of Annual average CO_2 rates and temperatures

Annual averages of monthly CO_2 rates are very highly correlated with several global and regional satellite measures of temperature since 1980 (the first year an annual change can be calculated from our time series). Examples are given in Table 4.

Table 4 Comparison of annual average CO_2 rate, or annual change in annual average CO_2 rate, and temperature series for 'Lower Troposphere' (UAH) temperature anomalies, July 1979 - December 2018.

Variables	**Timeframe**	**Linear correlation**	**p value**	**Fig. number**
Annual average CO_2 rate Mauna Loa vs Global temperature anomaly	July 1979 - Dec. 2018	Correlation = 0.710 adjusted $R^2 = 0.504$ n = 40 years	$p < 0.01$	19
Annual average CO_2 rate Mauna Loa vs Tropics ocean temperature anomaly	July 1979 - Dec. 2018			20

Figure 19

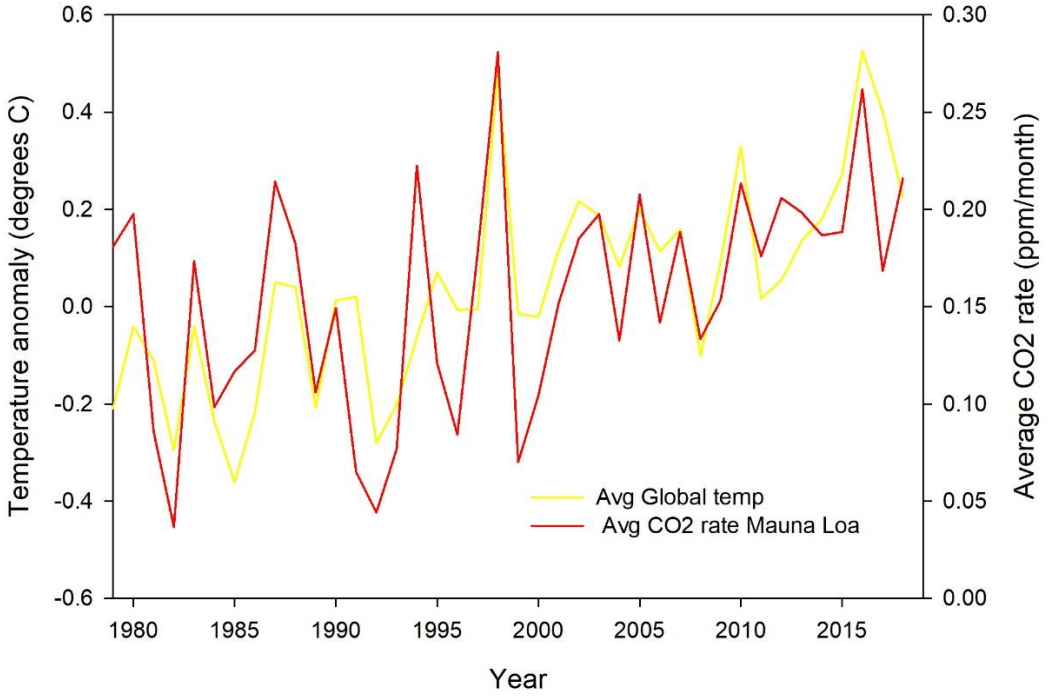

277 **Fig. 19** Annual average CO_2 rate Mauna Loa *vs* annual average Global Lower Tropospheric temperature anomaly
278 (UAH). Correlation = 0.710, adjusted $R^2 = 0.504$, n= 40 (years), significant at $p < 0.01$

Figure 20

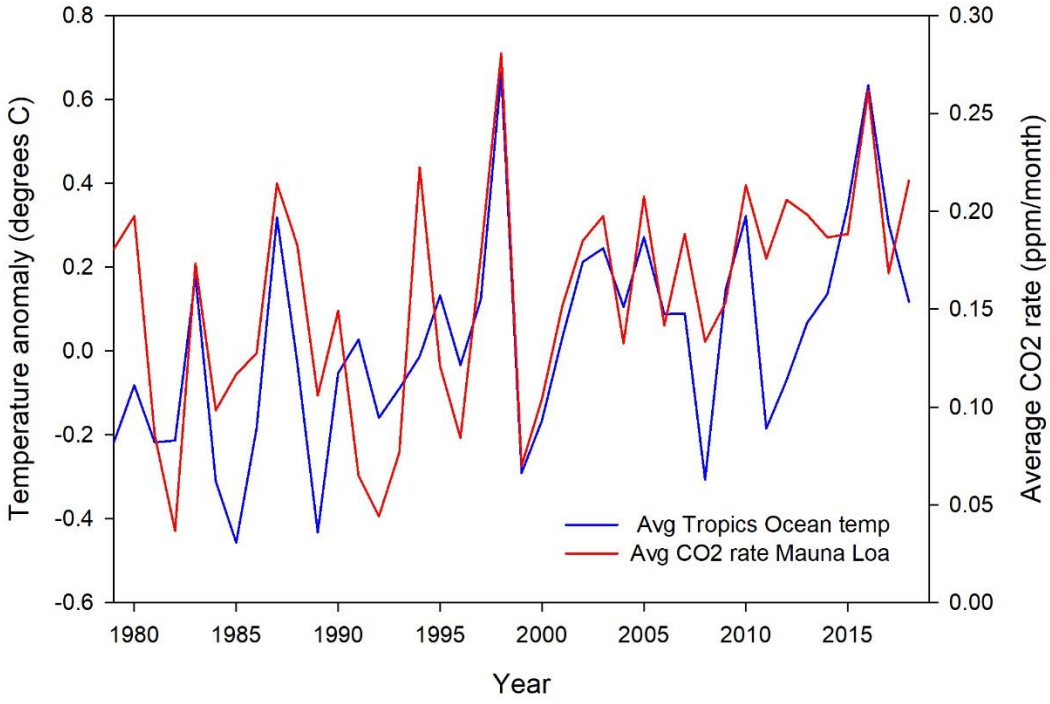

Fig. 20 Annual average CO_2 rate Mauna Loa *vs* annual average Tropics Ocean Lower Tropospheric temperature anomaly (UAH)

Discussion

We have found strong evidence that carbon cycle dynamics within years may have been misinterpreted, which therefore casts great uncertainty over the prevailing interpretation of the causes of atmospheric CO_2 change within and between years.

Within-year variation in CO_2 rates

The phenology of CO_2 at a recording station probably represents both local sources and sinks of CO_2 combined with strong but remote sources and sinks, and the balance is likely to vary with location (Keeling et al 2001; Keeling et al 2005; Le Quéré et al 2007; Francey et al 2019). Fine detail of CO_2 rates should prove helpful in identifying the possible location of a source or sink. CO_2 rates for sites that are strongly correlated plausibly share causation. Within the sites we studied, the amplitude of seasonal variation declines from Arctic to the South Pole (Figs. 1-11), typically attributed to there being more land in the Northern Hemisphere (e.g. Zhao and Zeng 2014).

Visual comparison (Figs. 4 and 5) shows the monthly CO_2 data for Barrow from NOAA are smoothed in comparison with the Scripps data from May 2018; this smoothing has lost detail in the signal and reduced the similarity with the Greenland Sea ice extent rate. Smoothing occurs during processing of Scripps data, as between 2017 (Fig. 5a) and 2018 (Fig. 5b). Retaining raw data will be of extreme importance. We predict other unprocessed CO_2 data (if still available) for other Northern Hemisphere recording sites will reveal very strong correlations with Greenland Sea ice.

The extremely tight covariation of Barrow CO_2 rate and Arctic sea ice extent rate suggests a marine phenomenon closely related to the edge of the sea ice or to recently ice-free sea. Similarly, the South Pole and Palmer Station CO_2 rates suggest local conditions, particularly sea ice, may dominate the pattern of within-year variation in high-latitude sites in the Southern Hemisphere.

The monthly Arctic ice volume rate has extraordinarily high predictive value for monthly CO_2 rates at Mauna Loa (r = 0.907 and Barrow (r = 0.920). It is possible that such a high correlation results in part from the smoothing in the modelling processes used to create both the ice volume and CO_2 data.

The twin peaks of CO_2 rate at Mauna Loa (highland Hawaii) are relatively even in amplitude and we propose they result from the combined influences of sea ice cycles at the Antarctic and Arctic (Fig. 8). Notably, Cape Kumukahi (lowland Hawaii, Fig. 9b) has very close similarity to the Greenland sea ice rate suggesting what we term 'Greenland-type phenology' (GTP) may dominate at low altitudes in the Northern Hemisphere.

Oceanic and planktonic influences have generally been dismissed as a cause of the annual CO_2 cycle. For example, it has been stated that "oceanic CO_2 exchange has only a small, or a negligible effect on the seasonal cycle of atmospheric CO_2" at Mauna Loa (Keeling et al 2001). It has been assumed or concluded from models that there are comparatively small oceanic CO_2 fluxes in the high latitudes (Gruber et al 2009; Haverd et al 2020) including from planktonic activity (Monroe 2013a). A temperature dependent Arctic flux of CO_2 has been previously identified (*e.g.* Semiletov et al 2004, 2007; Nomura et al 2010; Geilfus et al 2012; Brown et al 2015). However, this has been suggested to contribute less than 16% of the high latitude open ocean air-sea CO_2 flux (Brown et al 2015).

Abiotic forcing of CO_2 rates

Very high correlations as in Table 2 are rare in our experience of ecological time series but might be expected from basic physics or chemical processes. We propose that abiotic processes dominate CO_2 sources and sinks at high latitudes, contrary to current paradigm and the IPCC (2013). We also suggest that the crucial difference between the Northern and Southern Hemisphere CO_2 recording sites is the very substantial change in some regional sea temperatures near Greenland and the North Pole, with associated rapid changes in regional sea ice in the Arctic that are not possible near the South Pole. Reactive carbonate minerals in meltwater from Greenland (Sejr et al 2011) may also be particularly important. We argue this imprints a high-amplitude seasonal pattern of CO_2 release and drawdown near Greenland, and this pattern attenuates southwards, whilst effects of Southern Ocean sea ice increase southwards. Several other Arctic sea ice regions (MASIE data) have visual similarity to typical Northern Hemisphere CO_2 rates, such as synchronous peaks or troughs (Appendix, section E). Monte-Carlo analysis of all combinations of regions might identify other seas which significantly improve the fit to CO_2 rates but would be computationally intensive.

Very strong correlations between rates of change of CO_2 and sea ice volume rates could result from a process whereby a rapid change in one factor leaves another far from equilibrium. For example, the rate of outgassing or dissolution of gas in water will decline if the temperature remains constant; this is consistent with the low mid-winter CO_2 rate at Barrow and Alert. A strong correlation of CO_2 rate with ice extent rate or volume rate is consistent with degassing and solution of CO_2 during the freeze-thaw cycle and with experimental tank results showing synchrony of CO_2 release and sea ice formation (Nomura et al 2006). Strong correlations between untransformed sea ice rates and CO_2 rates suggest that if one is a causal process it has a linear relationship to the response variable. A wide survey of Arctic seas in July and August 2011 (Prytherch et al 2017) found air-sea CO_2 transfer velocity varied near linearly with decreasing sea ice concentration; the generally negative rates were consistent with negative CO_2 rates at Barrow and Alert in July (and August) of that year. Results also indicate a linear relationship between CO_2 transfer velocity and fractional ice cover in the Southern Ocean (Butterworth and Miller 2016).

Sea ice is important in ocean-atmosphere CO_2 fluxes (Semiletov et al 2004, 2007; Vancoppenolle et al 2013; Delille et al 2014; Tison et al 2017; Ouyang et al 2020). In the northern mid-winter, we find CO_2 rates at northern high latitudes are near zero, coinciding with near zero sea ice rates and a sea ice and snow cap which impedes gas exchange with the Arctic ocean (Loose et al 2009; Vancoppenolle 2013; Brown et al 2015; Nomura et al 2018). Melting ice has high undersaturation of CO_2 (Geilfus et al 2012). Arctic sea ice melt is associated with low surface water pCO_2 regionally and seasonally (Ahmed et al 2019). Arctic and Antarctic sea ice zones can be a sink for atmospheric CO_2, at least during the snow melt period (Nomura et al 2013). Observed variations in pCO_2 in the atmosphere are generally small compared to those in sea ice, suggesting the driving factor for the CO_2 flux between ice and atmosphere is the pCO_2 at the sea ice surface (Nomura et al 2013). Nelson and Nelson (2016) showed local atmospheric CO_2 declines can follow sea ice melt and suggest that this is a result of two processes: cold meltwaters (which are very low in CO_2) dissolving CO_2, and dissolution of calcium carbonate ($CaCO_3$, mostly ikaite) crystals released from the ice. When sea ice forms calcium carbonate can crystallise in the ice whilst brine is rejected beneath it (Papadimitriou et al 2004; Miller et al 2011; Vancoppenolle et al 2013; Papakyriakou and Miller 2011). There can be an efflux of CO_2 from young sea ice probably due to degassing from upward expulsion of brine and from calcium carbonate precipitation (Geilfus et al 2013).

In the Arctic, calcium carbonate precipitation / dissolution and brine rejection can dominate the sea ice CO_2 flux, at least regionally as near Greenland, and may have been underappreciated (Miller et al 2011; Søgaard et al 2013, 2019). In the Canadian Arctic Archipelago (CAA) observed from 2010 to 2016 sea ice dominated a seasonal cycle of pCO_2 in surface waters (Ahmed et al 2019). Waters were undersaturated with pCO_2 in July to mid August, followed by saturation to supersaturation in mid August to mid September, with a significant correlation to sea surface temperature and influenced by other regional processes. Moreover, the dense, extensive ice cap likely

reduces upwelling of CO_2 laden cold waters in the Northwest Pacific (Zhabin et al 2017; Gray WR et al 2018). Studies of Arctic surface waters (Nansen Basin, the slopes north of Svalbard, and Yermak Plateau) found them to be undersaturated in CO_2 (relative to the atmosphere) in January to June 2015 (Fransson et al 2017); the "major" contribution of calcium carbonate dissolution to CO_2 undersaturation was greater than the contribution of biological production. Although calcium carbonate dissolution was observed to be a minor factor in CO_2 drawdown in at least some areas of the Southern Ocean (Bakker et al 2008) higher concentrations of ikaite have been reported elsewhere (G. Dieckmann quoted in Bakker et al 2008).

Use of Greenland Sea ice data alone would be an excellent predictor of CO_2 variation at Barrow (r = 0.833) and a very good predictor at Mauna Loa (Fig. 9a) with a 1 month lag behind the sea ice rate). Inclusion of sea ice regions such as Kara and Barents seas may make very marginal improvements in prediction of the Barrow CO_2 rate (Hambler and Henderson, unpublished data); these are adjacent seas, strongly influenced by very substantial and rapidly-changing heat fluxes into the Arctic basin via Fram Strait (Beszczynska-Möller et al 2012; Kawasaki and Hasumi 2016). We suggest it is no coincidence that the high-latitude North Atlantic can be a particularly intense oceanic CO_2 sink (Takahashi et al 2009). The surface waters of the central Greenland Sea were observed to have general undersaturation of CO_2 with respect to the atmosphere but a "dramatic" seasonal cycle of Dissolved Inorganic Carbon (DIC) and little interannual variability (Miller et al 1999). Similarly, waters of Young Sound were undersaturated all year round (Sejr et al 2011). The very sharp fall in DIC around the start of May, and an inflection to a sharp rise in mid August (Miller et al 1999), are consistent with typically highly negative CO_2 rates between May and August at Barrow and Alert and with very rapid spring ice melt rates in the Greenland Sea (Figs. 4 and 5). Samples taken in March in Young Sound (Greenland Sea) suggest melting of sea ice and dissolution of abundant calcium carbonate crystals would result in meltwater far below atmospheric pCO_2 (Rysgaard et al 2013).

It would be worth investigating the contribution from the Greenland land mass (providing cold meltwater, glacial discharge and minerals) to the negative CO_2 flux in the summer. Peak meltwater discharge rates in are highly seasonal, with a narrow peak around July (*e.g.* Van As et al 2014) as with peak snow decline rate (Hambler and Henderson unpublished); this is consistent with high CO_2 drawdown in that month in Barrow and Alert. In the Greenland Sea / Young Sound, particularly low values of pCO_2 were reported in summer between melting ice floes and where there was glacial runoff, and a link with minerals in meltwater was suggested (Sejr et al 2011).

In the Antarctic, temperature influences carbon dynamics in a similar way to the Arctic, through modifications to salinity, CO_2 solubility, ice dynamics and productivity (Semiletov et al 2007; Bakker et al 2008; Takahashi et al 2009; Delille et al 2014; Geilfus et al 2014; Nomura at al 2014; Legge et al 2015; Butterworth and Miller 2016; Tison et al 2017; Vancoppenolle and Tedesco 2017; Gray AR et al 2018). Warming increases the permeability of sea ice which switches sharply from being a CO_2 source to a CO_2 sink as the ice melts in the spring-summer period (Delille et al 2014; Tison et al 2017). The Southern Ocean has generally been considered a CO_2 net sink (Butterworth and Miller 2016) and this is assumed in some climate models (Gray AR et al 2018) but is in fact a either a CO_2 source or sink dependent on location and season (Ishii et al 2002; Nomura et al 2014; Butterworth and Miller 2016; Gray AR et al 2018; Bushinsky et al 2019). Year-round observations show a seasonal CO_2 source in all regions of the Southern Ocean, particularly in winter (Gray AR et al 2018). Data from floats (May 2014 - April 2017) for the Southern Ice Zone show a sink in late spring to summer, with weak outgassing in autumn before formation of sea ice (Gray AR et al 2018). We suggest such observations, combined with the generally positive CO_2 rates at the South Pole (Fig. 10) and Palmer Station (Fig. 11) are consistent with a nearly continuous source of oceanic CO_2 in the Antarctic waters. We hypothesise this background source is interrupted by small, short-lived and regional CO_2 sinks developing when sea ice melts or plankton blooms.

Very rapid onset and declines in CO_2 rates imply non-linear causal processes, which are anticipated with albedo feedbacks of snow and ice melt (IPCC 2013; Ouyang et al 2020). The inflections which reverse the main seasonal

rise or fall in atmospheric CO_2 could coincide with an abiotic variable that varies in a non-linear way. Candidates include: brine volume fraction in ice reaching c. 5% which can lead to an order of magnitude increase in permeability (Nomura et al 2018); ice cover reaching a critical extent; ice cover reaching a critical depth; freezing water in swamps or tundra reaching a critical depth; snow on the tundra reaching a critical depth; albedo declining during Greenland terrestrial ice melt. In the Antarctic spring (when temperatures rise above about -5ºC) ice permeability increases and release of CO_2 to the atmosphere begins (Semiletov et al 2007). In the CAA maximum CO_2 drawdown occurs when sea ice permeability passes a critical threshold around May, permitting vertical brine movement through the ice (Papakyriakou and Miller 2011) and this threshold is consistent with a sharp inflection of atmospheric CO_2 rates at Barrow and Alert at this time. Flux (drawdown) of CO_2 where there is patchy sea ice may be much greater than over open water, possibly due to greater turbulence (Prytherch et al 2017).

It is possible that during some seasons the temperature dependent transition from CO_2 efflux to CO_2 absorption in ice and water can be observed even within a daily cycle (Semiletov et al 2007; Papakyriakou and Miller 2011; Nomura et al 2013; Geilfus et al 2014).

Biotic forcing of CO_2 rates

Temperature dependent biotic forcing of monthly CO_2 rates cannot be completely discounted, given photosynthesis in both marine and terrestrial regions is low in winter. A plausible candidate, planktonic productivity in high latitudes, is extremely seasonal with suitably narrow peaks in some regions after ice melt (Leu et al 2015). Tight coupling of CO_2 drawdown as Arctic ice retreats could include ice-edge and sub-ice algae with close synchrony to ice melt and to peak sea temperature (Semiletov et al 2004; 2007; Barber et al 2015; Tremblay et al 2012; Bai et al 2019). However, ice-edge algal productivity is apparently very low compared to total phytoplankton productivity of the Arctic (Barber et al 2015; Vancoppenolle et al 2013). Arctic sea ice extent and phenology is a major driver of local planktonic productivity, with ice inhibiting productivity (Ji et al 2013; Geilfus et al 2012; Tremblay et al 2012, 2015) especially if covered with snow (Leu et al 2015) or if ice melt causes stratification (Ouyang et al 2020). Studies which ascribe at least some drawdown of CO_2 to phytoplankton include: Ishii et al (2002); Bakker et al (2008); Nomura et al (2014); Legge et al (2015); Roden et al (2016); Ouyang et al 2020). Phytoplankton productivity is the conventional explanation for a strong seasonal CO_2 sink in the Antarctic region (Takahashi et al 2009).

It is difficult to test large-scale phytoplankton phenology against CO_2 rate phenology because there are severe limitations in regional data (Gregg et al 2014; Roden et al 2016; Hammond et al 2017; Rosso et al 2017; Frey et al 2018; Bai et al 2019) especially in the high latitudes where satellite, surface and submarine measurements of productivity are very sparse or absent. In contrast to the extremely tight synchrony of ice melt with CO_2 rates, phytoplankton typically start blooming after ice disintegration is well advanced (Leu et al 2015). In the CAA there is little evidence for strong marine primary productivity as a driver of seawater pCO_2 (Ahmed et al 2019). Arguably, unlike the rather consistent phenology of CO_2 and sea ice rates (Figs. 1 - 11) the phenology and magnitude of marine productivity varies substantially between years - often dependent on temperature, stratification, sporadic upwelling currents, seasonal fluxes of rivers, and winds (McGowan et al 1998; Goes et al 2004; Corbière et al 2007; Semiletov et al 2007; Mathis et al 2010; Mundy et al 2009; Wang et al 2009; Sejr et al 2011; Tremblay et al 2011, 2012; Kim 2012; Rosso et al 2017; Del Castillo et al 2019).

There is also a superficial similarity between the phenology of Northern Hemisphere terrestrial productivity and CO_2 flux (Figs. 13 - 18) and such similarity generated the common paradigm for the causal mechanism of the carbon cycle annual phenology (*e.g.* Keeling et al 2001; Ciais et al 2013). It has been suggested (Buermann et al 2007) the amplitude of seasonal variation in the Mauna Loa CO_2 curve reflected a terrestrial North American sink and a Eurasian source, whilst others ascribe most of the dynamics to Siberian forests (Monroe 2013b). The very sharp seasonal CO_2 decline, and very sharp inflection towards CO_2 growth, suggest a very highly seasonal high latitude

sink. A greater amplitude of seasonal variation is indeed seen in NDVI for more northerly latitudinal belts (Fig. 12) associated with very highly seasonal vegetation productivity nearer the Arctic. However, terrestrial net annual productivity per unit area is low in high latitudes, limiting their potential role in CO_2 drawdown.

Monthly CO_2 rates for Barrow and Mauna Loa show relatively weak synchrony with inverted NDVI rate (Figs. 13 - 17), other than CO_2 rates being most negative when NDVI rate and photosynthesis is high in the Northern Hemisphere summer - which may be coincidental. The phenology of the NDVI rate is very similar for the latitudinal belts we tested or for virtually the whole Northern Hemisphere terrestrial surface (Fig. 12). The rapid increase in photosynthetic activity in the Northern Hemisphere spring is months earlier than the rapid drawdown of CO_2. At Mauna Loa and Barrow, peak negative monthly CO_2 rates are within a period with peak inverted NDVI level (Fig. 18) and there might be changes in biotic drawdown rate unrelated to NDVI. However, the rapid summer decrease in CO_2 drawdown before NDVI drops is difficult to explain. For Mauna Loa, vegetation appears more likely to be involved in net drawdown than emission (Fig. 15). For Barrow, it is difficult to fit simultaneously both peaks and troughs in NDVI and CO_2 rates (Figs. 16, 17), unlike with sea ice rates (Figs. 4 and 5).

Identifying drivers of CO_2 rates

It is not clear how globally representative the patterns of CO_2 rates we describe are, although some are evidently very widespread. Whilst there are tens of sites recording CO_2 which provide suitable monthly data (Dlugokencky et al 2019) these are not systematically nor randomly distributed on the planet. For example, the Southern Hemisphere is very poorly represented. We have not attempted a thorough review of CO_2 flux studies (including in-situ measurements) and anticipate many local observations will be inconsistent with the larger pattern: we invite others to identify and discuss these. There may be stronger correlations than we have calculated (*e.g.* Appendix, section D).

We have made preliminary comparisons (Appendix, sections A and C) of monthly flask data for CO_2 from NOAA for all sites with data since January 2003, to compare with the sea ice data available since January 2003. These suggest a thorough systematic comparison would be worthwhile. We find the Greenland-type Phenology (GTP) to be near-universal in the recording sites of the Northern Hemisphere.

GTP is evident, in possibly residual or degraded form, in a few Southern Hemisphere sites. However, in the Southern Hemisphere high latitudes sites, Antarctic sea ice rate phenology more closely resembles CO_2 rate phenology (such as on the Antarctic continent or in Drake Passage). More widely in the Southern Hemisphere, relatively irregular phenologies are common and we suggest relate to weak and widespread influences from the Arctic and Antarctic ice interacting with strong, local and highly variable oceanic fluxes of CO_2.

Whilst still having some similarity to GTP, high altitude sites (subjectively defined here as over 1000 m) are more likely to exhibit a twin peaked CO_2 rate phenology similar to Mauna Loa. In such sites there are often better visual fits with the combined Arctic plus Antarctic sea ice rates, lagged by about 5 - 7 months (Appendix, section B). We suggest such sites are receiving well-mixed air imprinted with the combined effects of Arctic plus Antarctic sea ice. Mahé, a lowland site in the tropical equatorial Indian Ocean with a twin-peaked phenology may also be receiving such air.

Observations showing large changes in CO_2 rates at a site months *before* similar changes in rate at Barrow or Alert would be inconsistent with our interpretation if representative of a sufficiently large-scale and if not attributable to the combined effect of regional fluxes and sea ice. We believe some sites may be slightly ahead of Barrow or Greenland Sea ice due to their local sea ice or terrestrial sinks. Such sites include Park Falls, Wisconsin, USA, but

these typically are in tight synchrony with the Arctic sea ice volume rate; Arctic sea ice volume loss slightly precedes sea ice extent loss. Some such continental sites may be influenced by local forest drawing CO_2 down early in the year. In Hegyhatsal, Hungary, we suggest it is also possible freeze and thaw of the large freshwater Lake Balaton may be involved in advancing and modifying the GTP, and the lake's seasonal carbonate chemistry would be worth investigating, as would meltwater *p*CO2 from local mountains. In Namibia, which has a highly erratic CO_2 rate we suggest calcareous desert sands and rainfall might influence CO_2 phenology, so carbonate mineral crystallisation processes would be worth investigation; satellite observations suggest some deserts to have surprisingly high CO_2 flux rates (Mearns 2015).

Studies of sea ice and CO_2 dynamics with phenologies we find broadly consistent with our paradigm include: Ishii et al 2002; Semiletov et al 2007; Bakker et al 2008; Nomura et al 2010, 2013, 2014; Sejr et al 2011; Fransson et al 2011, 2017; Shadwick et al 2011; Vancoppenolle et al 2013; Geilfus et al 2013, 2014, 2015, 2018; Roden 2016; Brown et al 2015; Butterworth and Miller 2016; Prytherch et al 2017; Tison et al 2017; Nomura et al 2010, 2018; Vancoppenolle and Tedesco 2017; Gray AR et al 2018; Søgaard et al 2019; Ouyang et al 2020. This selection of studies provides examples of the types of research that will be necessary to test predictions on larger, representative spatial and temporal scales. It also illustrates the need to quantify air flow and lags between CO_2 sources and sinks and CO_2 recording stations. Improved coverage of the high latitudes by large-scale monitoring of CO_2 will help test our proposal. Isotope ratios for $^{13}C/^{12}C$ show very similar patterns by latitude and season as CO_2 rates (Keeling et al 2005) and could be tested for consistency with isotopic fractionation occurring at the ice edge by abiotic processes.

The mechanisms for a high observed flux of CO_2 during the sea ice cycle remain to be explained (Tison et al 2017). Direct observations for CO_2 flux and concentrations for ice and seawater are sparse in the difficult environment of the sea ice (Vancoppenolle et al 2013; Barber et al 2015; Nomura et al 2018) making analysis of mechanisms difficult. Samples obtained when logistically possible may be unrepresentative. A major study in the Arctic (MOSAiC 2019) illustrates the practical challenges but we predict successful year-round monitoring would detect rapid drawdown of CO_2 near the North Pole around July.

Whilst the relative sizes of biotic and abiotic fluxes will take many years to identify, we propose that contributions of atmospheric CO_2 from sources other than sea ice, including humans, are dwarfed by the signal from the melting of sea ice and subsequent re-emission of CO_2 when Arctic melt water warms.

Between year variation

There must be relationships linking within-year variation and between-year CO_2 increments (or future declines). We find a very close relationship between annual average Lower Tropospheric temperature anomaly and the annual average of monthly CO_2 rate over the period 1979-2018 (Fig. 19). Indeed, the temperature anomaly of the Lower Troposphere over the tropical oceans also has high similarity to annual global CO_2 rates (Fig. 20). The rate of change of atmospheric CO_2 has previously been associated with global temperature (Reichenau and Esser 2003; Soares 2010; The Oil ConunDRUM 2011, 2012; MacRae 2019). Evolution of CO_2 with the integral of temperature implies a temperature dependent change in sources and / or sinks of CO_2 (Salby 2016).

Temperature dependence within the annual cycle of CO_2 may lead to temperature dependence in the net accumulation or loss of CO_2 between years. Amongst other factors, variation in insolation, clouds, sea ice, winds, river flows, El Nino parameters, currents and precipitation on short timescales could force some of the inter-annual variation in CO_2. For example, the discharge from the Amur river varies between years (Kim 2012). Warm years with warm discharges potentially reduce sea ice in the North Pacific (Ogi et al 2001) and could thus increase CO_2 upwelling releases. In glacial / interglacial cycles, cold periods with extensive sea ice probably have reduced

deepwater ventilation of CO_2 due to reduced ocean circulation (Uemura et al 2018; Marzocchi and Jansen 2019). The role of sea ice may have been neglected because its impact on CO_2 flux was thought to be small compared to other sources such as vegetation (*e.g.* Ciais et al 2013). As with intra-annual variation, we propose that the role of biological activity has been greatly overestimated.

If temperature predominantly drives CO_2 through oceanic outgassing, mediated by sea ice, higher increments would be predicted in warm years, as observed (Fig. 19; Soares 2010; Salby 2012, 2016; Humlum et al 2013; IPCC 2013). Moreover, CO_2 levels are rising whilst productivity as measured by 'global greening' is occurring (Zhu et al 2016; Chen et al 2019; Winkler et al 2019; Haverd et al 2020). Arctic planktonic activity also had an increasing trend for 2003-2018, with low ice associated with increased chlorophyll levels (Frey et al 2018). Similarly, the Southern Ocean gained in chlorophyll concentration between 2002 and 2010 (Del Castillo et al 2019). These contrasts suggest the physical processes of CO_2 dissolution may be more important a sink than is terrestrial or marine productivity, as per Soares (2010). Previous explanations for higher CO_2 increments in warm years are somewhat convoluted (Keeling et al 2001) and it is possible that several surface processes (such as greater thermal outgassing from warm water, reduced sea ice cover, soil respiration, more fires, or permafrost melting) lead to greater CO_2 emission in warm years. We suggest the possible influence of extent and volume of sea ice be investigated further, including its influences on marine vertical transport through upwelling and brine rejection - although short time series may constrain detection of trends.

Polar oceans support most of the estimated (and assumed) global oceanic CO_2 uptake (Takahashi et al 2009) and may be important in intra- and inter-annual variation in CO_2 level increments (or declines), particularly through sinking to depth of brine rich in CO_2 (Vancoppenolle et al 2013) and through regional effects of stratification (Ouyang et al 2020). A temperature dependent inorganic carbon pump in polar regions may inject large amounts of carbon to the deep ocean (Rysgaard et al 2007; Tison et al 2017; Ahmed et al 2019) which might be influenced by sea ice dynamics. Sea ice may also have relevance to the lag of CO_2 behind temperature on Milankovitch cycles (Uemura et al 2018). In the Greenland Sea, inter-annual variation in gas exchange is "significantly" influenced by the duration of ice cover (Sejr et al 2011). Substantial inter-annual variation of air-sea CO_2 fluxes in the North Atlantic subpolar gyre was explained by temperature (solubility) and productivity (Corbière et al 2007). Comparing monthly time series for temperature and CO_2 flux over several decades, Soares (2010) deduced the mechanism of CO_2 increase in the atmosphere was temperature dependent solubility, but that this did not cause the decrease. This paradox may be removed if the warming air causes rapid ice melt, cooling the water.

We suggest heat flux into the Arctic basin from the Atlantic (Kawasaki and Hasumi 2016) and Pacific (Okkonen et al 2009; Ouyang et al 2020) could influence monthly and annual CO_2 fluxes. Ice and ocean current dynamics in the Fram Strait near Greenland may be particularly influential, based on the relatively strong correlation of monthly CO_2 rates to Greenland Sea ice extent rates.

Conclusions

A new paradigm is required regarding causality of changes in CO_2 levels. We argue CO_2 is a response variable to temperature, not a forcing variable, on some timescales. The importance of some bidirectional sea ice and marine fluxes has been very seriously neglected due to over-confidence in the magnitude of terrestrial drawdown of CO_2. Furthermore, we believe the significance of sea ice has not been recognised previously because of the focus on Mauna Loa, where the strong Arctic CO_2 signal is partly obscured by that from the Antarctic. We argue scientific understanding of the carbon cycle is extremely poor, with dominant annual sources and sinks inadequately sampled and quantified. Our results suggest that within the annual cycle the influence on CO_2 of the terrestrial biota, including human activity, may be trivial compared to massive fluxes due to sea ice. Surprisingly, terrestrial productivity (as measured by NDVI) appears largely irrelevant to CO_2 levels within the annual cycle. Our work has implications for conclusions based on CO_2 residence times in the atmosphere - which could be shorter in the

presence of strong regional marine sinks which react quickly to temperature and which may lead to long-term carbon sequestration in sediments.

We hypothesize that for recent decades much of the annual pattern of the 'global' CO_2 level is generated by sea ice dynamics about a relatively stable trend of CO_2 emission from a very large global marine source with high thermal inertia. The particularly strong correlations between ice melt and CO_2 drawdown leave little need to infer effects of other sources and sinks. Unless a stronger correlation can be found with a biotic variable, we suggest a temperature dependent abiotic mechanism dominates the annual cycle of CO_2. Basic physics and chemistry could provide the mechanisms for a lagged response of CO_2 level to temperature (Humlum et al 2013) at all timescales. Candidates include: thermally-induced outgassing as solubility declines with sea temperature (*e.g.* Wiesenburg and Guinasso 1979; Takahashi et al 1993; Soares 2010); temperature dependent upwelling of CO_2 rich water (which may be impeded by ice caps, Zhabin et al 2017; Gray WR et al 2018; Marzocchi and Jansen 2019); and brine rejection (Detlef et al 2018; Gray WR et al 2018). Ocean temperature has previously been implicated in carbon cycle dynamics but with no clear mechanism (*e.g.* Keeling et al 2001, 2005). Solar forcing is argued to have a strong influence on global temperature (Zharkova et al 2019) and might link sea ice and CO_2 rates.

Whilst sea ice extent and volume have proved adequate to detect strong correlations, causation cannot be clarified. In particular, there are too few long-term monitoring stations providing consistent and simultaneous information on surface and sub-surface sea temperatures, currents, productivity or carbon dynamics. The CO_2 record we downloaded from two providers for at least one recording station (Barrow) is somewhat inconsistent, presumably due to data smoothing; there is a risk such processing obscures interesting pattern. The possibility of feedbacks causing a lag of temperature behind CO_2 (van Nes et al 2015; Stips et al 2016) appears unlikely in our timeseries, because conspicuous synchronous very high peaks of the annual rate of change of CO_2 and temperature (Fig. 19) suggest there are no dominant lags of over a year within the studied period (1979-2018 inclusive). Whilst some causes of CO_2 rise could be eliminated by the phase relationship, the actual causes are impossible to assign and there is a risk of unknown covariates.

Much further research is required on the timing and location of variation in CO_2 fluxes and on marine productivity which can be hard to detect under ice through remote sensing (Tremblay et al 2011, 2012). Large-scale experimental manipulation of sea ice might elucidate causality. Disentangling causal mechanisms has been impeded by the 'scientific consensus' strongly reinforced by recent IPCC reports, which has led to limited examination of alternative correlates and drivers of climate and carbon dynamics. We believe there has been great overconfidence in extrapolation from very small sample sizes (flux measurement sites) and in complex climate models and associated carbon cycle models which are poorly parameterised. 'Earth system' models and many climate models incorporate representations of biogeochemical cycles (Steiner et al 2013; Notz and Bitz, 2017) which influence the outcome of policy scenarios (Hausfather 2019).

Substantial adjustments to assumed or measured CO_2 fluxes have corresponding implications for the global carbon cycle and climate prediction, based on constraints from net atmospheric CO_2 accumulation. There are enormous opportunity costs and ecological impacts of climate policy attempting to modify carbon fluxes, so critical evaluation of our work is urgent. We argue all climate models incorporating CO_2 fluxes need to be reparametrized, whilst all associated predictions, attributions and policies require re-analysis.

Acknowledgements

Acknowledgements do not imply agreement with our argument or methods. We thank Marian Dawkins, Tom Hart, Martin Speight, Branden Thornhill-Miller and William Wint for very stimulating discussion, and for polite,

professional constructive criticism; their views very often conflict strongly with our own. Download and processing of MODIS satellite imagery was implemented by Environmental Research Group Oxford, Ltd. The website WoodForTrees (http://www.woodfortrees.org/) enabled easy visualisation, analysis and early detection of the main patterns. Datasets in the tables are the work of numerous dedicated researchers and organisations over many years, including: DMI; NOAA and sources they acknowledge; NSIDC; Scripps institution of Oceanography. We thank all sources listed or indicated in the metadata on the hosting websites and in Table 1.

Declarations

Funding None.

Conflict of interest / Competing interest The authors declare they have no conflict of interest / competing interests.

Availability of data and material Data are available from the online providers indicated in the Methods.

Code availability R code can be provided upon reasonable request

Open Access

References

Ahmed, M., Else, B., Burgers, T. & Papakyriakou, T. (2019) Variability of surface water pCO_2 in the Canadian Arctic Archipelago from 2010 to 2016. *Journal of Geophysical Research: Oceans,* **124,** 1876-1896.

Ahmed, M. & Else, B.G. (2019) The Ocean CO_2 Sink in the Canadian Arctic Archipelago: a present-day budget and past trends due to climate change. *Geophysical Research Letters,* **46,** 9777-9785.

Bai, Y., Sicre, M.-A., Chen, J., Klein, V., Jin, H., Ren, J., Li, H., Xue, B., Ji, Z. & Zhuang, Y. (2019) Seasonal and spatial variability of sea ice and phytoplankton biomarker flux in the Chukchi sea (western Arctic Ocean). *Progress in oceanography,* **171,** 22-37.

Bakker, D., Hoppema, M., Schröder, M., Geibert, W. & De Baar, H.J. (2008) A rapid transition from ice covered CO_2-rich waters to a biologically mediated CO_2 sink in the eastern Weddell Gyre. *Biosciences,* **5,** 1373-1386.

Barber, D.G., Hop, H., Mundy, C.J., Else, B., Dmitrenko, I.A., Tremblay, J.-E., Ehn, J.K., Assmy, P., Daase, M. & Candlish, L.M. (2015) Selected physical, biological and biogeochemical implications of a rapidly changing Arctic Marginal Ice Zone. *Progress in Oceanography,* **139,** 122-150.

Barlow, J., Palmer, P., Bruhwiler, L. & Tans, P. (2015) Analysis of CO_2 mole fraction data: first evidence of large-scale changes in CO_2 uptake at high northern latitudes. *Atmospheric Chemistry and Physics,* **15,** 739-713.

Beszczynska-Möller, A., Fahrbach, E., Schauer, U. & Hansen, E. (2012) Variability in Atlantic water temperature and transport at the entrance to the Arctic Ocean, 1997–2010. *ICES Journal of Marine Science,* **69,** 852-863.

Brown, K.A., Miller, L.A., Mundy, C.J., Papakyriakou, T., Francois, R., Gosselin, M., Carnat, G., Swystun, K. & Tortell, P.D. (2015) Inorganic carbon system dynamics in landfast Arctic sea ice during the early-melt period. *Journal of Geophysical Research: Oceans,* **120,** 3542-3566.

Buermann, W., Lintner, B.R., Koven, C.D., Angert, A., Pinzon, J.E., Tucker, C.J. & Fung, I.Y. (2007) The changing carbon cycle at Mauna Loa Observatory. *Proceedings of the National Academy of Sciences,* **104,** 4249-4254.

Bushinsky, S.M., Landschützer, P., Rödenbeck, C., Gray, A.R., Baker, D., Mazloff, M.R., Resplandy, L., Johnson, K.S. & Sarmiento, J.L. (2019) Reassessing Southern Ocean air sea CO_2 flux estimates with the addition of biogeochemical float observations. *Global Biogeochemical Cycles,* **33,** 1370-1388.

Butterworth, B.J. & Miller, S.D. (2016) Air-sea exchange of carbon dioxide in the Southern Ocean and Antarctic marginal ice zone. *Geophysical Research Letters,* **43,** 7223-7230.

Chavez, F., Strutton, P., Friederich, G., Feely, R., Feldman, G., Foley, D. & Mcphaden, M. (1999) Biological and chemical response of the equatorial Pacific Ocean to the 1997-98 El Niño. *Science,* **286,** 2126-2131.

Chen, J.M., Ju, W., Ciais, P., Viovy, N., Liu, R., Liu, Y. & Lu, X. (2019) Vegetation structural change since 1981 significantly enhanced the terrestrial carbon sink. *Nature Communications,* **10,** 1-7.

Ciais, P., Sabine, C., Bala, G., Bopp, L., Brovkin, V., Canadell, J., Chhabra, A., Defries, R., Galloway, J., Heimann, M., Jones, C., Le Quéré, C., Myneni, R.B., Piao, S & Thornton, P. (2013) Carbon and other biogeochemical cycles. In: *Climate change 2013: the physical science basis. Contribution of Working Group I to the Fifth Assessment Report of the Intergovernmental Panel on Climate Change* (ed. by T. Stocker, D. Qin, G.-K. Plattner, M. Tignor, S. Allen, J. Boschung, A. Nauels, Y. Xia, V. Bex & P. Midgley), pp. 465-570. Cambridge University Press, Cambridge, United Kingdom.

Corbière, A., Metzl, N., Reverdin, G., Brunet, C. & Takahashi, T. (2007) Interannual and decadal variability of the oceanic carbon sink in the North Atlantic subpolar gyre. *Tellus B: Chemical and Physical Meteorology,* **59,** 168-178.

Del Castillo, C.E., Signorini, S.R., Karaköylü, E.M. & Rivero-Calle, S. (2019) Is the Southern Ocean getting greener? *Geophysical Research Letters,* **46,** 6034-6040.

Delille, B., Vancoppenolle, M., Geilfus, N.X., Tilbrook, B., Lannuzel, D., Schoemann, V., Becquevort, S., Carnat, G., Delille, D. & Lancelot, C. (2014) Southern Ocean CO_2 sink: The contribution of the sea ice. *Journal of Geophysical Research: Oceans,* **119,** 6340-6355.

Denning, A.S., Fung, I.Y. & Randall, D. (1995) Latitudinal gradient of atmospheric CO_2 due to seasonal exchange with land biota. *Nature,* **376,** 240-243.

Detlef, H., Belt, S., Sosdian, S., Smik, L., Lear, C.H., Hall, I., Cabedo-Sanz, P., Husum, K. & Kender, S. (2018) Sea ice dynamics across the Mid-Pleistocene transition in the Bering Sea. *Nature Communications,* **9,** 1-11.

Dettinger, M.D. & Ghil, M. (1998) Seasonal and interannual variations of atmospheric CO_2 and climate. *Tellus B,* **50,** 1-24.

DeVries, T. (2014) The oceanic anthropogenic CO_2 sink: Storage, air-sea fluxes, and transports over the industrial era. *Global Biogeochemical Cycles,* **28,** 631-647.

Didan, K. (2019) MOD13C2 MODIS/Terra Vegetation Indices Monthly L3 Global 0.05Deg CMG V006. 2015, distributed by NASA EOSDIS Land Processes DAAC. https://doi.org/10.5067/MODIS/MOD13C2.006. Accessed 16 December 2019.

Dlugokencky, E.J., Mund, J.W., Crotwell, A.M., Crotwell, M.J. & Thoning, K.W. (2019) Atmospheric carbon dioxide dry air mole fractions from the NOAA ESRL Carbon Cycle Cooperative Global Air Sampling Network, 1968-2018, Version: 2019-07. https://doi.org/10.15138/wkgj-f215 Accessed 11 May 2020.

Faes, L., Nollo, G., Stramaglia, S. & Marinazzo, D. (2017) Multiscale granger causality. *Physical Review E,* **96,** 042150.

Fetterer, F., Knowles, K., Meier, W.N., Savoie, M. & Wn, W. (2017) Updated daily. Sea Ice Index, Version 3. monthly North and South. Boulder, Colorado USA. NSIDC: National Snow and Ice Data Center. https://doi.org/10.7265/N5K072F8. Accessed 26 February.

Francey, R.J., Frederiksen, J.S., Steele, L.P. & Langenfelds, R.L. (2019) Variability in a four-network composite of atmospheric CO_2 differences between three primary baseline sites. *Atmospheric Chemistry and Physics,* **19,** 14741-14754.

Fransson, A., Chierici, M., Skjelvan, I., Olsen, A., Assmy, P., Peterson, A.K., Spreen, G. & Ward, B. (2017) Effects of sea-ice and biogeochemical processes and storms on under-ice water fCO_2 during the winter-spring transition in the high Arctic Ocean: Implications for sea-air CO_2 fluxes. *Journal of Geophysical Research: Oceans,* **122,** 5566-5587.

Fransson, A., Chierici, M., Yager, P.L. & Smith Jr, W.O. (2011) Antarctic sea ice carbon dioxide system and controls. *Journal of Geophysical Research: Oceans,* **116**, C12035.

Frey, K., Comiso, J., Cooper, L., Grebmeier, J. & Stock, L.V. (2018) Arctic ocean primary productivity: The response of marine algae to climate warming and sea ice decline. https://www.arctic.noaa.gov/Report-Card/Report-Card-2018/ArtMID/7878/ArticleID/778/Arctic-Ocean-Primary-Productivity-The-Response-of-Marine-Algae-to-Climate-Warming-and-Sea-Ice-Decline. Accessed 26 March 2020

Geilfus, N.X., Carnat, G., Dieckmann, G.S., Halden, N., Nehrke, G., Papakyriakou, T., Tison, J.L. & Delille, B. (2013) First estimates of the contribution of $CaCO_3$ precipitation to the release of CO_2 to the atmosphere

during young sea ice growth. *Journal of Geophysical Research: Oceans,* **118,** 244-255.
Geilfus, N.X., Carnat, G., Papakyriakou, T., Tison, J.L., Else, B., Thomas, H., Shadwick, E. & Delille, B. (2012) Dynamics of pCO_2 and related air ice CO_2 fluxes in the Arctic coastal zone (Amundsen Gulf, Beaufort Sea). *Journal of Geophysical Research: Oceans,* 117, C00G10.
Geilfus, N.-X., Galley, R., Crabeck, O., Papakyriakou, T., Landy, J., Tison, J.-L. & Rysgaard, S. (2015) Inorganic carbon dynamics of melt-pond-covered first-year sea ice in the Canadian Arctic. *Biogeosciences,* **12,** 2047-2061.
Geilfus, N.-X., Pind, M., Else, B., Galley, R., Miller, L., Thomas, H., Gosselin, M., Rysgaard, S., Wang, F. & Papakyriakou, T. (2018) Spatial and temporal variability of seawater pCO_2 within the Canadian Arctic Archipelago and Baffin Bay during the summer and autumn 2011. *Continental Shelf Research,* **156,** 1-10.
Geilfus, N.-X., Tison, J.-L., Ackley, S., Galley, R., Rysgaard, S., Miller, L. & Delille, B. (2014) Sea ice pCO_2 dynamics and air–ice CO_2 fluxes during the Sea Ice Mass Balance in the Antarctic (SIMBA) experiment–Bellingshausen Sea, Antarctica. *Cryosphere,* **8,** 2395-2407.
Goes, J.I., Sasaoka, K., Gomes, H.D.R., Saitoh, S.-I. & Saino, T. (2004) A comparison of the seasonality and interannual variability of phytoplankton biomass and production in the western and eastern gyres of the subarctic Pacific using multi-sensor satellite data. *Journal of oceanography,* **60,** 75-91.
Graven, H., Keeling, R., Piper, S., Patra, P., Stephens, B., Wofsy, S., Welp, L., Sweeney, C., Tans, P. & Kelley, J. (2013) Enhanced seasonal exchange of CO_2 by northern ecosystems since 1960. *Science,* **341,** 1085-1089.
Gray, A.R., Johnson, K.S., Bushinsky, S.M., Riser, S.C., Russell, J.L., Talley, L.D., Wanninkhof, R., Williams, N.L. & Sarmiento, J.L. (2018) Autonomous biogeochemical floats detect significant carbon dioxide outgassing in the high latitude Southern Ocean. *Geophysical Research Letters,* **45,** 9049-9057.
Gray, W.R., Rae, J.W., Wills, R.C., Shevenell, A.E., Taylor, B., Burke, A., Foster, G.L. & Lear, C.H. (2018) Deglacial upwelling, productivity and CO_2 outgassing in the North Pacific Ocean. *Nature Geoscience,* **11,** 340-344.
Gregg, W.W. & Rousseaux, C.S. (2014) Decadal trends in global pelagic ocean chlorophyll: A new assessment integrating multiple satellites, in situ data, and models. *Journal of Geophysical Research: Oceans,* **119,** 5921-5933.
Gruber, N., Gloor, M., Mikaloff Fletcher, S.E., Doney, S.C., Dutkiewicz, S., Follows, M.J., Gerber, M., Jacobson, A.R., Joos, F. & Lindsay, K. (2009) Oceanic sources, sinks, and transport of atmospheric CO_2. *Global Biogeochemical Cycles,* **23. (**GB1005).
Hammond, M.L., Beaulieu, C., Sahu, S.K. & Henson, S.A. (2017) Assessing trends and uncertainties in satellite-era ocean chlorophyll using space-time modeling. *Global Biogeochemical Cycles,* **31,** 1103-1117.
Harde, H. (2019) What humans contribute to atmospheric CO_2: comparison of carbon cycle models with observations. *Earth Sciences,* **8,** 139-159.
Hausfather, Z. (2019) CMIP6: the next generation of climate models explained. CarbonBrief. https://www.carbonbrief.org/cmip6-the-next-generation-of-climate-models-explained. Accessed 12 February 2020.
Haverd, V., Smith, B., Canadell, J.G., Cuntz, M., Mikalof-Fletcher, S., Farquhar, G., Woodgate, W., Briggs, P.R. & Trudinger, C.M. (2020) Higher than expected CO_2 fertilization inferred from leaf to global observations. *Global Change Biology,* **26**, 2390–2402.
Humlum, O., Stordahl, K. & Solheim, J.-E. (2013) The phase relation between atmospheric carbon dioxide and global temperature. *Global and Planetary Change,* **100,** 51-69.
IPCC (2013) *Climate Change 2013: The physical science basis. Contribution of Working Group I to the Fifth Assessment Report of the Intergovernmental Panel on Climate Change* (ed. by T. Stocker, D. Qin, G.-K. Plattner, M. Tignor, S. Allen, J. Boschung, A. Nauels, Y. Xia, V. Bex & P. Midgley), Cambridge University Press, Cambridge, United Kingdom.
Ishii, M., Inoue, H.Y. & Matsueda, H. (2002) Net community production in the marginal ice zone and its importance for the variability of the oceanic pCO_2 in the Southern Ocean south of Australia. *Deep Sea Research Part II: Topical Studies in Oceanography,* **49,** 1691-1706.
Ji, R., Jin, M. & Varpe, Ø. (2013) Sea ice phenology and timing of primary production pulses in the Arctic Ocean. *Global Change Biology,* **19,** 734-741.
Karkauskaite, P., Tagesson, T. & Fensholt, R. (2017) Evaluation of the plant phenology index (PPI), NDVI and EVI for start-of-season trend analysis of the Northern Hemisphere boreal zone. *Remote Sensing,* **9,** 485.
Kawasaki, T. & Hasumi, H. (2016) The inflow of Atlantic water at the Fram Strait and its interannual variability.

Journal of Geophysical Research: Oceans, **121,** 502-519.
Keeling, C., Piper, S., Bacastow, R., Wahlen, M., Whorf, T., Heimann, M. & Meijer, H. (2001) Exchanges of atmospheric CO_2 and $13CO_2$ with the terrestrial biosphere and oceans from 1978 to 2000. In: *Exchanges of atmospheric* CO_2 *and 13*CO_2 *with the terrestrial biosphere and oceans from 1978 to 2000. I. Global aspects, SIO Reference Series, No. 01-06,* pp. 1-88. Scripps Institution of Oceanography, San Diego.
Keeling, C.D. (1960) The concentration and isotopic abundances of carbon dioxide in the atmosphere. *Tellus,* **12,** 200-203.
Keeling, C.D., Bacastow, R.B., Bainbridge, A.E., Ekdahl Jr, C.A., Guenther, P.R., Waterman, L.S. & Chin, J.F. (1976) Atmospheric carbon dioxide variations at Mauna Loa observatory, Hawaii. *Tellus,* **28,** 538-551.
Keeling, C.D., Bacastow, R.B., Carter, A., Piper, S.C., Whorf, T.P., Heimann, M., Mook, W.G. & Roeloffzen, H. (1989) A three-dimensional model of atmospheric CO_2 transport based on observed winds: 1. Analysis of observational data. *Aspects of climate variability in the Pacific and the Western Americas,* **55,** 165-236.
Keeling, C.D., Piper, S.C., Bacastow, R.B., Wahlen, M., Whorf, T.P., Heimann, M. & Meijer, H.A. (2005) Atmospheric CO_2 and $^{13}CO_2$ exchange with the terrestrial biosphere and oceans from 1978 to 2000: Observations and carbon cycle implications. In: *A history of atmospheric* CO_2 *and its effects on plants, animals, and ecosystems,* (ed. by J.R. Ehleringer. T.E. Cerling, & M.D. Dearing), pp. 83-113. Springer, New York.
Keeling, R.F. (2008) Recording Earth's vital signs. *Science,* **319,** 1771-1772.
Khatiwala, S., Primeau, F. & Hall, T. (2009) Reconstruction of the history of anthropogenic CO_2 concentrations in the ocean. *Nature,* **462,** 346-349.
Kim, S.T. (2012) A review of the Sea of Okhotsk ecosystem response to the climate with special emphasis on fish populations. *ICES Journal of Marine Science,* **69,** 1123-1133.
Le Quéré, C., Rödenbeck, C., Buitenhuis, E.T., Conway, T.J., Langenfelds, R., Gomez, A., Labuschagne, C., Ramonet, M., Nakazawa, T. & Metzl, N. (2007) Saturation of the Southern Ocean CO_2 sink due to recent climate change. *Science,* **316,** 1735-1738.
Legge, O.J., Bakker, D.C., Johnson, M.T., Meredith, M.P., Venables, H.J., Brown, P.J. & Lee, G.A. (2015) The seasonal cycle of ocean-atmosphere CO_2 flux in Ryder Bay, west Antarctic Peninsula. *Geophysical Research Letters,* **42,** 2934-2942.
Leu, E., Mundy, C., Assmy, P., Campbell, K., Gabrielsen, T., Gosselin, M., Juul-Pedersen, T. & Gradinger, R. (2015) Arctic spring awakening–Steering principles behind the phenology of vernal ice algal blooms. *Progress in oceanography,* **139,** 151-170.
Loose, B., Mcgillis, W., Schlosser, P., Perovich, D. & Takahashi, T. (2009) Effects of freezing, growth, and ice cover on gas transport processes in laboratory seawater experiments. *Geophysical Research Letters,* **36**, L05603.
MacRae, A.M.R. (2019) CO_2, GLOBAL WARMING, CLIMATE AND ENERGY. https://wattsupwiththat.com/2019/06/15/CO_2-global-warming-climate-and-energy-2/. Accessed 15 June 2019.
Marzocchi, A. & Jansen, M.F. (2019) Global cooling linked to increased glacial carbon storage via changes in Antarctic sea ice. *Nature Geoscience,* **12,** 1001-1005.
Mathis, J., Cross, J., Bates, N., Bradley Moran, S., Lomas, M., Mordy, C. & Stabeno, P. (2010) Seasonal distribution of dissolved inorganic carbon and net community production on the Bering Sea shelf. *Biogeosciences,* **7,** 1769-1787.
McGowan, J.A., Cayan, D.R. & Dorman, L.M. (1998) Climate-ocean variability and ecosystem response in the Northeast Pacific. *Science,* **281,** 210-217.
Mearns, E. (2015). CO2 - The view from space - update. http://euanmearns.com/co2-the-view-from-space-update/ Accessed 28 May 2020.
Messié, M. & Chavez, F.P. (2012) A global analysis of ENSO synchrony: The oceans' biological response to physical forcing. *Journal of Geophysical Research: Oceans,* **117**, C09001.
Miller, L.A., Chierici, M., Johannessen, T., Noji, T.T., Rey, F. & Skjelvan, I. (1999) Seasonal dissolved inorganic carbon variations in the Greenland Sea and implications for atmospheric CO_2 exchange. *Deep Sea Research Part II: Topical Studies in Oceanography,* **46,** 1473-1496.
Miller, L.A., Papakyriakou, T.N., Collins, R.E., Deming, J.W., Ehn, J.K., Macdonald, R.W., Mucci, A., Owens, O., Raudsepp, M. & Sutherland, N. (2011) Carbon dynamics in sea ice: A winter flux time series. *Journal of Geophysical Research: Oceans,* **116**, C02028.
Monroe, R. (2013a) Why does atmospheric CO_2 peak in May?

https://scripps.ucsd.edu/programs/keelingcurve/2013/06/04/why-does-atmospheric-CO_2. Accessed 26 March 2020.

Monroe, R. (2013b) Why-are-seasonal-CO_2-fluctuations-strongest-in-northern-latitudes? https://scripps.ucsd.edu/programs/keelingcurve/2013/05/07/why-are-seasonal-CO_2-fluctuations-strongest-in-northern-latitudes/. Accessed 26 March 2020.

Moreau, S., Vancoppenolle, M., Bopp, L., Aumont, O., Madec, G., Delille, B., Tison, J.-L., Barriat, P.-Y. & Goosse, H. (2016) Assessment of the sea-ice carbon pump: Insights from a three-dimensional ocean-sea-ice biogeochemical model (NEMO-LIM-PISCES). *Elementa: Science of the Anthropocene,* **4,** 000122.

MOSAiC (2019) The key to the Arctic puzzle. from https://www.mosaic-expedition.org/science/arctic-climate/. Accessed 29 October 2019.

Mundy, C., Gosselin, M., Ehn, J., Gratton, Y., Rossnagel, A., Barber, D.G., Martin, J., Tremblay, J.É., Palmer, M., Arrigo, K.R., Darnis, G., Fortier ,L., Else, B, & Papakyriakou, T. (2009) Contribution of under-ice primary production to an ice-edge upwelling phytoplankton bloom in the Canadian Beaufort Sea. *Geophysical Research Letters,* **36**, L17601.

Nelson, M.D. & Nelson, D.B. (2016) Oceans, ice & snow and CO_2 rise, swing and seasonal fluctuation. *International Journal of Geosciences,* **7,** 1232-1282.

Newell, R.E., Navato, A.R. & Hsiung, J. (1978) Long-term global sea surface temperature fluctuations and their possible influence on atmospheric CO_2 concentrations. *Pure and Applied Geophysics,* **116,** 351-371.

Newell, R.E. & Weare, B.C. (1977) A relationship between atmospheric carbon dioxide and Pacific sea surface temperature. *Geophysical Research Letters,* **4,** 1-2.

Nomura, D., Eicken, H., Gradinger, R. & Shirasawa, K. (2010) Rapid physically driven inversion of the air–sea ice CO_2 flux in the seasonal landfast ice off Barrow, Alaska after onset of surface melt. *Continental Shelf Research,* **30,** 1998-2004.

Nomura, D., Granskog, M.A., Assmy, P., Simizu, D. & Hashida, G. (2013) Arctic and Antarctic sea ice acts as a sink for atmospheric CO_2 during periods of snowmelt and surface flooding. *Journal of Geophysical Research: Oceans,* **118,** 6511-6524.

Nomura, D., Granskog, M.A., Fransson, A., Chierici, M., Silyakova, A., Ohshima, K.I., Cohen, L., Delille, B., Hudson, S.R. & Dieckmann, G.S. (2018) CO_2 flux over young and snow-covered Arctic pack ice in winter and spring. *Biogeosciences,* **15,** 3331-3343.

Nomura, D., Yoshikawa-Inoue, H., Kobayashi, S., Nakaoka, S., Nakata, K. & Hashida, G. (2014) Winter-to-summer evolution of pCO_2 in surface water and air–sea CO_2 flux in the seasonal ice zone of the Southern Ocean. *Biogeosciences,* **11,** 5749-5761.

Nomura, D., Yoshikawa-Inoue, H. & Toyota, T. (2006) The effect of sea-ice growth on air–sea CO_2 flux in a tank experiment. *Tellus B: Chemical and Physical Meteorology,* **58,** 418-426.

Notz, D. & Bitz, C.M. (2017) Sea Ice in Earth System Models. In: *Sea ice*, 3rd edn. (ed. by D. Thomas), pp. 304-325. Wiley, New Jersey.

Ogi, M., Tachibana, Y., Nishio, F. & Danchenkov, M.A. (2001) Does the fresh water supply from the Amur River flowing into the Sea of Okhotsk affect sea ice formation? *Journal of the Meteorological Society of Japan. Ser. II*, **79,** 123-129.

Okkonen, S., Ashjian, C., Campbell, R.G., Maslowski, G., Wieslaw, C., Kinney, J. & Potter, R. (2009) Intrusion of warm Bering/Chukchi waters onto the shelf in the western Beaufort Sea. *Journal of Geophysical Research: Oceans,* **114,** 2156-2202.

Ouyang, Z., Qi, D., Chen, L., Takahashi, T., Zhong, W., DeGrandpre, M.D., Chen, B., Gao, Z., Nishino, S., Murata, A., Sun, H., Robbins, L.L, Jin, M. & Cai, W.-J. (2020) Sea-ice loss amplifies summertime decadal CO_2 increase in the western Arctic Ocean, *Nature Climate Change*. https://doi.org/10.1038/s41558-020-0784-2 Accessed 18 June 2020.

Papadimitriou, S., Kennedy, H., Kattner, G., Dieckmann, G. & Thomas, D. (2004) Experimental evidence for carbonate precipitation and CO_2 degassing during sea ice formation. *Geochimica et Cosmochimica Acta,* **68,** 1749-1761.

Papakyriakou, T. & Miller, L. (2011) Springtime CO_2 exchange over seasonal sea ice in the Canadian Arctic Archipelago. *Annals of Glaciology,* **52,** 215-224.

Peterson, J.T., Komhyr, W., Waterman, L., Gammon, R., Thoning, K. & Conway, T. (1987) Atmospheric CO_2 variations at Barrow, Alaska, 1973–1982. *Journal of Atmospheric Chemistry,* **4,** 491-510.

Prytherch, J., Brooks, I.M., Crill, P.M., Thornton, B.F., Salisbury, D.J., Tjernström, M., Anderson, L.G., Geibel, M.C. & Humborg, C. (2017) Direct determination of the air-sea CO_2 gas transfer velocity in Arctic sea ice

regions. *Geophysical Research Letters*, **44,** 3770-3778.
Reichenau, T.G. & Esser, G. (2003) Is interannual fluctuation of atmospheric CO_2 dominated by combined effects of ENSO and volcanic aerosols? *Global Biogeochemical Cycles*, **17,** 1094.
Resplandy, L., Keeling, R., Rödenbeck, C., Stephens, B., Khatiwala, S., Rodgers, K., Long, M., Bopp, L. & Tans, P. (2018) Revision of global carbon fluxes based on a reassessment of oceanic and riverine carbon transport. *Nature Geoscience*, **11,** 504-509.
Robinson, D.A., Estilow, T. & Al., E. (2012) NOAA Climate Data Record (CDR) of Northern Hemisphere (NH) Snow Cover Extent (SCE), Version 1. Monthly: N. America; N. America no Greenland. NOAA National Centers for Environmental Information. Retrieved 27 March 2020.
Roden, N.P., Tilbrook, B., Trull, T.W., Virtue, P. & Williams, G.D. (2016) Carbon cycling dynamics in the seasonal sea ice zone of East Antarctica. *Journal of Geophysical Research: Oceans*, **121,** 8749-8769.
Rosso, I., Mazloff, M.R., Verdy, A. & Talley, L.D. (2017) Space and time variability of the Southern Ocean carbon budget. *Journal of Geophysical Research: Oceans,* **122,** 7407-7432.
Rysgaard, S., Glud, R.N., Sejr, M., Bendtsen, J. & Christensen, P. (2007) Inorganic carbon transport during sea ice growth and decay: A carbon pump in polar seas. *Journal of Geophysical Research: Oceans,* **112**, C03016.
Rysgaard, S., Søgaard, D.H., Cooper, M., Pućko, M., Lennert, K., Papakyriakou, T., Wang, F., Geilfus, N., Glud, R.N. & Ehn, J. (2013) Ikaite crystal distribution in winter sea ice and implications for CO_2 system dynamics. *Cryosphere*, **7,** 707-718.
Salby, M. (2012) *Physics of the atmosphere and climate*, 2nd edn. Cambridge University Press, Cambridge, United Kingdom.
Salby, M. (2016) Prof Salby: Atmospheric Carbon. https://www.youtube.com/watch?v=3q-M_uYkpT0. Accessed 18 February 2020.
Schaefer, K., Denning, A.S. & Leonard, O. (2005) The winter Arctic Oscillation, the timing of spring, and carbon fluxes in the Northern Hemisphere. *Global Biogeochemical Cycles*, **19**, GB3017.
Sejr, M.K., Krause-Jensen, D., Rysgaard, S., Sørensen, L.L., Christensen, P.B. & Glud, R.N. (2011) Air-sea flux of CO_2 in Arctic coastal waters influenced by glacial melt water and sea ice. *Tellus B: Chemical and Physical Meteorology*, **63,** 815-822.
Semiletov, I. (1999) Aquatic sources and sinks of CO_2 and CH_4 in the polar regions. *Journal of the Atmospheric Sciences*, **56,** 286-306.
Semiletov, I., Makshtas, A., Akasofu, S.I. & L Andreas, E. (2004) Atmospheric CO_2 balance: The role of Arctic sea ice. *Geophysical Research Letters*, **31**, L05121.
Semiletov, I.P., Pipko, I.I., Repina, I. & Shakhova, N.E. (2007) Carbonate chemistry dynamics and carbon dioxide fluxes across the atmosphere–ice–water interfaces in the Arctic Ocean: Pacific sector of the Arctic. *Journal of Marine Systems*, **66,** 204-226.
Shadwick, E.H., Thomas, H., Chierici, M., Else, B., Fransson, A., Michel, C., Miller, L., Mucci, A., Niemi, A. & Papakyriakou, T. (2011) Seasonal variability of the inorganic carbon system in the Amundsen Gulf region of the southeastern Beaufort Sea. *Limnology and Oceanography*, **56,** 303-322.
Sigman, D.M., Hain, M.P. & Haug, G.H. (2010) The polar ocean and glacial cycles in atmospheric CO_2 concentration. *Nature*, **466,** 47-55.
Soares, P.C. (2010) Warming power of CO_2 and H_2O: correlations with temperature changes. *International Journal of Geosciences,* **1,** 102-112.
Søgaard, D.H., Deming, J.W., Meire, L. & Rysgaard, S. (2019) Effects of microbial processes and $CaCO_3$ dynamics on inorganic carbon cycling in snow-covered Arctic winter sea ice. *Marine Ecology Progress Series,* **611,** 31-44.
Søgaard, D.H., Thomas, D.N., Rysgaard, S., Glud, R.N., Norman, L., Kaartokallio, H., Juul-Pedersen, T. & Geilfus, N.-X. (2013) The relative contributions of biological and abiotic processes to carbon dynamics in subarctic sea ice. *Polar Biology*, **36,** 1761-1777.
Spencer, R., Christy, J. & Braswell, W. (2015) Version 6.0 of the UAH Temperature Dataset Released: New LT Trend = +0.11 C/decade. https://www.drroyspencer.com/2015/04/version-6-0-of-the-uah-temperature-dataset-released-new-lt-trend-0-11-cdecade/. Accessed 15 April 2020.
Steiner, N., Lee, W. & Christian, J. (2013) Enhanced gas fluxes in small sea ice leads and cracks: Effects on CO_2 exchange and ocean acidification. *Journal of Geophysical Research: Oceans*, 118, 1195-1205.
Stips, A., Macias, D., Coughlan, C., Garcia-Gorriz, E. & San Liang, X. (2016) On the causal structure between CO_2 and global temperature. *Scientific Reports,* **6,** 1-9.
Takahashi, T., Olafsson, J., Goddard, J.G., Chipman, D.W. & Sutherland, S. (1993) Seasonal variation of CO_2 and

nutrients in the high-latitude surface oceans: A comparative study. *Global Biogeochemical Cycles,* **7**, 843-878.

Takahashi, T., Sutherland, S.C., Wanninkhof, R., Sweeney, C., Feely, R.A., Chipman, D.W., Hales, B., Friederich, G., Chavez, F. & Sabine, C. (2009) Climatological mean and decadal change in surface ocean pCO_2, and net sea–air CO_2 flux over the global oceans. *Deep Sea Research Part II: Topical Studies in Oceanography,* **56,** 554-577.

The Oil ConunDRUM (2011) The sensitivity of global temperature to CO_2. http://theoilconundrum.blogspot.co.uk/2011/09/sensitivity-of-global-temperature-to.html. Accessed 19 February 2020.

The Oil ConunDRUM (2012) CO_2 outgassing model (αβ). http://theoilconundrum.blogspot.com/2012/03/. Accessed 19 February 2020.

Tison, J.-L., Delille, B. & Papadimitriou, S. (2017) Gases in sea ice. In: *Sea ice,* 3rd edn. (ed. by D.N. Thomas), pp. 433-471. Wiley, New Jersey.

Tremblay, J.É., Bélanger, S., Barber, D., Asplin, M., Martin, J., Darnis, G., Fortier, L., Gratton, Y., Link, H. & Archambault, P. (2011) Climate forcing multiplies biological productivity in the coastal Arctic Ocean. *Geophysical Research Letters,* **38**, L18604.

Tremblay, J.-É., Anderson, L.G., Matrai, P., Coupel, P., Bélanger, S., Michel, C. & Reigstad, M. (2015) Global and regional drivers of nutrient supply, primary production and CO_2 drawdown in the changing Arctic Ocean. *Progress in Oceanography,* **139,** 171-196.

Tremblay, J.-É., Robert, D., Varela, D.E., Lovejoy, C., Darnis, G., Nelson, R.J. & Sastri, A.R. (2012) Current state and trends in Canadian Arctic marine ecosystems: I. Primary production. *Climatic Change,* **115,** 161-178.

Uemura, R., Motoyama, H., Masson-Delmotte, V., Jouzel, J., Kawamura, K., Goto-Azuma, K., Fujita, S., Kuramoto, T., Hirabayashi, M. & Miyake, T. (2018) Asynchrony between Antarctic temperature and CO_2 associated with obliquity over the past 720,000 years. *Nature Communications,* **9,** 1-11.

Van As, D., Andersen, M.L., Petersen, D., Fettweis, X., Van Angelen, J.H., Lenaerts, J.T., Van Den Broeke, M.R., Lea, J.M., Bøggild, C.E. & Ahlstrøm, A.P. (2014) Increasing meltwater discharge from the Nuuk region of the Greenland ice sheet and implications for mass balance (1960–2012). *Journal of Glaciology,* **60,** 314-322.

Van Nes, E.H., Scheffer, M., Brovkin, V., Lenton, T.M., Ye, H., Deyle, E. & Sugihara, G. (2015) Causal feedbacks in climate change. *Nature Climate Change,* **5,** 445-448.

Vancoppenolle, M., Meiners, K.M., Michel, C., Bopp, L., Brabant, F., Carnat, G., Delille, B., Lannuzel, D., Madec, G. & Moreau, S. (2013) Role of sea ice in global biogeochemical cycles: emerging views and challenges. *Quaternary Science Reviews,* **79,** 207-230.

Vancoppenolle, M. & Tedesco, L. (2017) Numerical models of sea ice biogeochemistry. In: *Sea ice,* 3rd edn. (ed. by D.N. Thomas), pp. 492-515. Wiley, New Jersey.

Verdy, A., Dutkiewicz, S., Follows, M., Marshall, J. & Czaja, A. (2007) Carbon dioxide and oxygen fluxes in the Southern Ocean: Mechanisms of interannual variability. *Global Biogeochemical Cycles,* **21**, GB2020.

Wang, J., Hu, H., Mizobata, K. & Saitoh, S.I. (2009) Seasonal variations of sea ice and ocean circulation in the Bering Sea: A model-data fusion study. *Journal of Geophysical Research: Oceans,* **114**, C02011.

Wiesenburg, D.A. & Guinasso Jr, N.L. (1979) Equilibrium solubilities of methane, carbon monoxide, and hydrogen in water and sea water. *Journal of Chemical and Engineering Data,* **24,** 356-360.

Winkler, A.J., Myneni, R.B., Alexandrov, G.A. & Brovkin, V. (2019) Earth system models underestimate carbon fixation by plants in the high latitudes. *Nature Communications,* **10,** 1-8.

Zhabin, I., Dmitrieva, E. & Vanin, N. (2017) Effects of the wind and ice conditions on the upwelling along the western Kamchatka coast (Sea of Okhotsk) based on the satellite data. *Izvestiya, Atmospheric and Oceanic Physics,* **53,** 965-972.

Zhao, F. & Zeng, N. (2014) Continued increase in atmospheric CO_2 seasonal amplitude in the 21st century projected by the CMIP5 Earth system models. *Earth System Dynamics,* **5**, 423-439.

Zharkova, V., Shepherd, S., Zharkov, S. & Popova, E. (2019) Oscillations of the baseline of solar magnetic field and solar irradiance on a millennial timescale. *Scientific Reports,* **9,** 1-12.

Zhu, Z., Piao, S., Myneni, R.B., Huang, M., Zeng, Z., Canadell, J.G., Ciais, P., Sitch, S., Friedlingstein, P. & Arneth, A. (2016) Greening of the Earth and its drivers. *Nature Climate Change,* **6,** 791-795.

Appendix

Monthly rate of change of CO_2 at NOAA Global Monitoring Laboratory sites vs. selected sea ice rates

Graphs of CO_2 rates from all NOAA recording sites in NOAA ESRL Carbon Cycle Cooperative Global Air Sampling Network (Dlugokencky et al 2019) where there are flask sample monthly data since January 2003, plotted against selected sea ice rates.

Dlugokencky, E.J., J.W. Mund, A.M. Crotwell, M.J. Crotwell, and K.W. Thoning (2019), Atmospheric Carbon Dioxide Dry Air Mole Fractions from the NOAA ESRL Carbon Cycle Cooperative Global Air Sampling Network, 1968-2018, Version: 2019-07, https://doi.org/10.15138/wkgj-f215 Retrieved 11 May 2020.

Section A: Sites in descending latitudinal order (for Pacific Ocean transect sites see section C below)

Section B: High-altitude (>1000 m) sites, in descending altitudinal order.

Section C: Pacific Ocean transect sites, in descending latitudinal order.

Section D: Selected examples of high visual similarities between CO_2 and sea ice rates.

Section E: Barrow CO_2 rate *vs.* all 16 Northern Hemisphere sea ice regions (MASIE data, mapped at ftp://sidads.colorado.edu/DATASETS/NOAA/G02186/), in numerical order.

Abbreviations for observatory site names (as per the NOAA database) are given in brackets in the graph caption.

Sea ice data sources as per main text: MASIE for 'Greenland Sea' and 'Arctic' (*ie* Northern Hemisphere) sea ice extent; NSIDC for 'Antarctic' and 'Arctic plus Antarctic' sea ice extent; DMI for Arctic sea ice volume.

A sea ice region (Greenland Sea, Northern Hemisphere, Antarctic, or Arctic plus Antarctic) is selected which gives a relatively strong visual fit to the CO_2 rate, or the Greenland Sea is used as a default. Some graphs show a CO_2 rate with a lag (in months) giving a relatively strong visual fit to the selected ice rate, as indicated in the caption.

Monthly rates calculated as per main text.

We thank the institutions and individuals above and acknowledged in the main text.

NOTE: Given the challenges and risk of errors in plotting numerous graphs under pandemic lockdown conditions, any individual graph in this Appendix should be treated as a draft - requiring confirmation before making firm conclusions about that site. However, the evidently recurrent relationship of sea ice rates to CO_2 rates is robust.

Section A: Global Monitoring Laboratory sites for which there are CO_2 data since January 2003 *vs.* selected sea ice region. (Most Pacific Ocean transect sites are in Section C)

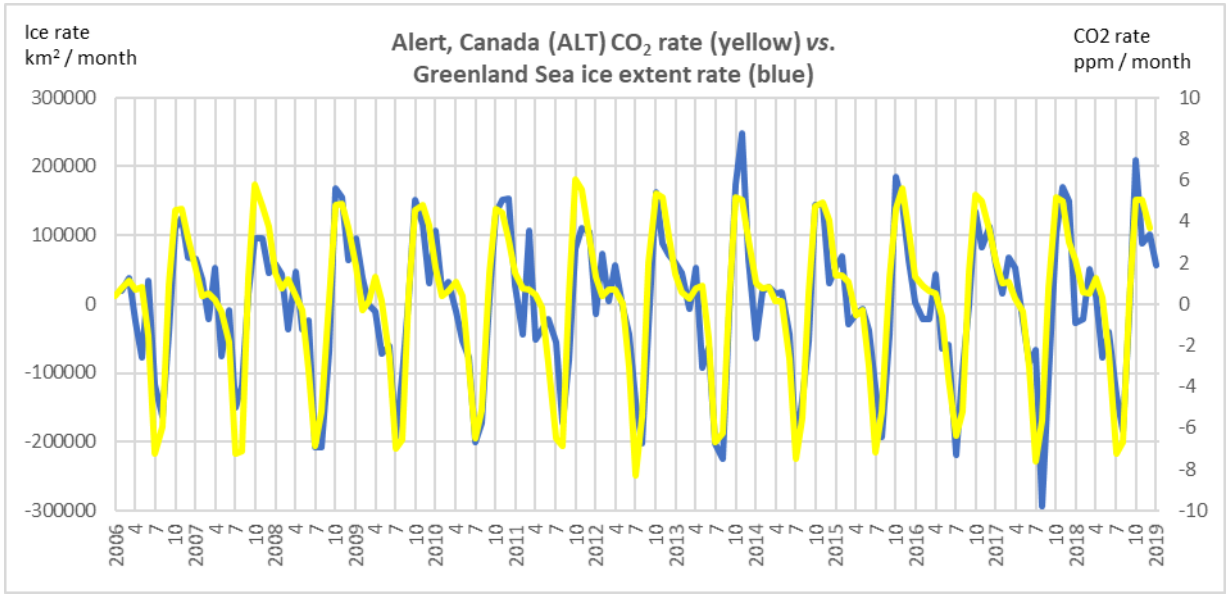

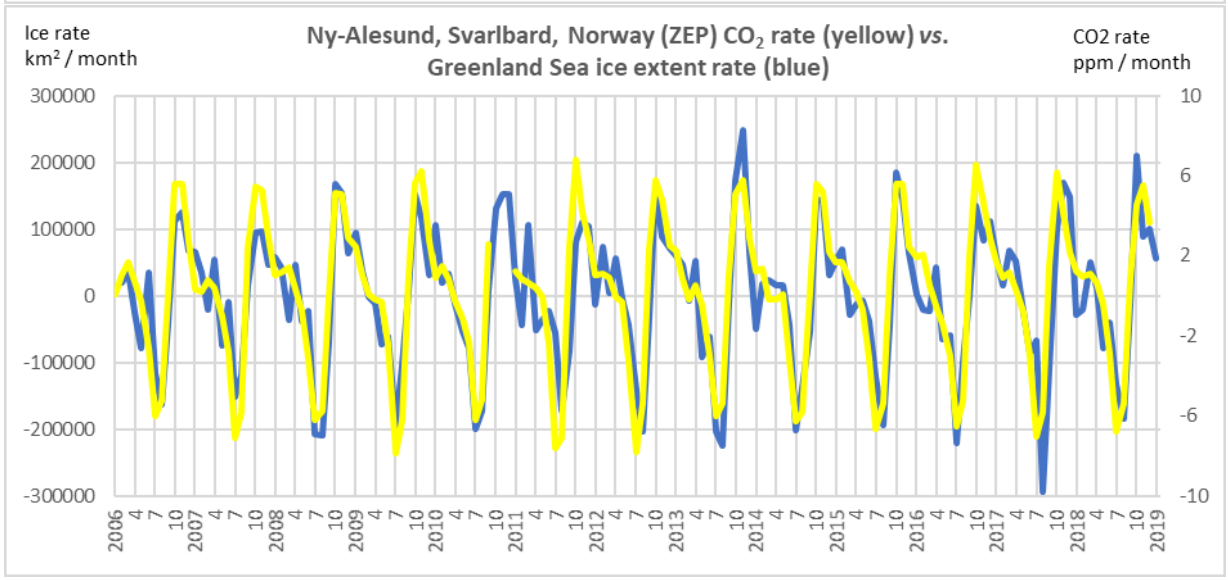

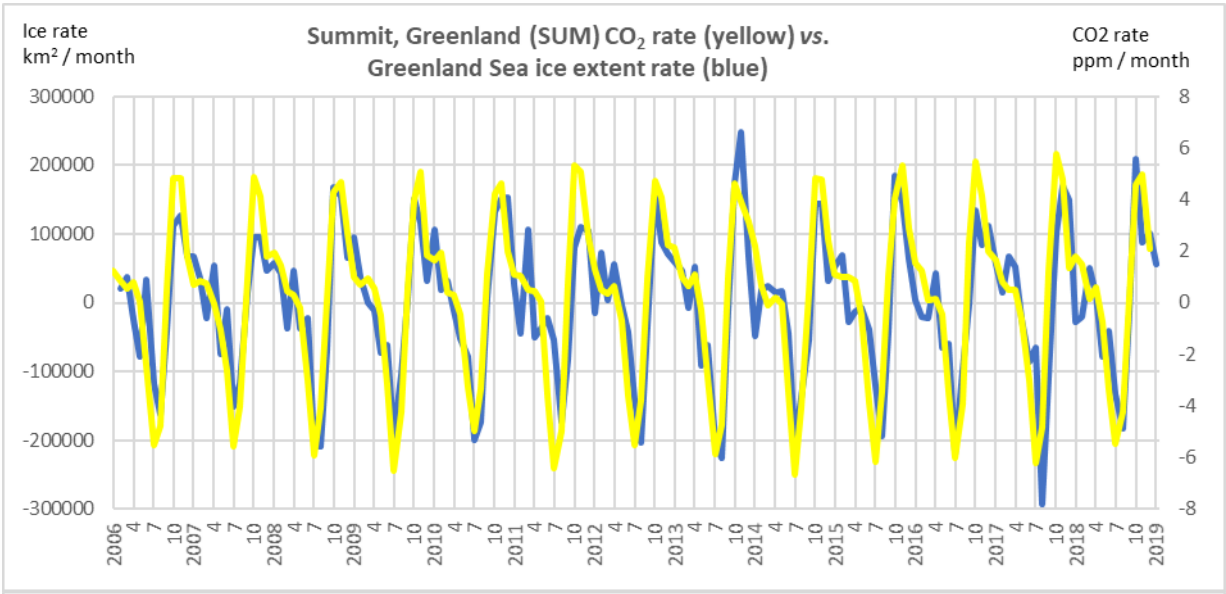

1064

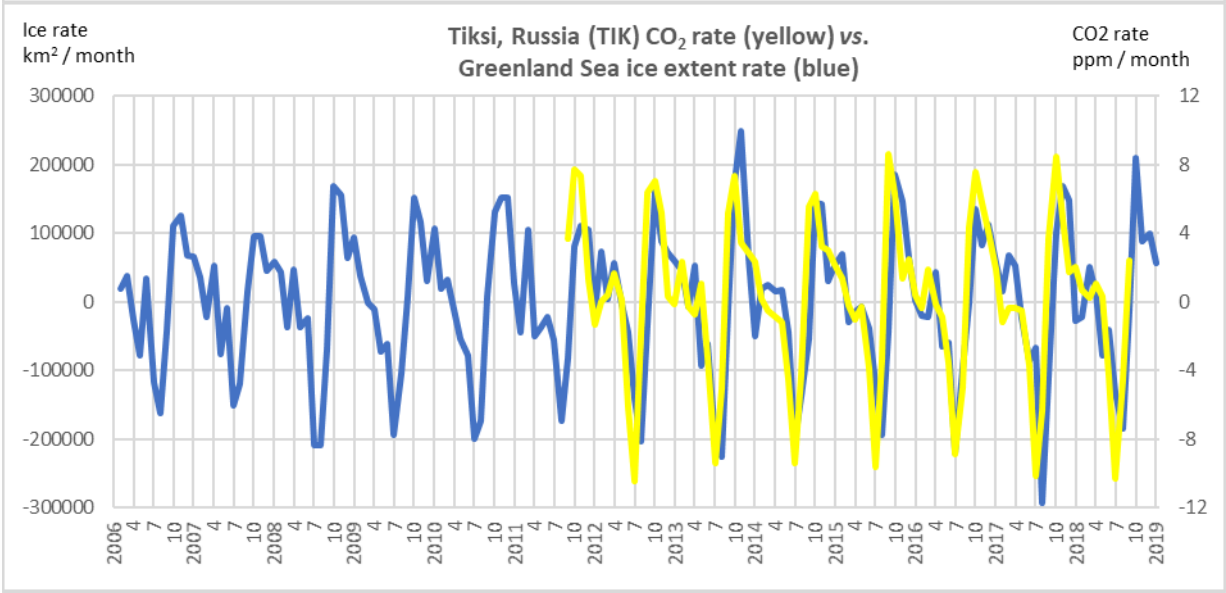

1065

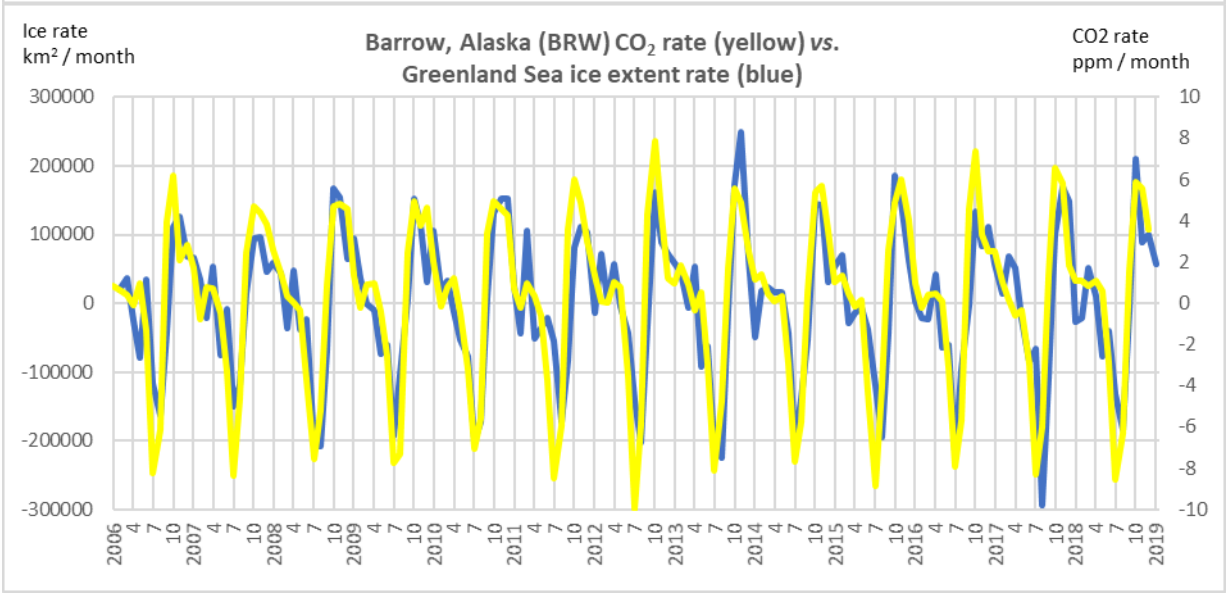

1066

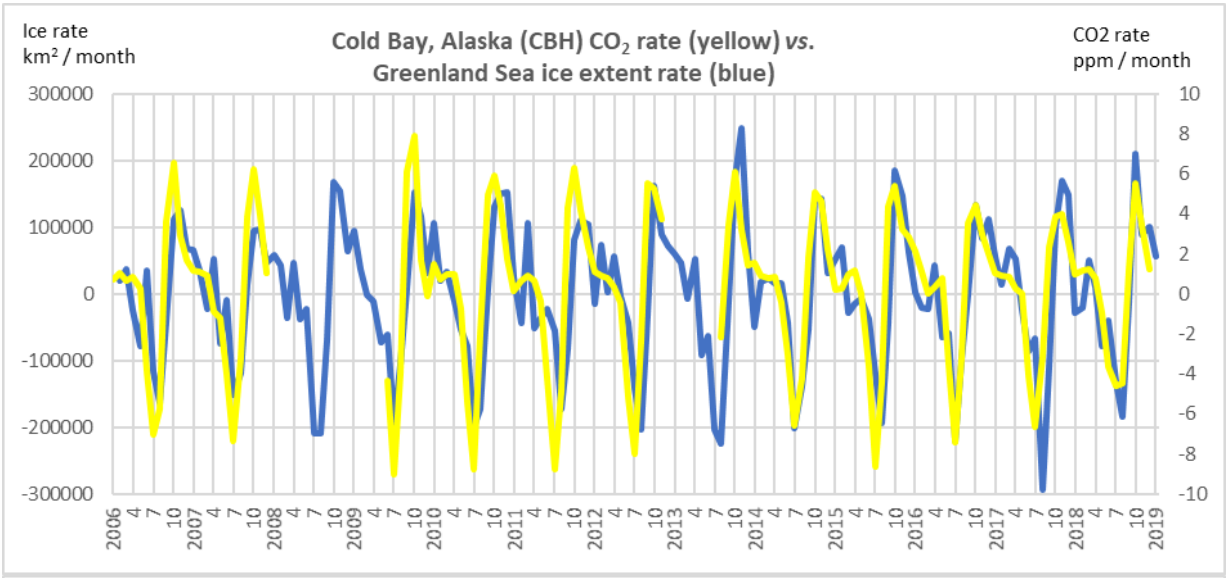

1067

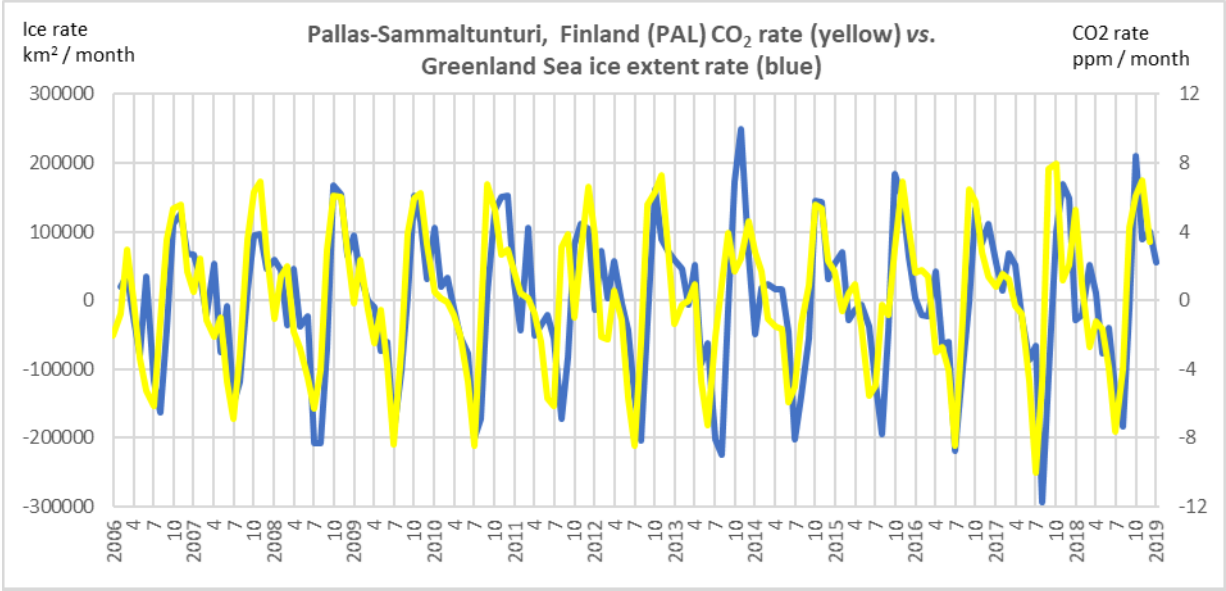

1068

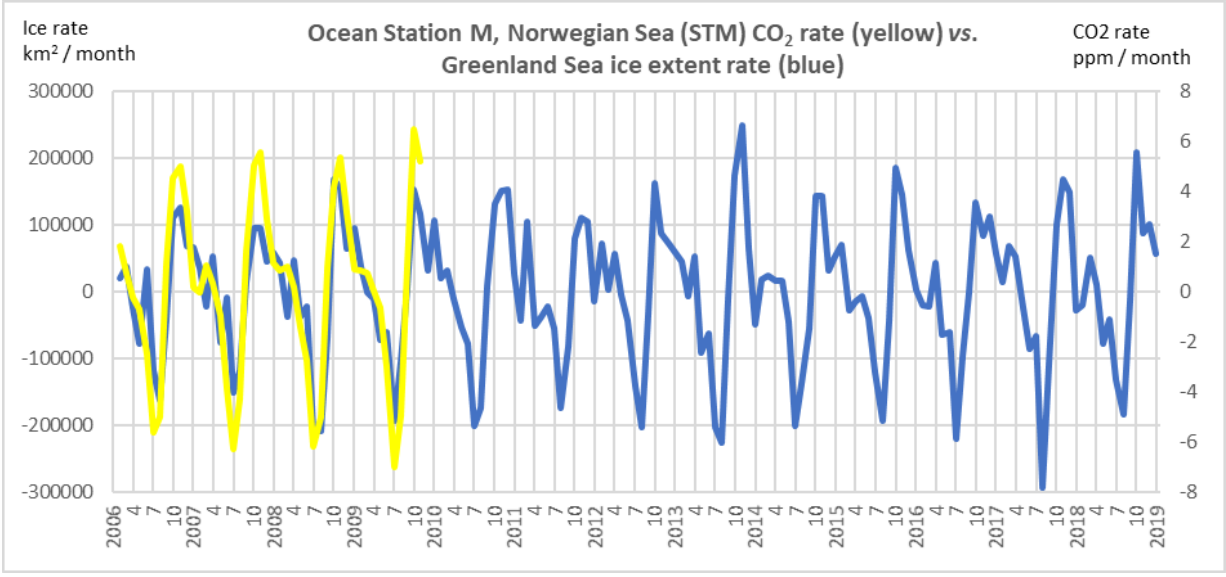

1069

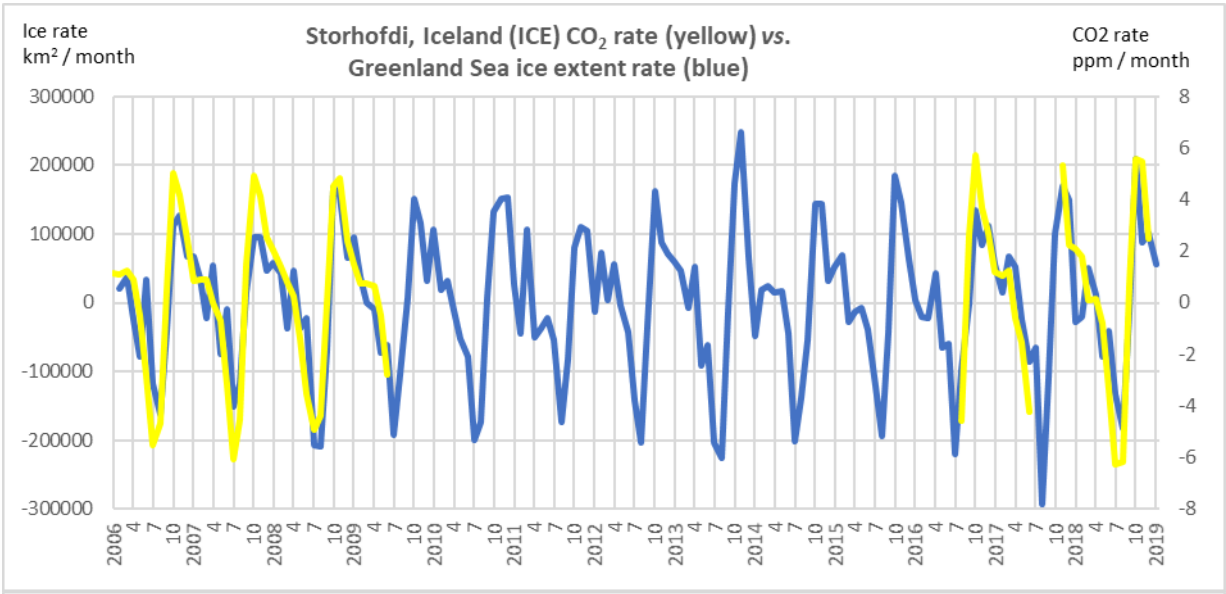

1070

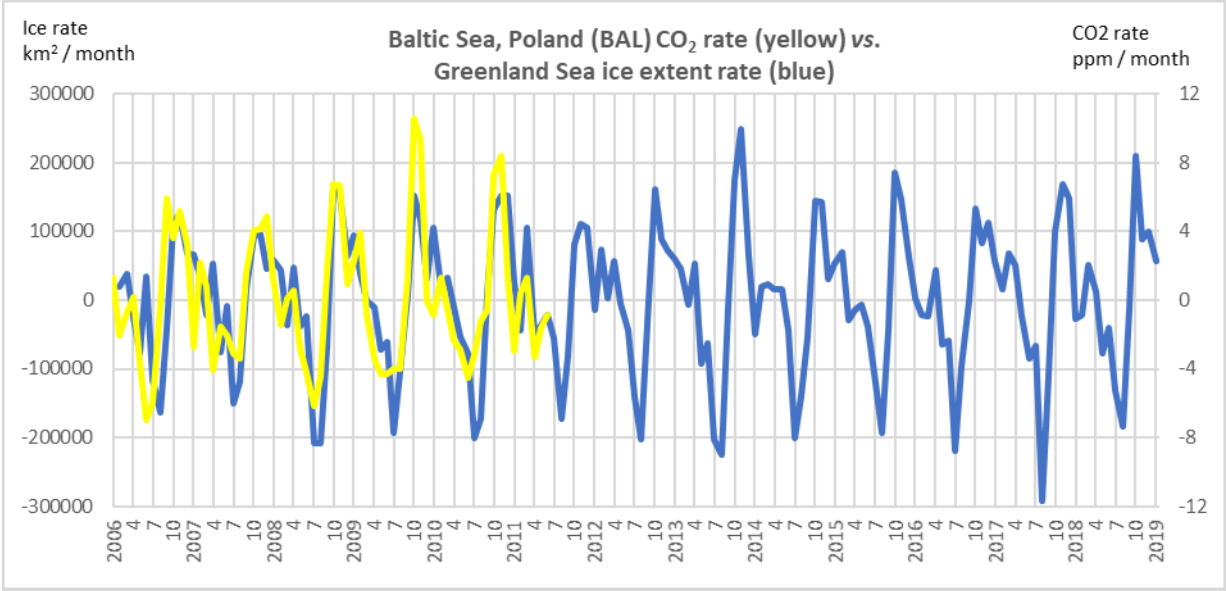

1071

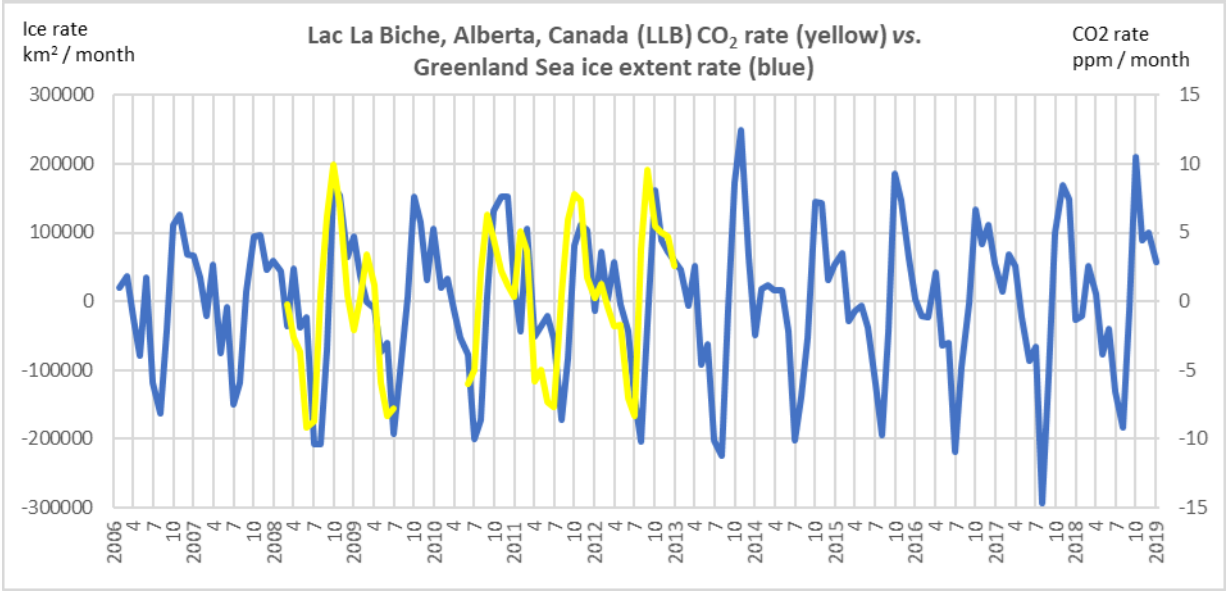

1072

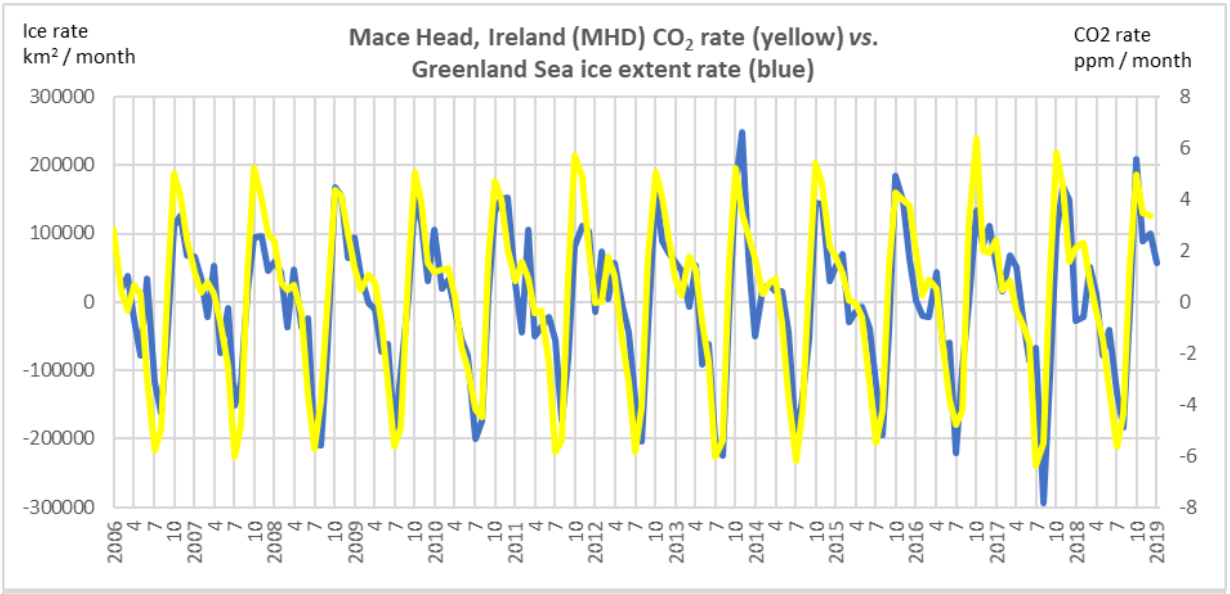

1073

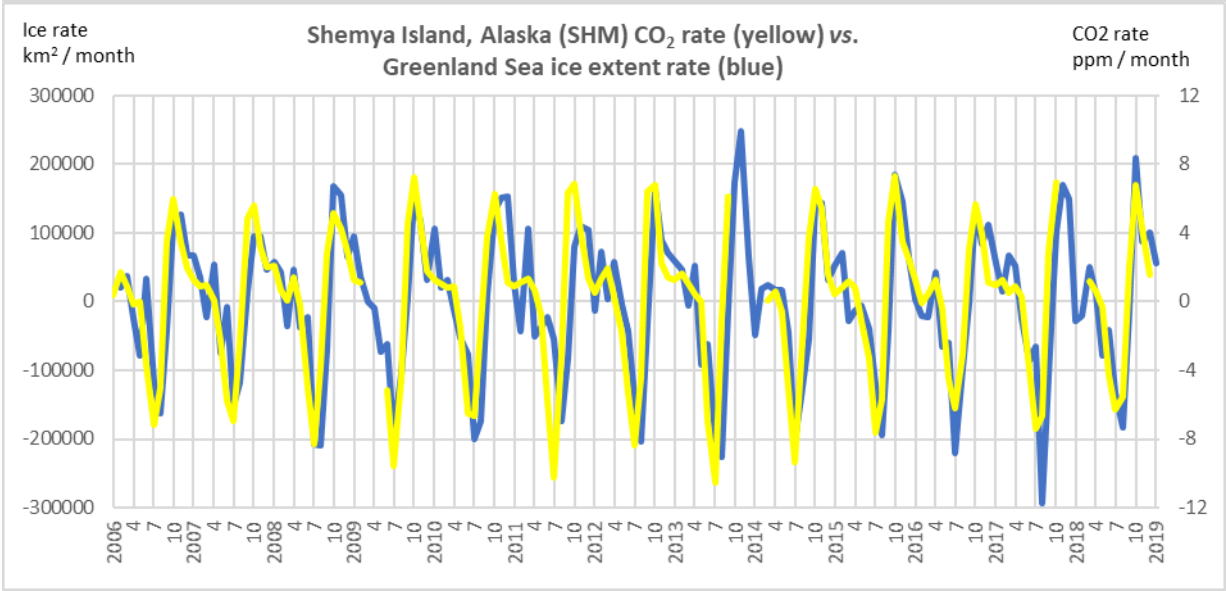

1074

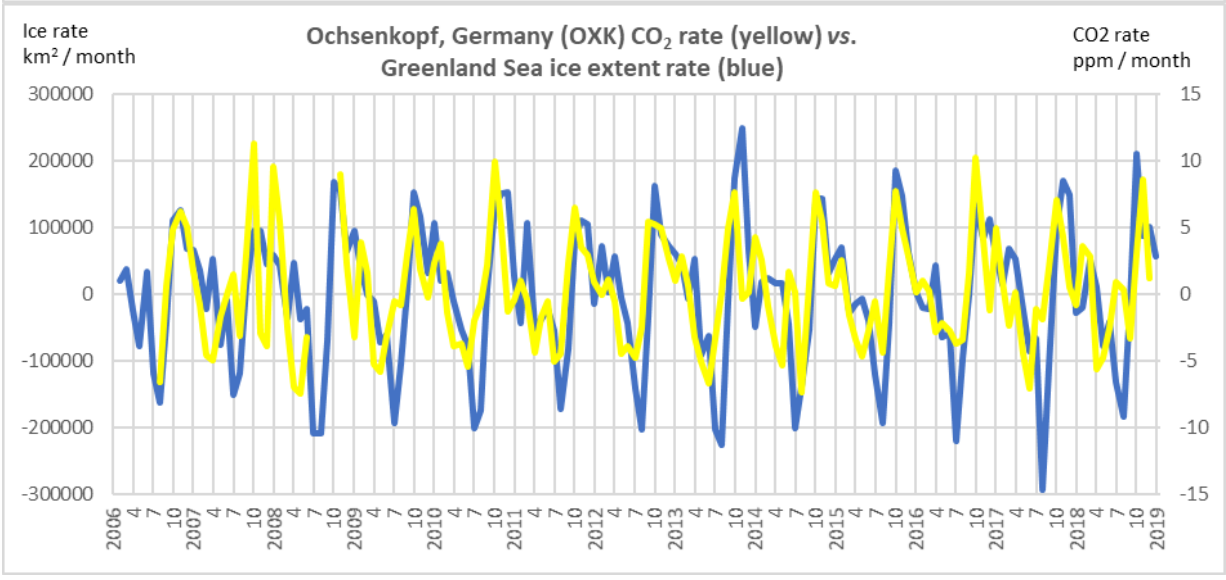

1075

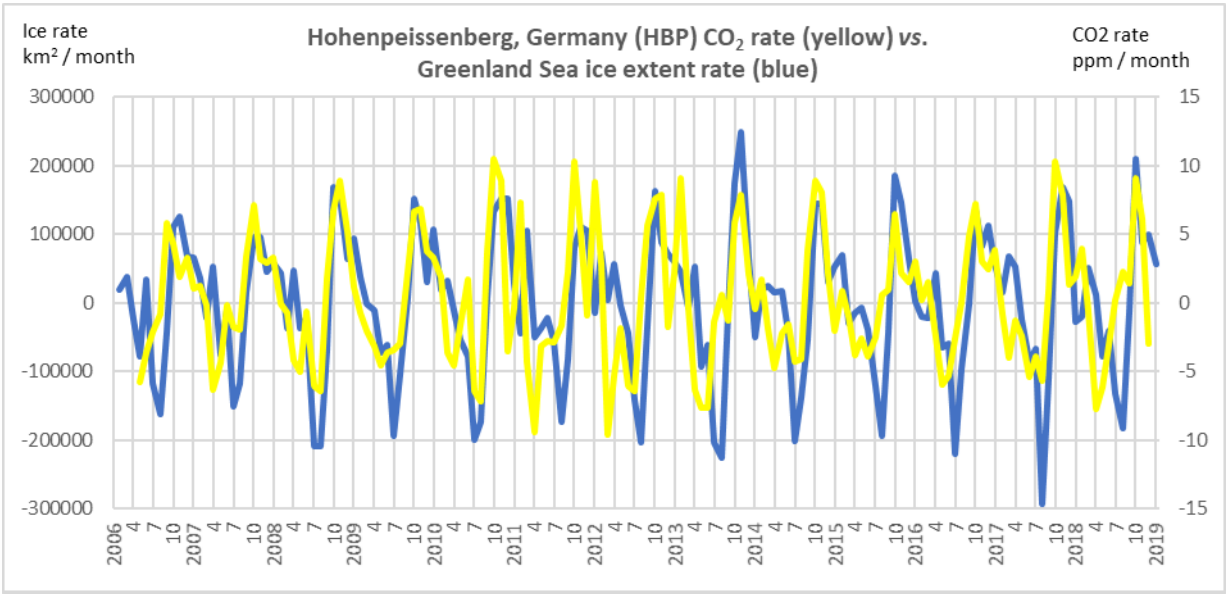

1076

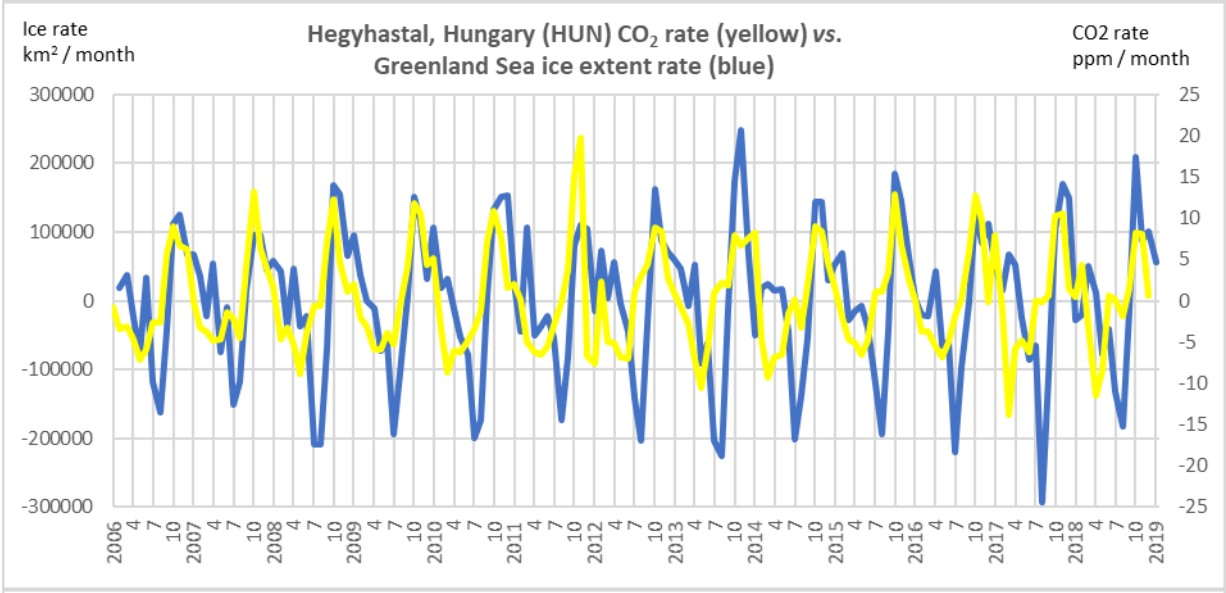

1077

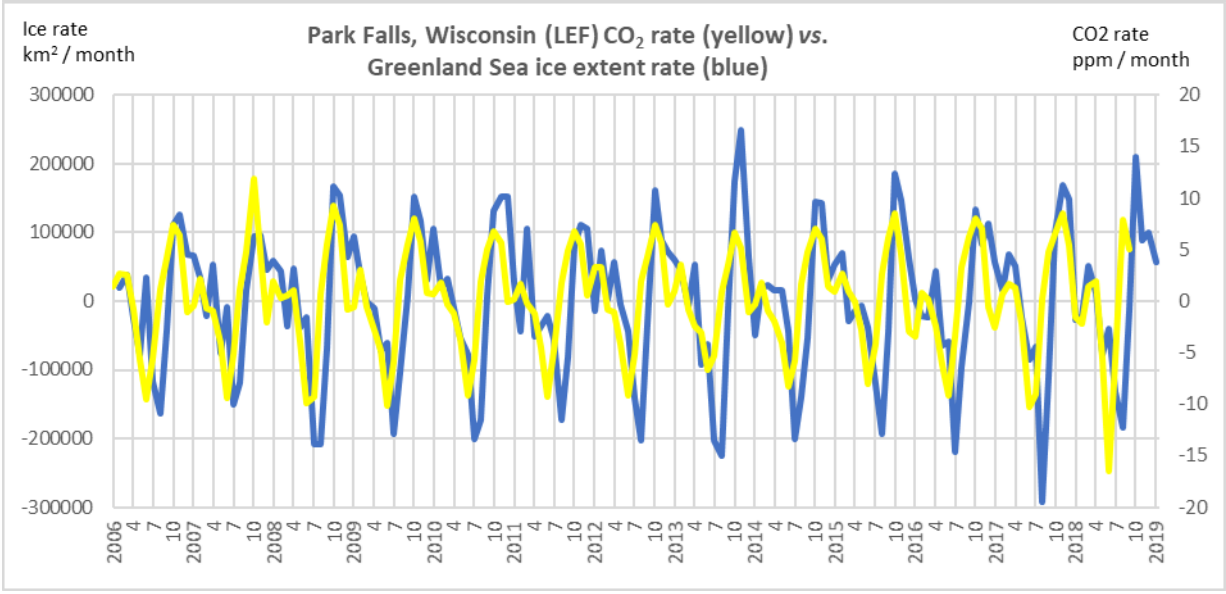

1078

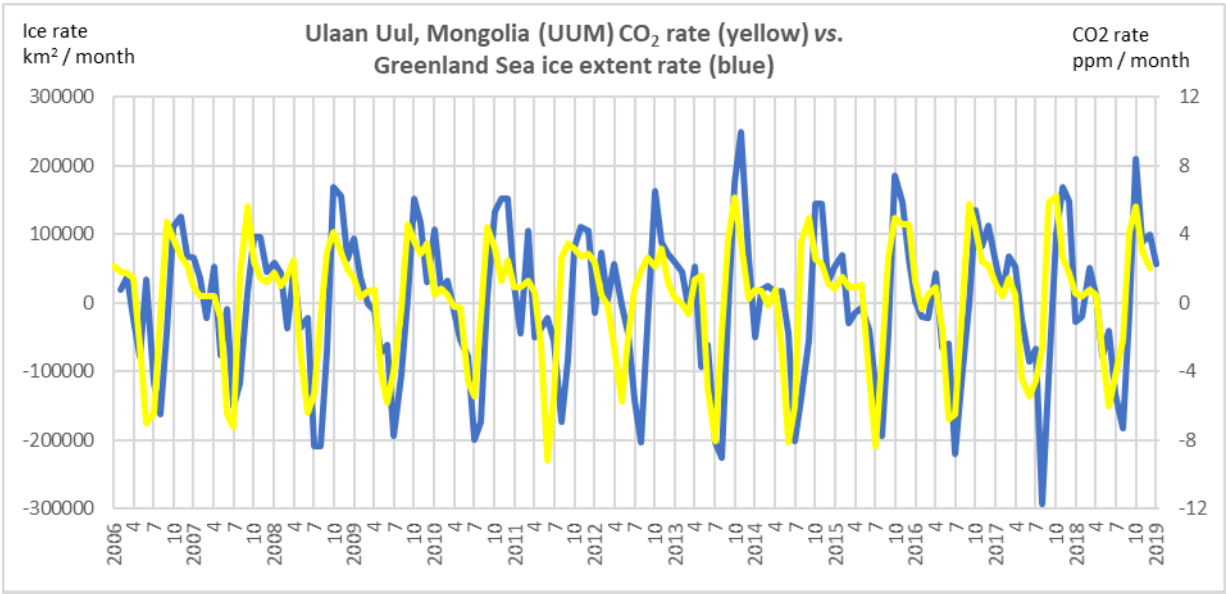

1079

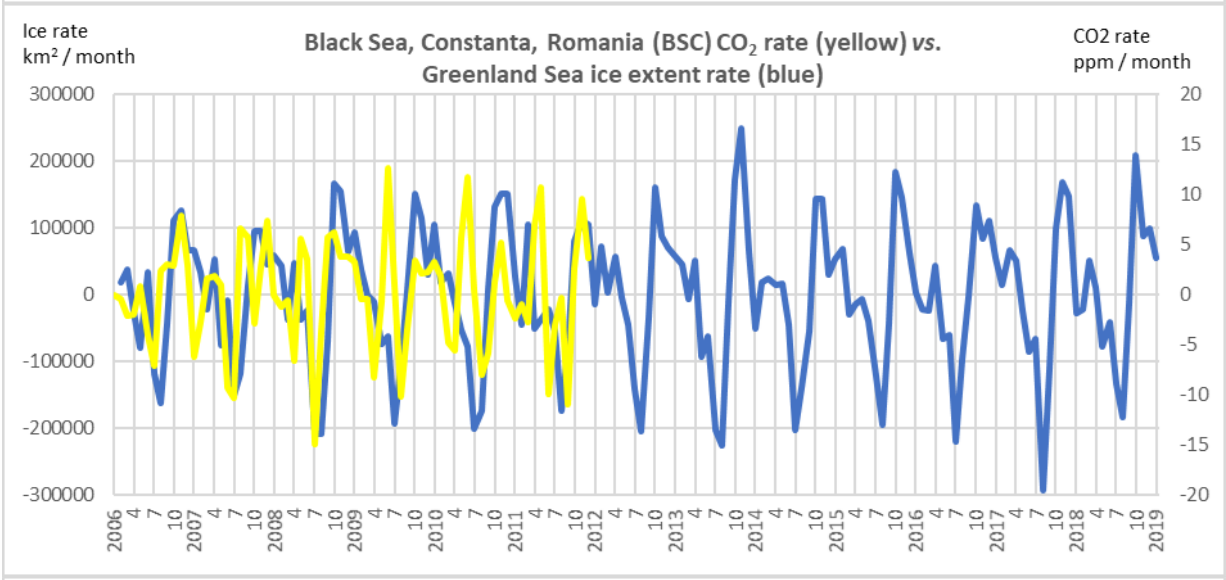

1080

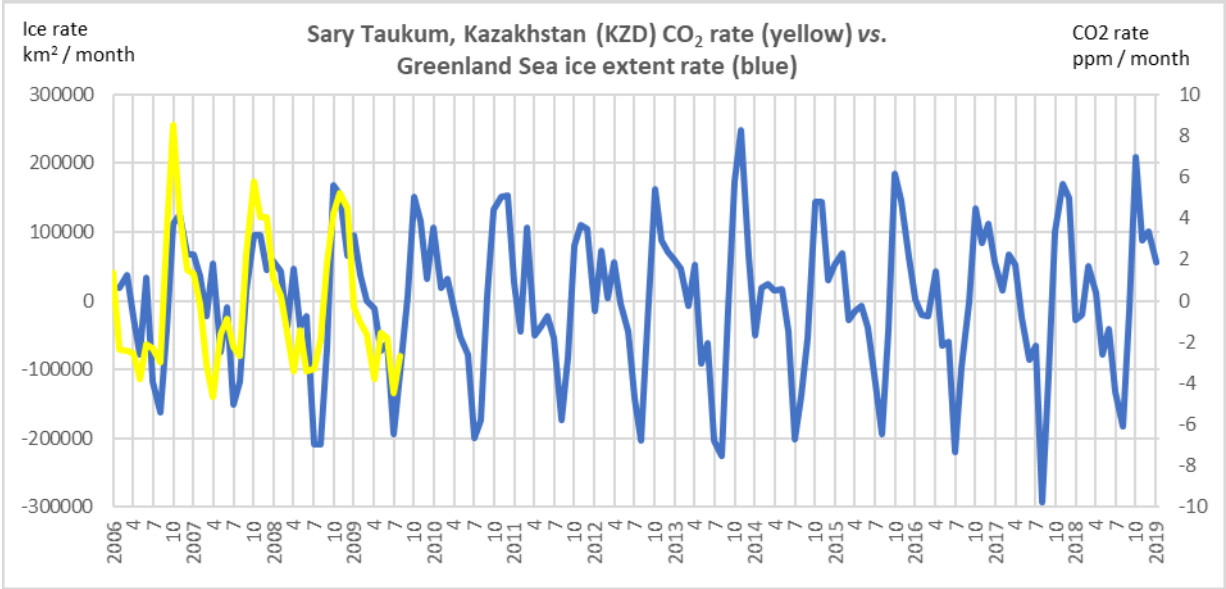

1081

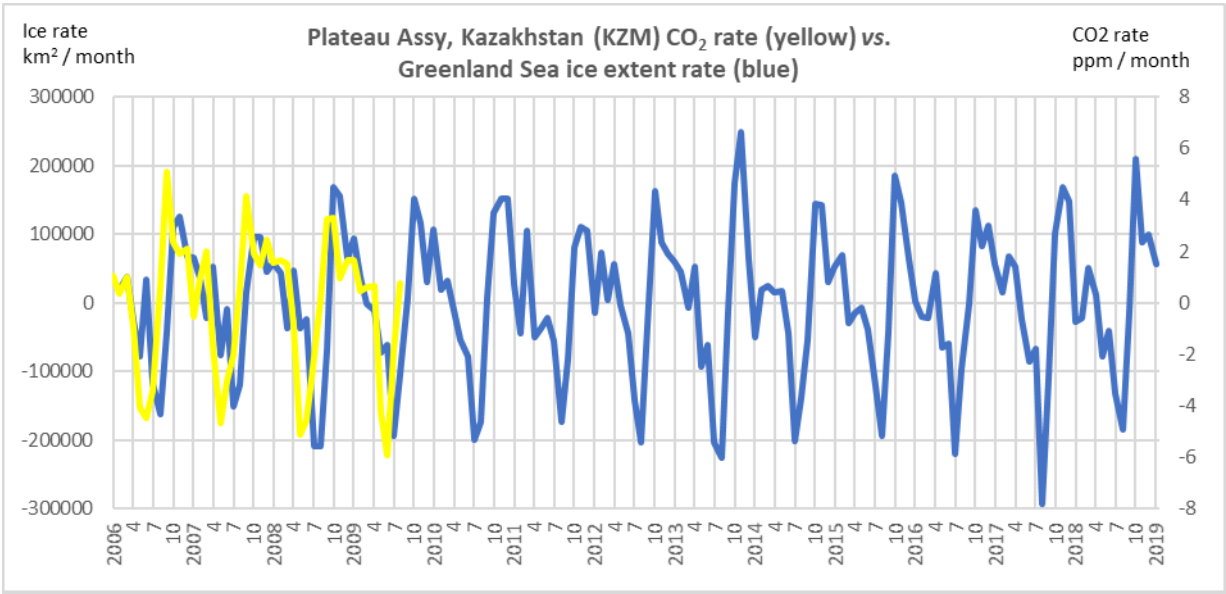

1082

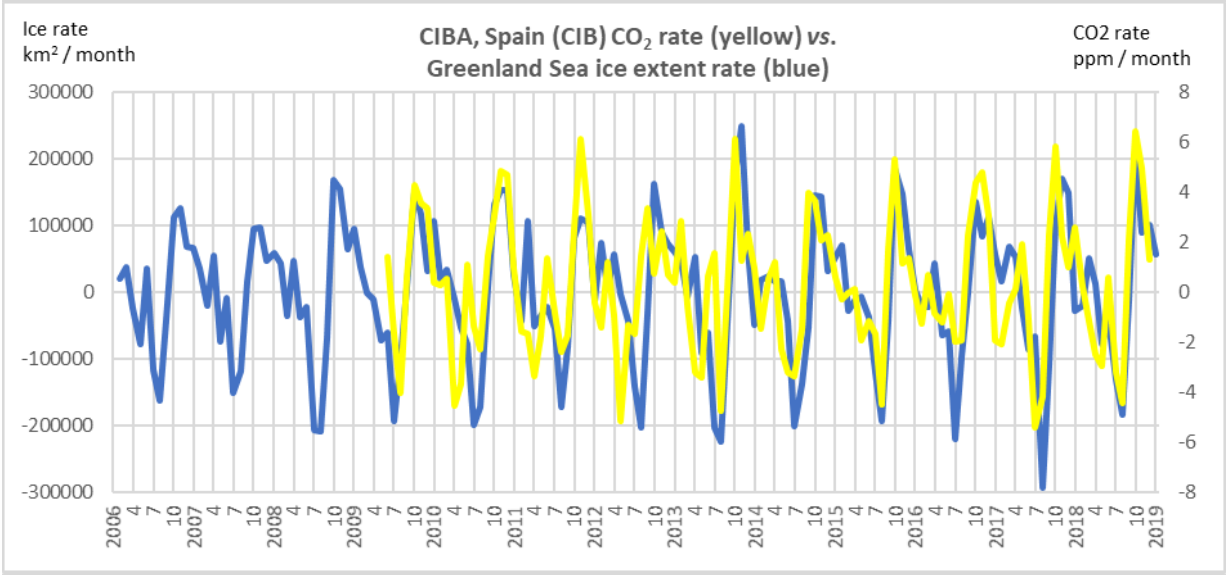

1083

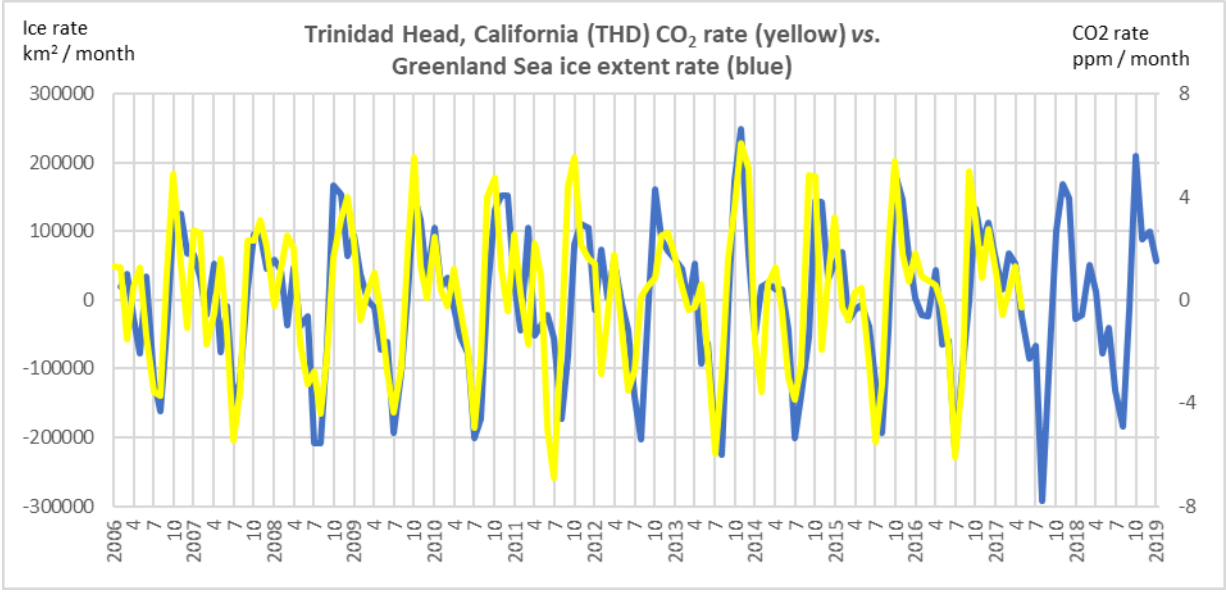

1084

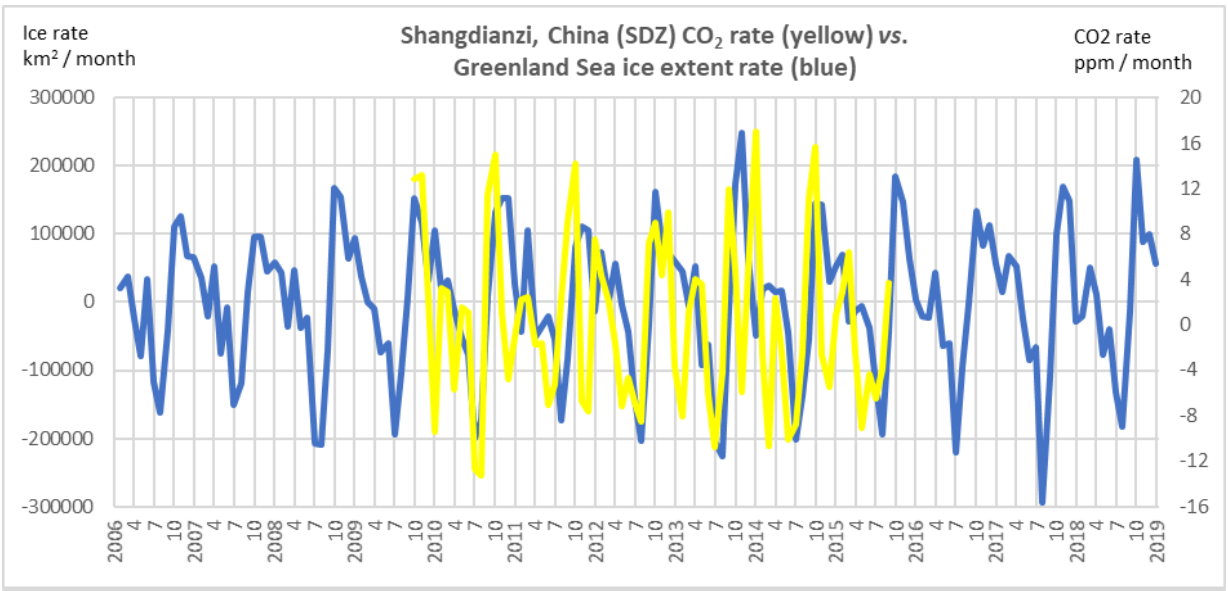

1085

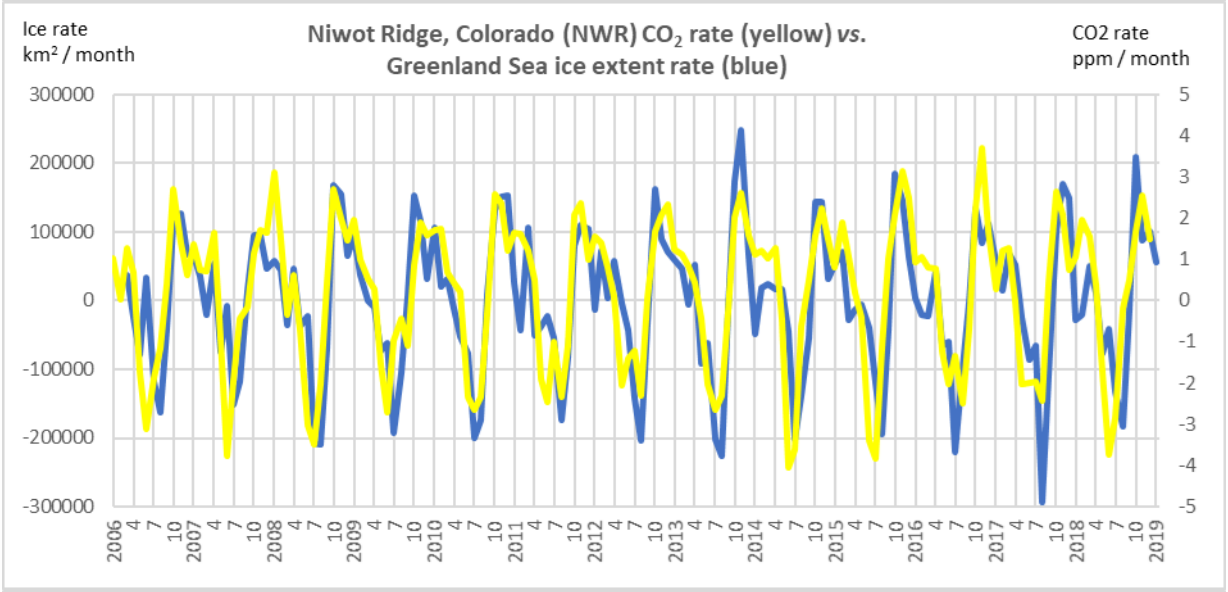

1086

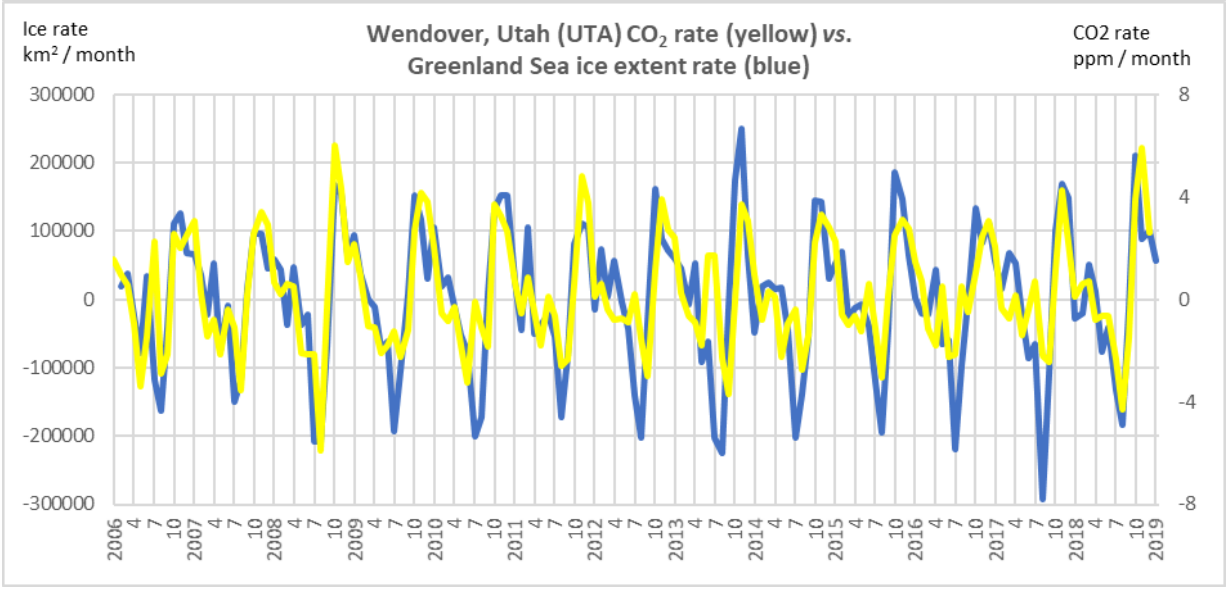

1087

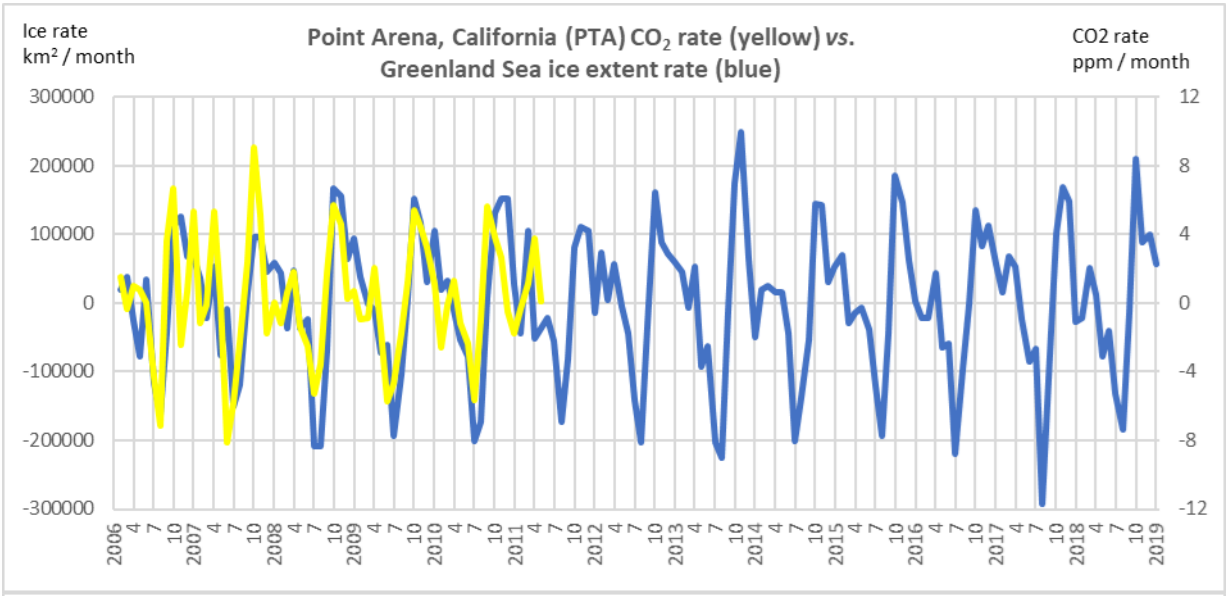

1088

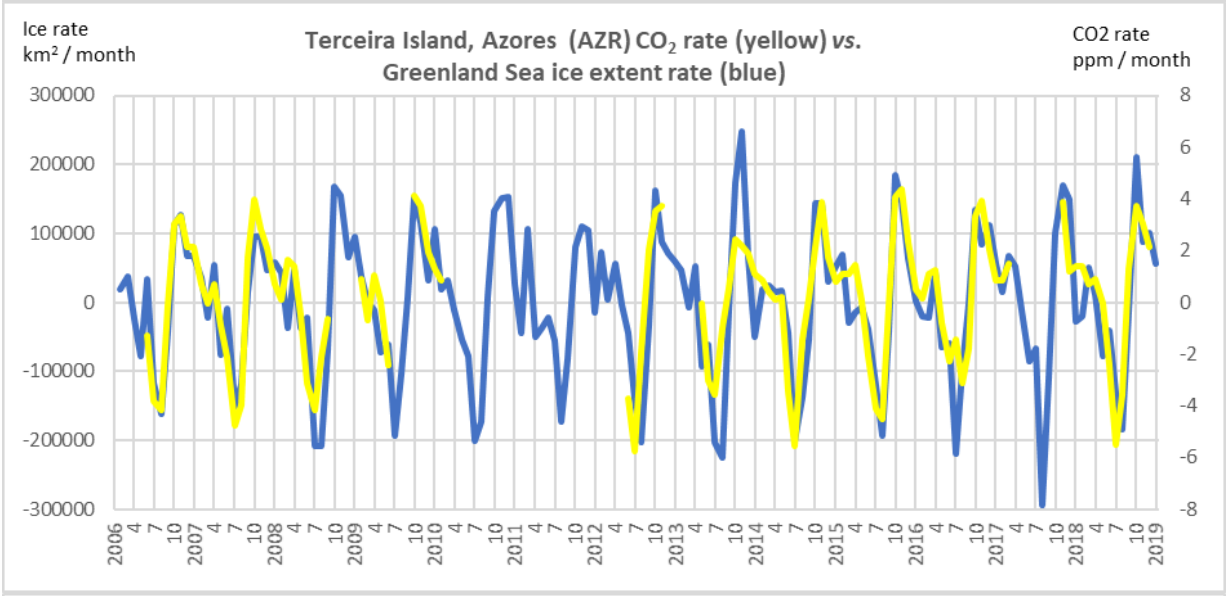

1089

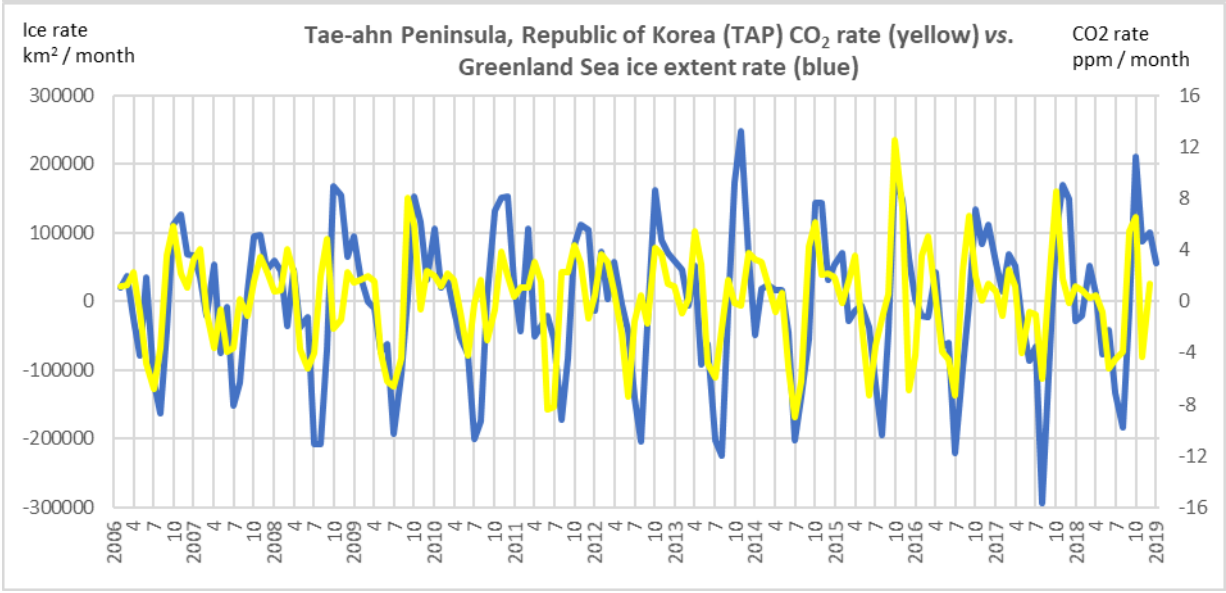

1090

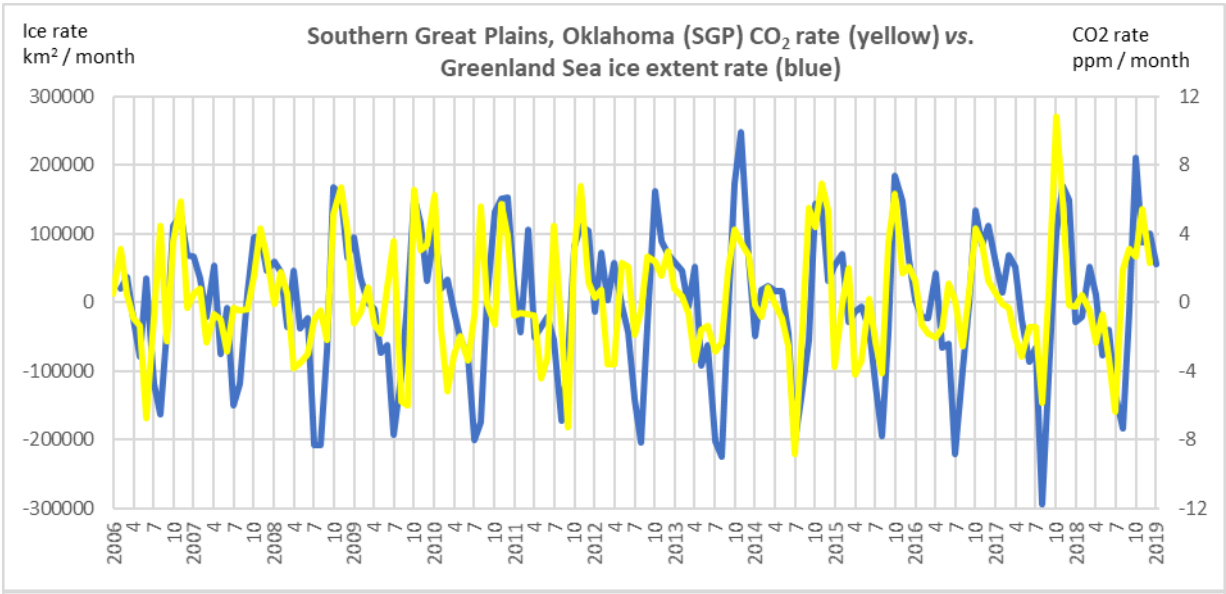

1091

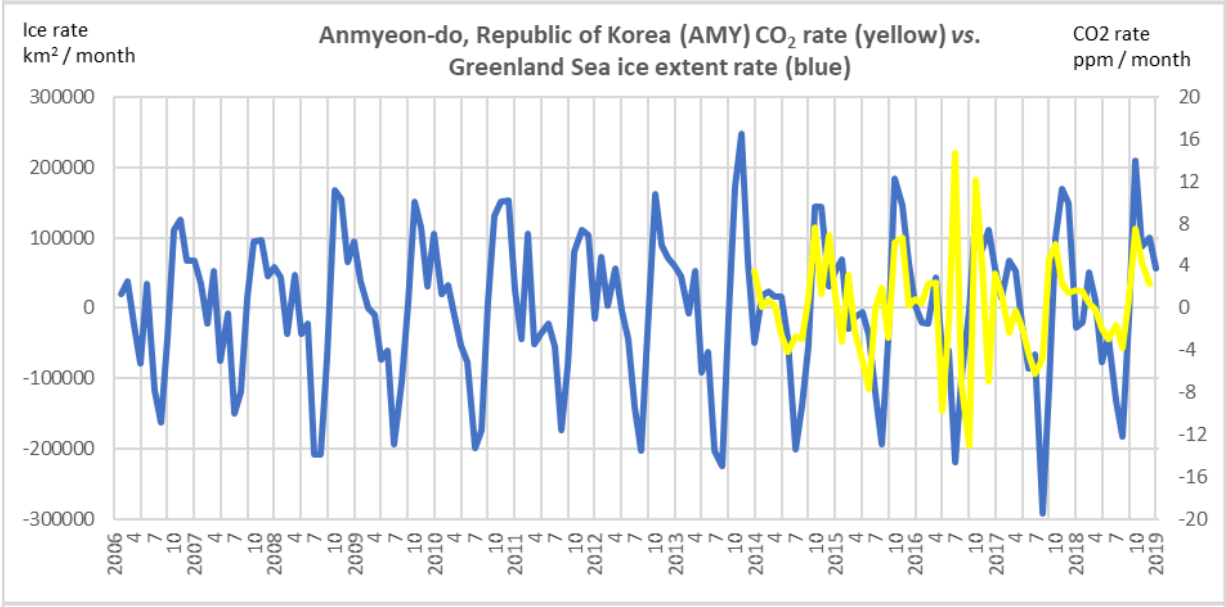

1092

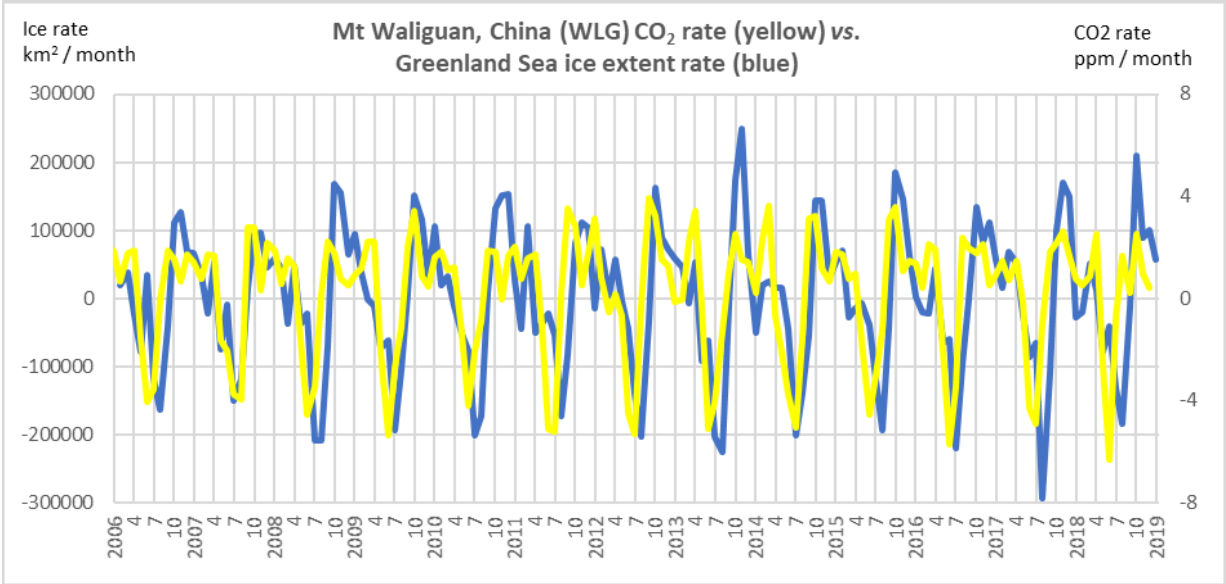

1093

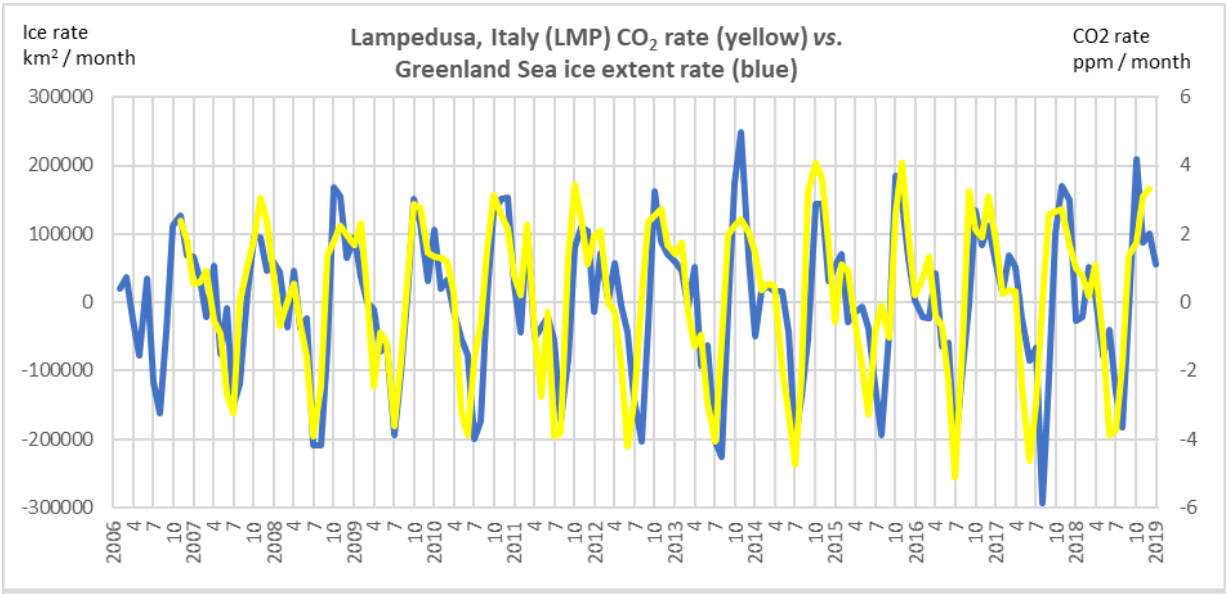

1094

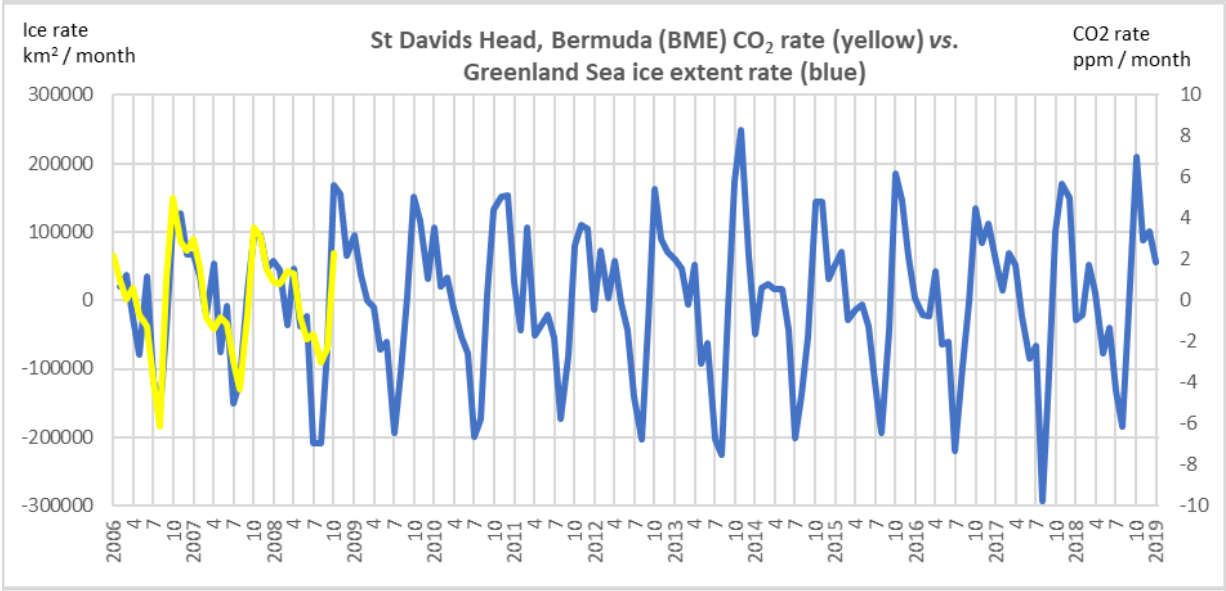

1095

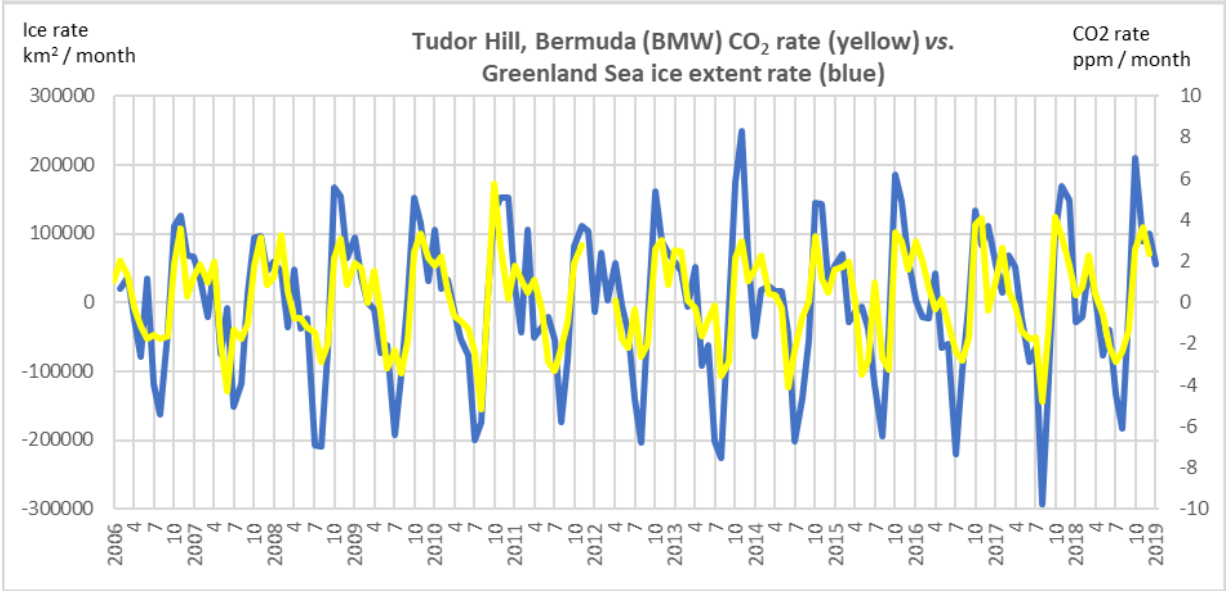

1096

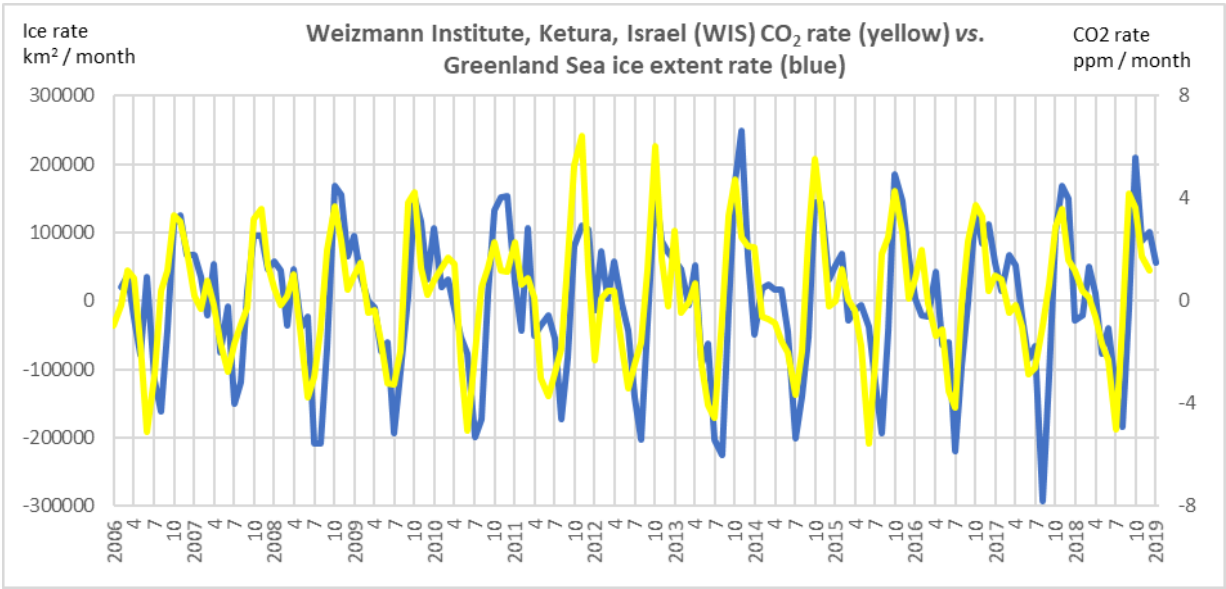

1097

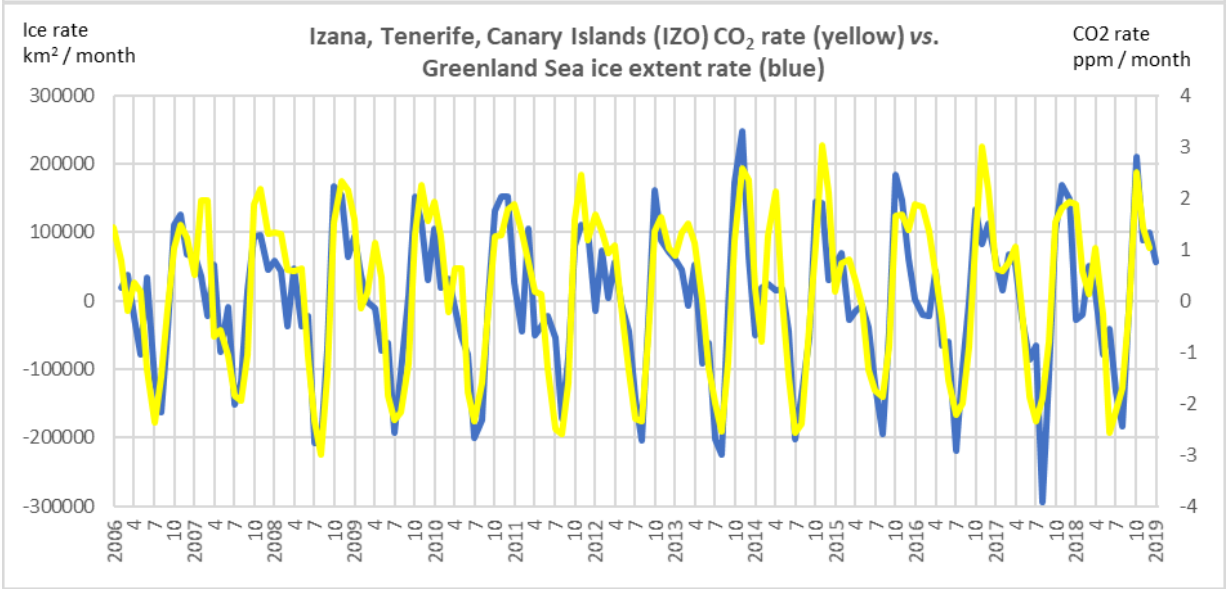

1098

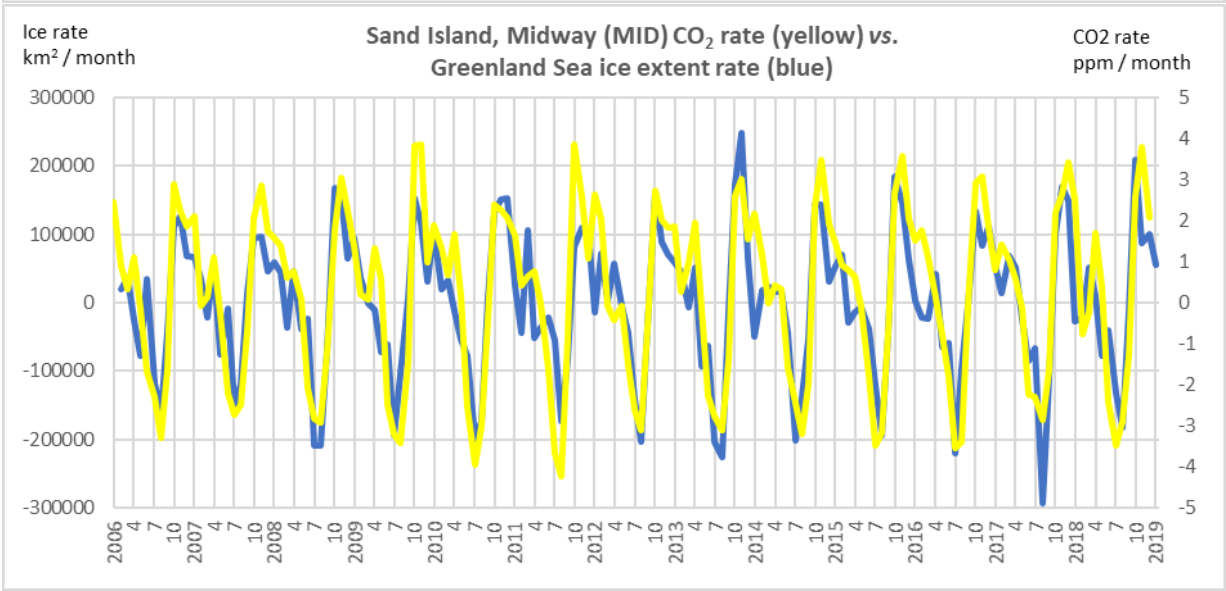

1099

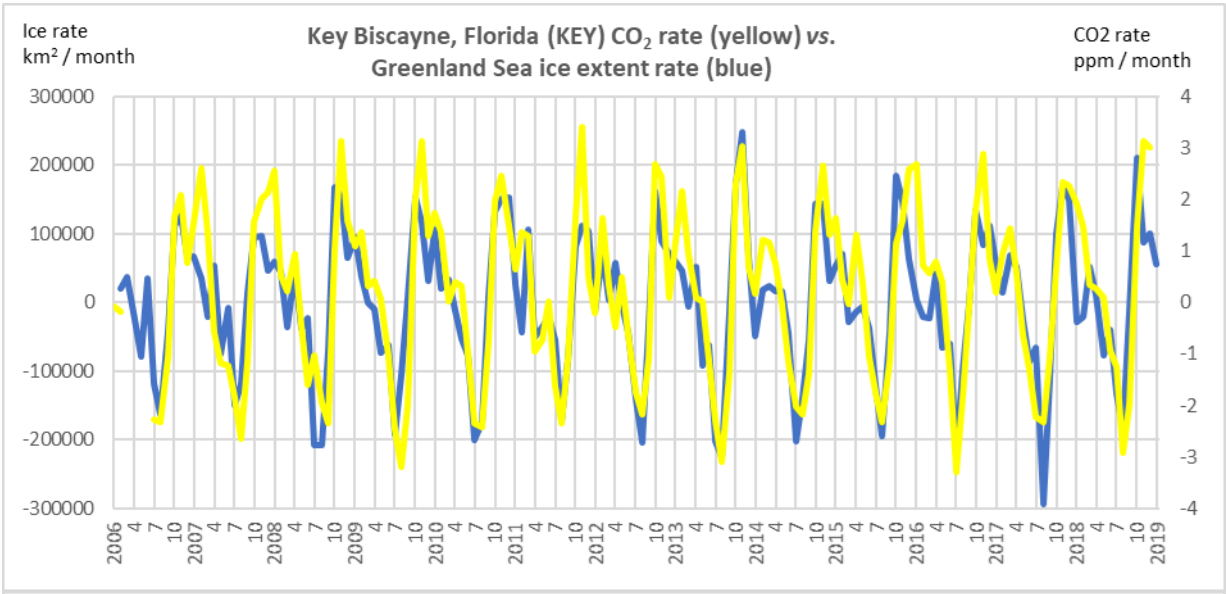

1100

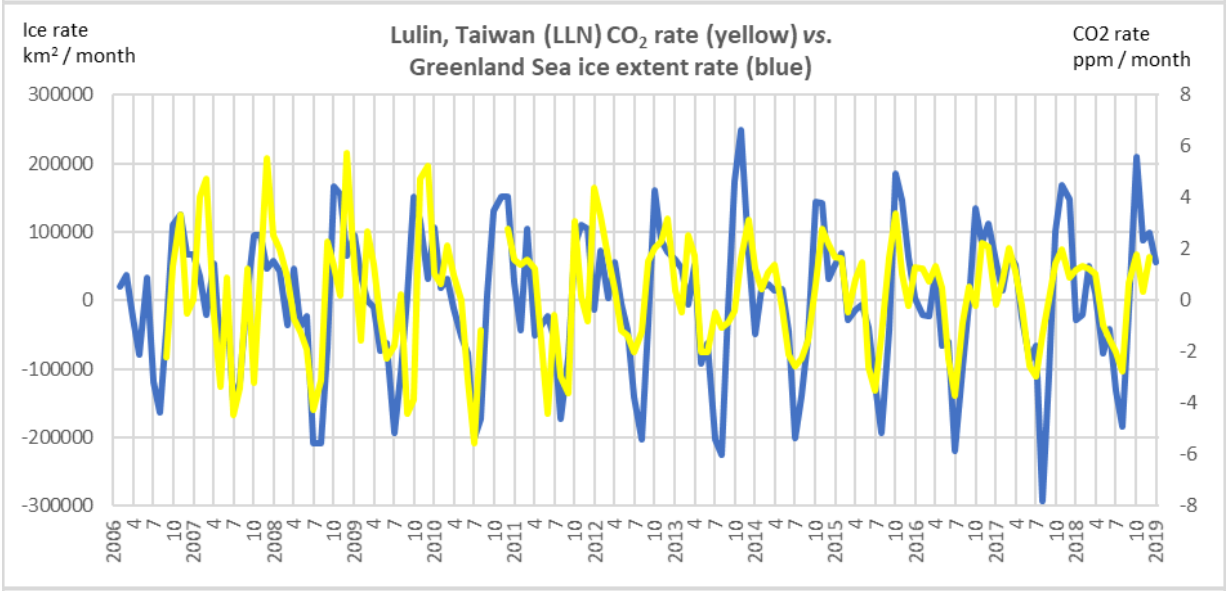

1101

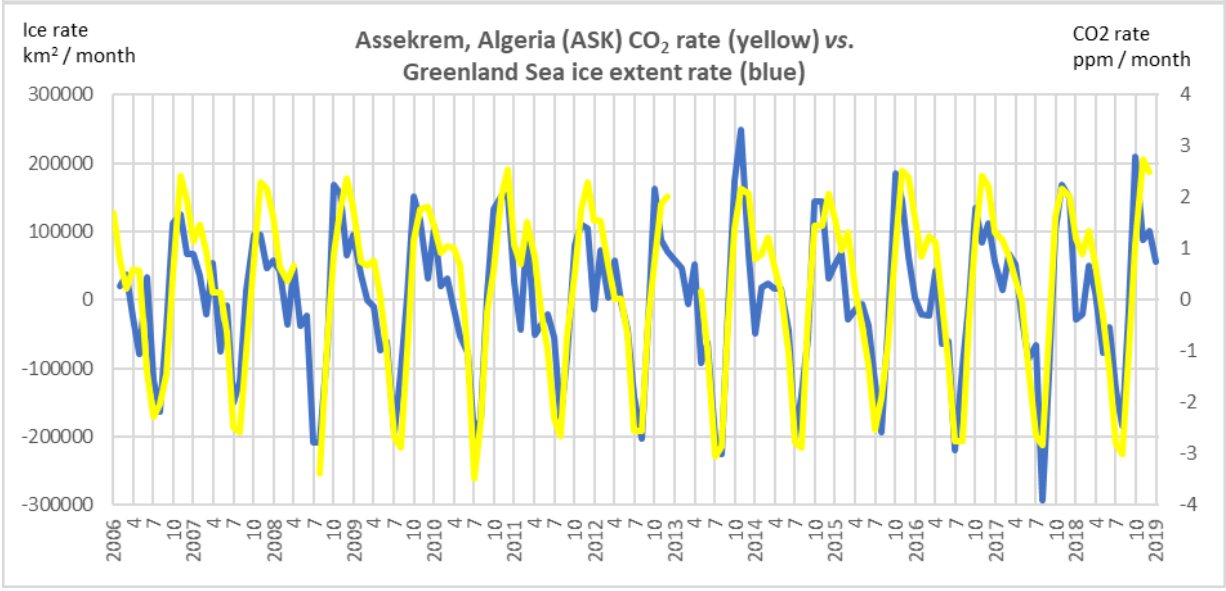

1102

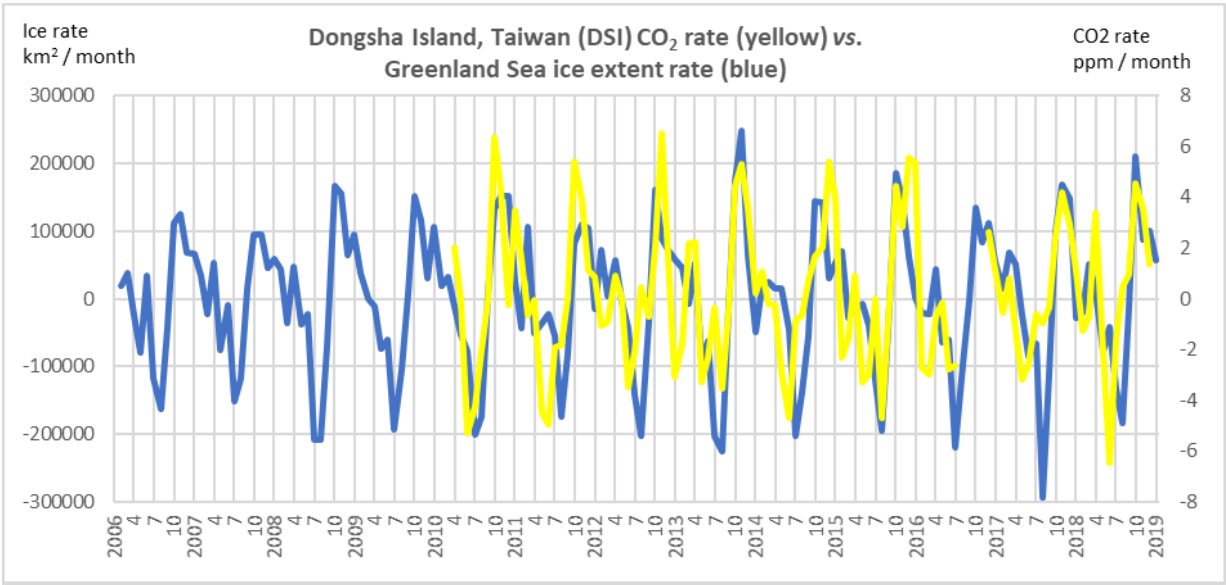

1103

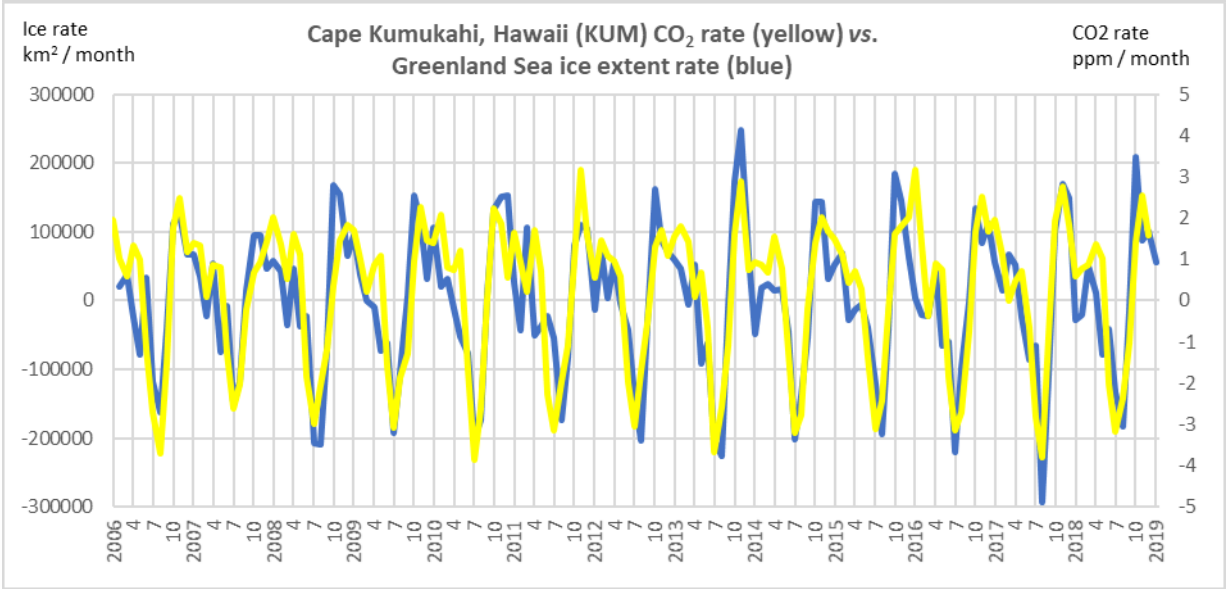

1104

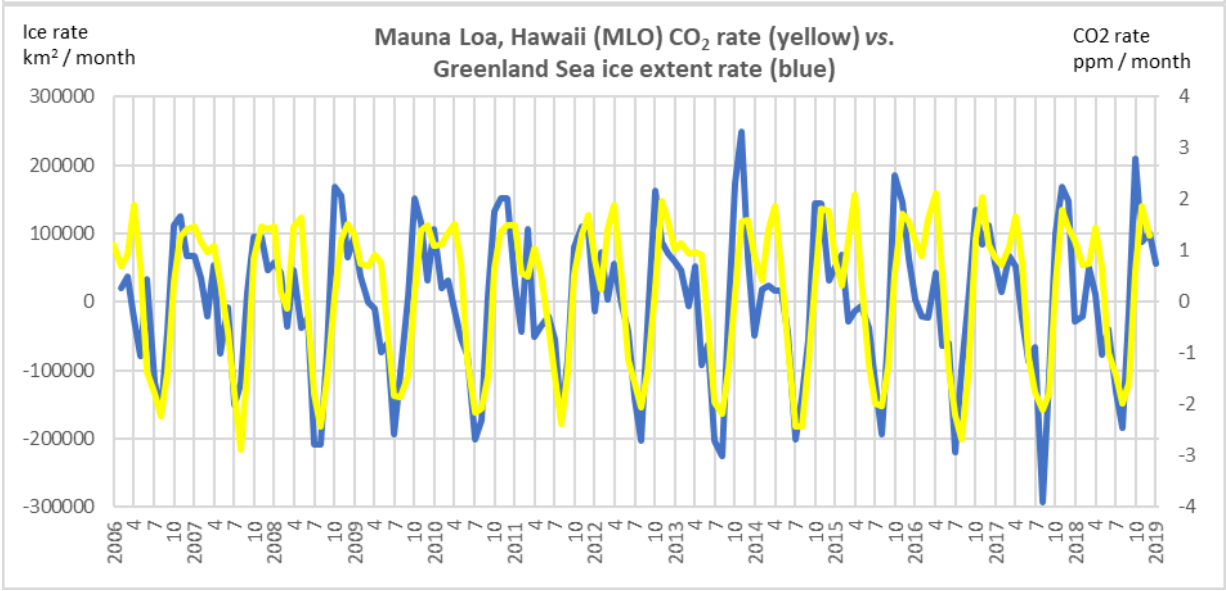

1105

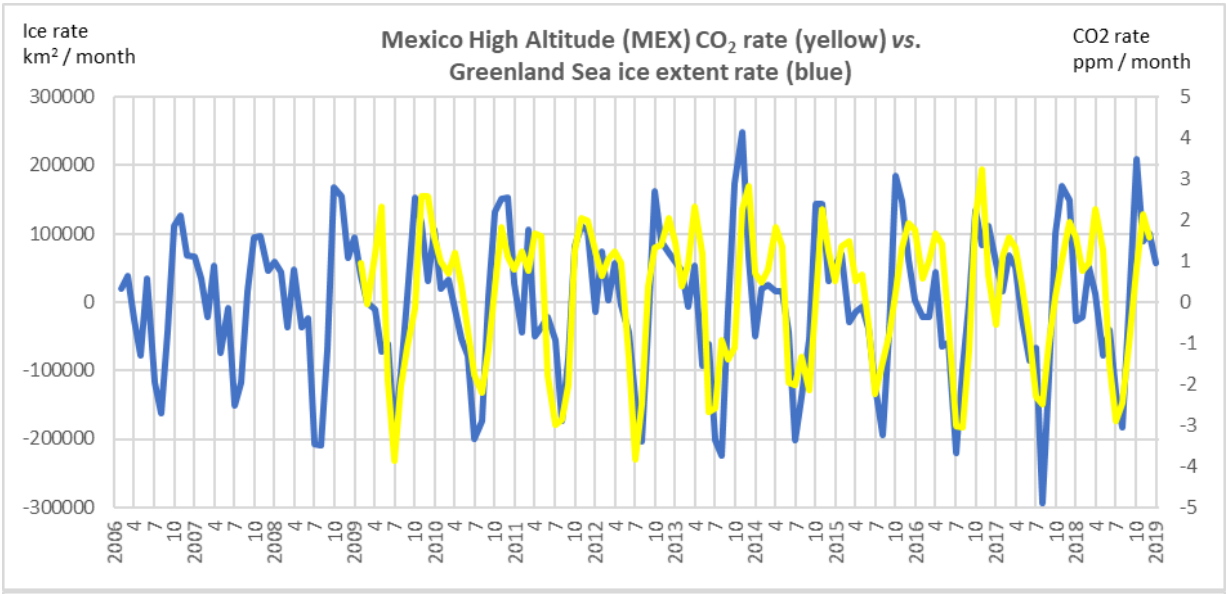

1106

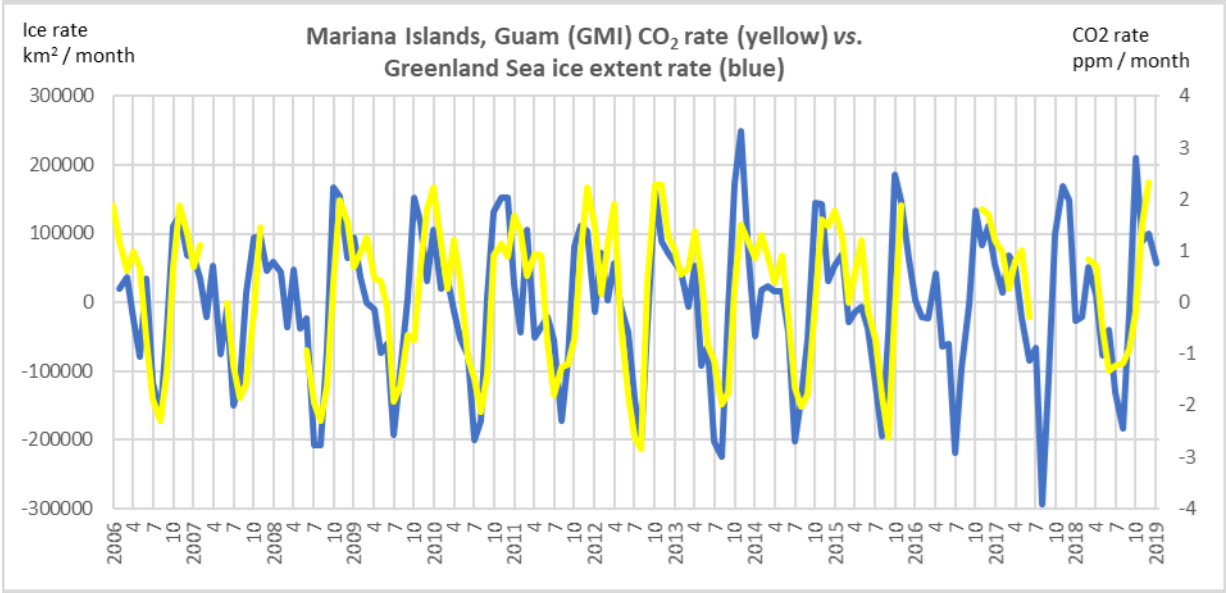

1107

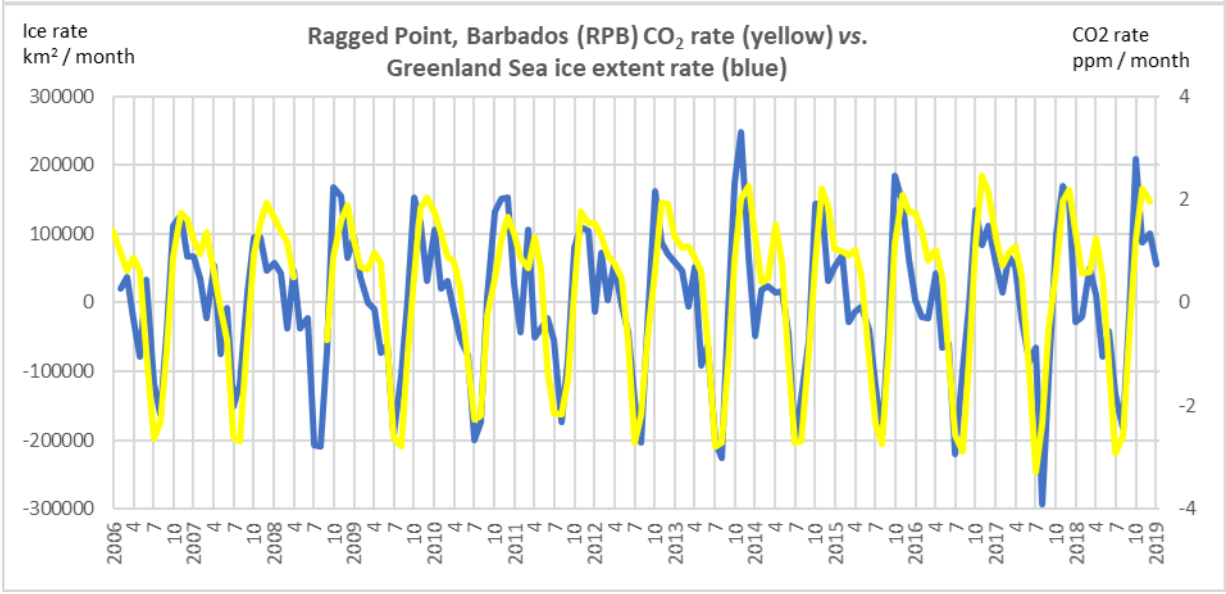

1108

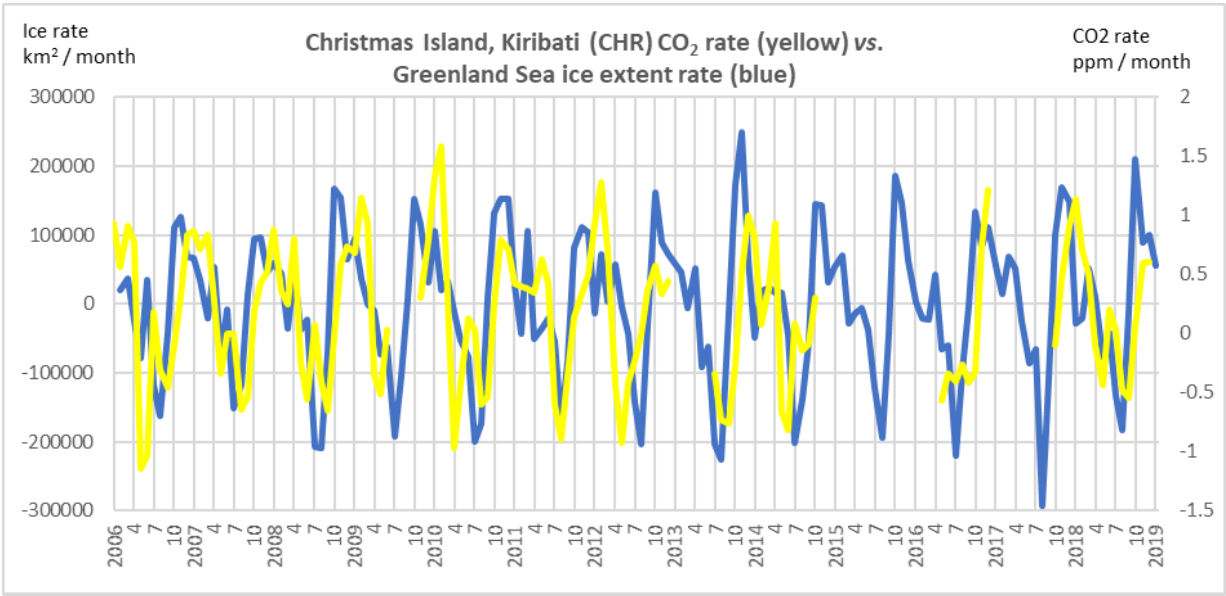

1109

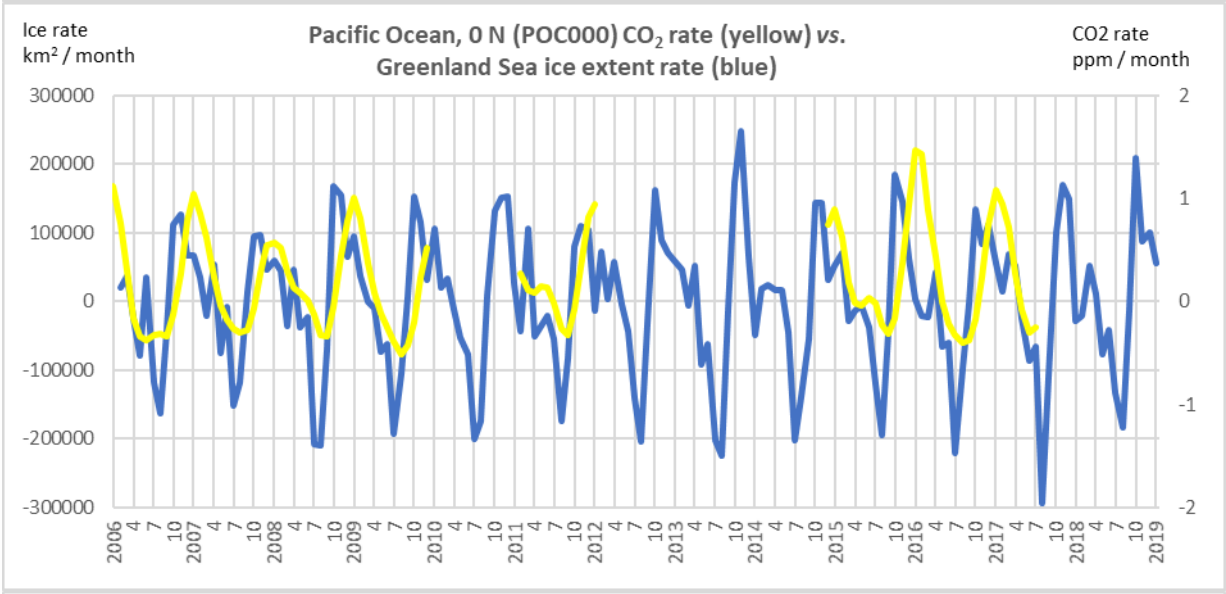

1110

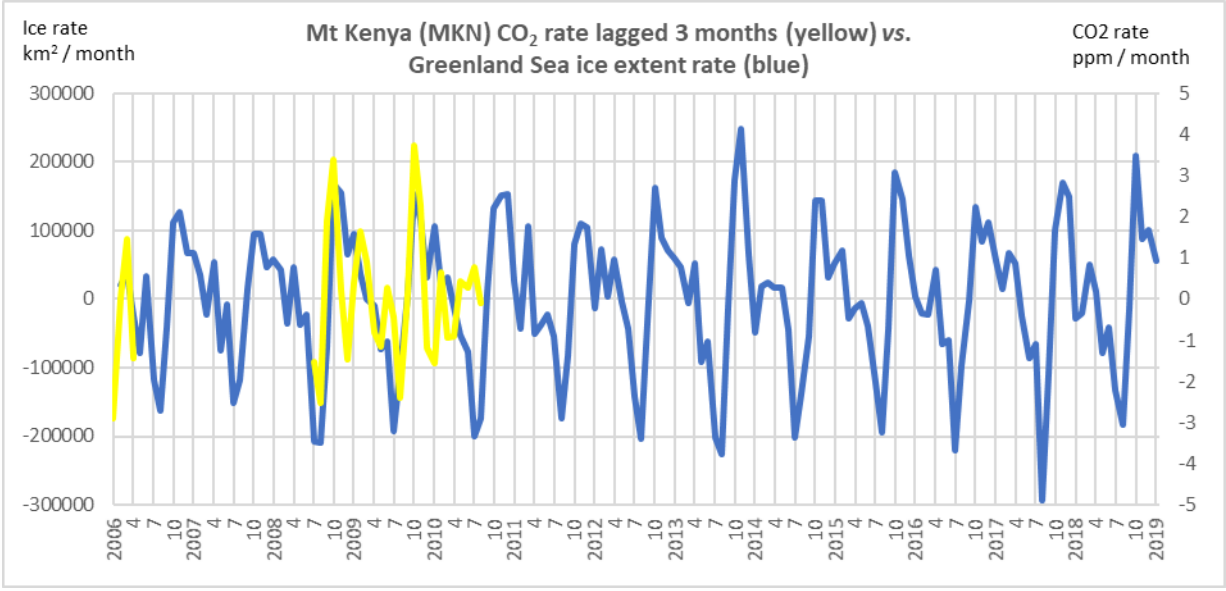

1111

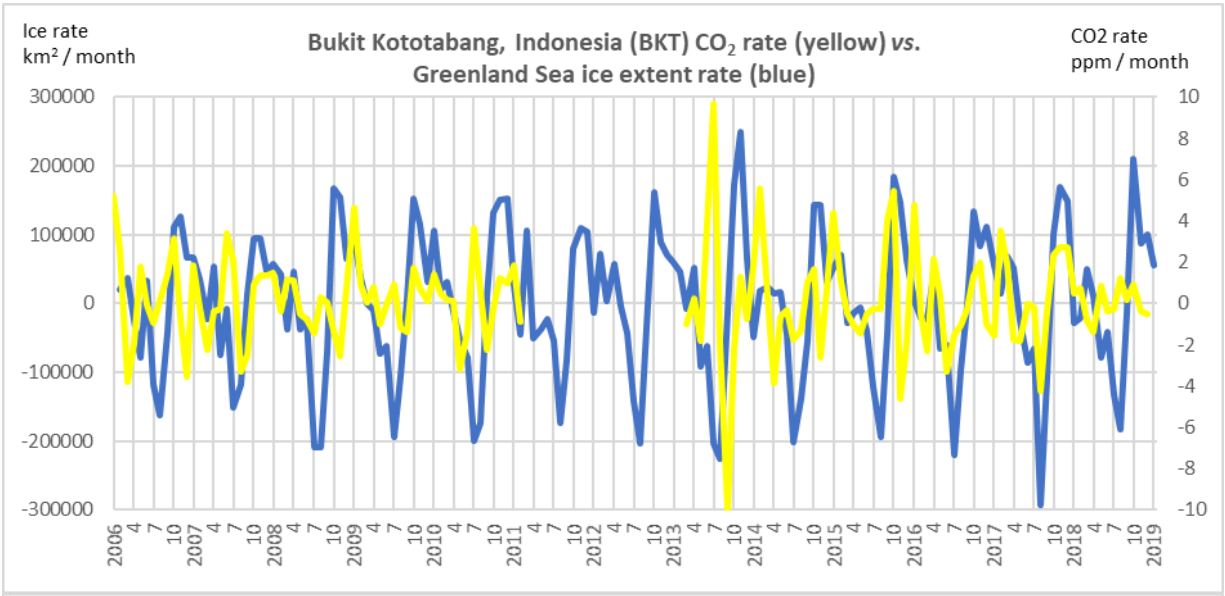

1112

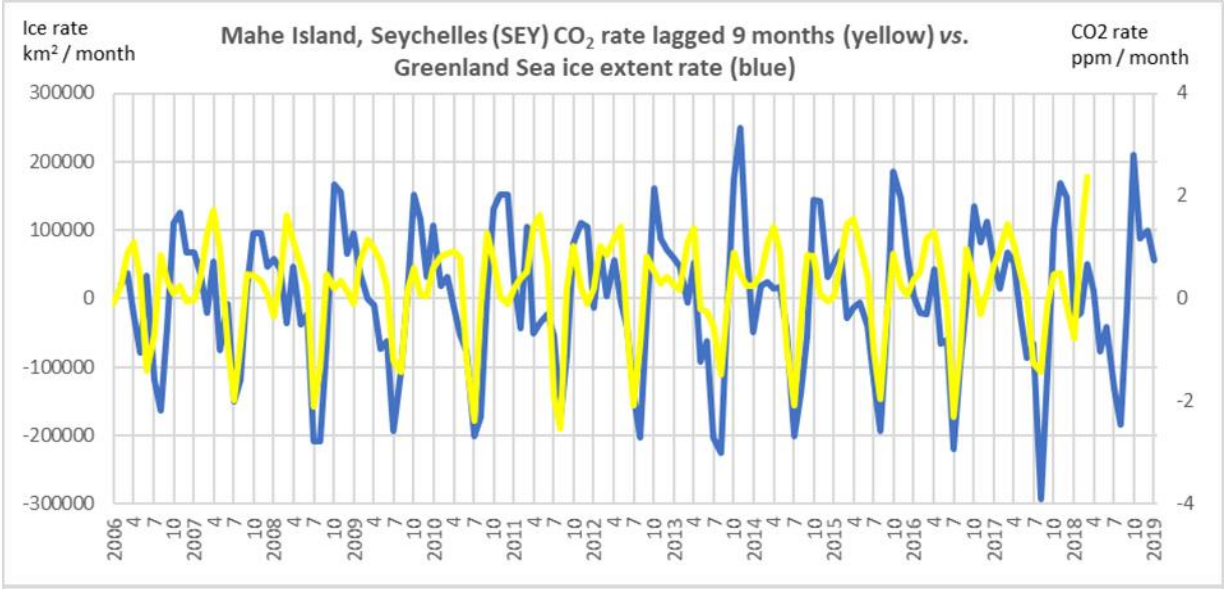

1113

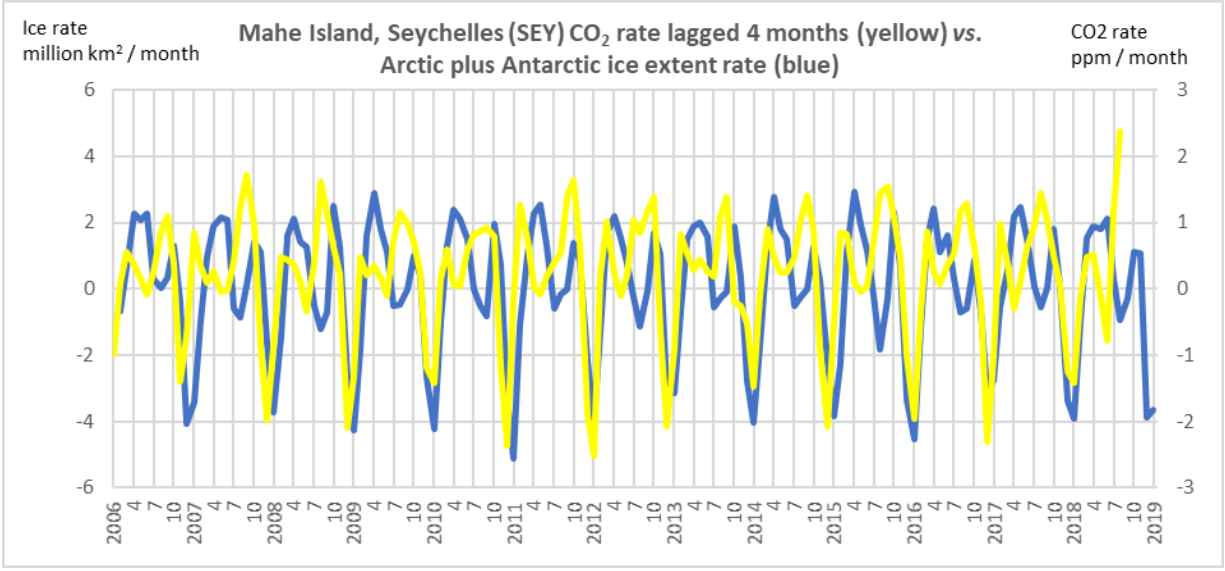

1114

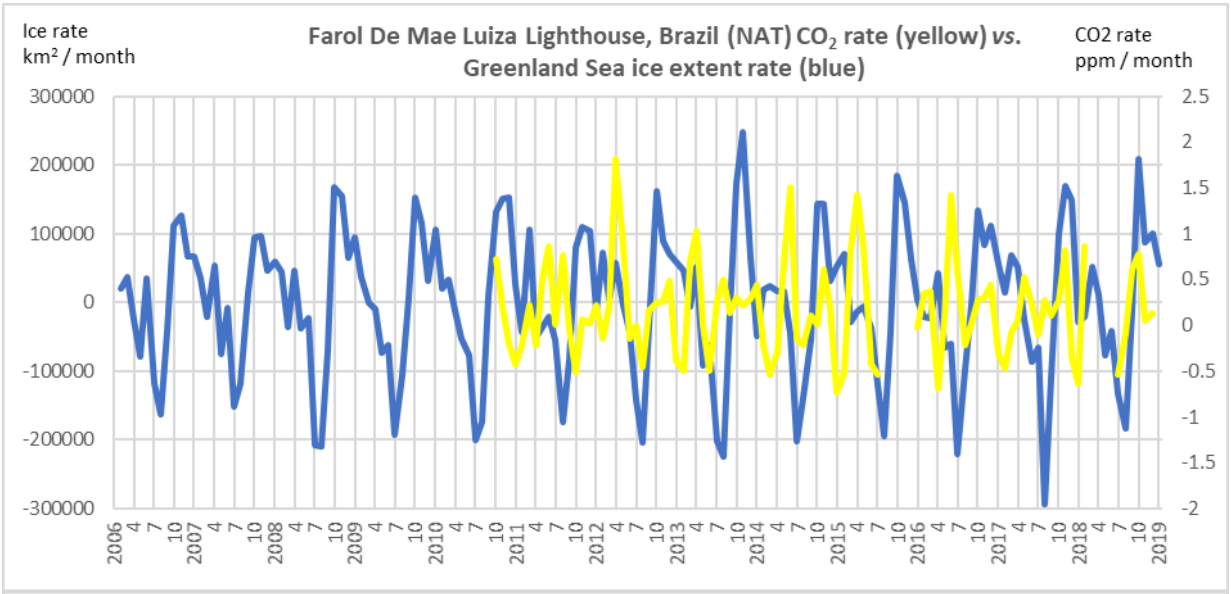

1115

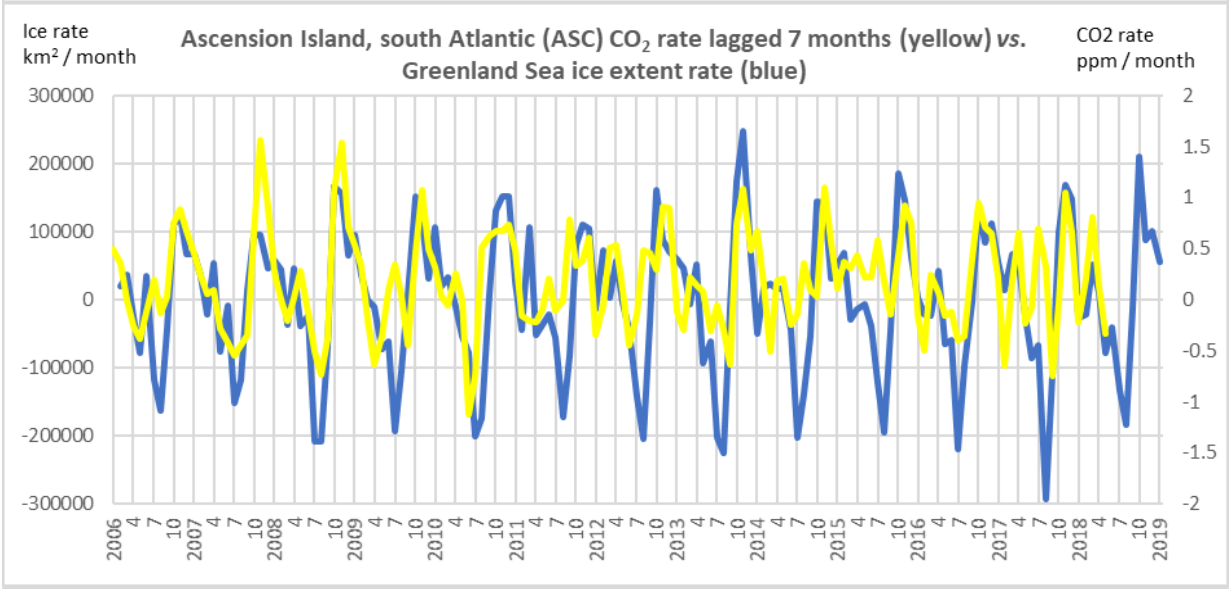

1116

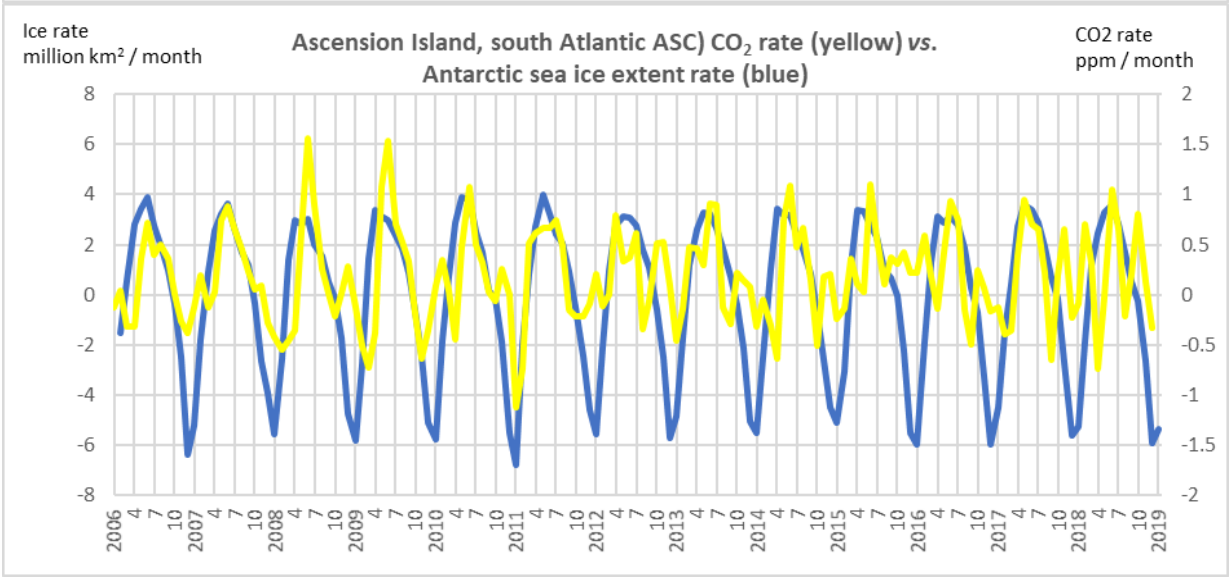

1117

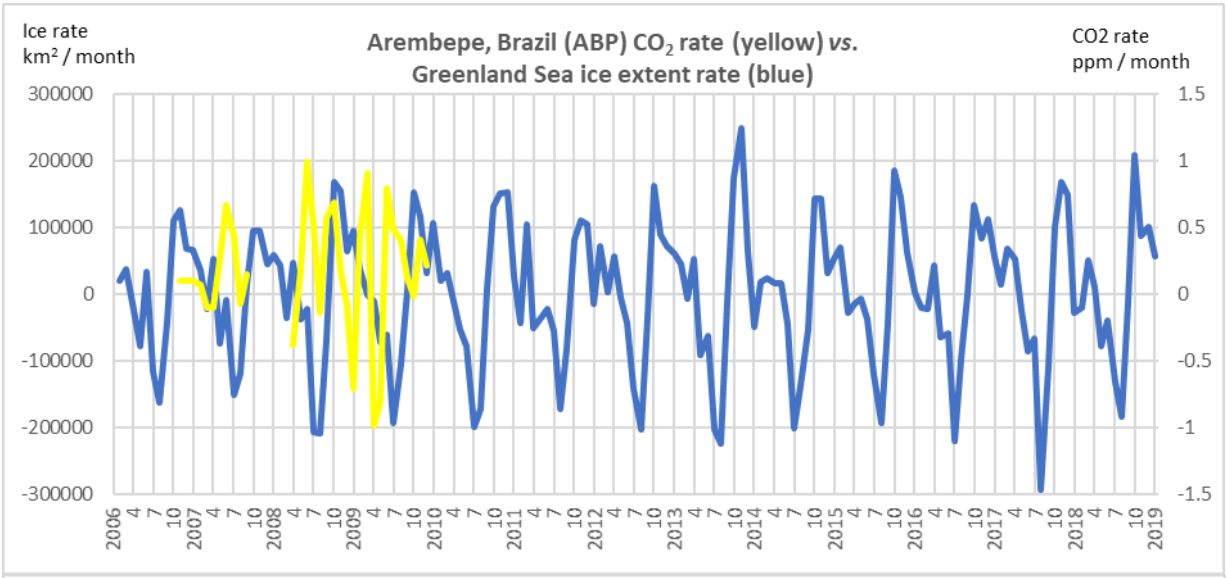

1118

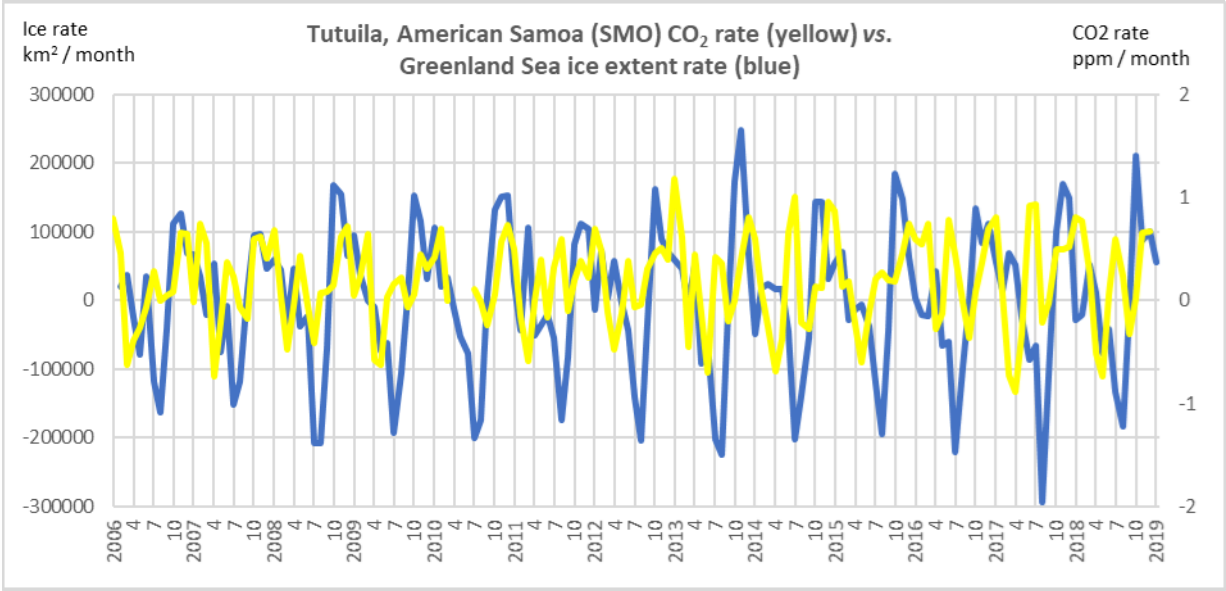

1119

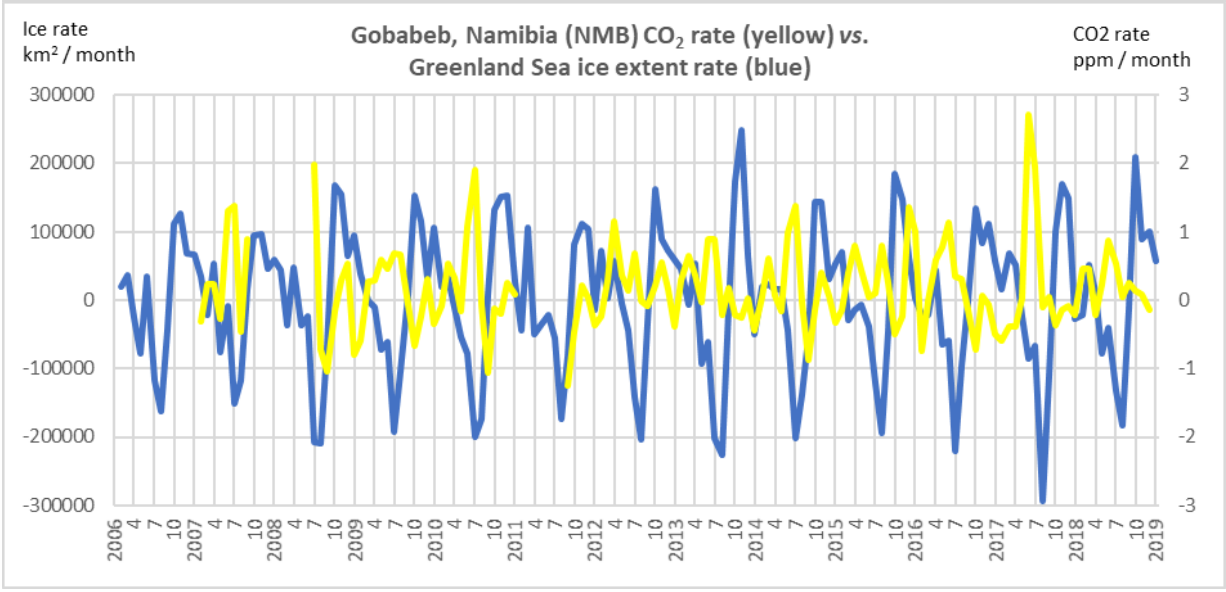

1120

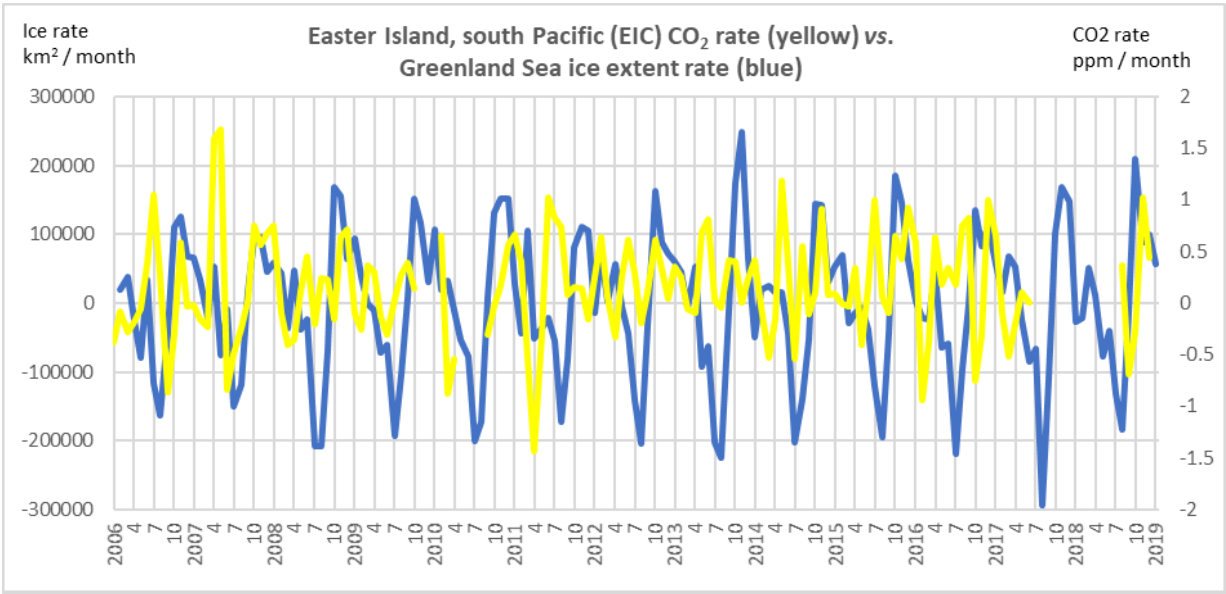

1121

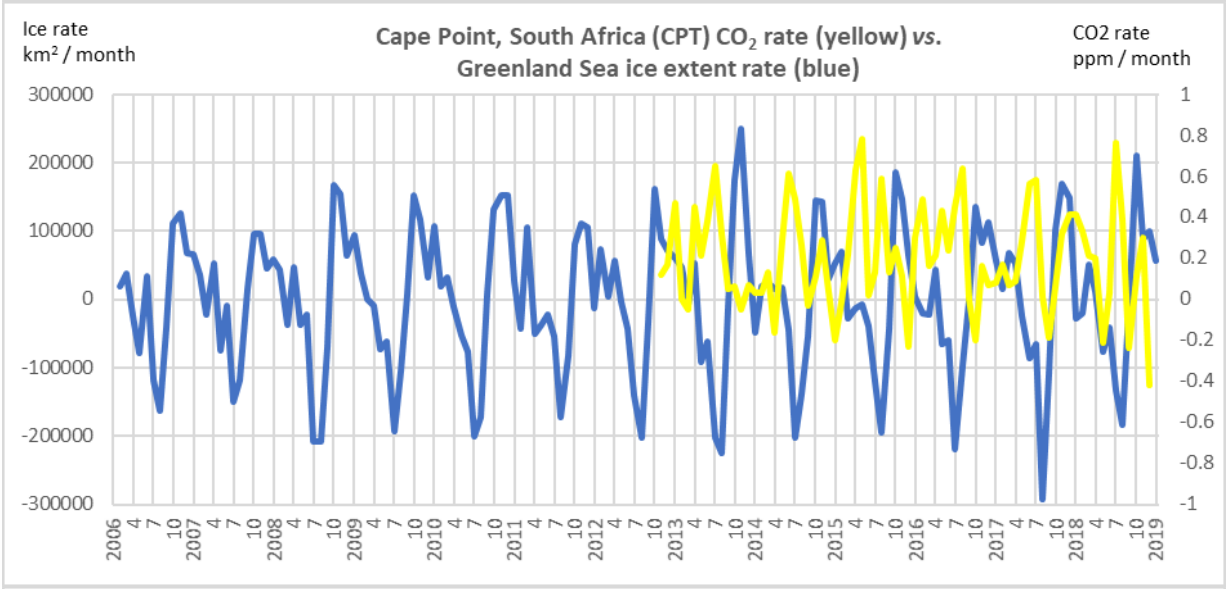

1122

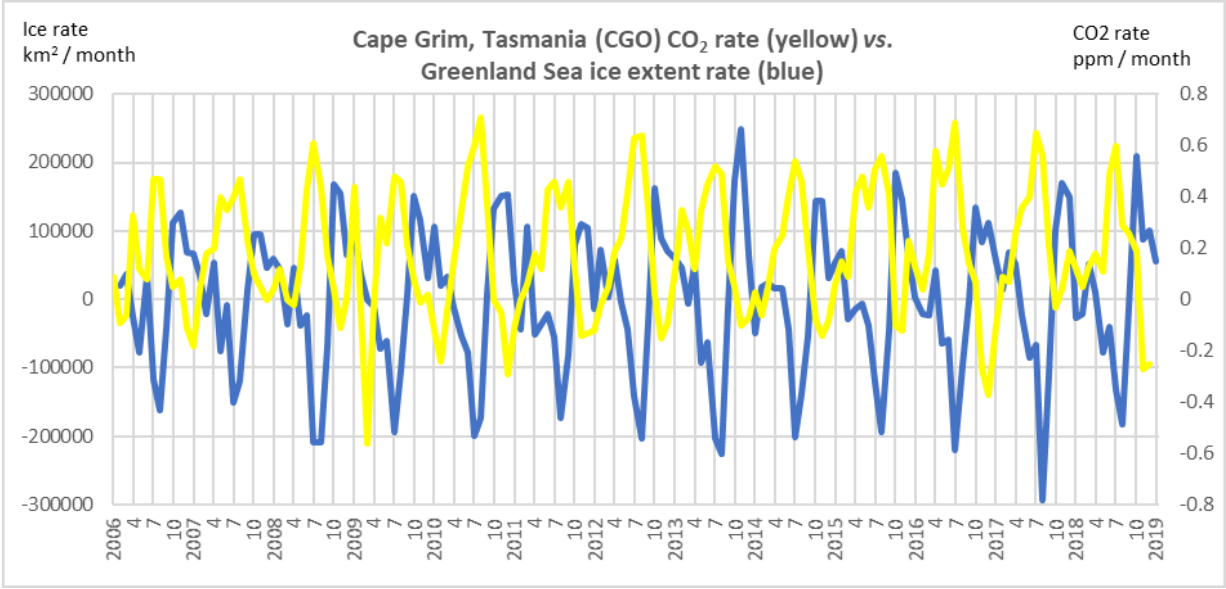

1123

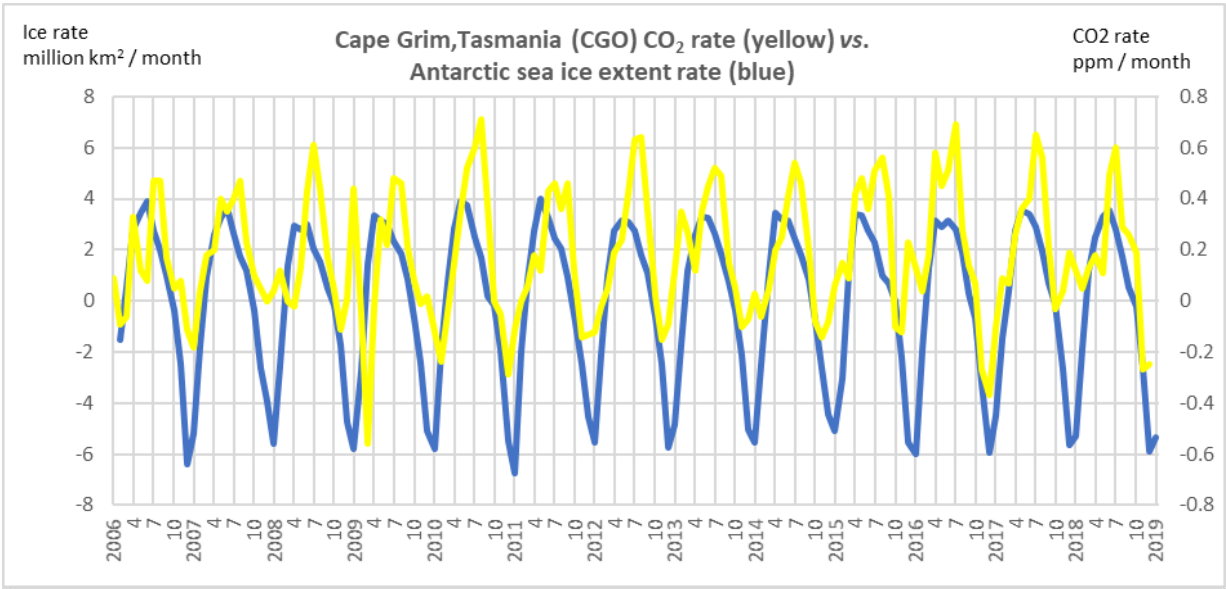

1124

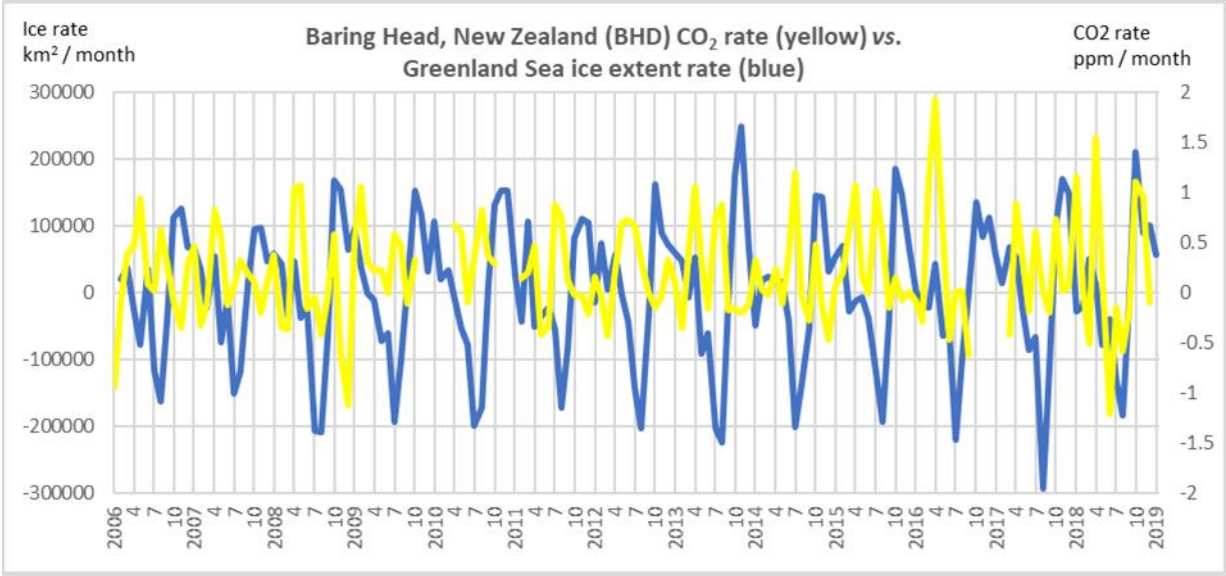

1125

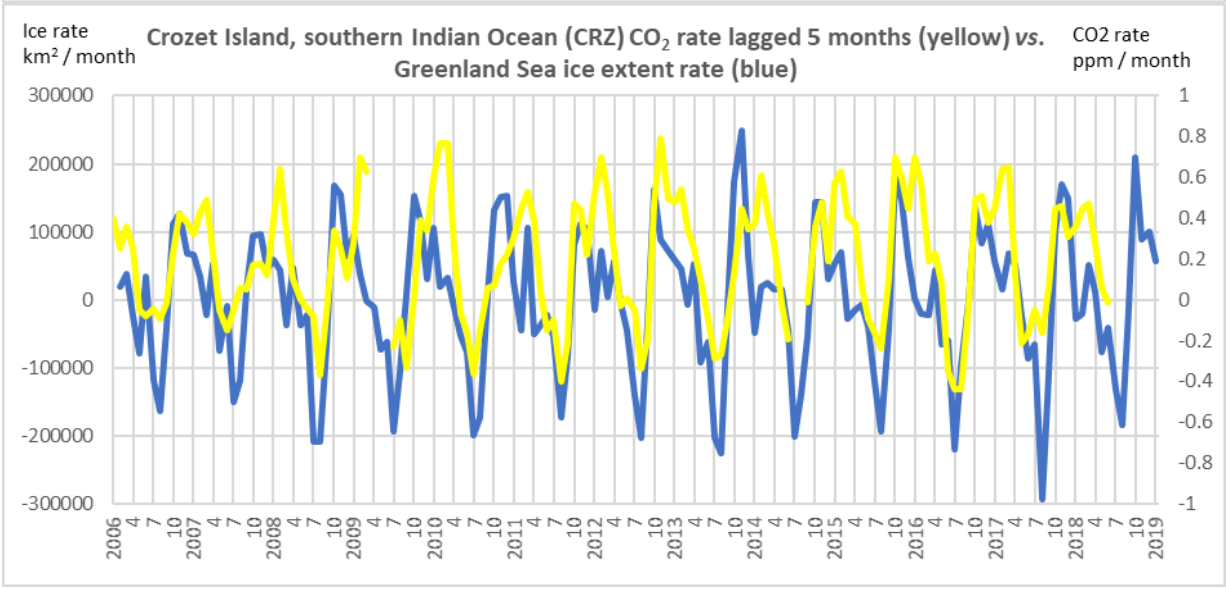

1126

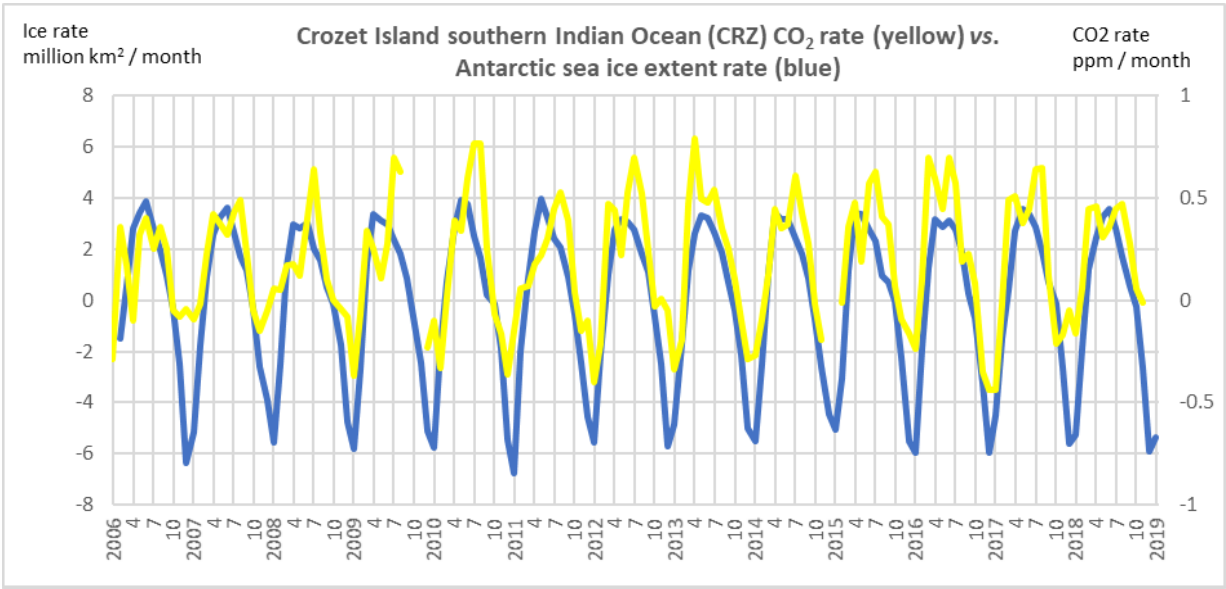

1127

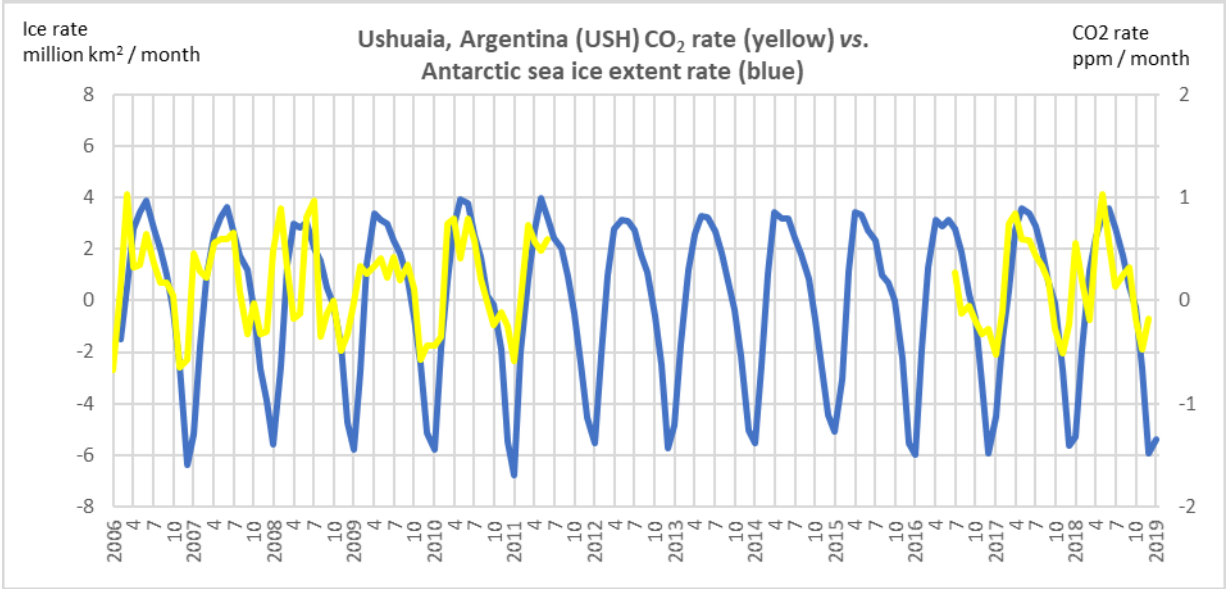

1128

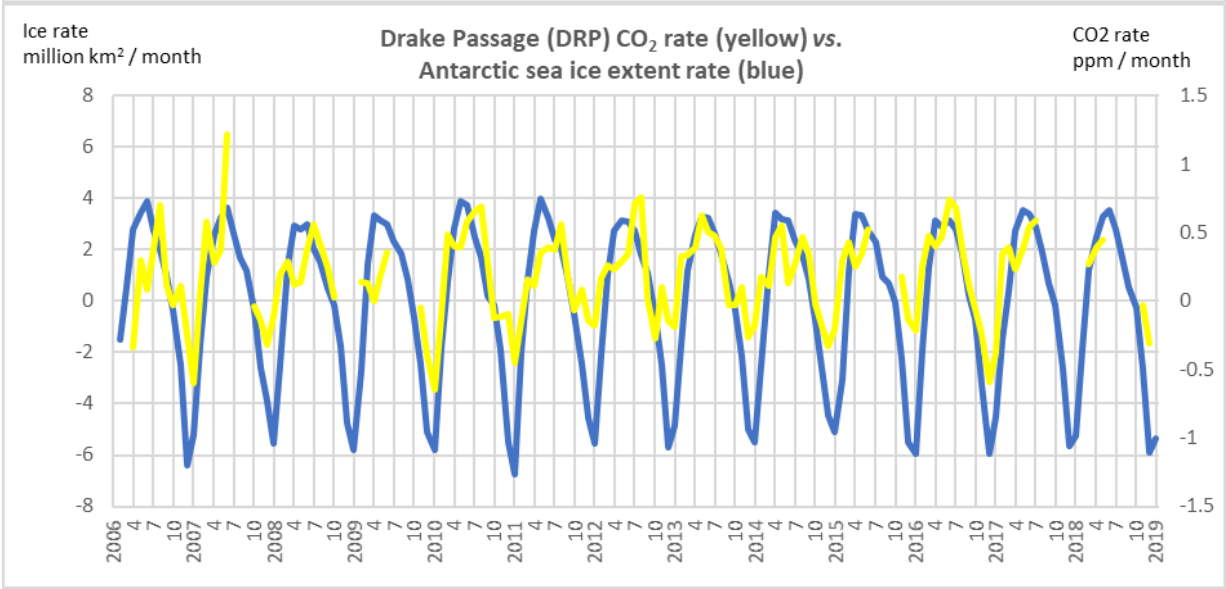

1129

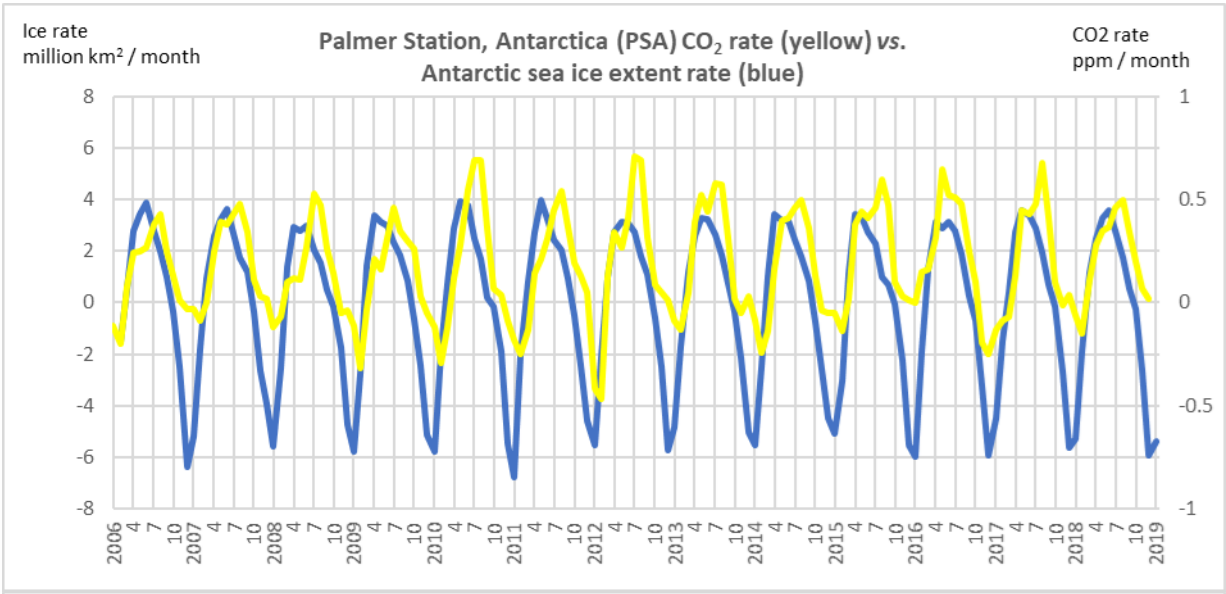

1130

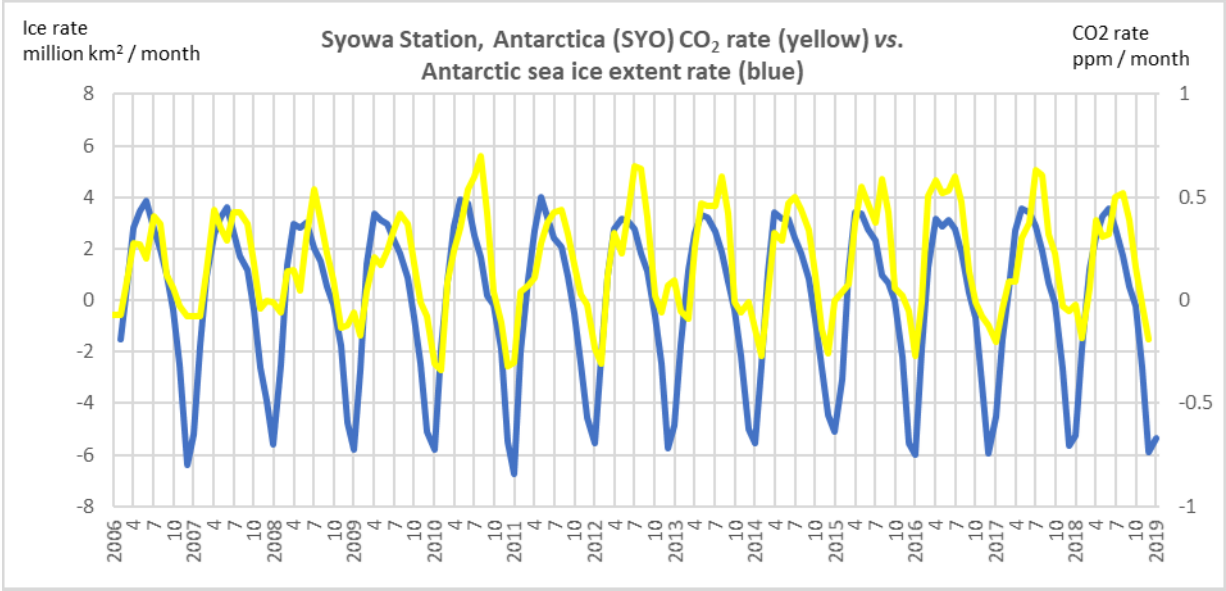

1131

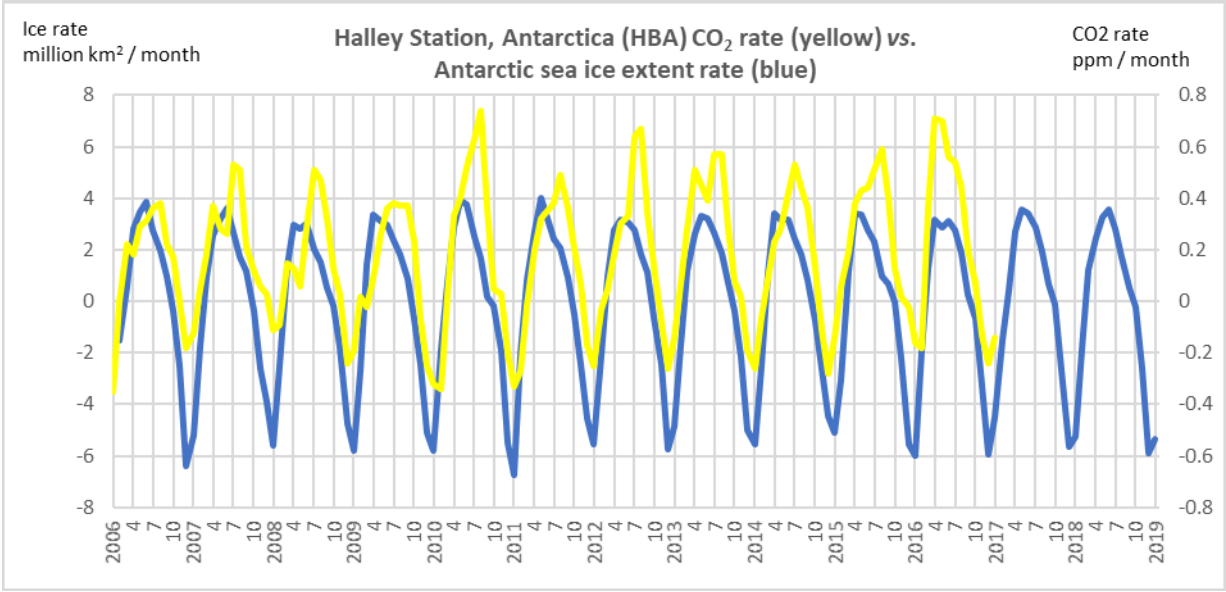

1132

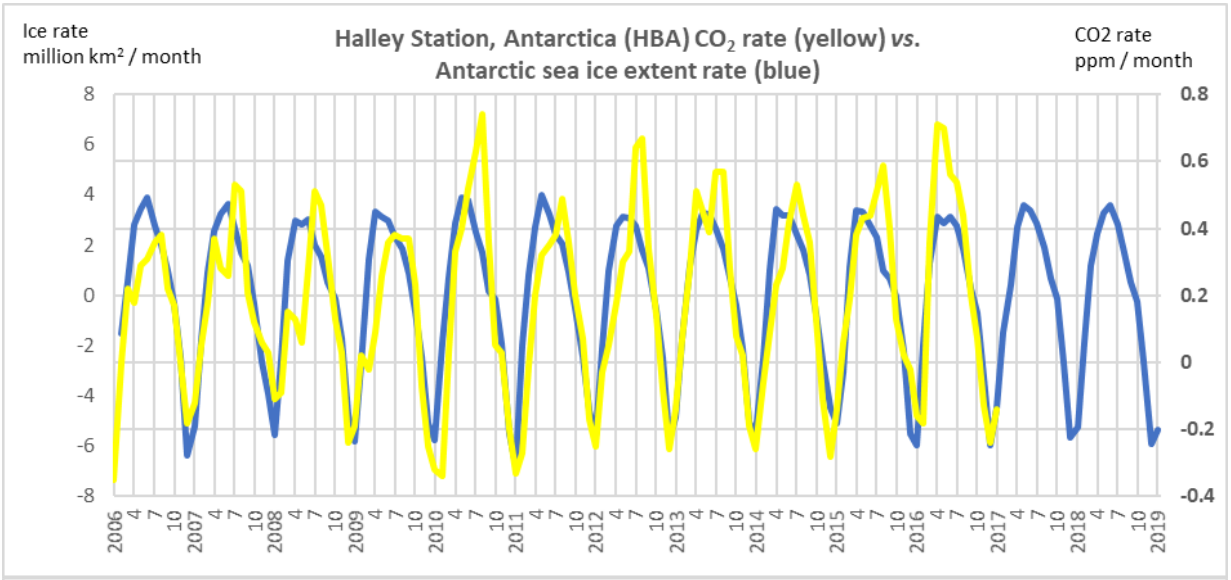

1133

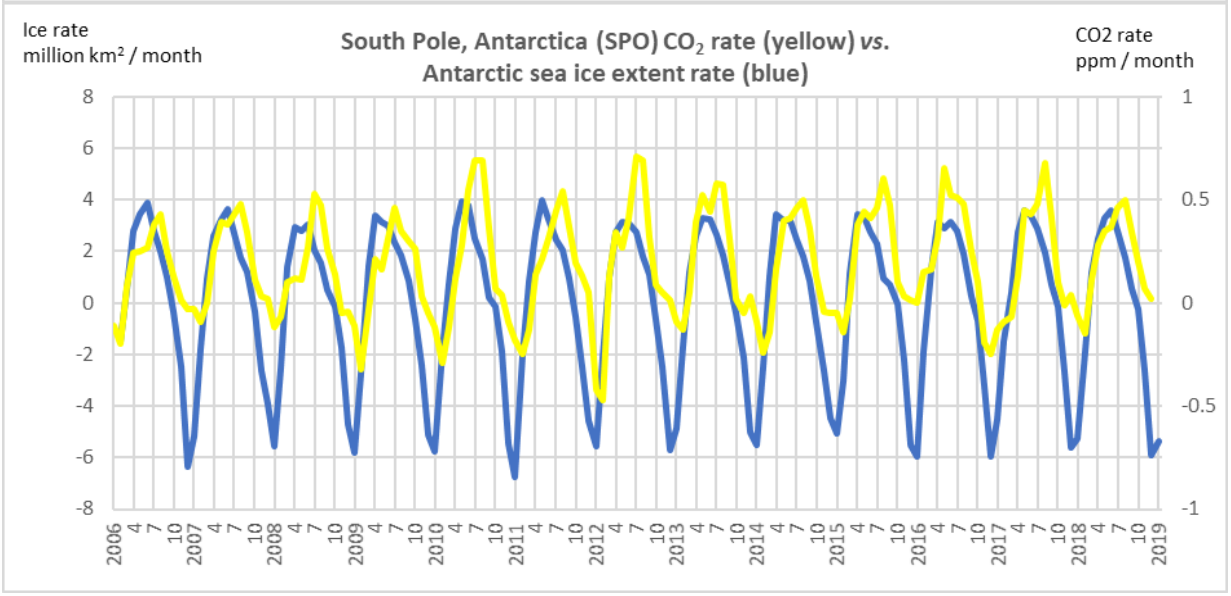

1134

1135

Section B: High altitude (>1000m) CO_2 recording sites, ordered by altitude

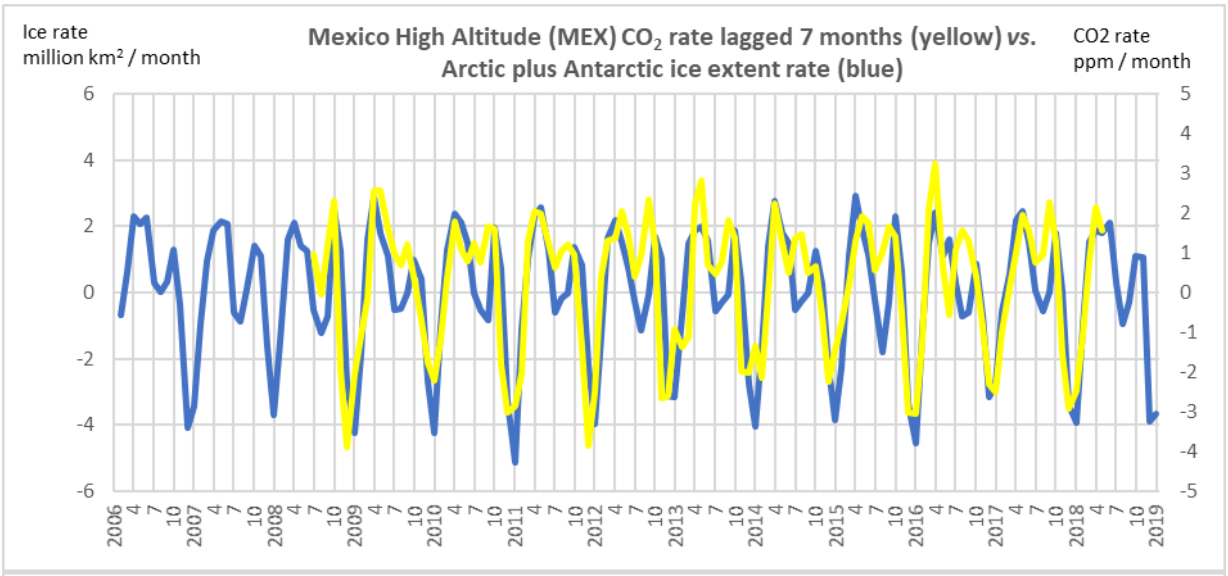

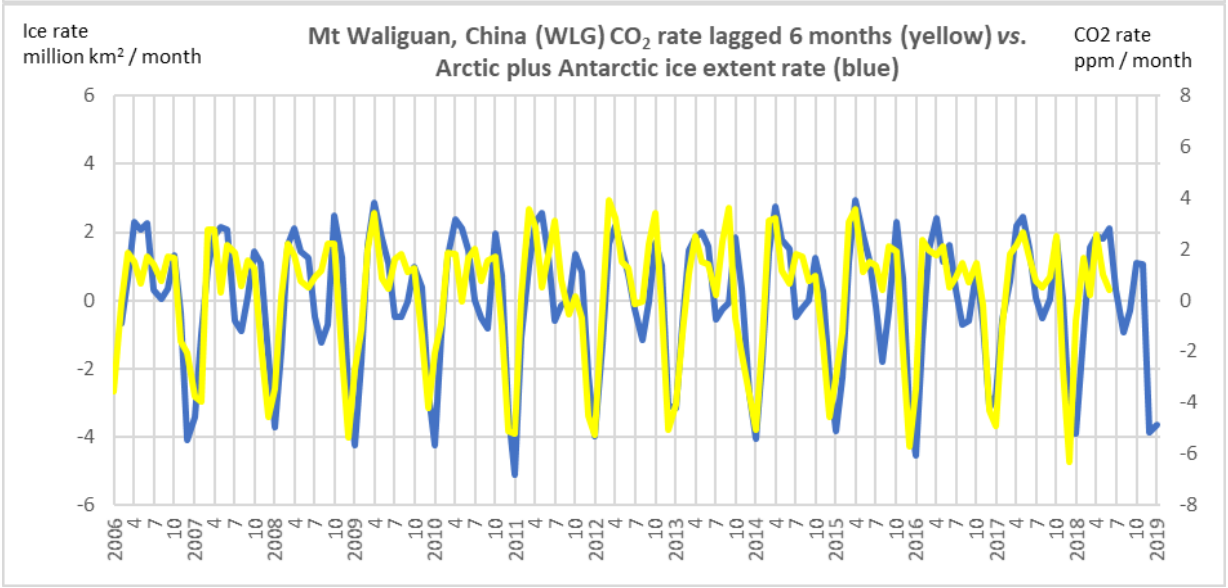

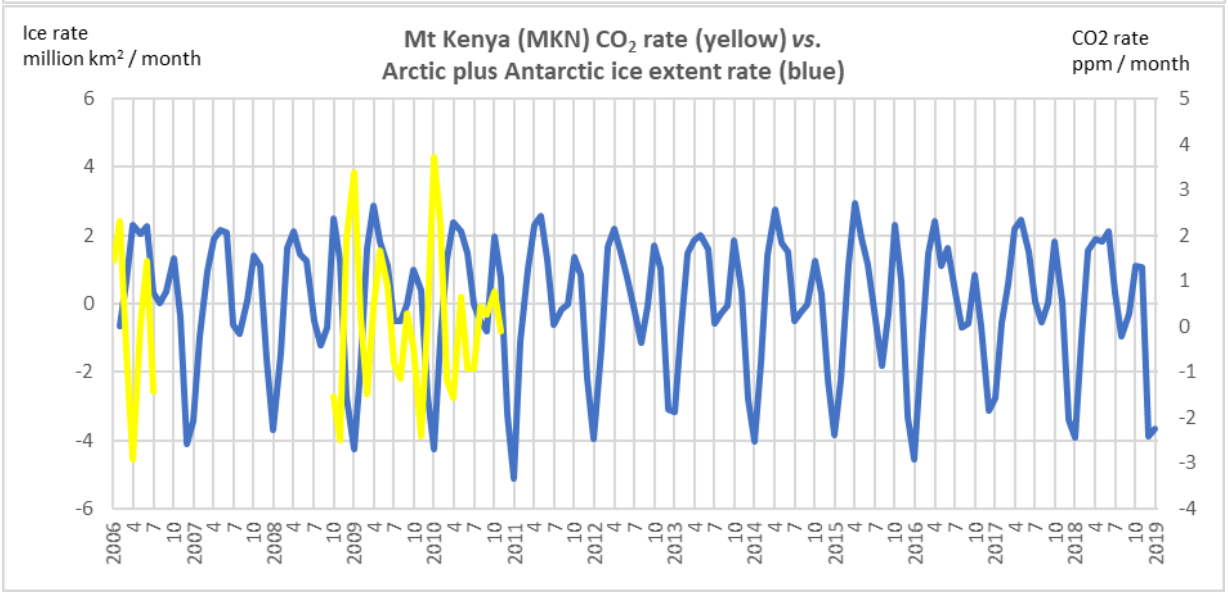

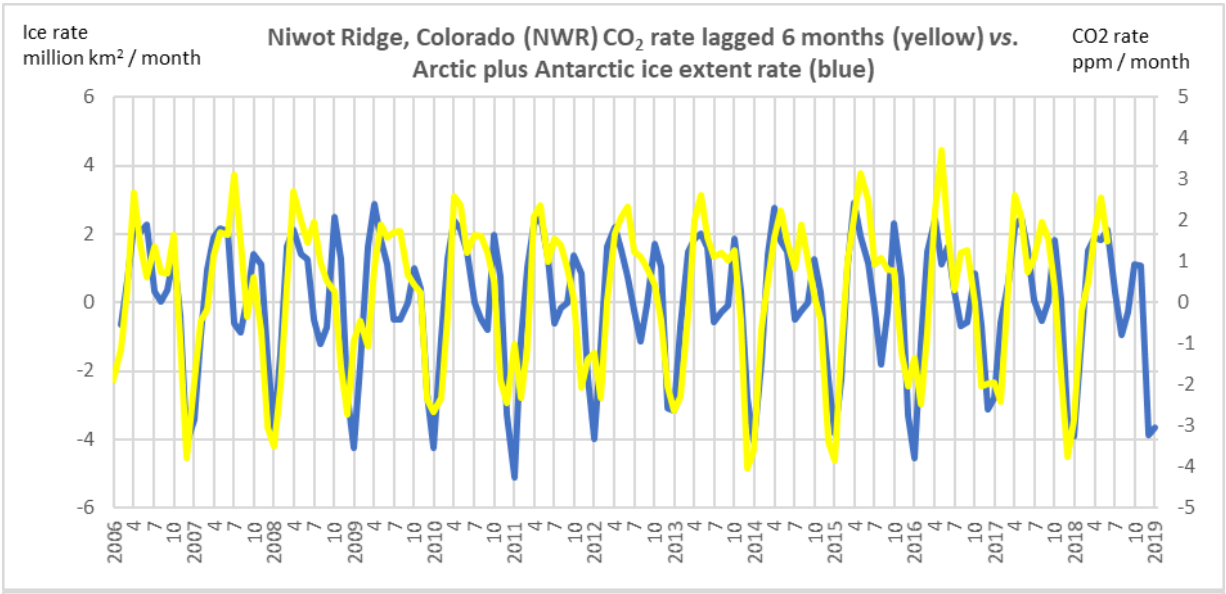

1141

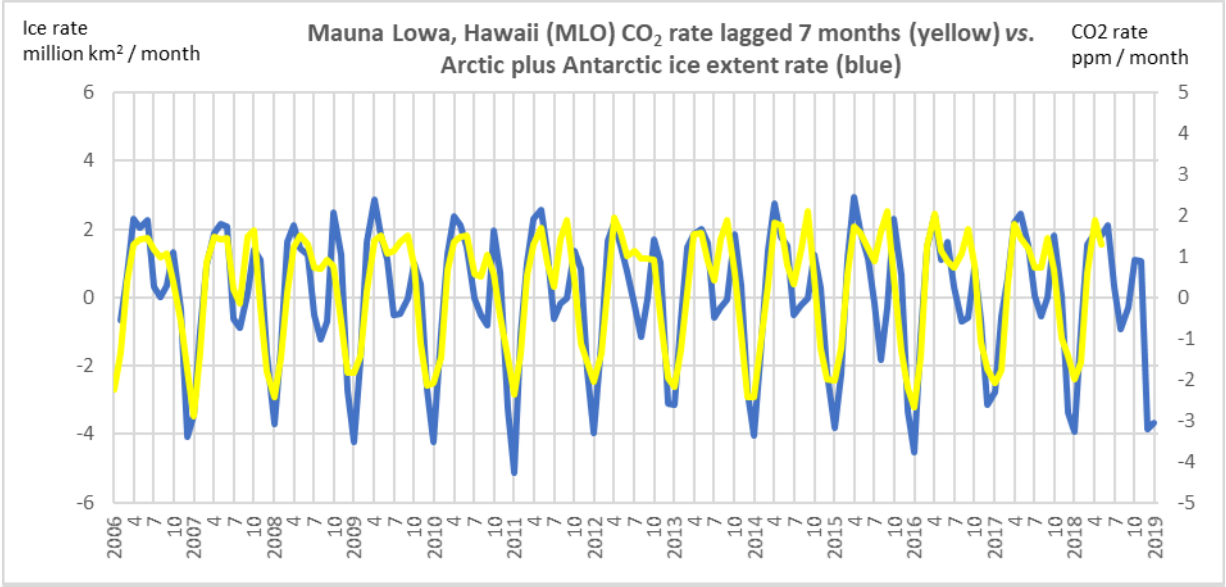

1142

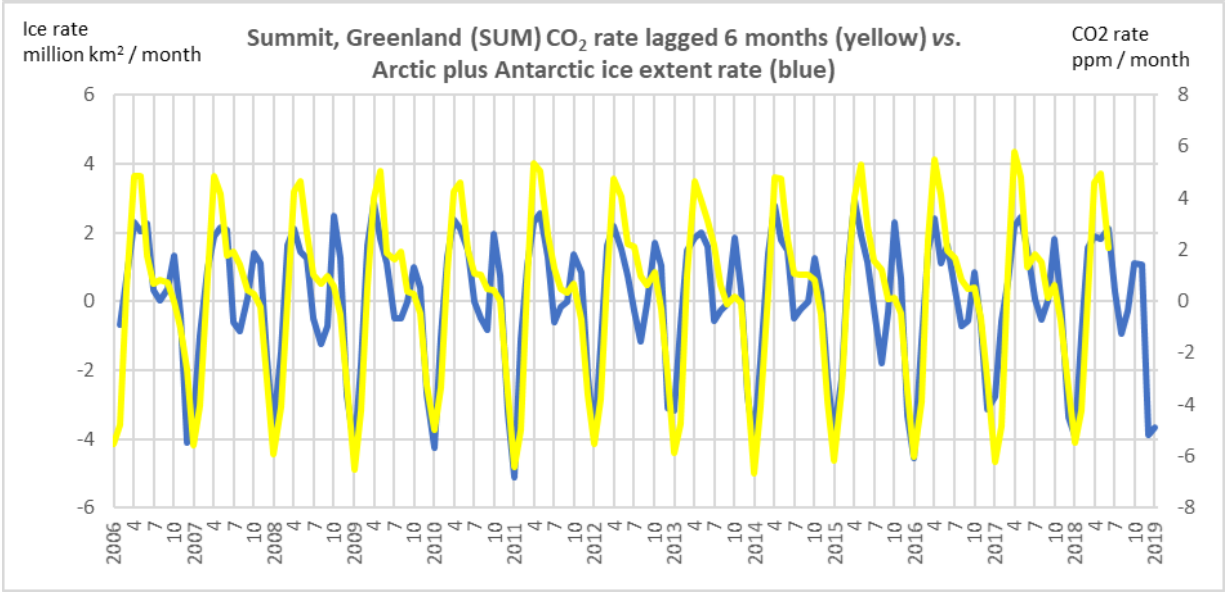

1143

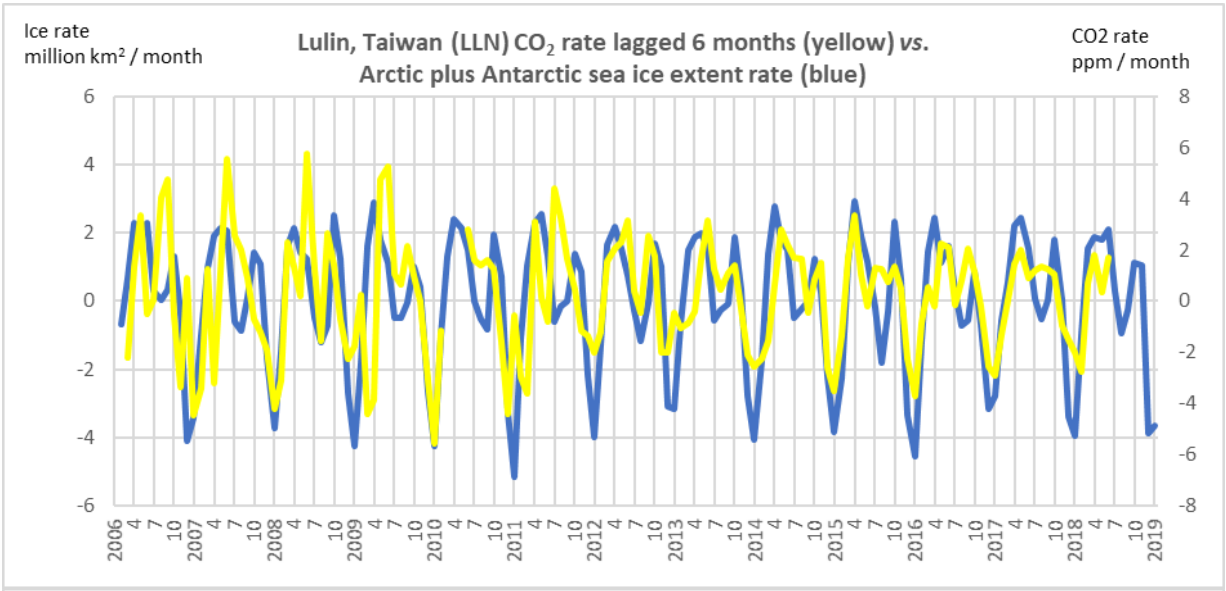

1144

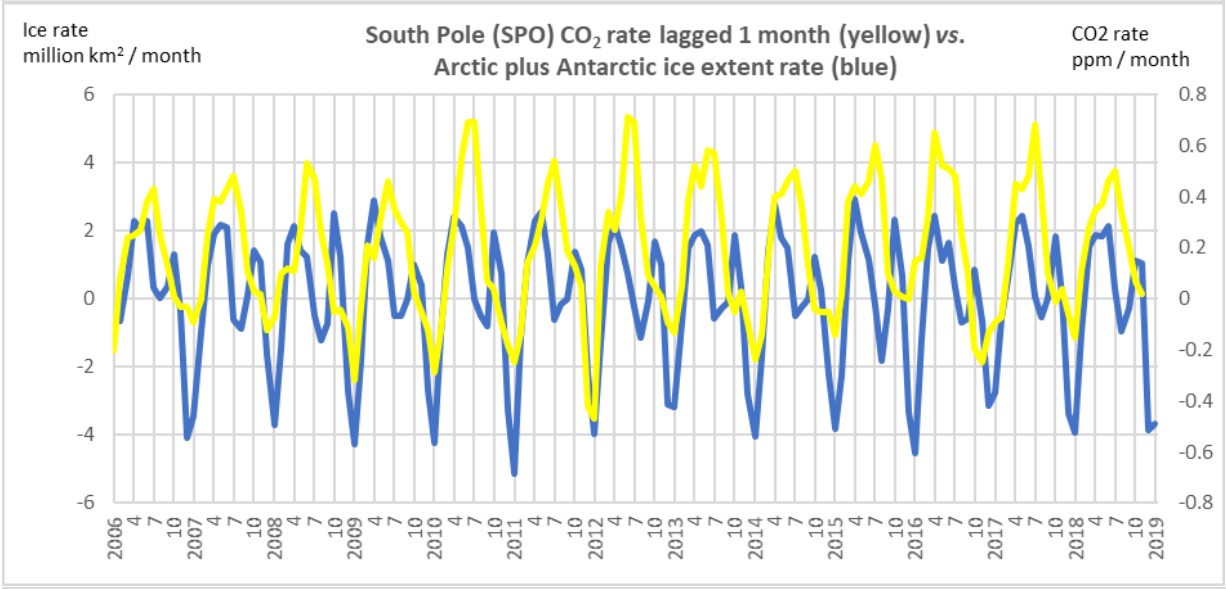

1145

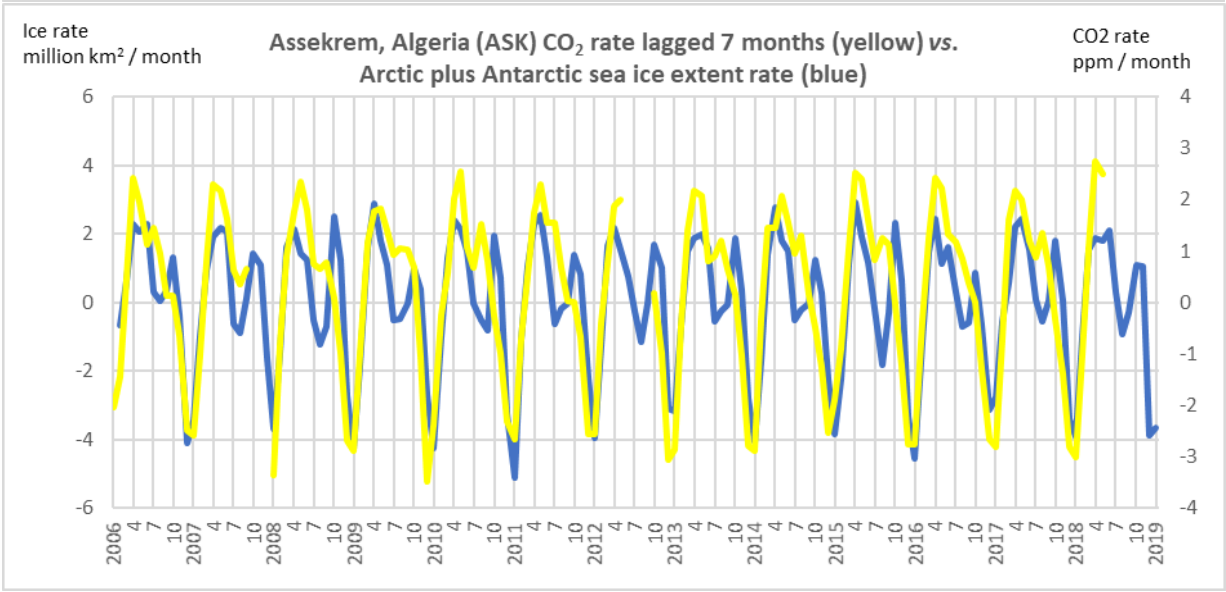

1146

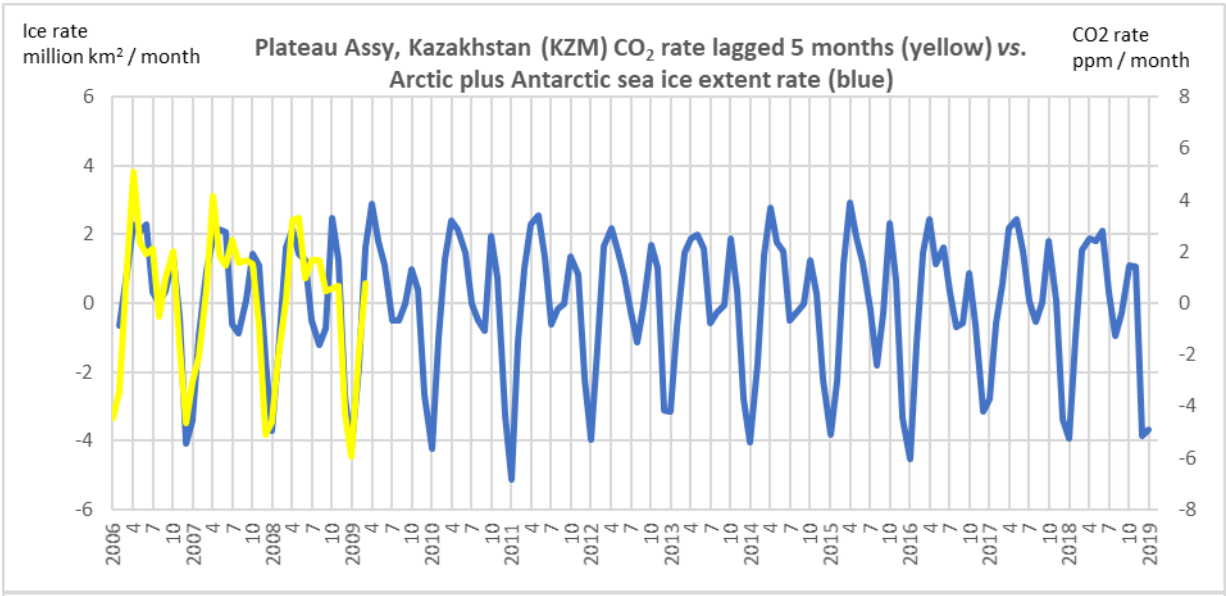

1147

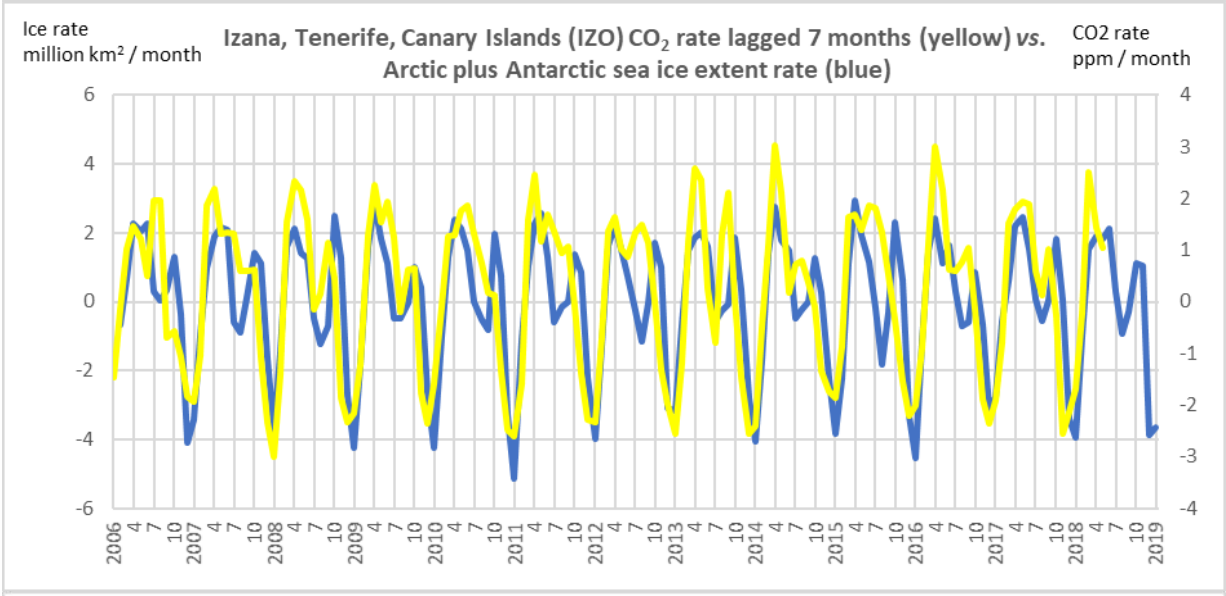

1148

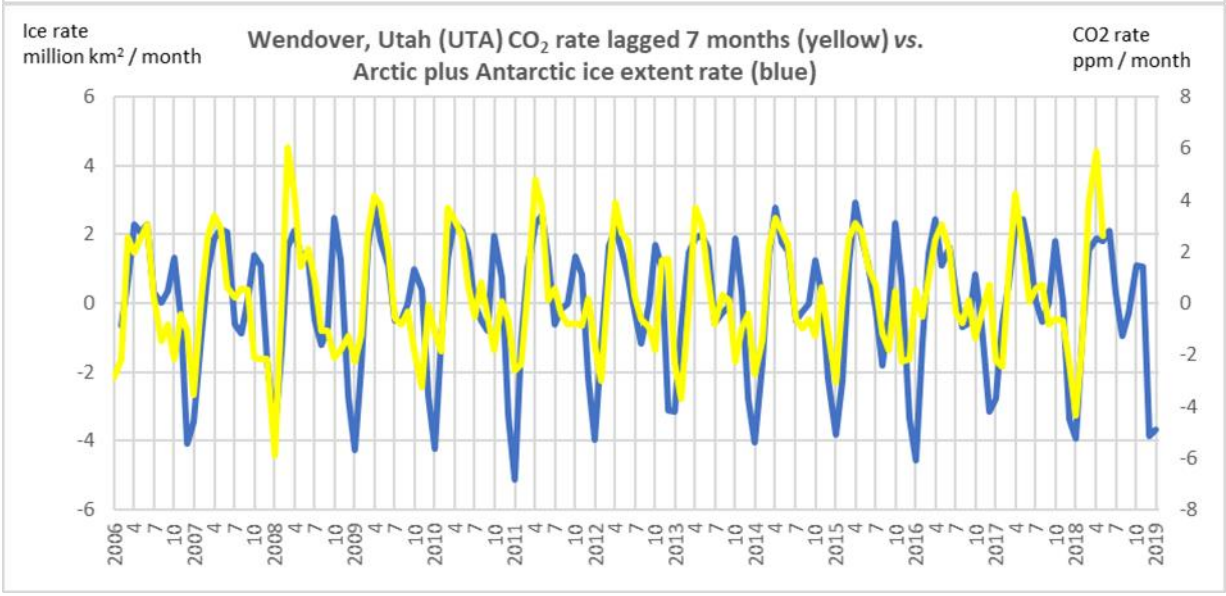

1149

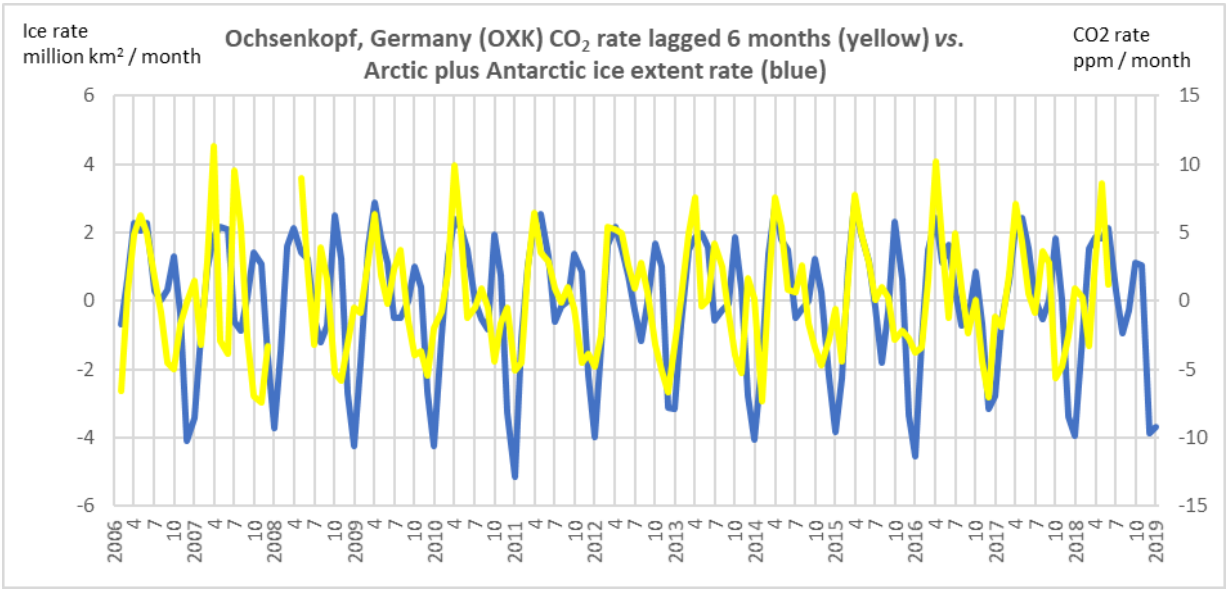

1150

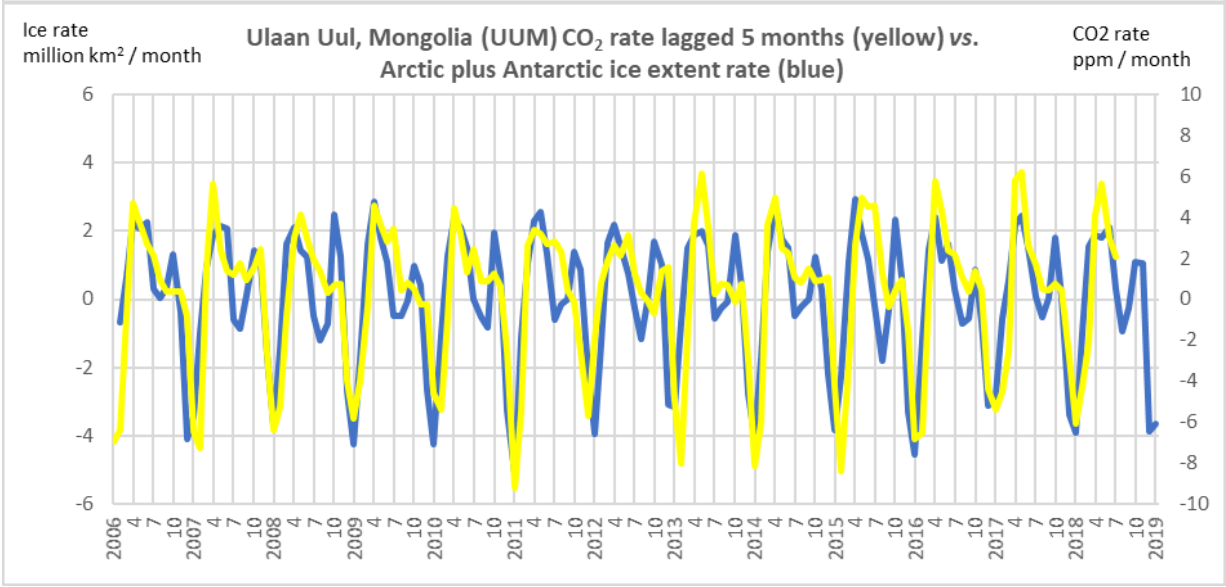

1151

1152

Section C: Pacific Ocean transect sites, in descending latitudinal order

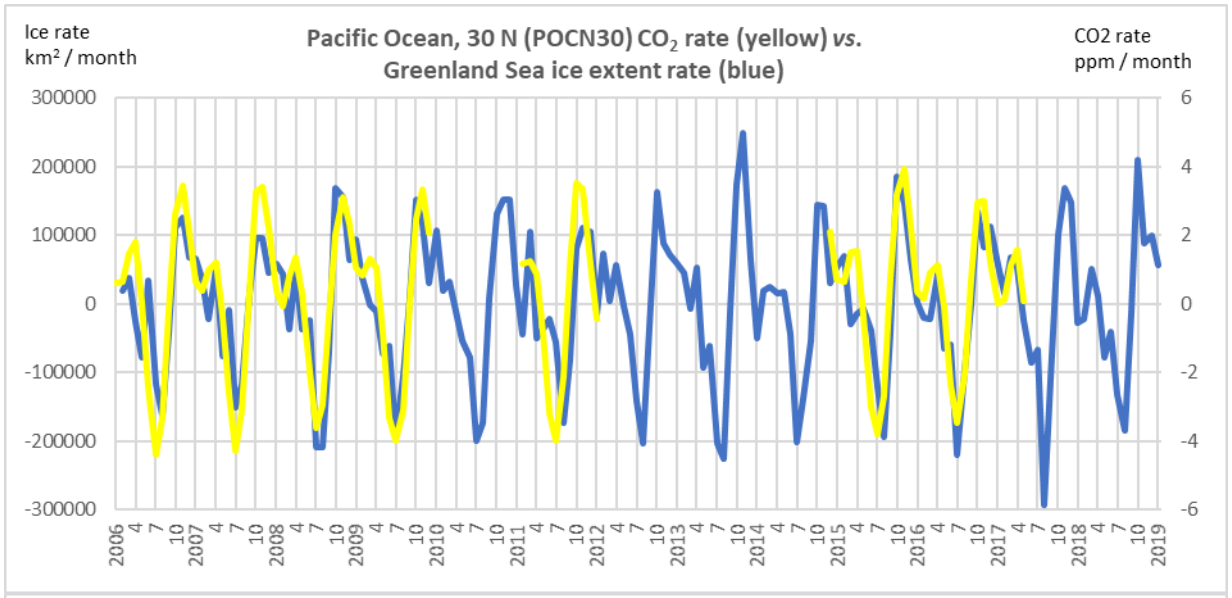

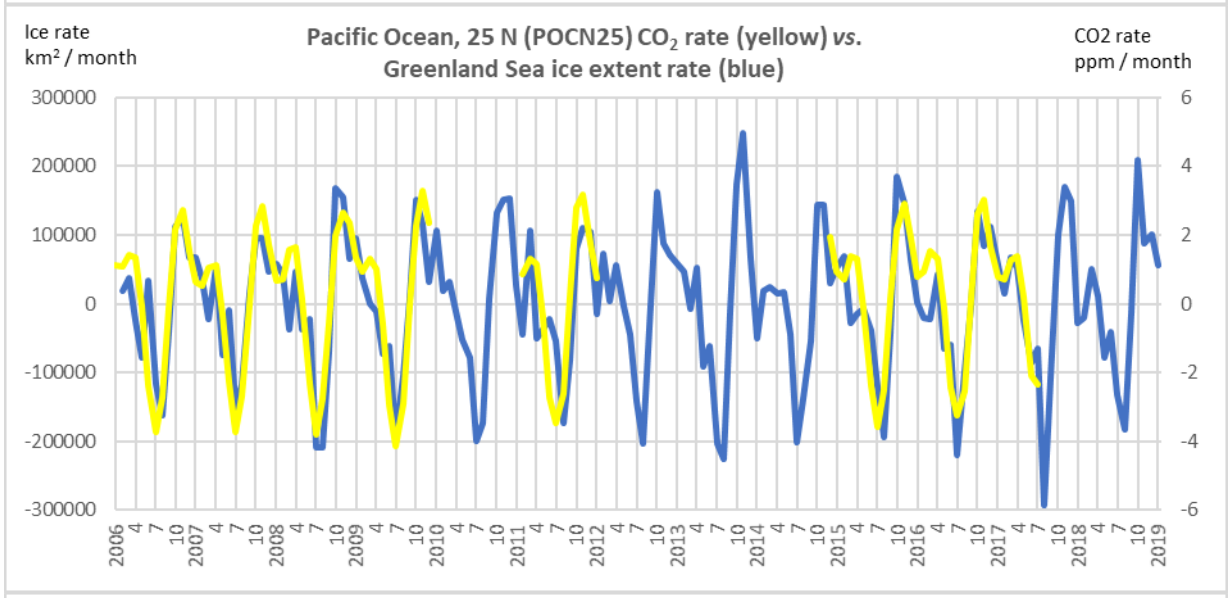

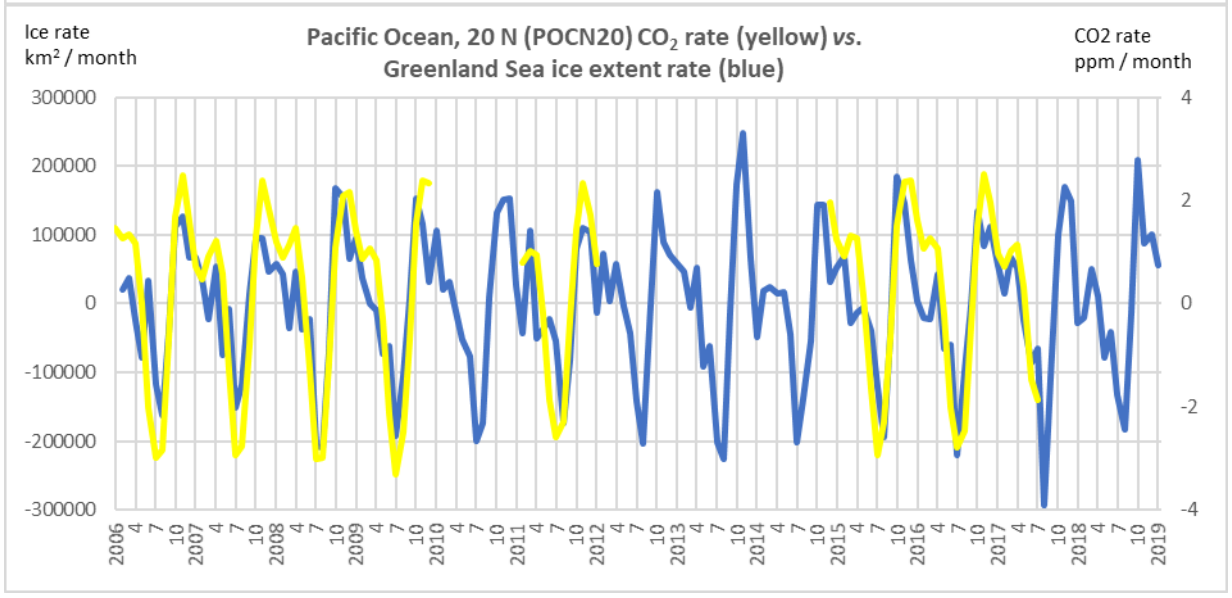

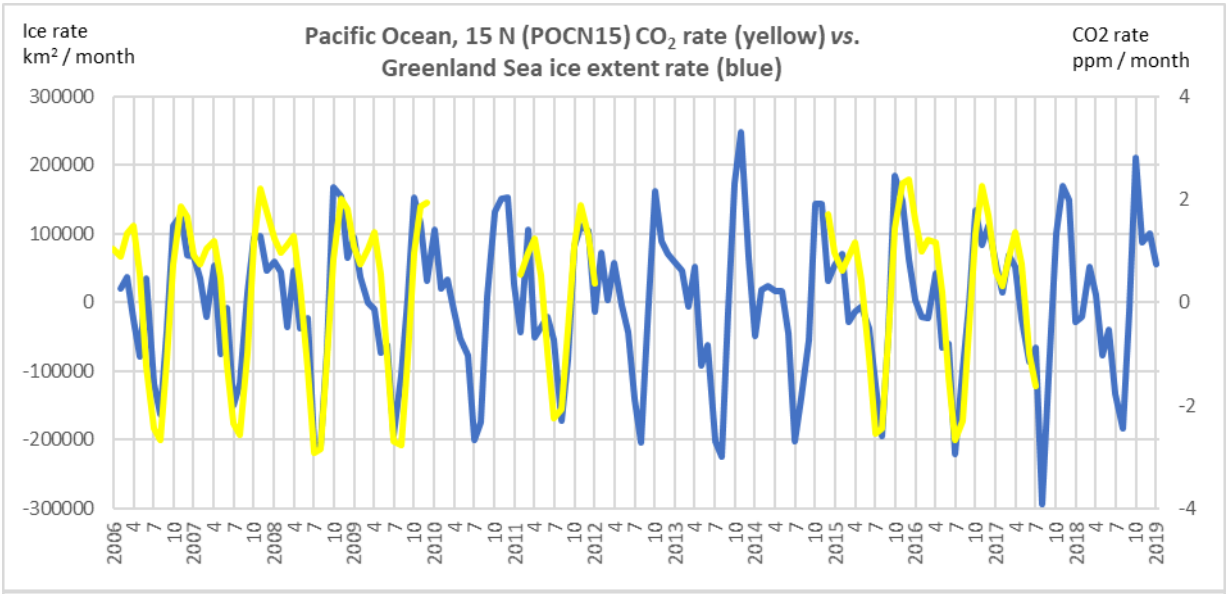

1158

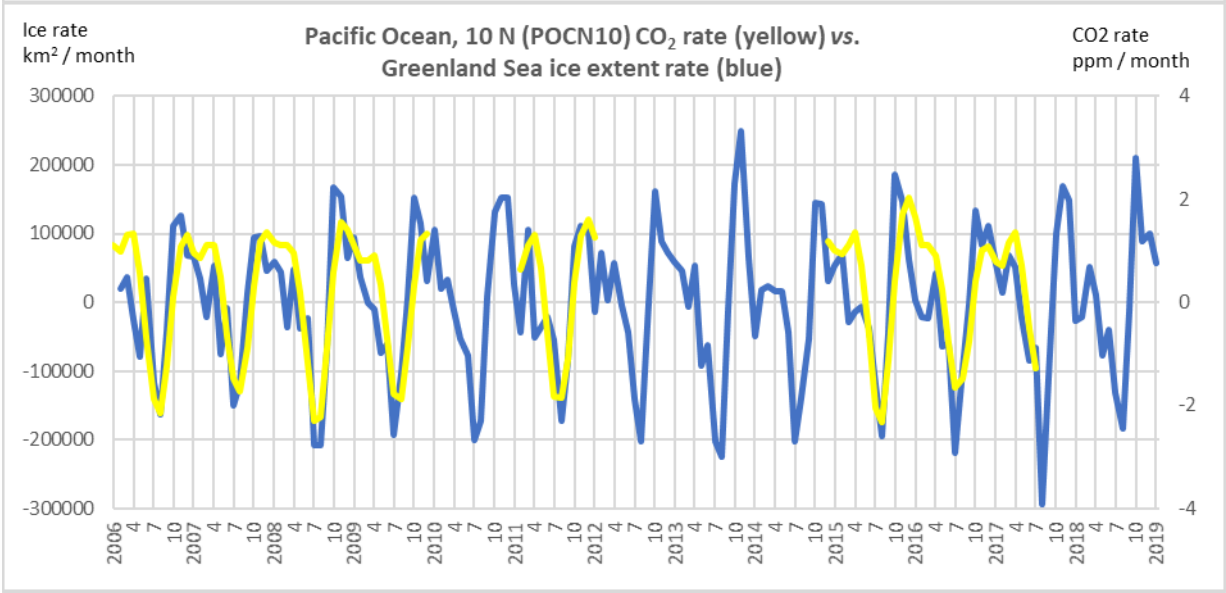

1159

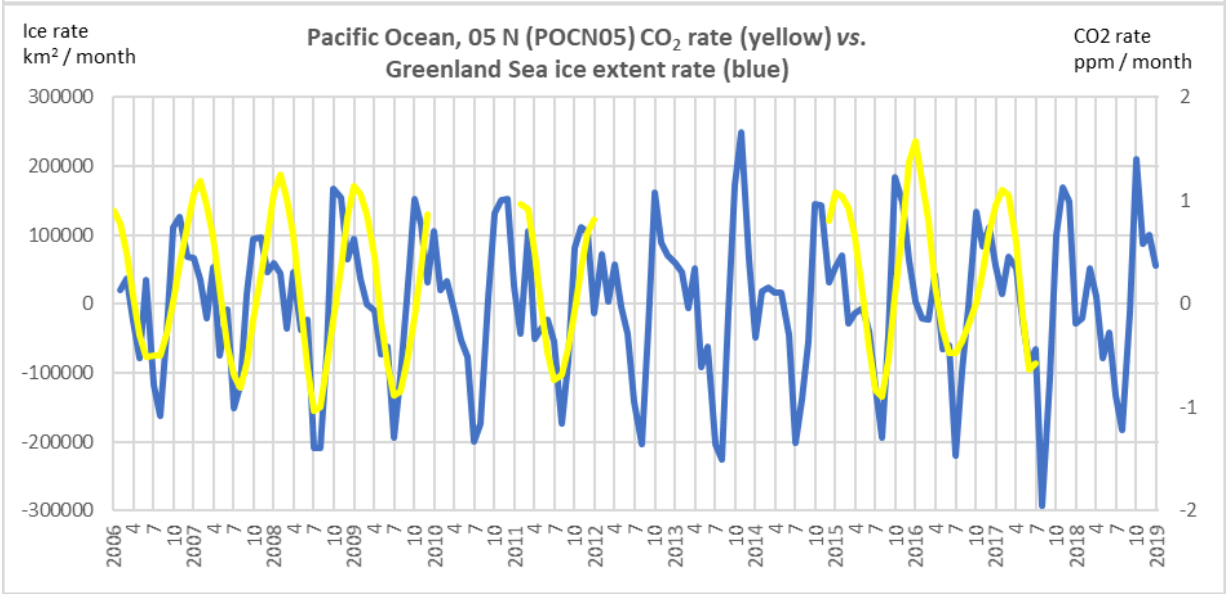

1160

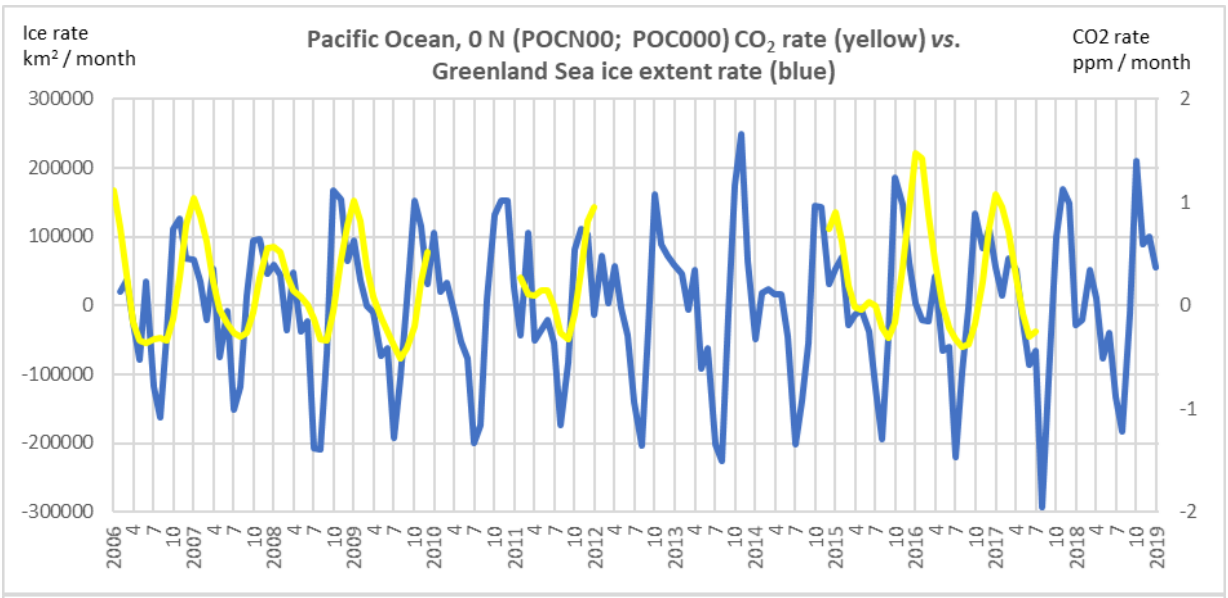

1161

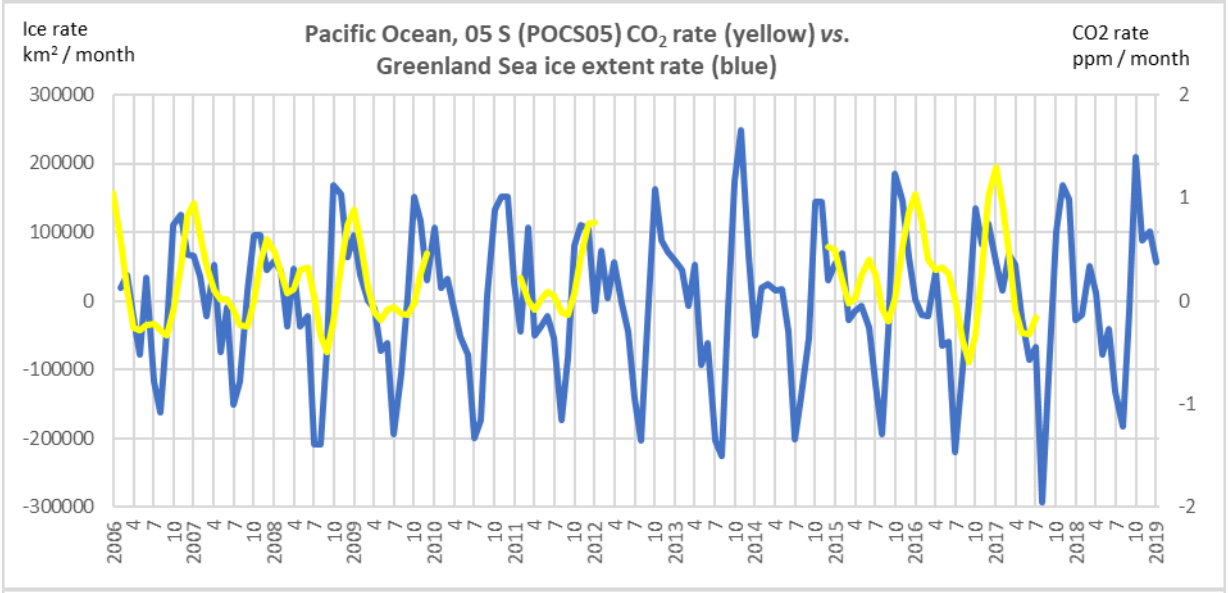

1162

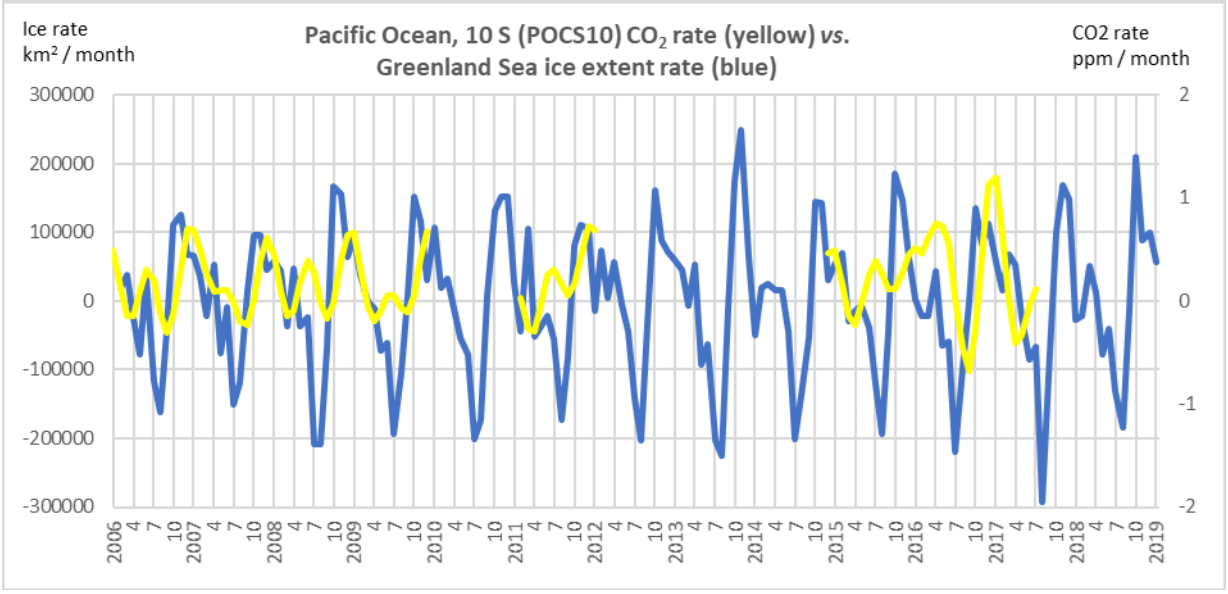

1163

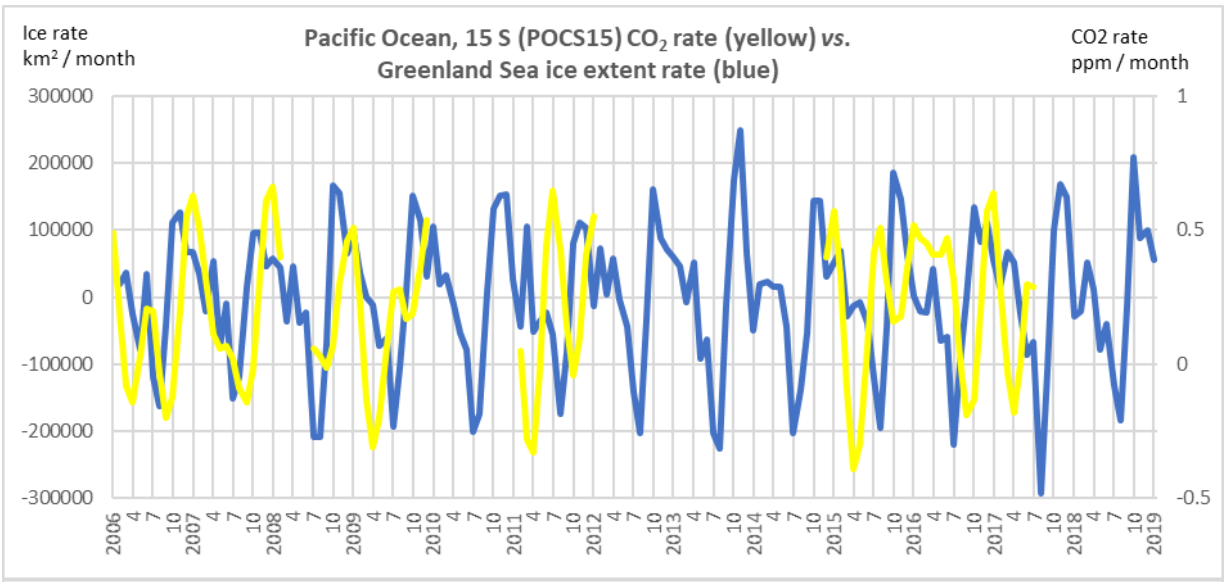

1164

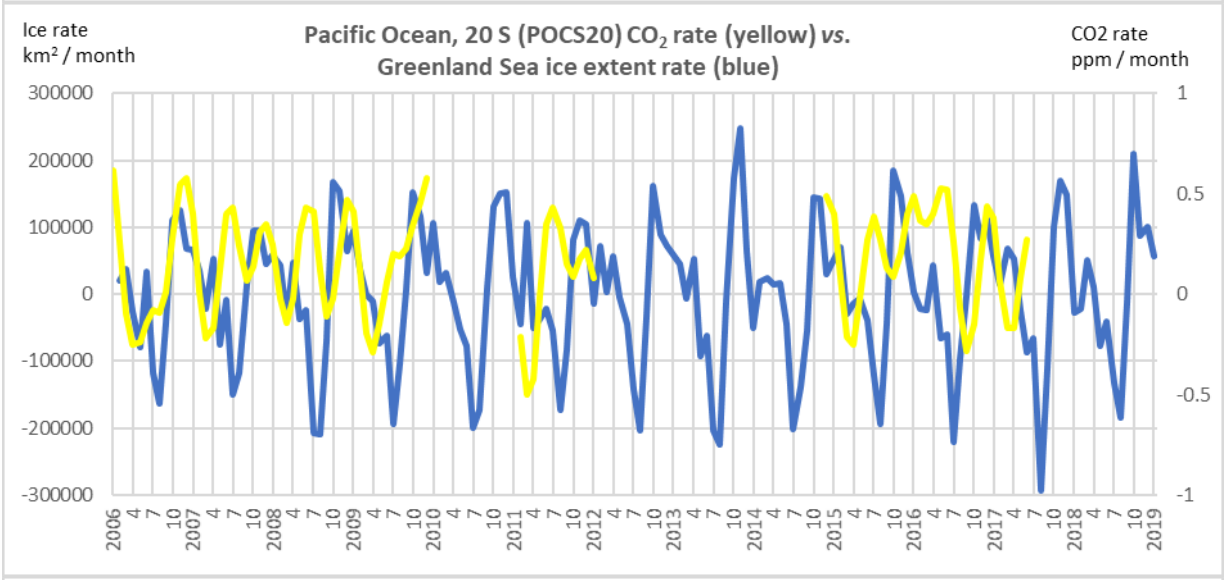

1165

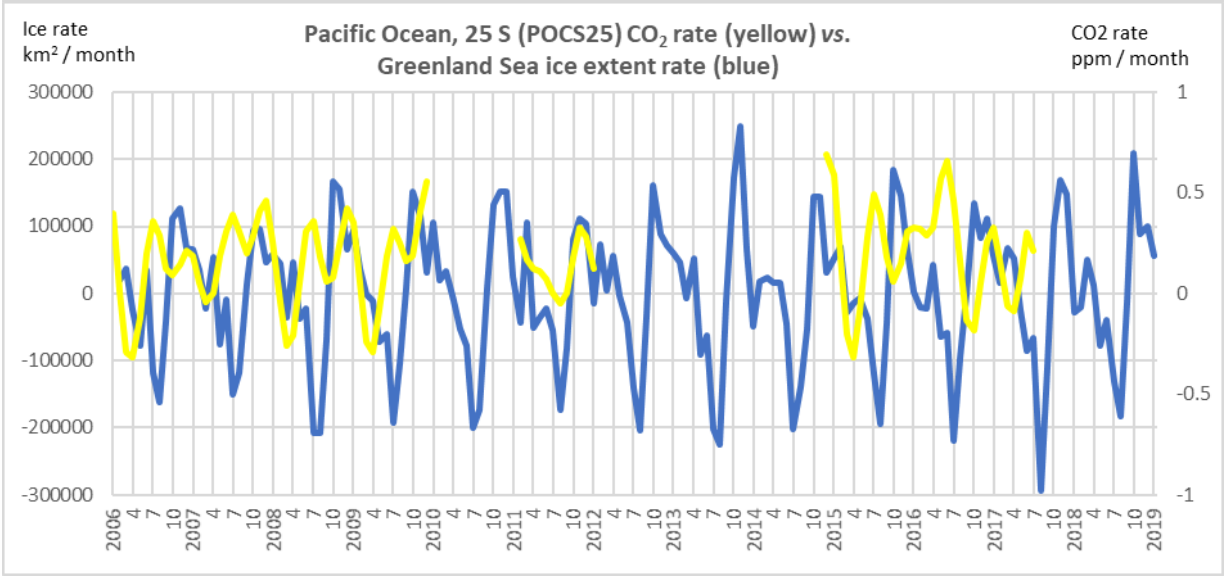

1166

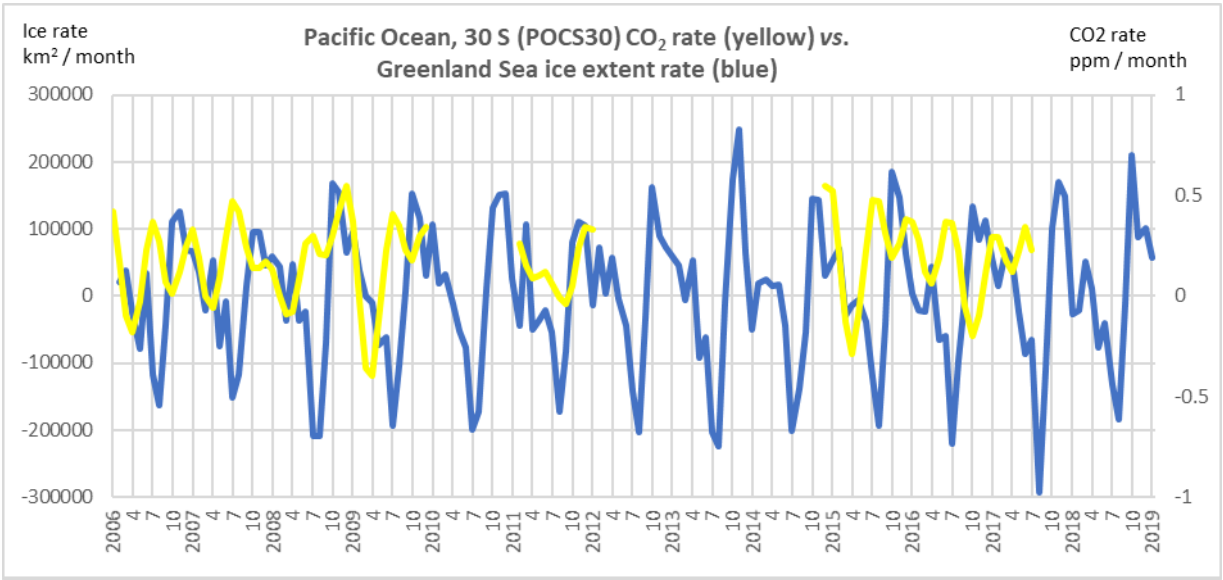

1167

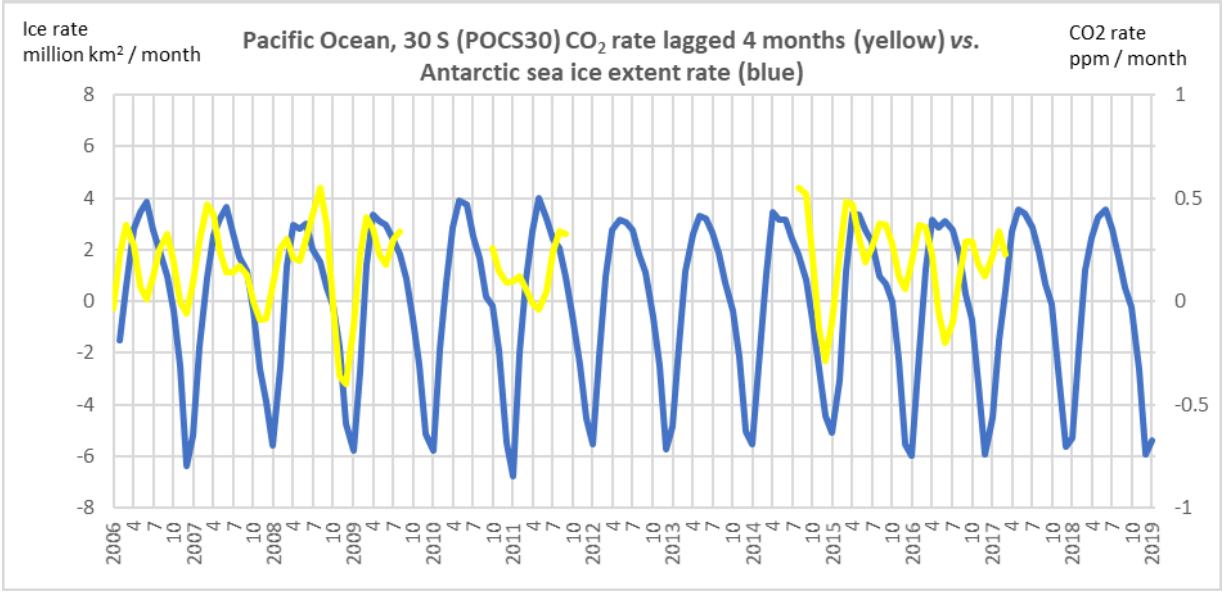

1168

1169

Section D: Selected examples of CO_2 rates and sea ice rates with high visual similarity

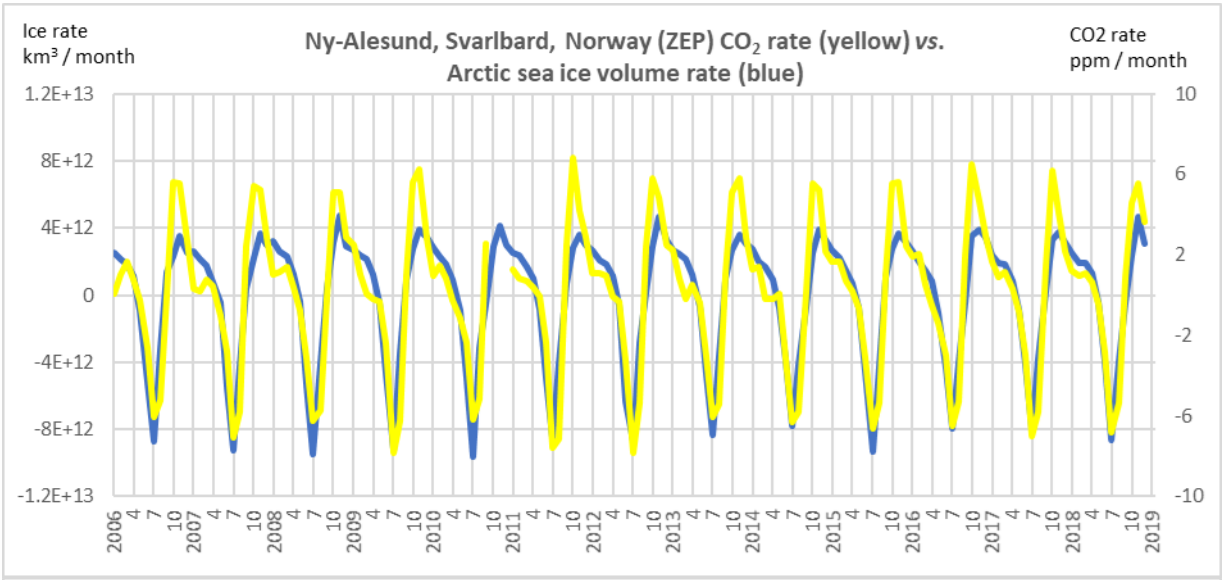

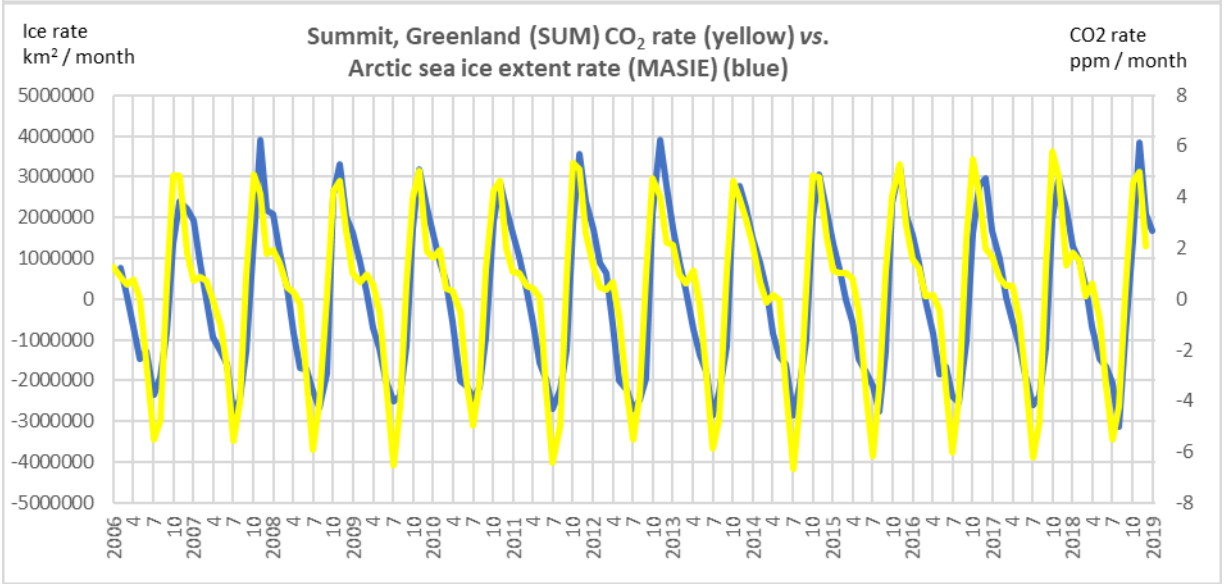

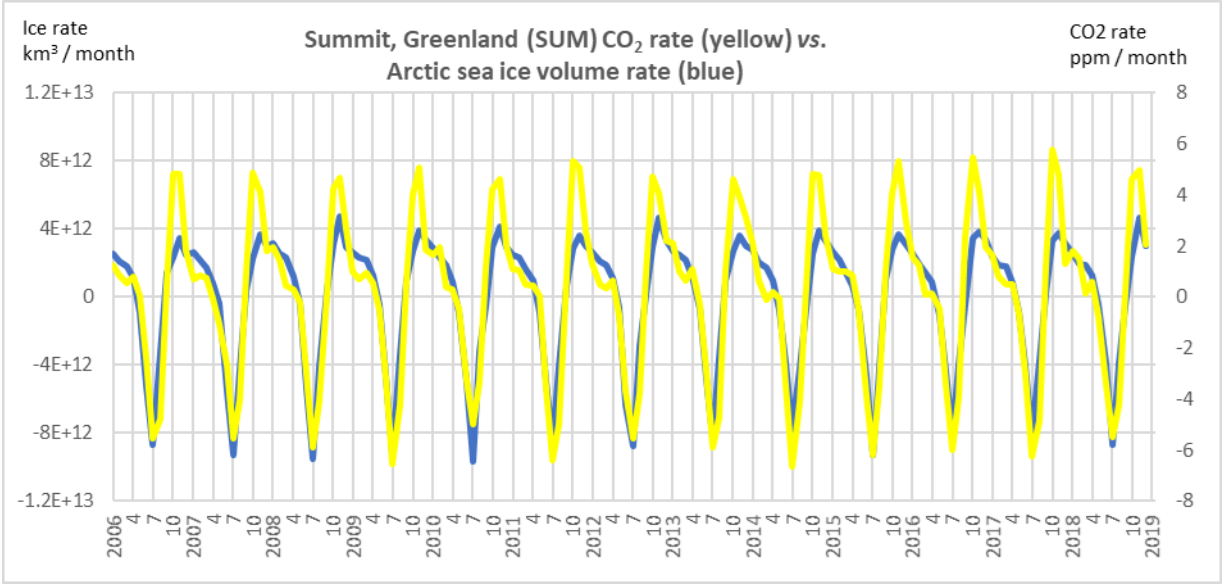

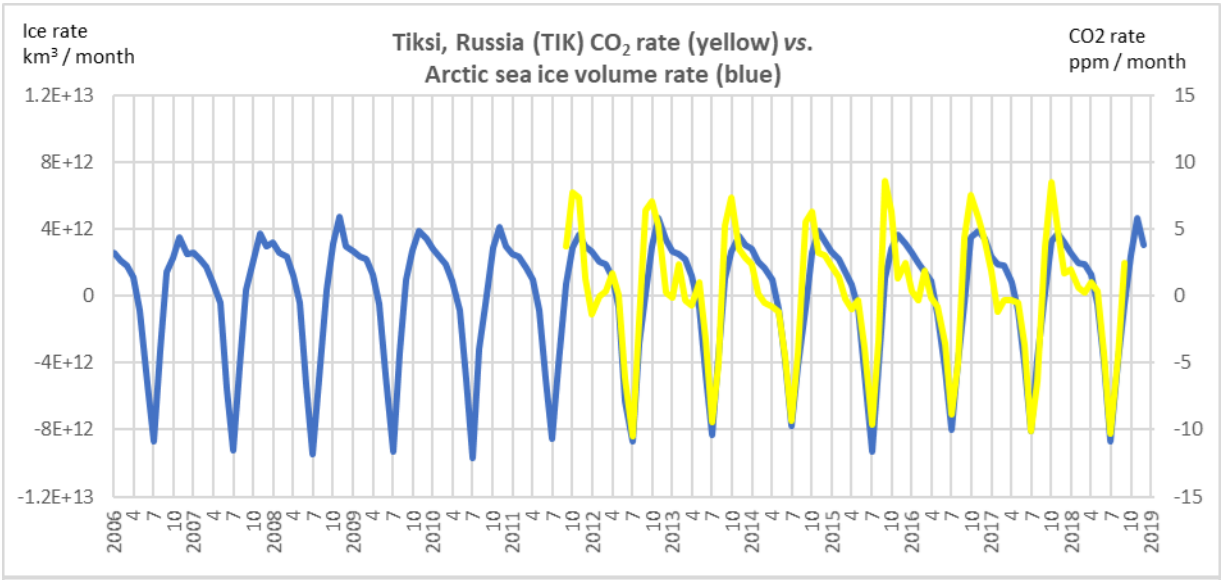

1176

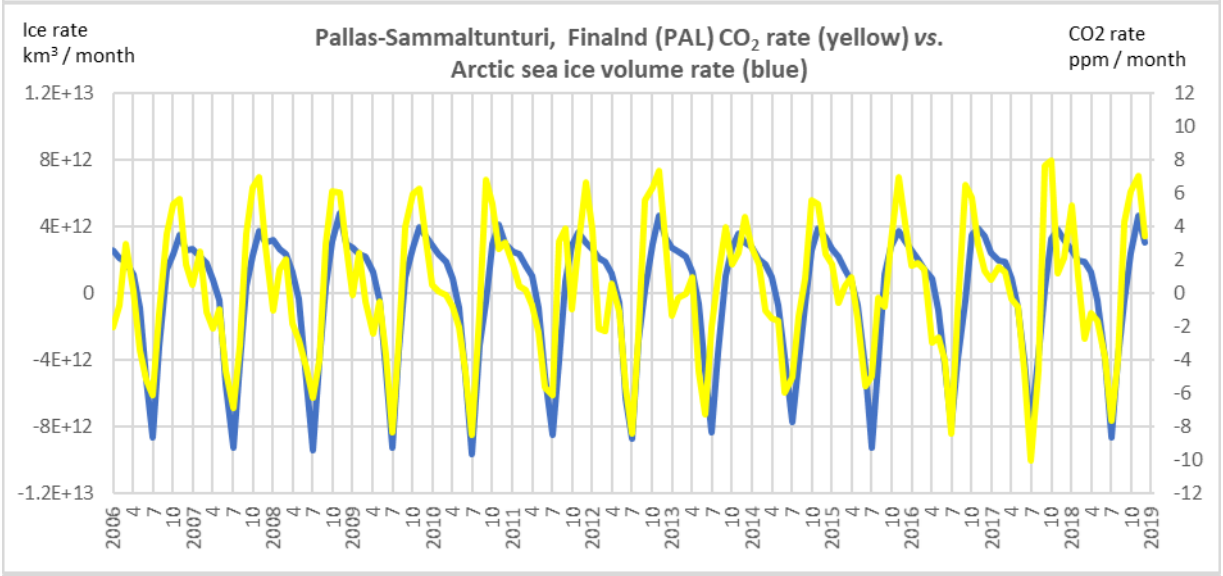

1177

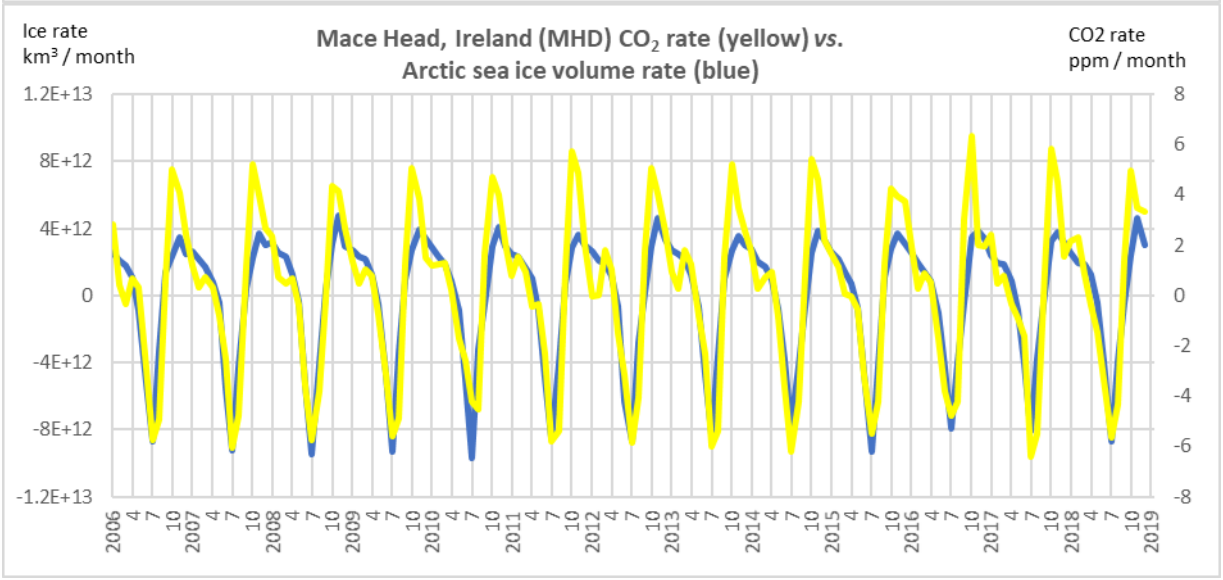

1178

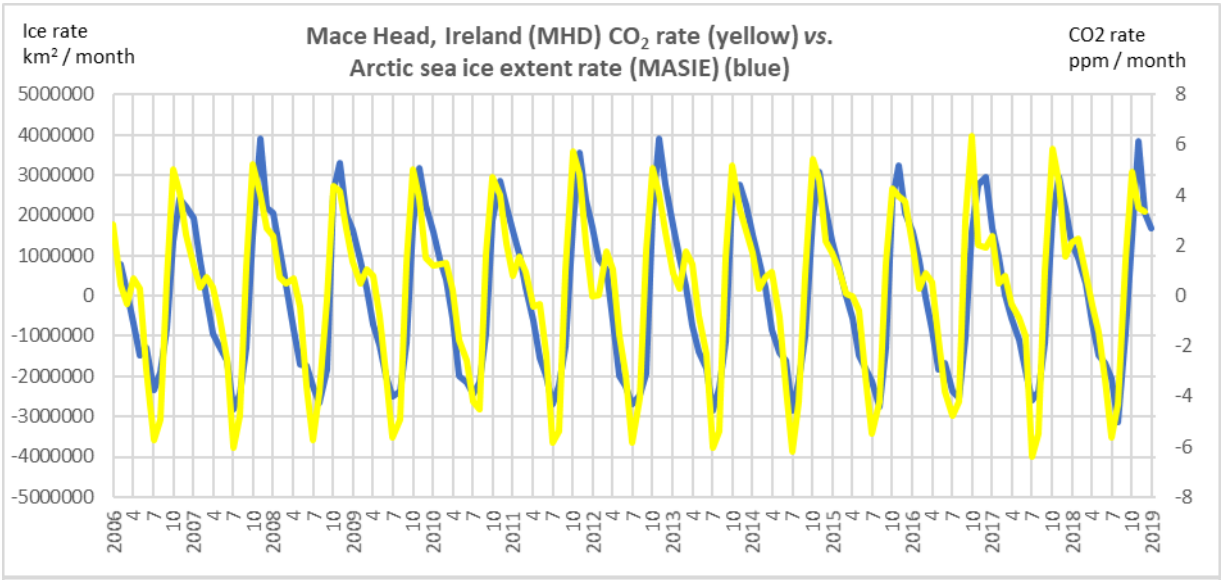

1179

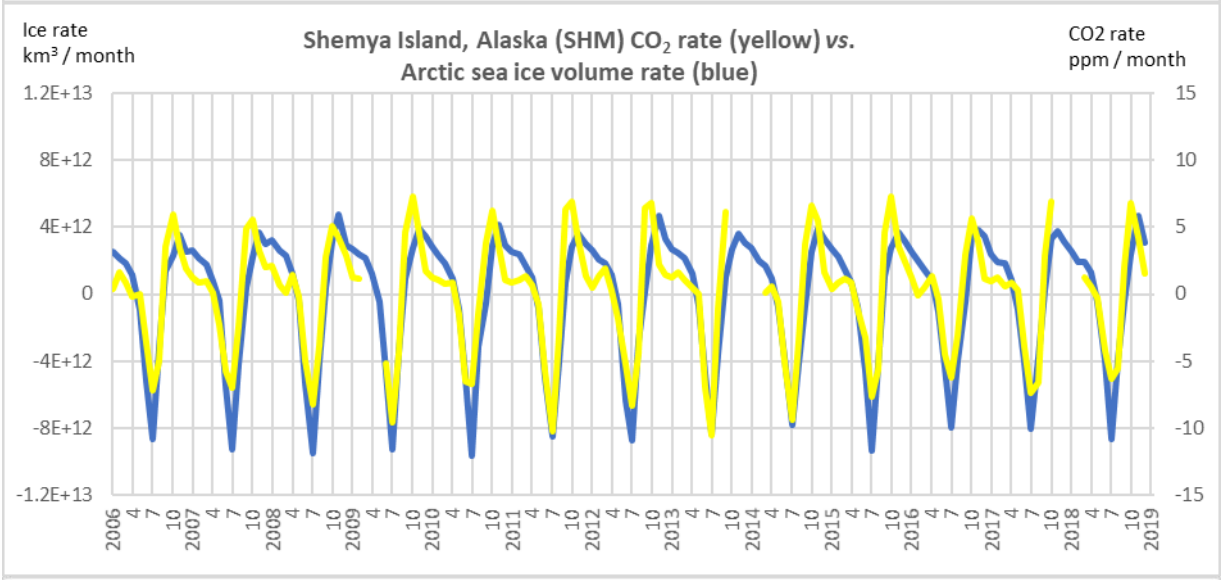

1180

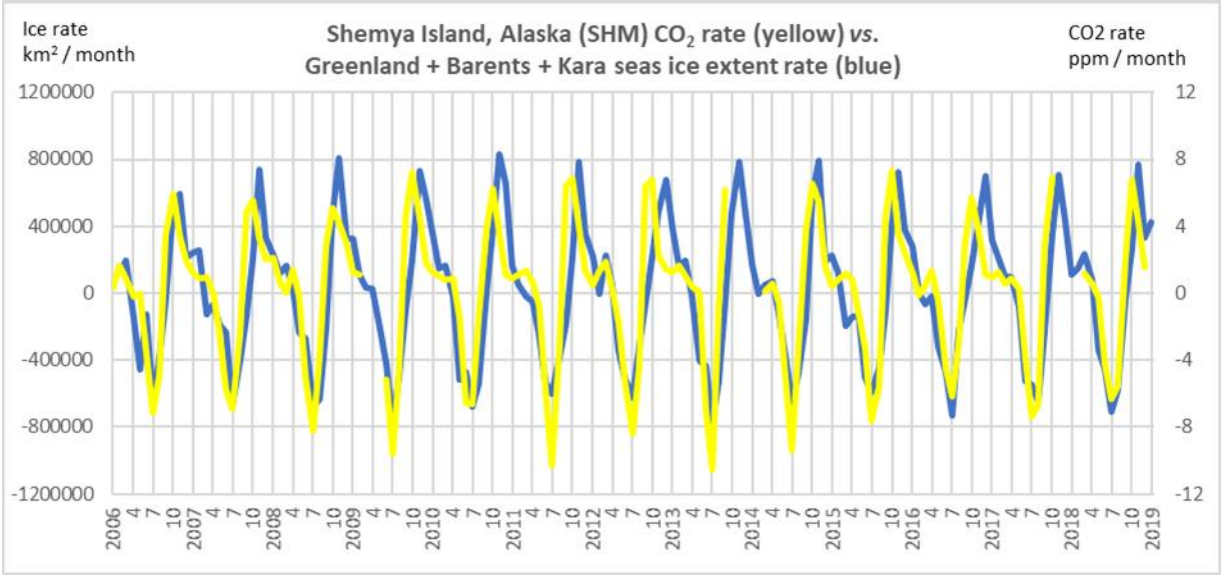

1181

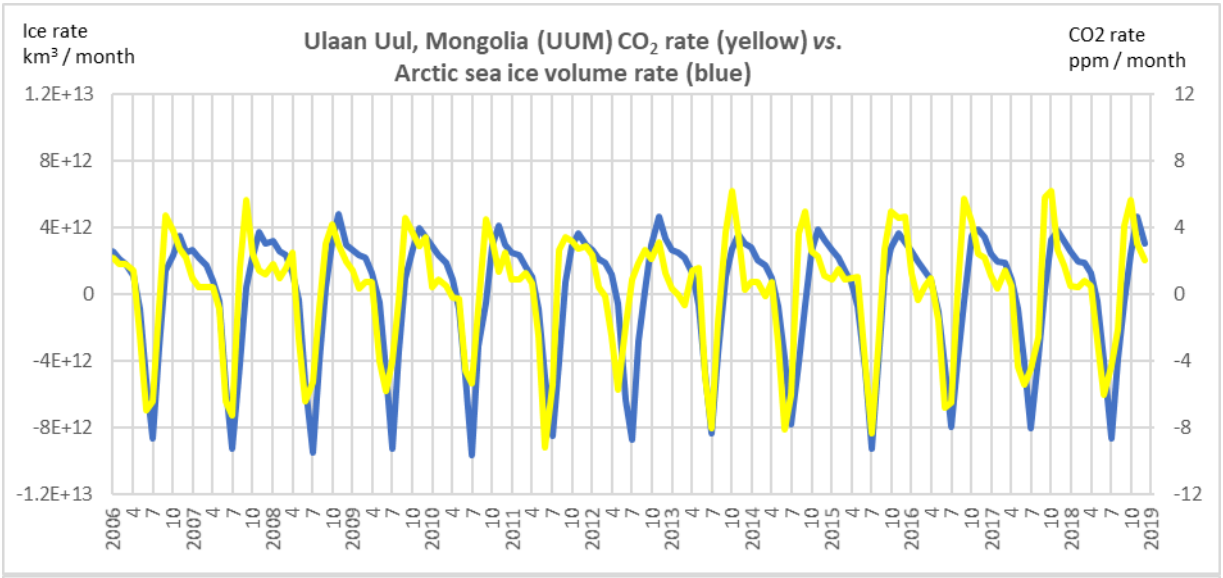

1182

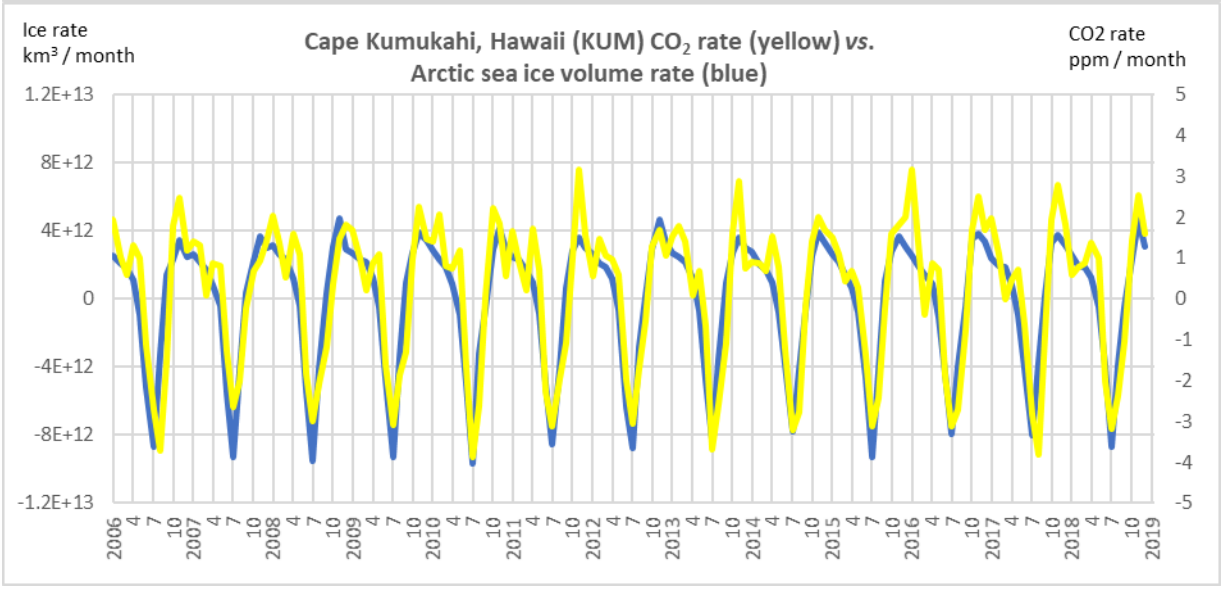

1183

1184

Section E: Barrow (BRW) CO_2 rate vs sea ice rate in Arctic regions (MASIE data and map)

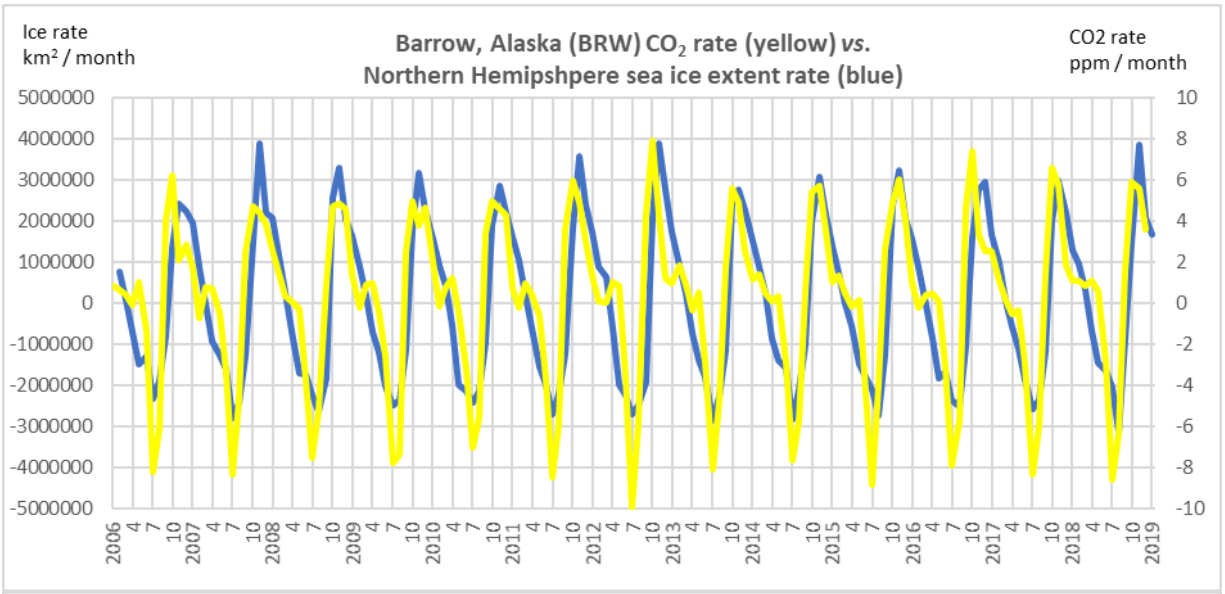

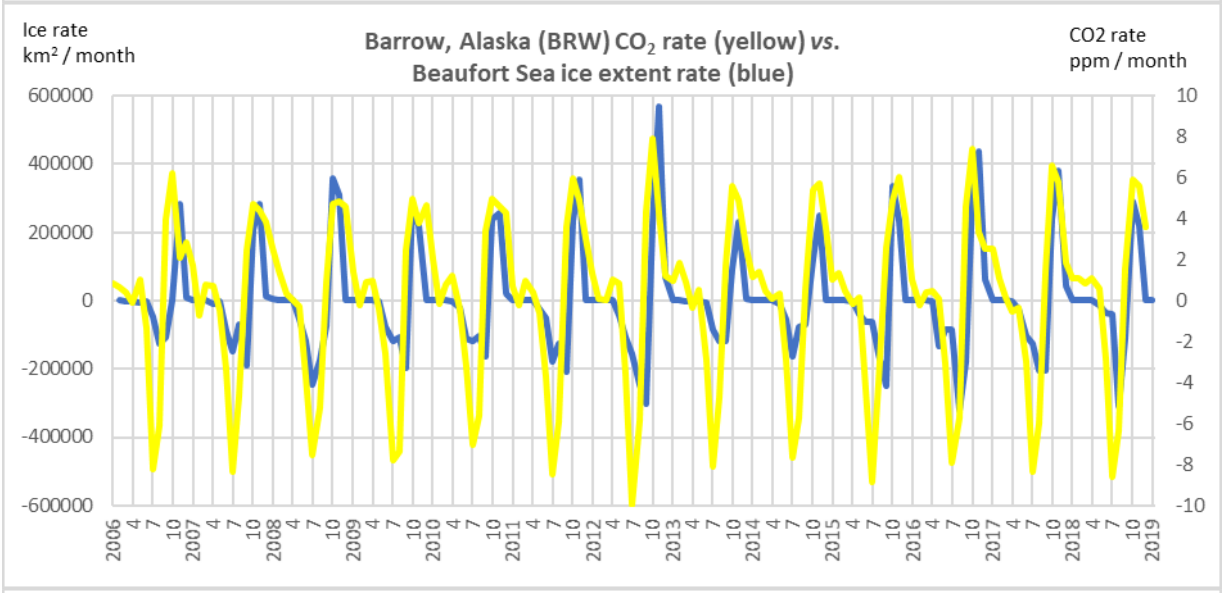

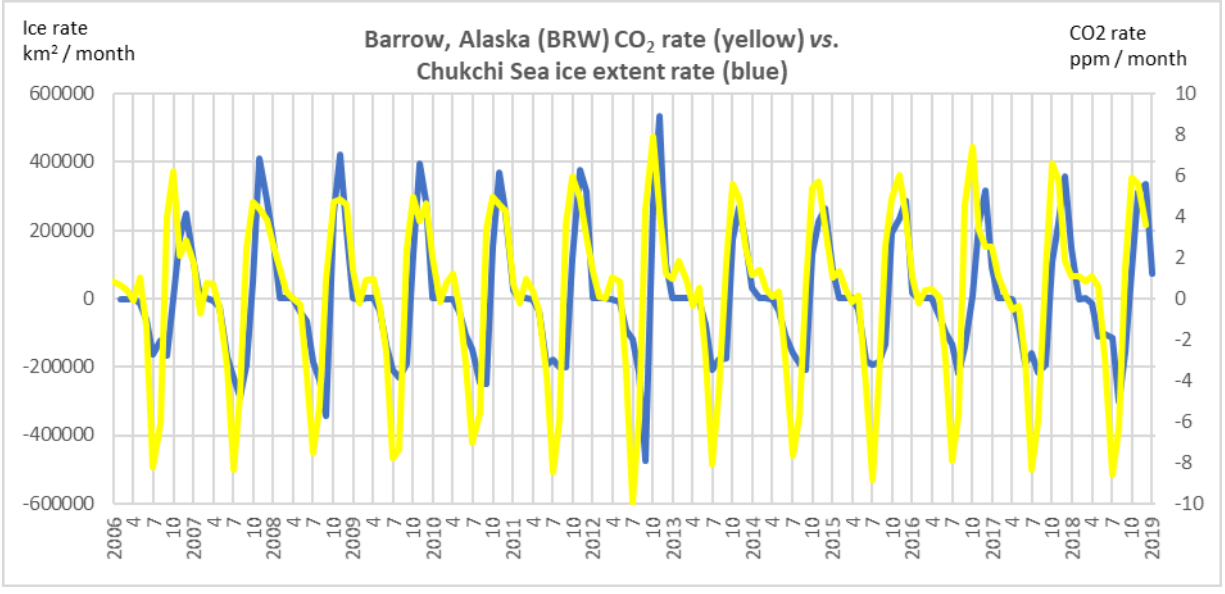

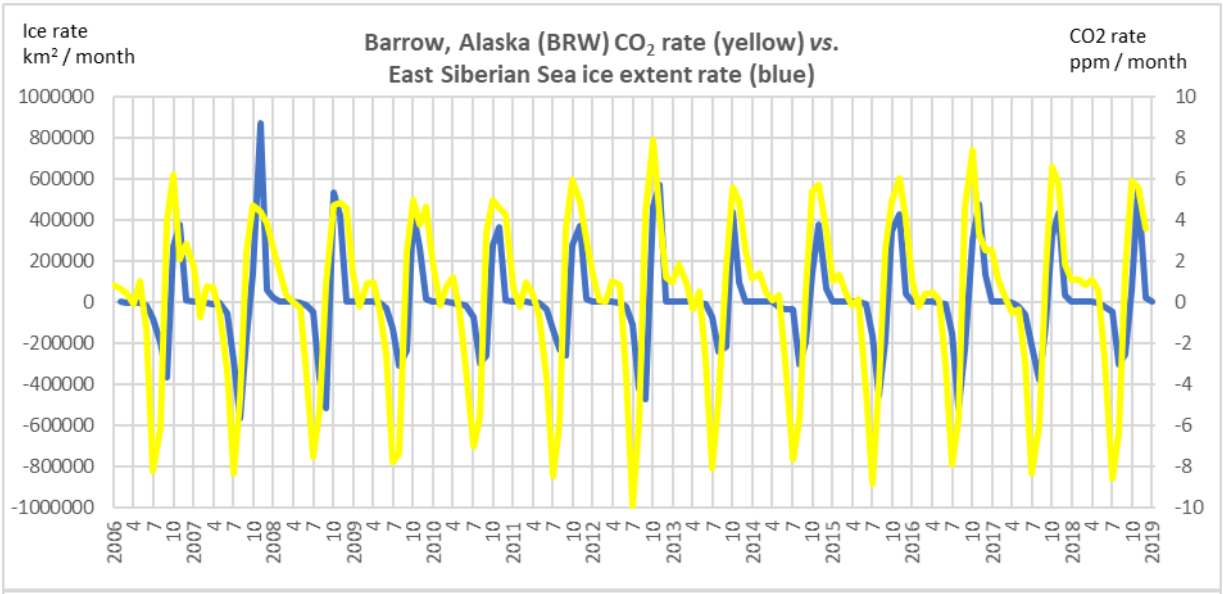

1190

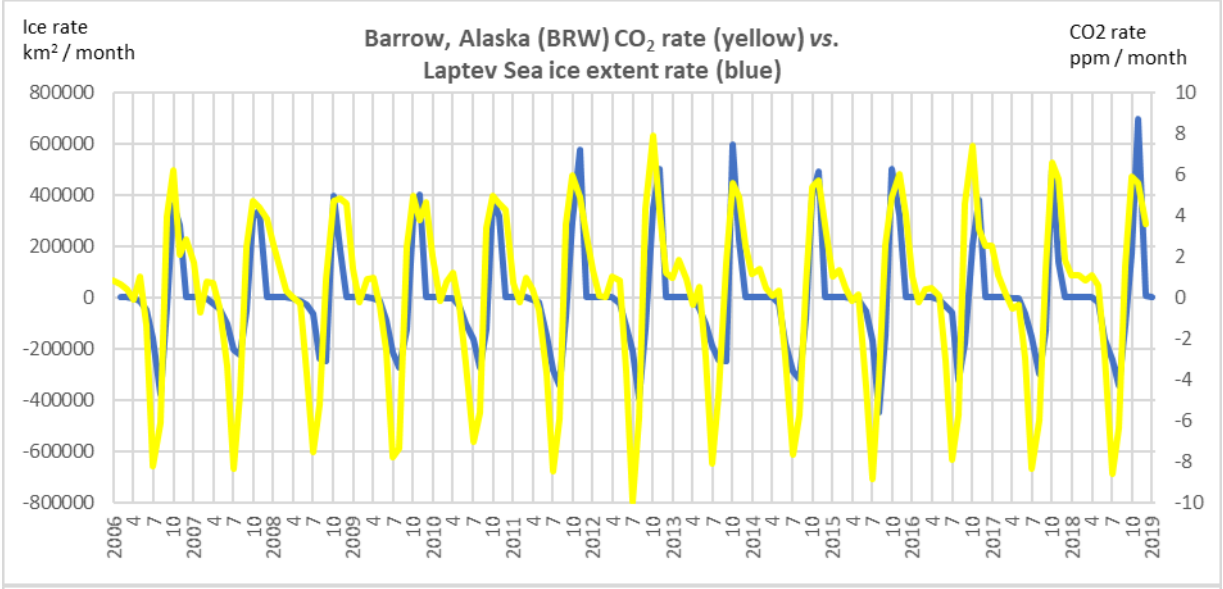

1191

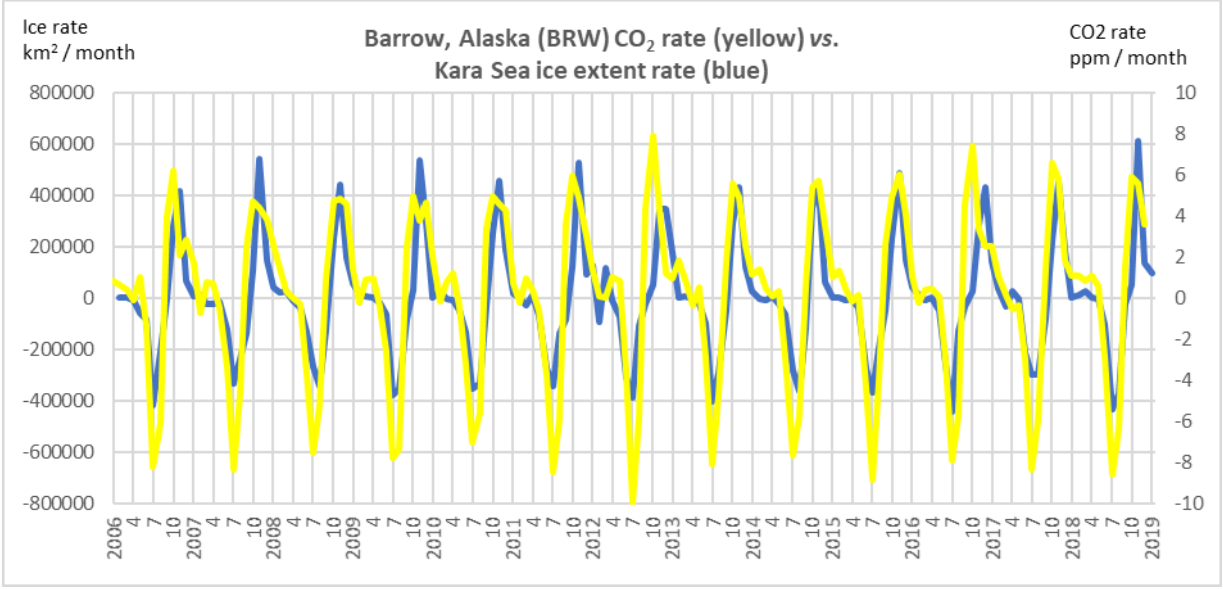

1192

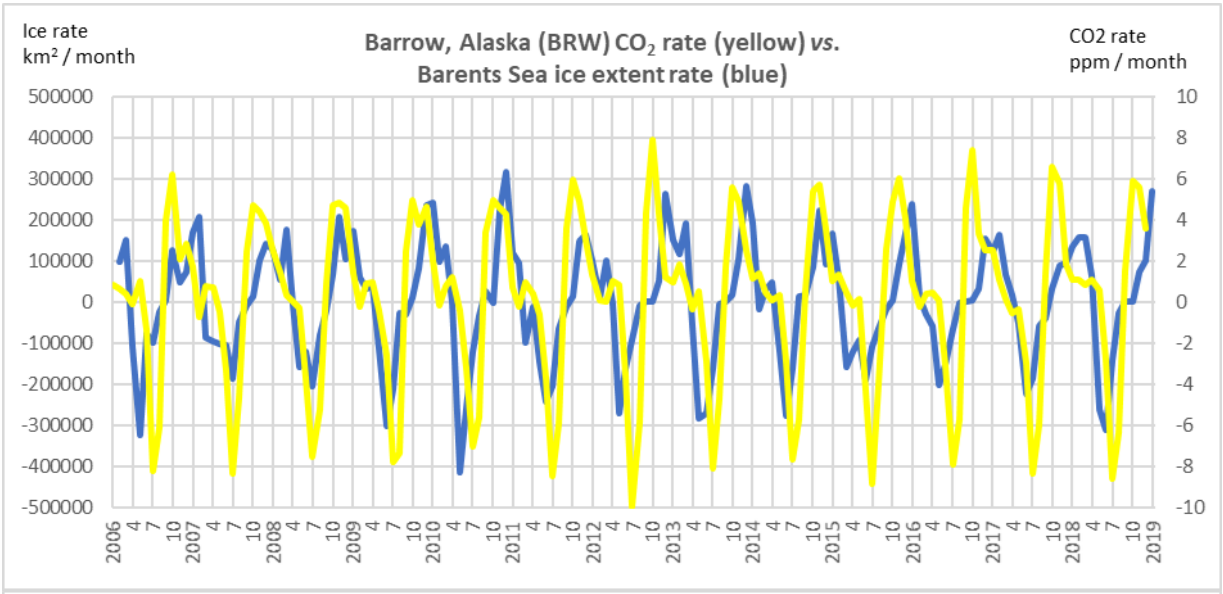

1193

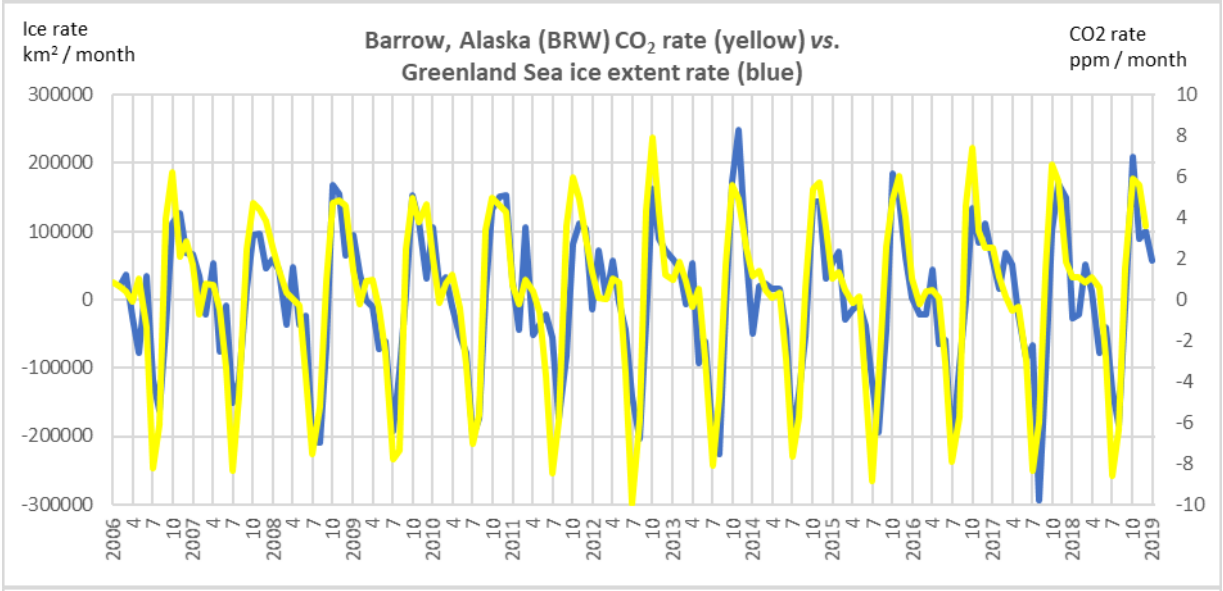

1194

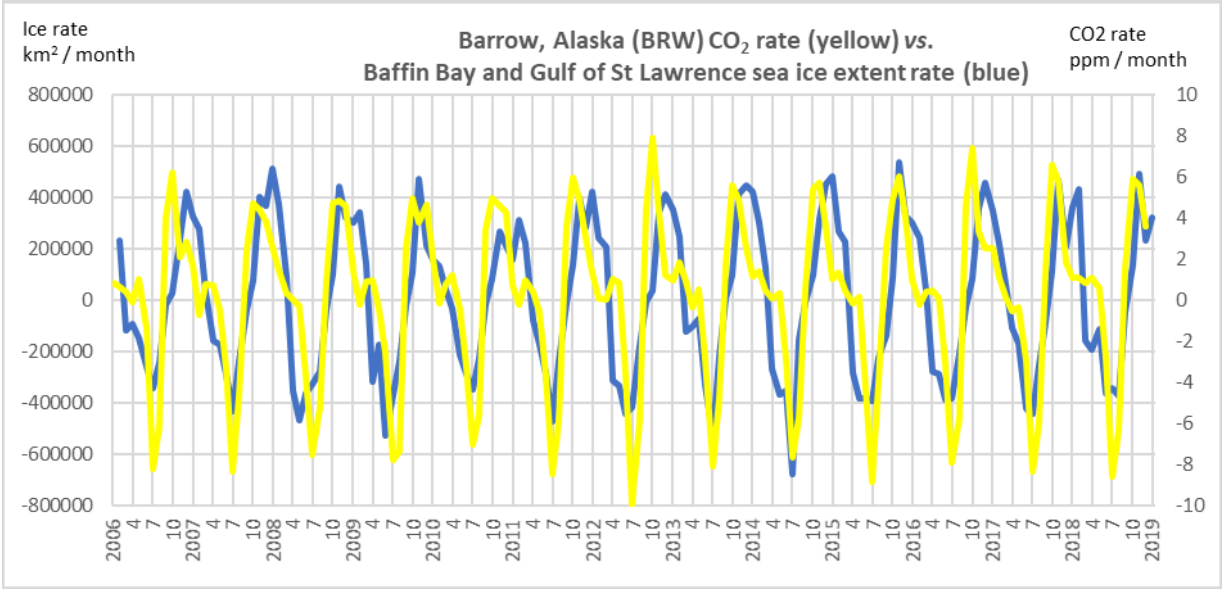

1195

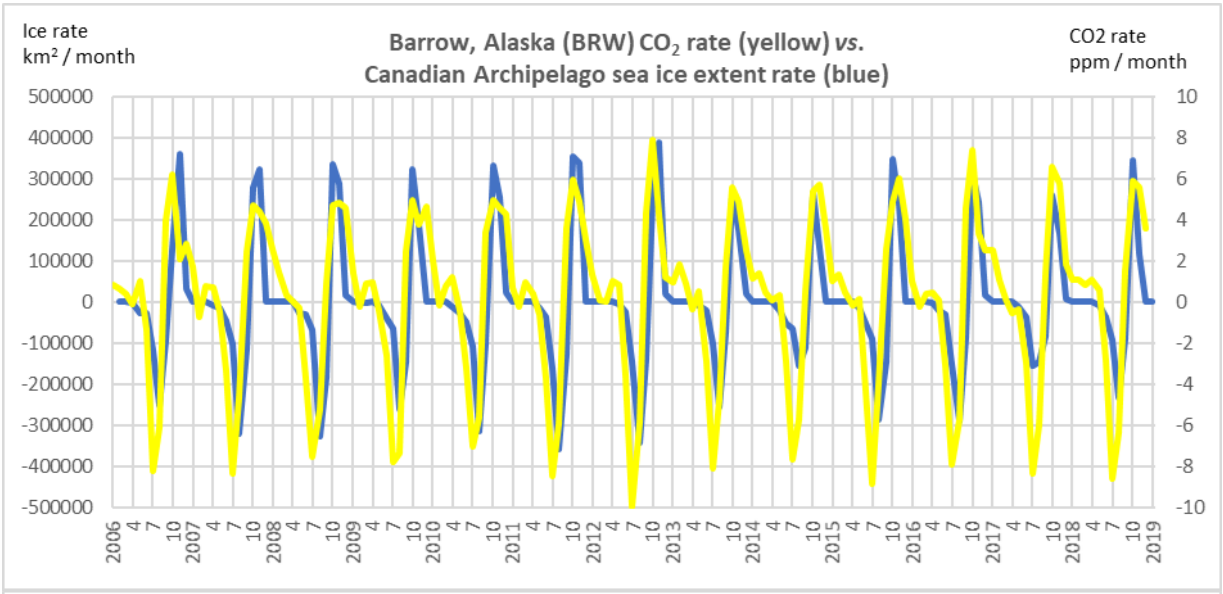

1196

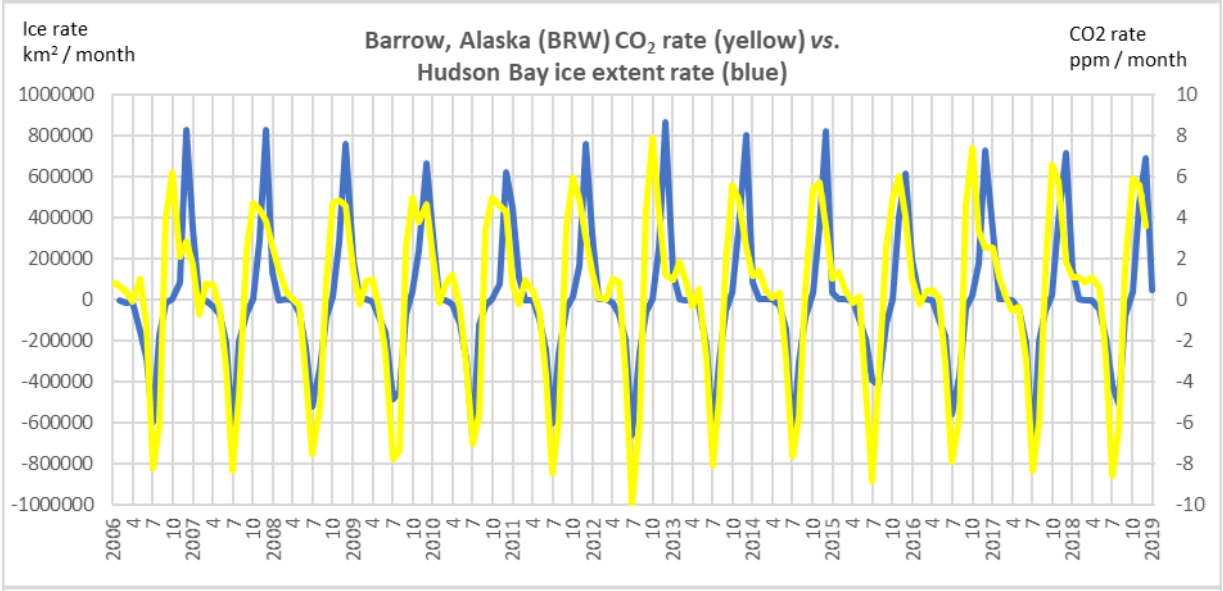

1197

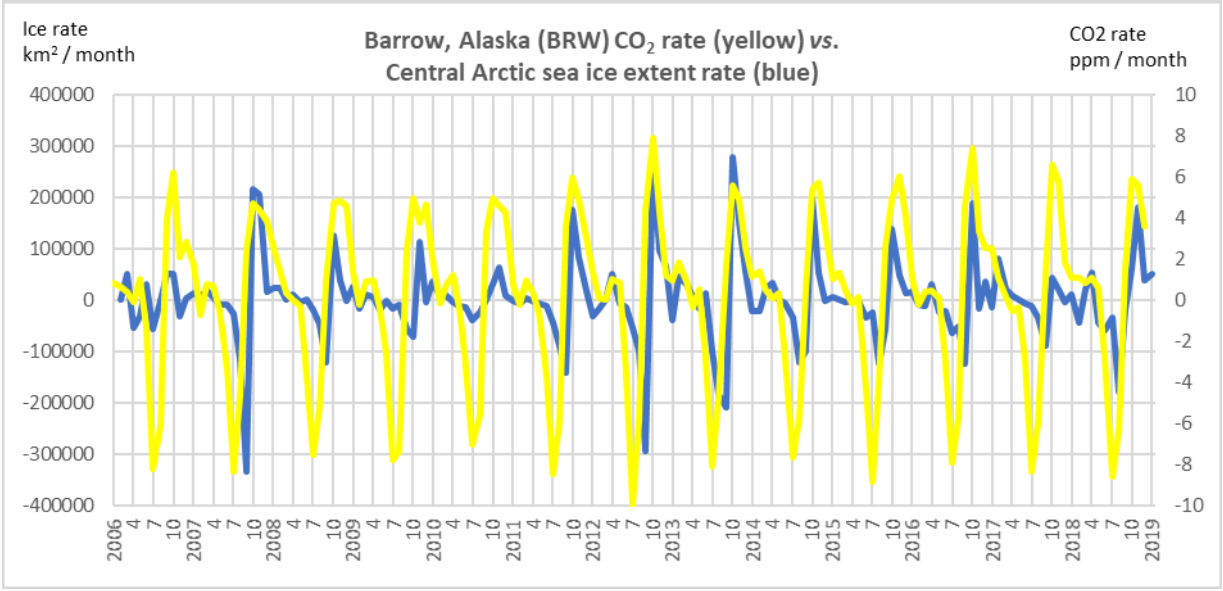

1198

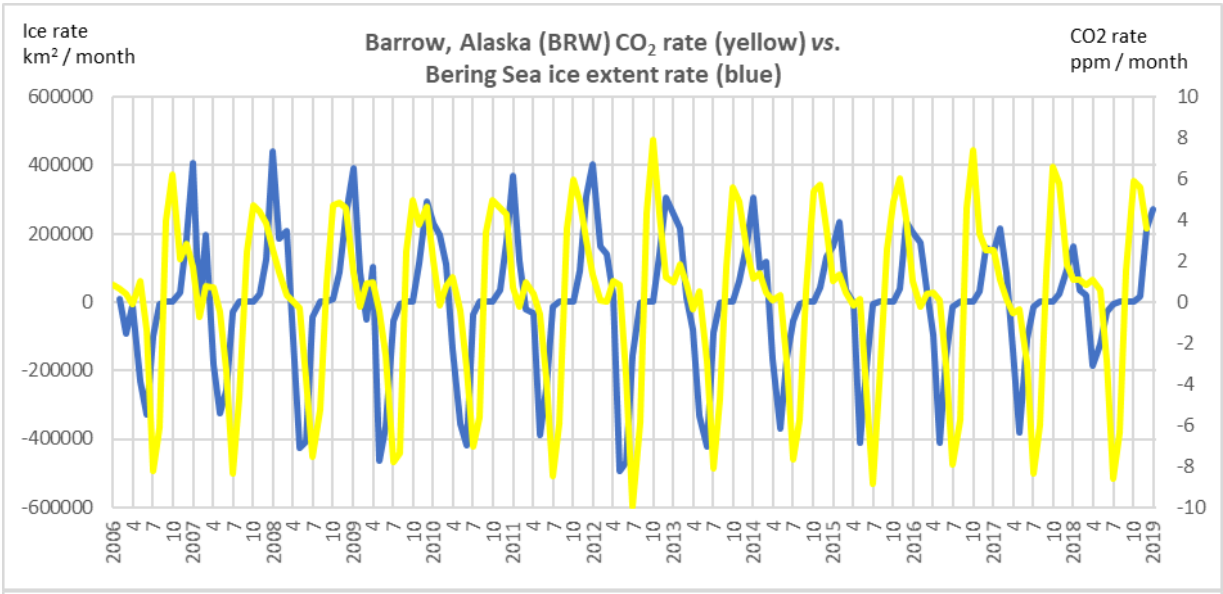

1199

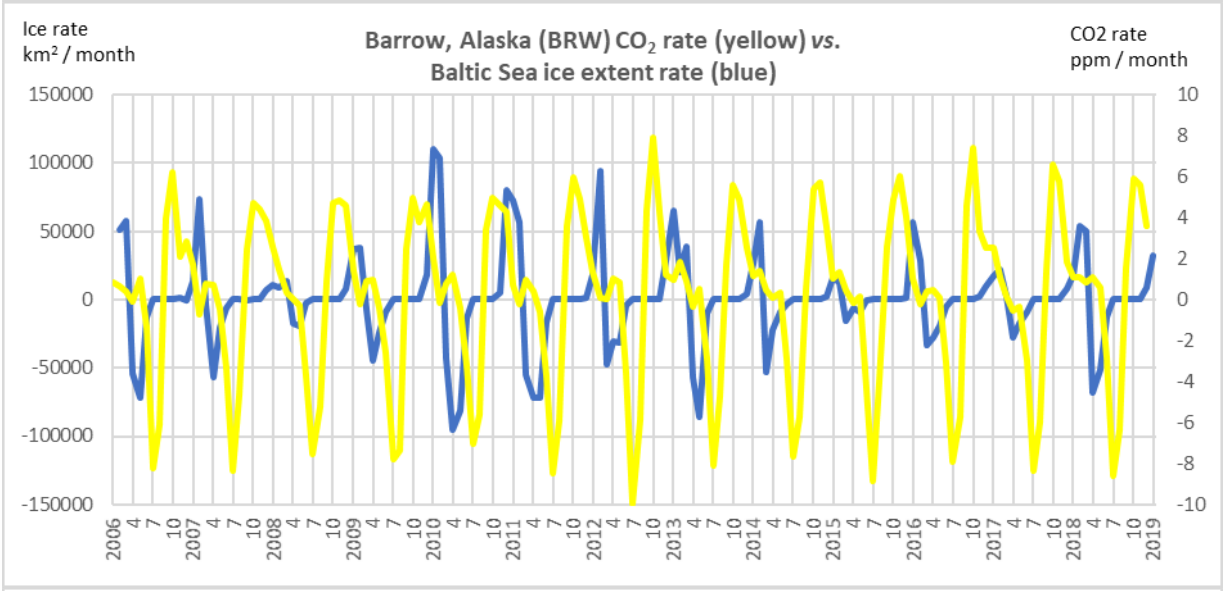

1200

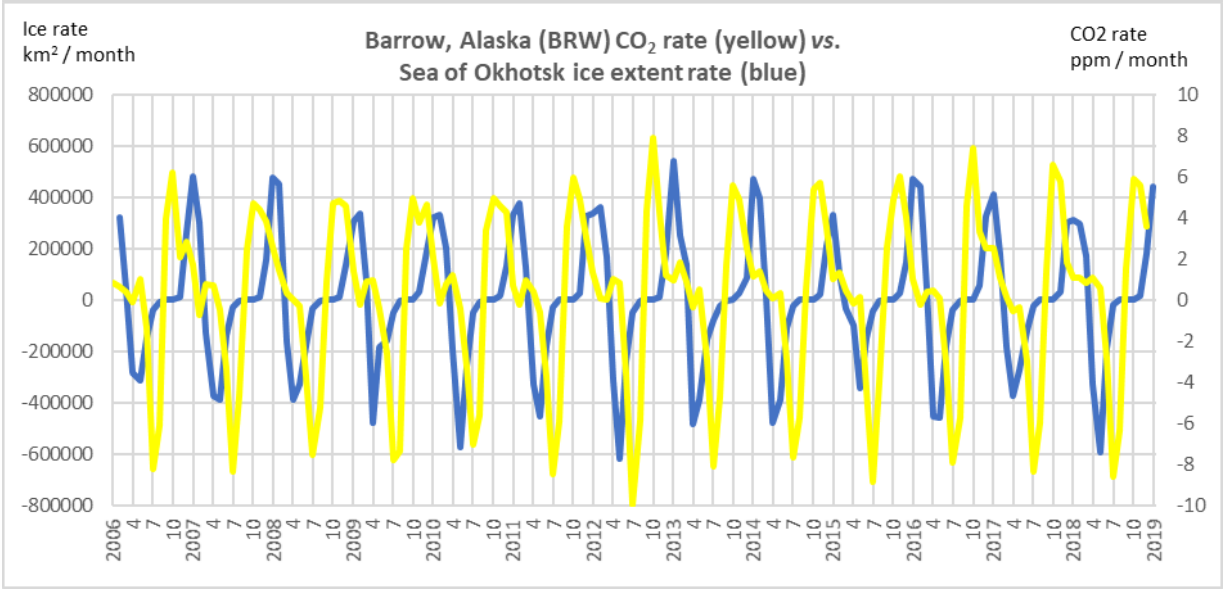

1201

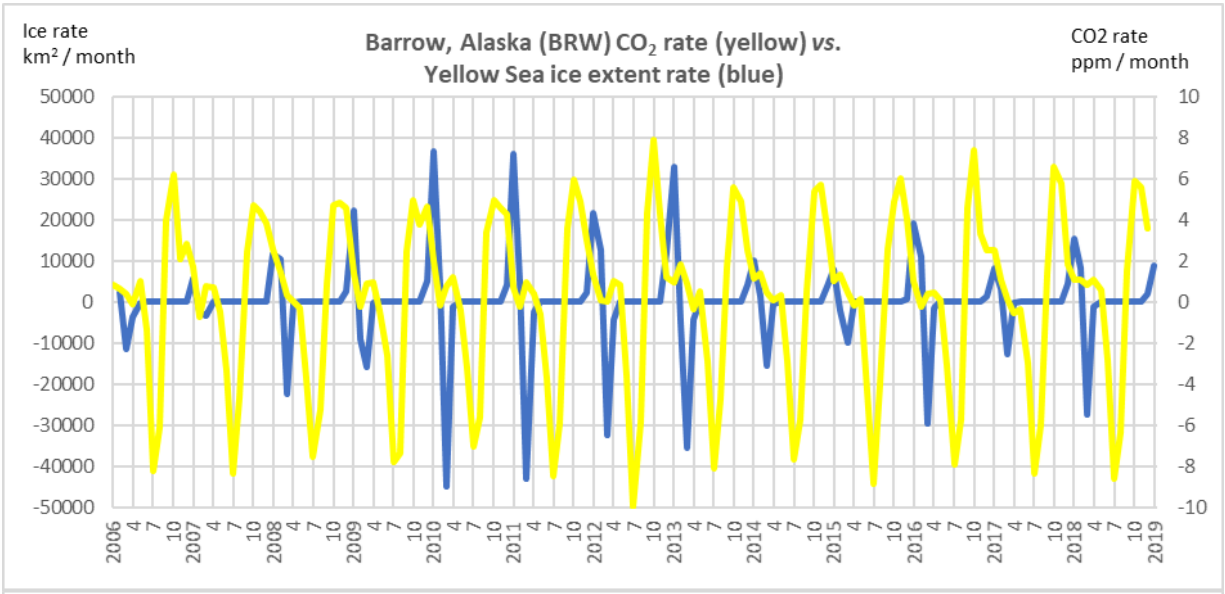

1202

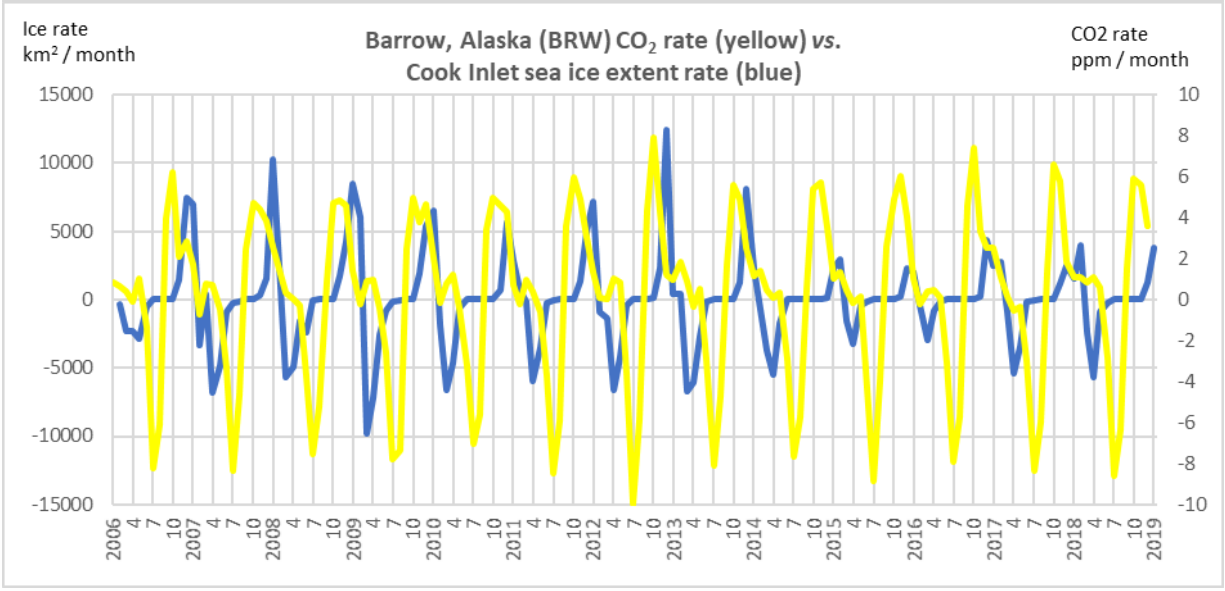

1203

1204